CHIRAL SEPARATION OF DRUGS AND DRUG INTERMEDIATES BY IMMOBILIZED BIOCATALYST

A

THESIS

SUBMITTED TO THE

UNIVERSITY OF PUNE

FOR THE DEGREE OF

DOCTOR OF PHILOSOPHY

IN

BIOTECHNOLOGY

BY

BHALCHANDRA K. VAIDYA

UNDER THE GUIDANCE OF

DR. B. D. KULKARNI

CHEMICAL ENGINEERING AND PROCESS DEVELOPMENT DIVISION, NATIONAL CHEMICAL LABORATORY

PUNE - 411008, INDIA

DECEMBER 2009

Chiral Separation of Drugs and Drug Intermediates by Immobilized Biocatalyst

A

THESIS

SUBMITTED TO THE

UNIVERSITY OF PUNE

FOR THE DEGREE OF

DOCTOR OF PHILOSOPHY

IN

BIOTECHNOLOGY

BY

BHALCHANDRA K. VAIDYA

UNDER THE GUIDANCE OF

DR. B. D. KULKARNI

CHEMICAL ENGINEERING AND PROCESS DEVELOPMENT DIVISION, NATIONAL CHEMICAL LABORATORY

PUNE - 411008, INDIA

DECEMBER 2009

राष्ट्रीय रासायनिक प्रयोगशाला
(वैज्ञानिक तथा औद्योगिक अनुसंधान परिषद)
डॉ. होमी भाभा मार्ग पुणे – 411 008. भारत
NATIONAL CHEMICAL LABORATORY
(Council of Scientific & Industrial Research)
Dr. Homi Bhabha Road, Pune - 411 008. India.

CERTIFICATE

This is to certify that the work incorporated in the thesis entitled '**Chiral Separation of Drugs and Drug Intermediates by Immobilized Biocatalyst**' submitted by **Mr. Bhalchandra K. Vaidya** was carried out by the candidate under my supervision/guidance at Chemical Engineering and Process Development Division, National Chemical Laboratory, Pune (India). Such material as has been obtained from other sources, has been duly acknowledged in the thesis.

Dr. Bhaskar D. Kulkarni **December 2009**

Deputy Director & Head,

Chemical Engineering & Process Development Division,

National Chemical Laboratory,

Pune - 411008 (India).

DECLARATION BY THE CANDIDATE

This is to certify that the work incorporated in the thesis entitled '**Chiral Separation of Drugs and Drug Intermediates by Immobilized Biocatalyst**' is my own work conducted under the supervision/guidance of **Dr. B. D. Kulkarni**, at Chemical Engineering and Process Development Division, National Chemical Laboratory, Pune (India). I further declare that to the best of my knowledge, this thesis does not contain any part of work, which has been submitted for the award of any degree either of this University or any other University without proper citation.

Mr. Bhalchandra K. Vaidya (*Research student*)

Dr. Bhaskar D. Kulkarni (*Research guide*)

Dedicated to

my parents & teachers ...

CONTENTS

Acknowledgements

This gives me immense pleasure to express a deep sense of respect and gratitude to Dr. B. D. Kulkarni, Deputy Director and Head of Chemical Engineering & Process Development Division, National Chemical Laboratory (NCL) Pune, for the responsibilities taken as my research guide. His rational approach, invaluable advice and constant support helped me to rise up to this level. I really consider myself honoured for having him as my guide.

I am equally obliged to my co-guide Dr. Sanjay Nene, Head of Biochemical Engineering Department, NCL-Pune who has put countless efforts for making this work successful. I express my earnest gratitude to Dr. Sanjay Nene for his keen interest, excellent guidance, valuable suggestions and parental care during my stay in NCL-Pune. Without his intellectual inputs, motivation and consistent support the objective would not have been accomplished. His creative thinking, administrative skills, unbiased nature and gracious personality inspired me a lot. Working with him was an enriching and enlivening experience.

I am extremely grateful to Dr. Alain Archelas, Directeur de Recherches au CNRS, Biosciences, Université Paul Cézanne, Marseille, France for allowing me to work in his laboratory for about six months. The work regarding epoxide hydrolase was successful solely because of his efforts, guidance and help. Starting form hostel arrangements up to getting a student residential card, he helped me in all my difficulties during my stay in Marseille, France. I would also like to thank Dr. Jose M. Guisán and Dr. Cesar Mateo, Departamento de Biocatálisis, Instituto de Catálisis, CSIC, Madrid, Spain for their assistance in epoxide hydrolase immobilization.

It is my pleasure to thank Dr. Surendra Ponrathnam for his valuable guidance regarding enzyme immobilization on functional polymers and membranes. His ideas, supervision and assistance gave a proper direction to the present research. The assistance from Dr. C. R. Rajan is gratefully acknowledged. I am sincerely indebted to Dr. R. V. Gadre and Mr. V. V. Jogdand for their technical suggestions and constructive discussions which indeed helped me to plan and execute my experiments. I thank all other scientists and staff members of Biochemical Engineering Group especially Dr. H. V. Adhikane and Dr. (Mrs.) Sangita Kasture for their timely help.

I take this opportunity to extend my heartfelt gratitude to my dear friends Anirudhha Deshpande, Ganesh Ingavale, Jahnvi Shah, Kiran Desai, Laxman Savargave, Narahari Pujari, Renuka Joshi, Sandeep Golegaonkar, Snehal Mutalik and Suyog Kuwar for helping me in my experimental work, for their valuable suggestions and moral support. I would like to thank all my friends and colleagues especially Abhijeet Karale, Amol Dive, D. M. Thakar, Gayatri Iyer, Geetanjali Lale, Hitesh Suthar, Kumar Babu, Mayura Dange-Deshpande, Santosh Dhule and Tushar Deshpande for their co-operation and providing a friendly working ambiance.

I wish to thank Dr. S. Shivram, the Director, National Chemical Laboratory for allowing me to work in this laboratory and to submit this work in the form of Ph. D. thesis.

The present research would not have been feasible without financial assistance from the Council of Scientific and Industrial Research (CSIR), New Delhi, India. The Senior Research Fellowship from CSIR-India is gratefully acknowledged. I would also like to acknowledge the funding from Department of Science and Technology (SERC Programme), New Delhi, India for part of the

work. I am grateful to the Science and Technology Service, Embassy of France in India, New Delhi, India for offering me a 'Sandwich Ph.D. Fellowship' to carry out part of my Ph.D. research in University of Paul Cézanne, Marseille, France.

Last but not the least, I would like to dedicate this moment of joy to my parents and dear sister, Vidya without their moral support the goal would not have been accomplished.

– B. K. Vaidya

LIST OF ABBRIVIATIONS

Prefixes:

d- or (+)-	Dextrorotatory enantiomer
l or (-)	Levorotatory enantiomer
dl- or (±)-	Equi molar mixture of dextrorotatory and levorotatory enantiomers (i.e. racemic mixture)
D-	*Dexter* enantiomer
L-	*Laevus* enantiomer
DL-	Equi molar mixture of *Dexter* and *Laevus* enantiomers (i.e. racemic mixture)
R- or (*R*)-	*Rectus* enantiomer
S- or (*S*)-	*Sinister* enantiomer
RS- or *(RS)*-	Equi molar mixture of *Rectus* and *Sinister* enantiomers (i.e. racemic mixture)
Rac-	Racemic mixture

Acronyms and abbreviations:

AGE	Allyl glycidyl ether
AGE-(C) polymer	Polymers synthesized using AGE (as monomer units) and cyclohexanol (as porogen)
AGE-(H) polymer	Polymers synthesized using AGE (as monomer units) and hexanol (as porogen)
AGE-(L) polymer	Polymers synthesized using AGE (as monomer units) and lauryl alcohol (as porogen)
AGE-Re	Agar entrapped *Rhodococcus erythropolis* cells
AIBN	2,20-Azobis(isobutyronitrile)
AL	*Alcaligens* lipase
ALG-Re	Alginate entrapped *Rhodococcus erythropolis* cells
ANOVA	Analysis of Variance
CLD	Cross-link density
CLE	Cross-linked enzyme
CLEA	Cross-linked enzyme aggregates
CLEC	Cross-linked enzyme crystal
CRL	*Candida rugosa* lipase
DKR	Dynamic kinetic resolution

DMSO	Dimethyl sofoxide
DoE	Design of Experiments
DOPA	3,4-Dihydroxy phenylalanine
DOPA-ester	3,4-Dihydroxy phenylalanine ethyl ester
DPC	Differential photocalorimeter
DVB	Divinyl benzene
EGDM	Ethylene glycol dimethacrylate
EH	Epoxide hydrolase
EMB	Enzyme membrane bioreactor
Enz	Native enzyme moiety
Enz^*, Enz_1^*, Enz_2^*	Partially deactivated enzyme moieties
Enz^D	Totally deactivated enzyme moiety
FCCCD	Face-centre central composite design
FID	Flame ionized detector
FT-IR	Fourier transform infrared spectroscopy
GA	Glyoxyl-agarose
GC	Gas chromatography
GLA	Glutaraldehyde
GMA	Glycidyl methacrylate
GMA-(C) polymer	Polymers synthesized using GMA (as monomer units) and cyclohexanol (as porogen)
HEMA	2-Hydroxyethyl methacrylate
HPA	Homophenylalanine
HPA-amide	Homophenylalanine amide
HPA-ester	Homophenylalanine ethyl ester
HPLC	High pressure liquid chromatography
LHRH	Luteinizing-hormone releasing hormone
MSD	Mean square deviation
MTCC	Microbial Type Culture Collection
NA	Naphthylalanine
NA-amide	Naphthylalanine amide
N-acetyl HPA	N-acetyl homophenylalanine
N-acetyl NA	N-acetyl naphthylalanine
N-acetyl PG	N-acetyl phenylglycine
NA-ester	Naphthylalanine ethyl ester
NMDA	N-methyl D-aspartate

PAGE	Polyacrylamide gel electrophoresis
PCL	*Pseudomonas cepacia* lipase
PG	Phenylglycine
PG-amide	Phenylglycine amide
PG-ester	Phenylglycine ethyl ester
p-NP	*p*-Nitro-phenol
p-NPP	*p*-Nitro-phenyl palmitate
PP	Polypropylene
PPL	Porcine pancreatic lipase
PTHF	Polytetrahydrofuran
PUA	Polyurethane
PUA-Re	Polyurethane entrapped *Rhodococcus erythropolis* cells
PVA-Re	Polyvinyl alcohol entrapped *Rhodococcus erythropolis* cells
PVP	Poly vinyl pyrrolidone
rpm	Rotations per minute
RRSSq.	Relative residual sum of squares
RSM	Response surface methodology
SDS	Sodium dodecyl sulphate
SEM	Scanning electron microscopy
SGDV	Styrene-Glycidyl methacrylate-Divinyl benzene
SMBC	Simulated moving bed chromatography
St-EH	*Solanum tuberosum* epoxide hydrolase
TLL	*Thermomyces languginous* lipase
w/w	Weight by weight
w/v	Weight by volume
v/v	Volume by volume
X	Adsorption parameter (i.e. mg of diol adsorbed per g of resin)

Symbols:

a	Residual enzyme activity (dimensionless)
a_c	Residual enzyme activity calculated by kinetic model (dimensionless)
a_e	Experimental residual enzyme activity (dimensionless)
A_{CLEA}	Activity expressed by CLEA
$A_{Immo.}$	Activity of 1 g of immobilized enzyme (U/g of support)
$A_{Membrane}$	Activity of 1 cm^2 of biocatalytic membrane (U/cm^2 of membrane)

A_{Free}	Activity of free enzyme (U/mL)
$A_{Residual}$	Activity of residual enzyme solution (U/mL)
C	Conversion ratio (dimensionless)
cc	Correlation coefficient
c_S^R	Concentration of *R*-enantiomer of substrate
c_S^S	Concentration of *S*-enantiomer of substrate
$c_{S(t)}^R$	Concentration of *R*-enantiomer of substrate at time *t*
$c_{S(t)}^S$	Concentration of *S*-enantiomer of substrate at time *t*
$c_{S(0)}^R$	Initial concentration of *R*-enantiomer of substrate (at t = 0)
$c_{S(0)}^S$	Initial concentration of *S*-enantiomer of substrate (at t = 0)
c_P^R	Concentration of *R*-enantiomer of product
c_P^S	Concentration of *S*-enantiomer of product
E	Enantiomeric ratio (dimensionless)
E_d	Deactivation energy (kJ $kmol^{-1}$ K^{-1})
ee	Enantiomeric excess (dimensionless)
ee_P	Enantiomeric excess of product (dimensionless)
ee_S	Enantiomeric excess of substrate (dimensionless)
K, K_1 and K_2	Thermal deactivation kinetic constants (min^{-1})
K_{cat}	Turnover number (s^{-1})
K_{cat}/K_m	Specificity constant ($mM^{-1} \cdot s^{-1}$)
k_d	Thermal deactivation rate constants in Arrhenius equation (min^{-1})
K_m	Michaelis constant (mM)
K_m^R	Michaelis constant for *R*-enantiomer (mM)
K_m^S	Michaelis constant for *S*-enantiomer (mM)
k_R	Rate of transformation of *R*--enantiomer of a substrate
k_S	Rate of transformation of *S*-enantiomer of a substrate
R	Universal gas constant (8.314×10^{-3} kJ $kmol^{-1}$ K^{-1})
R^2	Regression coefficient
[*S*]	Substrate concentration (mM)
t	Time
T	Temperature
$t_{1/2}$	Half-life (min)
${}^{Total}A_{Free.}$	Total activity of free enzyme loaded on 1 g of polymer beads (Units)
v	Initial velocity of enzymatic reaction (U/mg)
V_{Free}	Volume of free enzyme (mL)
V_{max}	Maximum reaction velocity (U/mg)

V_{max}^{R}	Maximum reaction velocity for *R*-enantiomer (U/mg)
V_{max}^{S}	Maximum reaction velocity for *S*-enantiomer (U/mg)
$V_{Residual}$	Volume of residual enzyme solution (mL)
α-(*R*) and β-(*R*)	Regioselectivity constants for *R*-epoxide (indicating preference of attack on more substituted and less substituted carbon atom of the oxirane ring respectively)
α-(*S*) and β-(*S*)	Regioselectivity constants for *S*-epoxide (indicating preference of attack on more substituted and less substituted carbon atom of the oxirane ring respectively)
β^*, β_1^* and β_2^*	Activity ratio (dimensionless)
ΔE_d	Difference in deactivation energies (kJ $kmol^{-1}$ K^{-1})
η	Efficiency coefficient (dimensionless)

Units: *

cal	Calorie
g	Gram
h	Hour
J	Joule
K	Kelvin
kDa	Kilo dalton
L	Liter
m	Meter
M or mol.	Mole
min	Minute
s	Second
U	Enzyme units *(as defined in respective chapters)*
W	Watt
°C	Degree centigrade

(Units with SI prefixes are not listed.)*

LIST OF FIGURES

Chapter 1:

Chapter 2:

Chapter 3:

Chapter 4:

Chapter 5:

Chapter 6:

Chapter 7:

Chapter 8:

LIST OF SCHEMES

Chapter 6:

Chapter 7:

LIST OF TABLES

Chapter 1:

Chapter 2:

Chapter 3:

Chapter 4:

Chapter 5:

Chapter 6:

Chapter 7:

CHAPTER

1

Introduction

Chirality has become a major theme in the design, discovery, development and marketing of new drugs [1-3]. The role of chirality in efficacy and safety of drugs has been thoroughly identified and implicated globally by pharmaceutical industries as well as concerned regulatory agencies. Thus, in order to accomplish efficacious and safe medication and also compliance with the guidelines set by the regulatory agencies, pharmaceutical industries are compelled to move towards manufacturing and marketing of chiral drugs essentially in single-enantiomer dosage forms. The worldwide sales of chiral drugs in single-enantiomer dosage forms continued growing at about 13% annual rate over past few years [3]. To respond the rising industrial demand of enantiopure drugs, search of new efficient methods of asymmetric synthesis and the strategic development of the available methods have been the center-stage of academic as well as industrial pharmaceutical research over the recent years [4].

The biocatalytic enantioselective synthesis of highly versatile chiral entities having prospective as drugs or drug intermediates is attempted in the present thesis. This chapter outlines the basic concepts of chirality, mechanism of chiral pharmacology and toxicity, various methods of enantioselective synthesis and the importance of biocatalysis in enantioselective synthesis. Further, this chapter delineates the scope of thesis and elaborates the specific research objectives.

1.1. ROLE OF CHIRALITY IN PHARMACEUTICALS

1.1.1. Basic concepts of chirality

Chirality (also sometimes called stereoisomerism or dissymmetry) is a property of an object which is non-superimposable with its mirror image. The word chiral is derived from Greek word '*cheir'*, which means 'handedness'. When a molecule cannot be superimposed on its mirror image, this molecule and its image are called chiral. It is like a pair of hands which are otherwise appear identical but in fact are non-superimosible on each other as demonstrated in Fig. 1.1 [5]. A chiral molecule contains at least one chiral center or asymmetric center, which is a central carbon atom to which four different atoms (or group of atoms) are attached. Carbon is not the only atom that can act as an asymmetric center. Sulfur, phosphorus and nitrogen can sometimes form chiral molecules such as omeprazole, cyclophosphamide and methaqualone, respectively [6].

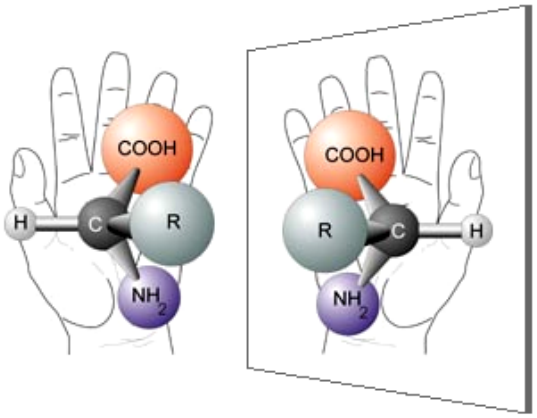

Fig. 1.1: Non-superimposible mirror images (enantiomers) of a chiral molecule [**Source:** Adapted from ref. **7**]

The origin of the chirality lies in stereoisomerism. Stereoisomers are isomers which differ from each other only by way of orientation of atoms (or group of atoms) in a three dimensional space. The classification of stereoisomers is given in Fig. 1.2.

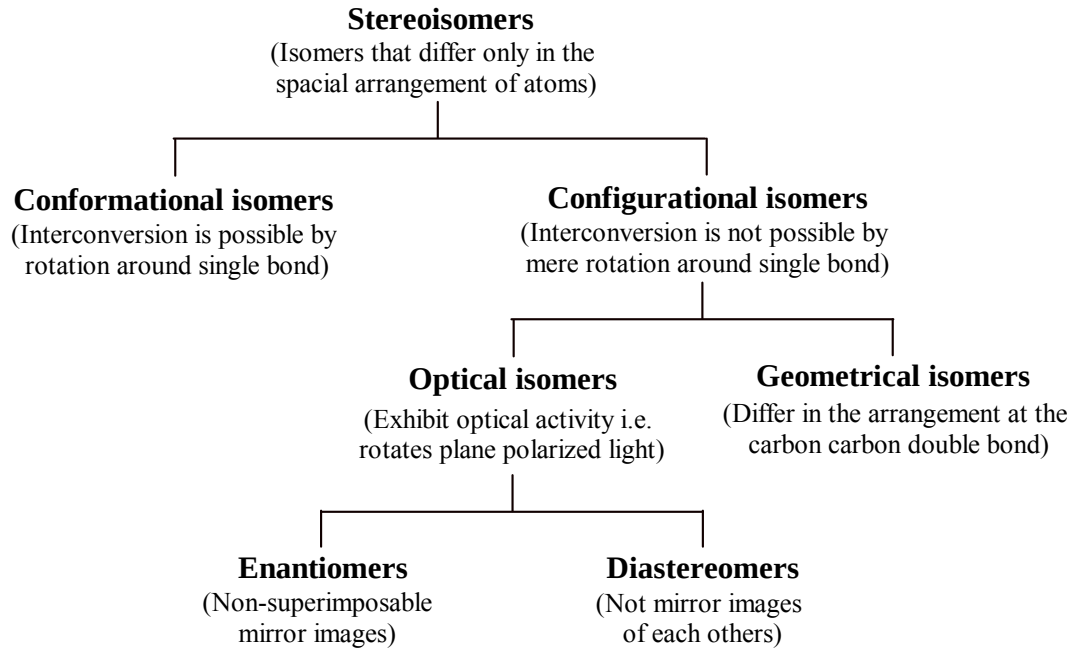

Fig. 1.2: Classification of stereoisomers

Stereoisomers which are non-superimposable mirror images of each others are called as enantiomers. Compounds which are chiral may exist as enantiomers while those which are achiral (non chiral) cannot exist as enantiomers. Thus chirality is the

necessary and sufficient condition for the existence of enantiomers [9]. The ability of chiral molecules to rotate plane polarized light is termed as optical activity. Enantiomers are therefore also sometimes referred as optical isomers. Two enantiomers of the same compound rotate plane polarize light in opposite direction. Depending on whether they rotate the plane-polarized light towards right (+) or left (-), the two enantiomers of compound may be classified as dextrorotary (*d*-isomer) or levorotary (*l*-isomer) respectively.

Enantiomers have identical physical properties (e.g melting point, boiling point, density etc.) except for the direction of rotation of plane polarized light and identical gross chemical properties (e.g. reactivity towards achiral acids and bases) except towards chiral (i.e. enantioselective) reagents/catalysts. An equimolar mixture (50:50) of the two enantiomers of a chiral compound is called a racemic mixture (racemate) that does not exhibit optical activity. Racemic mixture is denoted with sign (±) or (*dl*) or with prefix *rac* [5]. The arrangement of atoms (or group of atoms) that characterizes a particular stereoisomer is called its configuration. The configuration is indicated by use of prefixes *R* and *S* according to the Sequence Rule proposed by R.S. Cahn, C. Ingold and V. Prelog [9]. This system is based on a set of rules for ordering the priority to the substituents attached to the asymmetric atom. If the counting from the highest priority (highest atomic number or highest mass) to the lowest one, goes in a clockwise direction, the configuration is designated as *R* (Latin: *Rectus* means right); otherwise if counting goes in a counter clockwise direction, the configuration is designated as *S* (Latin: *Sinister* means left). A racemate is designated as *RS*. Depending upon the direction of plane polarized light towards right (+) or left (-), each *R*- and *S*-enatiomer is designated as *R*(+) or *R*(-) and *S*(+) or *S*(-) [5].

The stereoisomers that are not mirror images of each other are called as diastereomers. Unlike enantiomers, diastereomers exhibit different physical and chemical properties. Epimers are a special category of diastereoisomers. They are a pair of stereoisomers with more than one stereogenic center that differs in chirality at one and only one chiral center.

1.1.2. Chirality and biological activity

Although chirality is not a prerequisite for the biological activity, the chirality of bioactive compounds causes distinct differences in the biological activities of the

individual enantiomers. This is a general phenomenon and applies to all other bioactive substances, such as drugs, fragrances, flavours, insecticides and herbicides etc. [4]. For instance, (i) *d*-Popoxyphene (marketed as Darvon) has narcotic analgesic effects while *l*-propoxyphene (marketed as Novrad) has antitussive properties. (ii) (+)-Ascorbic acid has antiscorbic property while its optical isomer, (-)-ascorbic acid is inactive. (iii) *S,S*-Aspartame has sweet taste while its *R,R*-isomer is bitter. (iv) *R*-(-)-Limonene has orange-like flavour while *S*-(+)-limonene gives lemon-like flavour. (v) *S*-(+)-Carvone smells like caraway while *R*-(-)-carvone smells like spearmint. (vi) *d*-Bermethrine is potent insecticide while *l*-bermethrine is almost inactive. Thus, despite having identical chemical composition, the enantiomers of chiral bioactive compounds *surprisingly* exert dissimilar biological responses [6, 8].

1.1.3. Mechanism of chiral pharmacology and toxicity

Drugs work by binding to the specific biological sites (or drug binding sites), such as proteins (receptors, enzymes), nucleic acids (DNA and RNA) and biomembranes (phospholipids and glycolipids) present in the body. The pharmacological activity of drugs depends mainly on their interaction with these biological sites. All these sites are composed of homochial biomolecules having complex three-dimensional structures, capable of recognizing the chirality of the drug molecule [5]. Whereas, only one enantiomer of a chiral drug preferentially interacts with the binding site, the other enantiomer has a weak interaction with that receptor or interacts with some other receptor(s) in body. The enantiomer which gives a desirable therapeutic effect is termed as ‘eutomer’ while its antipode is termed as ‘distomer’ which is either less potent, inactive, or even exhibits severe side effects or drug toxicity [10]. The molecular mechanism of chiral pharmacology and toxicity is illustrated in Fig. 1.3, using a hypothetical example of a chiral drug and its chiral binding site. For the drug to have its desirable pharmacological effect, the portions of the drug labelled as A, B, and C must interact with the corresponding regions of the binding site labelled a, b, and c respectively. As shown in the Fig. 1.3, among the two enantiomers, only one enantiomer of the drug has a 3-dimensional structure that can be aligned with the binding site to allow A to interact with a, B to interact with b, and C to interact with c. In contrast, another enantiomer of the same drug cannot bind in the same manner no matter how it is rotated in space. Thus, the difference in their 3-

dimensional structures allows the eutomer while prevents the distomer to exert a desirable pharmacological effect [6].

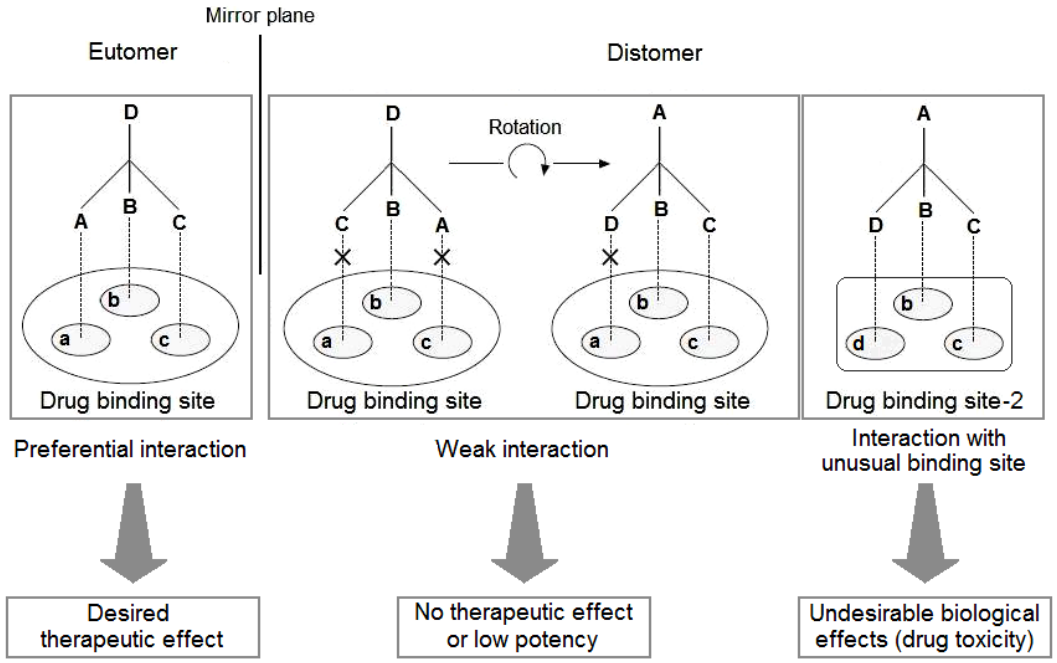

Fig. 1.3: Mechanism of chiral pharmacology and toxicity: the eutomer has a 3-dimensional structure that allows drug domain 'A' to interact with binding site domain 'a', 'B' to interact with 'b', and 'C' to interact with 'c' and therefore exerts a desirable biological effect (an active enantiomer). In contrast, the distomer cannot be aligned to bind these three binding sites simultaneously. As a result, it fails to exert a desirable effect (inactive or less active enantiomer or in few cases distomer interacts with an unusual binding site leading to undesirable biological effects i.e. drug toxicity). [**Source**: Adapted from ref. 6]

In rare cases, the chiral center(s) of a drug does not play an active role in drug-receptor interaction. In these instances, the individual enantiomers may display very similar or even identical pharmacological behaviour at their target site. However, the enantiomers may differ in their metabolic profiles as well as their affinities for other receptors, transporters, or enzymes. Hence, for a given chiral drug, it is appropriate to consider the two enantiomers as two separate drugs with different properties unless otherwise proven experimentally [6]. The examples of differential enantiomer potency and differential enantiomer toxicity of chiral drugs are enlisted in Table 1.1 and Table 1.2 respectively.

Table 1.1: Differential isomer potency of enantiomers of chiral drugs

Specific examples	Therapeutic action and application	Isomer potency
***Case 1:* One enantiomer is active while another is (almost) inactive**		
Albuterol, Salmeterol	Bronchodilators used in the treatment of asthma	*l*-Isomer is active whereas *d*-isomer is inactive [11,12]
Hexobarbital, Secobarbital	Hypnotics or sedative used in psychiatric treatment	*l*-Isomer is active whereas *d*-isomer is inactive [13,14]
Ketamine, isoflurane	Anesthetic	*d*-Isomer is active whereas *l*-isomer is almost inactive [15,16]
***Case 2:* One enantiomer is therapeutically active while another is less active**		
Verapamil, Nicardipine	Calcium channel antagonists used for cardiovascular therapy	*l*-Isomer is 10-20 times more active than *d*-isomer [17, 18]
Captopril, Benazepril	ACE inhibitors used as antihypertensive	*l*-Isomer is more potent than *d*-isomer [19]
Methadone	Analgesic for treatment of opiate dependence and cancer pain	*l*-Isomer is 25-50 times more potent than *d*-isomer [20, 21]
***Case 3:* Both enantiomers having equal therapeutic potency**		
Cyclo-phosphamide	Antineoplastic	Both enantiomers exhibit equal therapeutic activity [22]
Flecainide	Antiarrhythmic	Both enantiomers exhibit equal therapeutic activity [22]
Fluoxetine	Antidepressant	Both enantiomers exhibit equal therapeutic activity [22]
***Case 4:* Both enantiomers having different pharmacological activities**		
Propranolol	*d*-isomer reduces plasma concentrations of T3 cells and used to treat hyperthyroidism while *l*-somer is β-blocking drug used as antihypertensive	*d*-Isomer can inhibit the conversion of thyroxin (T4) to triiodothyronin (T3) which is opposite to the *l*-isomer [23, 24]
Propoxyphene	*d*-Propoxyphene (Darvon) is painkiller, whereas the *l*-propoxyphene (Novrad) is a cough suppressant.	*d*- and *l*-Isomers of propoxyphene have independent pharmacological activities [25]

Table 1.2: Differential isomer toxicity of enantiomers of chiral drugs

Specific examples	Therapeutic application of the eutomer	Isomer toxicity
***Case 1:* Eutomer is non-toxic while distomer shows toxic effect(s)**		
l-DOPA	Treatment of parkinsonism	*d*-Isomer gives agranulocytosis (or grave toxicity) [26, 27]
S,S-Ethambutol	Treatment of tuberculosis	*R,R*-Isomer causes optical neuritis that can lead to blindness [5]
***Case 2:* Eutomer is less toxic than distomer**		
l-Tetramisole (or Levamisole)	Nematocide	Toxicity (i.e. vertigo, vomiting, headache etc.) of *l*-isomer is less than *d*-isomer [27]
l-Bupivacaine	Local anaesthetic	*l*-Bupivacaine is less toxic than *d*-isomer [8]
***Case 3:* Eutomer is more toxic than distomer**		
l-Secobarbital	Anaesthetic	*l*-Isomer is a more potent and also more toxic than *d*-isomer [28]
***Case 4:* Eutomer and disomer are equally toxic**		
Cyclophosphamide	Antineoplastic	Both enantiomers exhibit same degree of toxicity [22]

1.1.4. Effect of chiral inversion

Some chiral drugs undergo *in vivo* and/or *in vitro* interconversion of enantiomers called as chiral inversion. This phenomenon greatly affects the differential potency and toxicity of such chiral drugs. Chiral inversion is categorized into two types: unidirectional inversion and bidirectional inversion [5].

2-Arylpropionic acids (ibuprofen, ketoprofen, fenprofen, benoxaprophen, etc. and collectively called as profens) are non-steroidal anti-inflammatory agents which undergo unidirectional *in vivo* chiral inversion. The *S*-enantiomer is therapeutically active (eutomer) while the *R*-enantiomer is weakly active or inactive (distomer). For example, (*S*)-ibuprofen is over 100-fold more potent as an inhibitor of cyclo-oxygenase I than (*R*)-ibuprofen. However, in the human body, only inactive *R*-enantiomer undergoes chiral inversion by hepatic enzymes into the active *S*-enantiomer and not vice-versa. This unique inversion process enhances the

effectiveness of racemic profen drugs. However, recent findings have revealed the undesirable biological effects of the *R*-enantiomer and thus emphasized the use of *S*-profens for a safe and effective treatment [26].

3-Hydroxy-benzodiazepines (oxazepam, lorazepam, temazepam) and thalidomide undergo bidirectional chiral inversion whereby the *R* and *S* enantiomers undergo racemization. 3-Hydroxy-benzodiazepines can racemize *in vitro* by aqueous solutions at elevated temperatures and thalidomide (a former sedative withdrawn from the market in the 1960s due to severe teratogenic effects) exhibits *in vitro* as well as *in vivo* bidirectional chiral inversion [5].

1.1.5. Potential advantages of using single enantiomer of drug [29]

- Improved therapeutic index – low (quantity and frequency of) dosage required
- Less complex pharmacokinetic profile
- Less complex pharmacodynamic profile
- Less complex relationship between plasma concentration and therapeutic effect
- Nil or less side effects/ drug toxicity
- Reduced potential for complex drug interactions

1.1.6. Emergence of chiral drugs

In view of heightened awareness regarding the differential biological and therapeutic behaviour of two enantiomers and the severe side effects associated with the non-functional enantiomer in the racemic drug, the drug stereochemistry has become an issue for the pharmaceutical industry as well as the regulatory authorities.

The first policy statement regarding the development of new stereoisomeric drugs was published by United States Food and Drug Administration in 1992 [30], which was closely followed by European guidelines in 1993 [31], which came into force in 1994. At present the decision regarding the stereoisomeric form, i.e. single enantiomer or racemic mixture, to be developed is left to the drug company. However, the decision taken requires scientific justification based on quality, safety and efficacy, together with the risk-benefit ratio and may be argued on a case-by-case basis [32, 33]. Further, the Food and Drug Administration (FDA) demands detailed documentation of pharmacological and pharmacokinetic behaviour of each enantiomer as well as their combined effects and permits only single-enantiomer

drugs to enter the market when the individual enantiomers show differences [34]. Indeed, the FDA guidelines had a major impact on the pharmaceutical industry resulting in the emergence of single-enantiomeric drugs from 1990's (Fig. 1.4). However it is interesting to note that, well before the enforcement of FDA guidelines – roughly since 1980's the single enantiomers were a significant component of approved drugs [1].

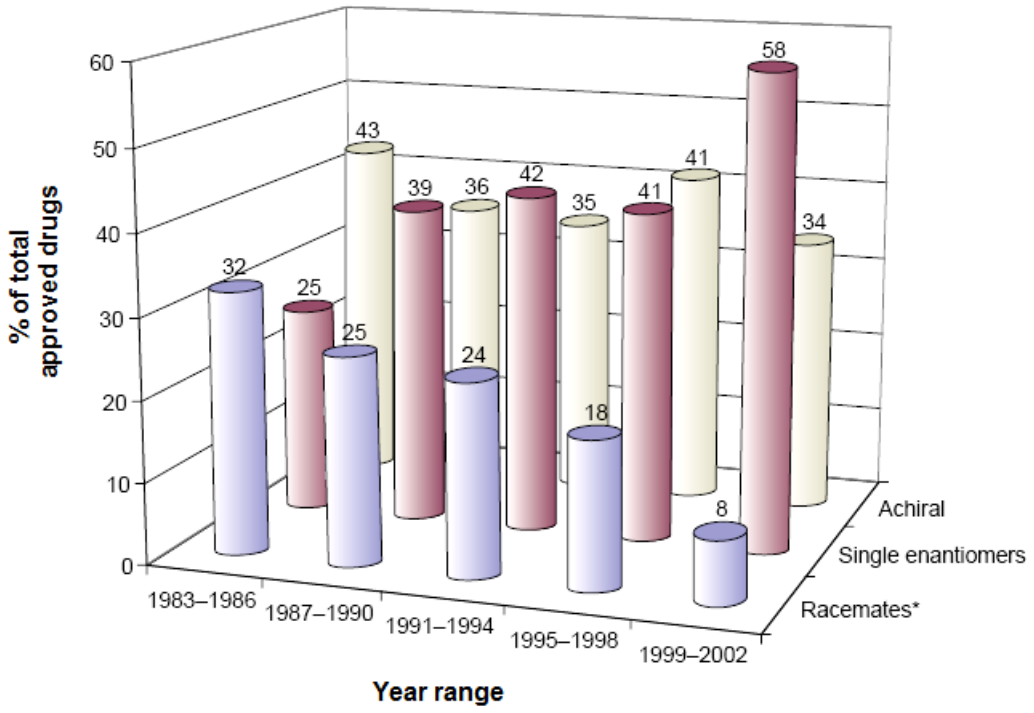

Fig. 1.4: Distribution of worldwide-approved drugs according to chirality character in four-year ranges; *data including diastereomeric mixtures. [**Source**: Adapted from ref. 1]

Since 1990's the chiral drugs have dominated the pharmaceutical business. More than 40% of all marketed drugs are currently sold in an enantiopure form [3]. The market share of chiral drugs is expected to rise sharply in the near future as approximately 80% of total drugs under development are chiral. About 70% of the new small-molecule drugs which received the approval by Food & Drug Administration in 2007 were chiral [35]. Past two decades have witnessed a significant expansion in the production of chiral drug molecules. A worldwide sinerio of emergence of single enantiomeric drugs over 20 years is given in Fig. 1.5.

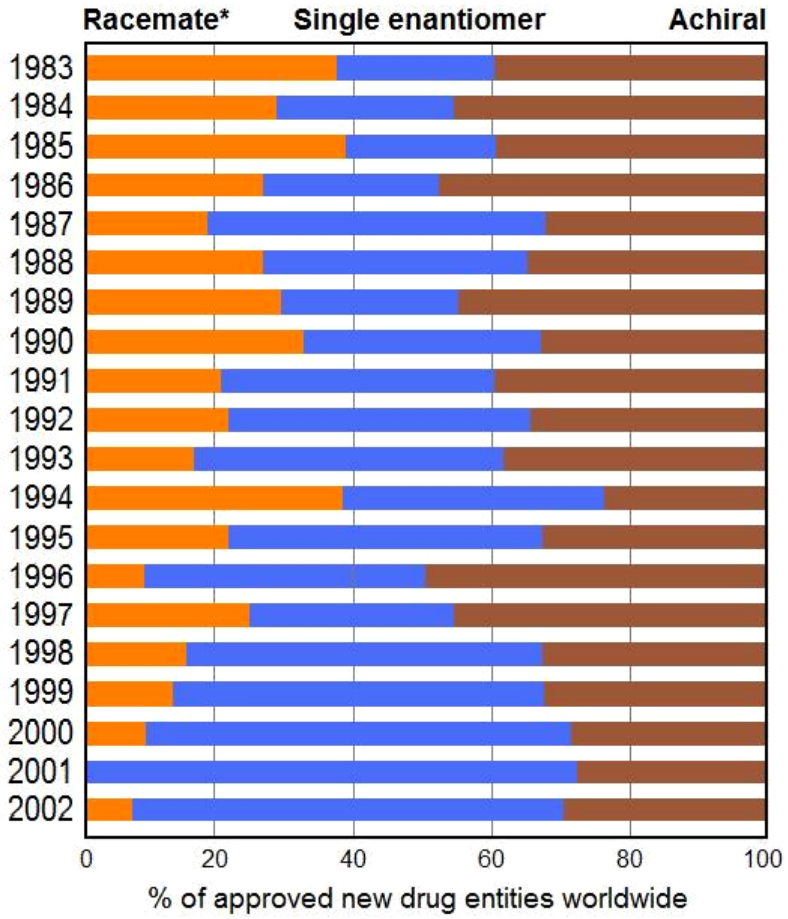

Fig. 1.5: Emergence of single enantiomeric drugs: A worldwide sinerio for 20 years; single enantiomers have dominated racemates since 1990; ***** data include diastereomeric mixtures. [**Source**: Adapted from ref. 36]

Besides development of new pharmaceuticals in single enantiomeric form, chiral technology (i.e. chirotechnology) has a crucial role in re-evaluation and re-marketing of single enantiomeric forms of existing racemic drugs (called Racemic switching) which permits additional years of market exclusivity (patent protection) [29]. According to Frost & Sullivan, worldwide revenues from chiral compounds destined for the drug industry amounted to $4.8 billion in 1999 and will be triple to $14.9 billion by 2009, with the average annual growth of 12% [37]. The global growth in revenues of pharmaceutical sector driven by chirotechnology over last 10 years is given in Table 1.3.

Today chiral technology is mainly driven by pharmaceutical industries. Besides pharmaceuticals, the 'chirality' is receiving attention from several business

sectors such as biochemicals, agrochemicals, aroma and flavour compounds, dyes and pigments and polymers. The industrial demand of enantiopure chemicals is therefore expected to show explosive growth in the coming years [3].

Table 1.3: The global growth in revenues of pharmaceutical sector from chiral technology

Year	**Revenue** ($ Billions)	**Annual growth** (%)
1999	4.80	-
2000	5.40	12.5
2001	6.10	13.0
2002	7.00	14.8
2003	7.74	10.6
2004	8.57	10.8
2005	9.53	11.1
2006	10.61	11.3
2007	11.85	11.7
2008	13.28	12.1
2009	14.94*	12.5

* predicted value; [**Source**: Adapted from ref 37]

1.2. METHODS OF ENANTIOSELECTIVE SYNTHESIS

The synthesis of enantiopure compound is generally initiated from (i) chiral pool; (ii) prochiral substrates; or (iii) racemates [34, 38]. The different methods of enantioselective synthesis from these three substrates are summarized in Fig. 1.6.

1.2.1. Chiral pool

The term ‘chiral pool’ refers to the many naturally available chiral molecules that exist in high enantiomeric purity. The most versatile chiral starting materials obtained from natural resources, in order of their industrial production per annum, are: carbohydrates, a-amino acids, terpenes, hydroxy acids and alkaloids. Other inexpensive chiral natural products are ascorbic acid, dextrose, ephedrine, limonene, quinidine and quinine, etc. [5, 34].

Further, these enantiopure compounds can be incorporated into the molecule to provide the desired chiral centre or to induce the desired chiral centre during

synthesis (chiral induction or diastereoselective synthesis). For example, naturally occurring enantiopure amino acids can be converted into antibacterials, cytotoxic agents and protease inhibitors (e.g. ritonavir) using this technology [39].

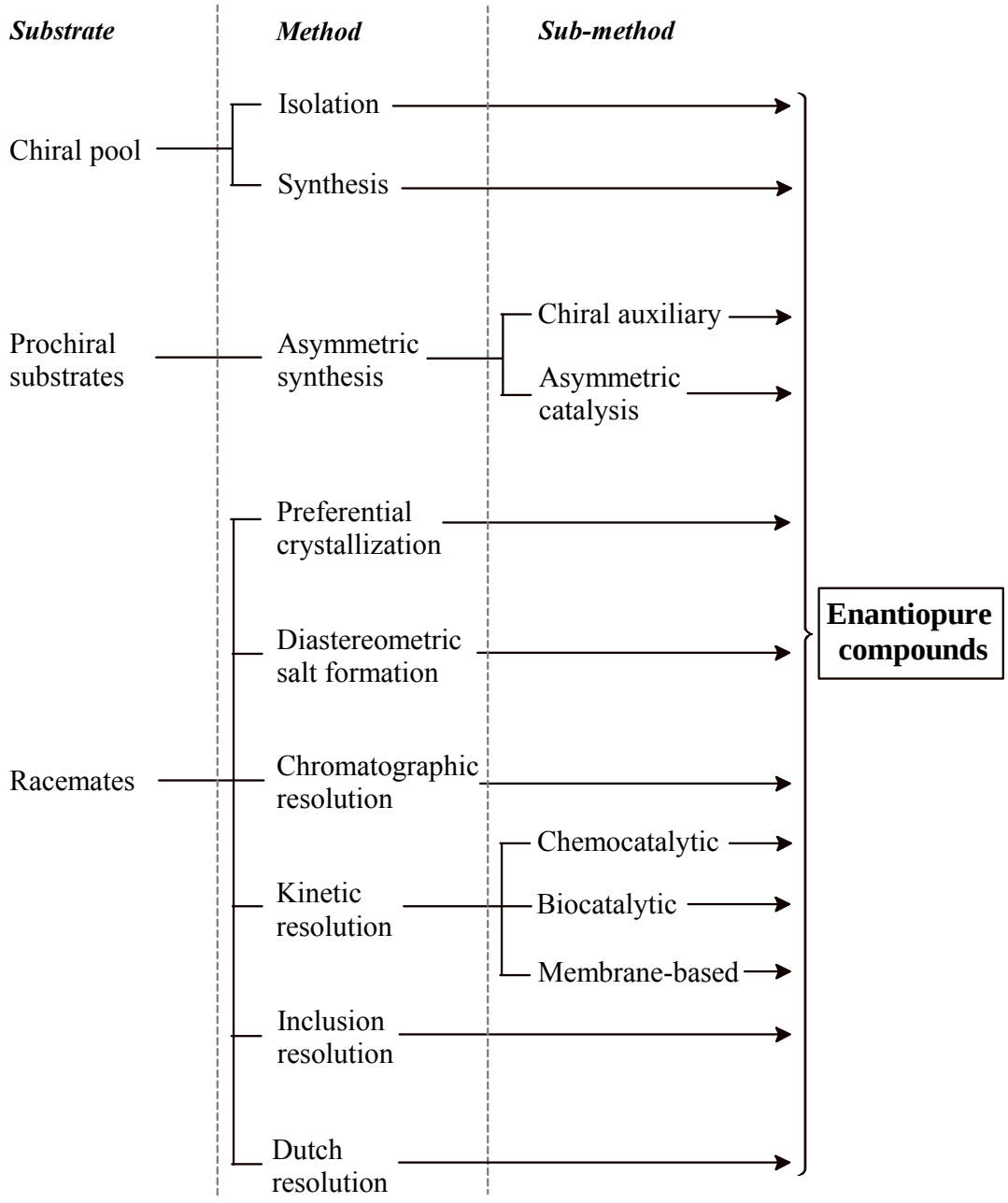

Fig. 1.6: Methods for synthesizing enantiopure compounds

1.2.2. Starting from prochiral substrate - Asymmetric synthesis

The term asymmetric synthesis refers to stereoselective synthesis of chiral product staring from non-chiral (or prochiral) substrate(s). Early innovations in

asymmetric catalysis were contributed by both industry and academia. The Nobel Prize-winning work of W. S. Knowles, R. Noyori, and K. B. Sharpless fostered many subsequent innovations in this field. Knowles's efforts led to the first industrial use of a chiral transition-metal complex to asymmetrically hydrogenate a prochiral substrate with high enantiomeric excess [35]. The asymmetric synthesis can be achieved either by means of a chiral auxiliary or using asymmetric catalyst [34].

(a) Chiral auxiliary

Chiral auxiliaries are a class of compounds which are used to modify the substrate molecule to introduce a stereogenic center. In the chiral auxiliary approach, the auxiliary is attached to the substrate, then stereoselective reaction is carried out and finally the auxiliary is removed or recycled.

(b) Asymmetric catalysis

An asymmetric catalyst as its name suggest catalyzes asymmetric reactions. Here no modification of the substrate is required (i.e. number of steps are reduced). Asymmetric catalysis can be achieved either by using a chemocatalyst or a biocatalyst.

1.2.3. Starting from the racemate – Resolutions

The separation of enantiomers of a compound from the racemic mixture is termed as resolution. It can be achieved by preferential crystallization, distereomeric salt formation, chromatographic resolution, kinetic resolution or inclusion resolution [34].

(a) Preferential crystallization

This method is based on the different crystallization pattern of two enantiomers. Only one enantiomer from the racemic mixture under specific conditions preferentially crystallizes in the form of a simple salt (e.g. hydrochloride). A mixture of crystals of individual enantiomers that can in principle be separated mechanically is termed as a conglomerate. Since approximately 7% of the racemic compounds form conglomerates and the manual 'crystal picking' is highly inconvenient and time consuming this method has poor industrial relevance. This method can be used for the

resolution of few tartarate salts and glutamate salts [34].

(b) Diastereomeric salt formation

The most practical and widely used technique via a 'classical' resolution of enantiomers is by diastereomeric salt formation. In this method, an acid-base reaction is involved between a racemate and a resolving agent, where two diastereomeric salts having dissimilar physical and chemical properties are formed. These two diastereomers obtained can be easily separated either by crystallization or by filtration if one is soluble and the other is insoluble. Finally, the salt is decomposed by treatment with either acid or base, when pure enantiomer is obtained [40]. The two diastereomers formed can also be separated by classical achiral liquid chromatography. This method has been used in the resolution of α-methyl-L-3,4-dihydroxy phenylalanine, aspargine and glutamic acid [8].

(c) Chromatographic resolution

The use of chromatographic techniques in the resolution of enantiomers to obtain large quantities of enantiomerically pure drugs and drug intermediates is a growing field. Chromatographic separation relies on a difference in affinity between a chiral stationary phase and a mobile phase. Simulated moving bed chromatography (SMBC) is a continuous chromatographic multi-column separation process wherein six to eight columns are run in series. In recent years, SMBC has become an alternative approach for the separation of enantiomers in quantities ranging from grams to several hundred kilograms [41,42]. A successful example of SMBC is in the commercial scale synthesis of enantiopure (R)-miconazole (used in treatment of skin diseases and tuberculosis) from a racemic intermediate.

(d) Kinetic resolution

Kinetic resolution can separate two enantiomers on the basis of their different reaction rates with a chiral entity. The chiral entity can be a chemocatalyst (e.g., a metal complex or an organic chiral catalyst) [43] or a biocatalyst (e.g., an enzyme or a microorganism) [44]. The main disadvantage of a kinetic resolution is the theoretical yield of the desired enantiomer can never exceed the limit of 50% of mole ratio. The Sharpless epoxidation and the lipase catalyzed kinetic resolution of racemic *sec*-

amines are the examples of chemocatalytic resolution and biocatalytic resolution respectively [45].

Kinetic resolution aided with *in-situ* racemization of slowly transformed enantiomer is called as 'Dynamic Kinetic Resolution' (DKR) which can, in principle, convert 100% of the racemate to the desired product. The *in-situ* racemization can be spontaneous or can be induced by using a racemization catalyst (transition metal catalyst or racemase enzymes) [34]. Industrial production of enantiopure D-amino acids currently practiced by DSM is based on a dynamic kinetic resolution process [45].

Enantioselective membranes can be employed for the kinetic resolution of enantiomers. These membranes are able to resolve optical isomers because of their chiral recognition sites (e.g., chiral side chains, chiral backbones, or chiral selectors). They act as selective barriers in the resolution process, and they selectively transport one enantiomer due to the stereospecific interaction between the enantiomer and chiral recognition sites, thereby producing a permeate solution enriched with one enantiomer. The separation of two enantiomers could result due to one or combination of following mechanisms *viz.* hydrogen bonding, hydrophobic, Coulombic forces, van der Waals interactions and steric effects with the chiral sites [46].

(e) Inclusion resolution

Inclusion resolution is a relatively novel method which is based on chiral discrimination and recognition in the crystalline phase [47]. A chiral host molecule forms an inclusion complex preferably with one of the enantiomers especially by means of hydrogen bonds. The most widely applied chiral host molecules are the derivatives of tartaric acid, succinamide and lactic acid. Recently, both enantiomers of 9,9'-spirobifluorene-1,1'-diol (used in synthesis of chiral ligand) were conveniently obtained by inclusion resolution with 2,3-dimethoxy-N,N,N',N'-tetracyclohexyl-succinamide [48].

(f) Dutch resolution

The crucial step in the development of a resolution procedure is to find a suitable resolving agent. The choice of resolving agent has been done by trial-and-error based on the prior experience rather than any mechanistic approach. In 1998, a

new approach to classical resolution was reported whereby, instead of using one resolving agent, mixtures of structurally closely related resolving agents (called as families of resolving agents) were added to the racemic mixture. This method was coined "Dutch Resolution"- a name which has been widely adopted [49]. Structurally related enantiopure derivatives of sulphonic acid, mandelic acid, 1-phenylethylamine etc. have been known to constitute families of resolving agents. With these families many resolutions have been carried out readily whereas with single resolving agents resolutions were either poor or failed. Dutch Resolution certainly has something of combinatorial characteristics in it; upon the simultaneous addition of a family of resolving agents, higher de (diastereomeric excess) values of the first salts were obtained via this method.

DL-threo-(4-methylthiophenyl) serine amide could be successfully resolved by using 1 mol equivalent of the family of cyclic phosphoric acids. The resolved amide can be used as an intermediate in the synthesis of thiamphenicol [50], which is an antimicrobial substance used for the treatment of infectious diseases in cattle, pigs and poultry.

1.2.4. Comparison of chiral pool, asymmetric synthesis and resolution processes

Each method of enantioselective synthesis has specific advantages and disadvantages. The selection of appropriate method depends on several factors such as availability of substrate, scale of synthesis, cost of synthesis, desired enantiopurity and use of the chiral product.

The need of enantiopure compounds in bulk amount with considerably high optical purity at low cost can be accomplished easily via chiral pool. In the early 1990s, almost 80% of chiral drugs were derived from chiral-pool materials, whereas today, just 25% come from the chiral pool and rest use different chiral technologies *viz.* asymmetric synthesis or resolution procedures [51].

Asymmetric synthesis, either by chiral auxiliaries or by asymmetric catalysis, should be the most cost-effective method for producing single enantiomers since it has a theoretical yield of 100%. However use of chiral auxiliary is hampered by several factors *viz.* (i) unavailability of both enantiomers of the chiral auxiliary, (ii) additional steps required for attachment-detachment of an auxiliary to the substrate and (iii) difficulties in the removal of the auxiliary. Synthesis by asymmetric catalysis

often requires lengthy procedures such as selection of suitable catalyst and optimization of process parameters. Furthermore, the chemocatalytic process gives low enantiopurity. On the other hand, requirement of very low quantity of the catalyst and high efficiency of the process are some of the attractive features of asymmetric catalysis. Recently, the introduction of high-throughput experimentation has drastically accelerated the screening procedures for choosing the appropriate catalyst for certain process [52].

Despite the theoretical yield being 50%, resolution is one of the most common methods for laboratory or industrial scale synthesis of enantiopure compounds. Almost all resolution methods are simple, easy to scale up and therefore can be readily incorporated into an industrial process. If the unwanted isomer can find a profitable use or can be racemized in situ (e.g. dynamic kinetic resolution), the resolution method becomes even more advantageous.

1.3. BIOCATALYSTS FOR ENANTIOSELECTIVE SYNTHESIS

Enzymes are remarkable catalysts in terms of selectivity, specificity and efficiency. In the last decade, employing biocatalysts (enzymes) for organic synthesis has proved to be a valuable alternative to conventional chemical methods. Enzymes quite often catalyze reactions with exceptionally high chiral (enantio-) and positional (regio-) selectivities without formation of (unwanted) by-products. As a result, biocatalysts can be used in both simple and complex transformations without the need for the tedious blocking-deblocking steps that are common in enantio- and regioselective chemo-catalytic organic synthesis. The high selectivity and specificity of enzymes make them attractive catalysts especially for synthesis of pharmaceuticals, where the demand for enantiomerically pure molecules is continuously increasing [53].

Moreover, enzyme-catalyzed reactions are carried out generally under mild conditions (of pH temperature and pressure) that minimize problems like isomerization, racemization or epimerization of product. Enzymes are far more efficient than chemical catalysts. The initial reaction rates of enzymatic transformations are roughly 10^{10} to 10^{20} times higher than that of chemo-catalyzed reactions. In addition, biocatalytic processes are less hazardous, less polluting (environmentally benign) and consume less energy than conventional chemo-catalytic

processes, especially those which use heavy-metal catalysts [54].

Further, the recent advancements in the field of molecular biology is causing a revolution in the industrial utilization of biocatalysts due to following reasons: (i) availability of a wide range of expression hosts to produce biocatalysts cost effectively; (ii) rapid discovery of enzyme tool boxes through genome mining as a result of widespread availability of gene sequences; (iii) robust directed evolution (rational, semi-rational or random) and screening technologies to improve enzyme properties to meet process requirements [55].

In spite of the promising features, the industrial applications of many enzymes are hindered because of two inherent limitations (which are exhibited by almost all enzymes): (i) lack of (operational and storage) stability and (ii) high cost. The immobilization of enzyme is simple but equally effective method to overcome these limitations [56].

1.3.1. Immobilized enzyme

Immobilized enzymes are used as heterogeneous catalyst which can be easily recovered and reused. Immobilized enzymes are defined as enzymes that are physically confined or localized, with retention of their catalytic activity [57]. The physical confinement remarkably alters the physical, chemical, mechanical, catalytic and kinetic properties of an enzyme.

Immobilization is also useful in providing stability to the enzyme against denaturation by preventing conformational changes and protecting it in a confined microenvironment. Besides enhanced stability, immobilization of enzymes provides several advantages such as ease of separation from a reaction mixture, repeated or continuous use, possible modulation of the catalytic properties, prevention of microbial contaminations, easy handling and extended storage life, enabling greater control over catalytic processes and process economics [58].

1.3.2. Immobilization methods

A wide range of methods (e.g. non-covalent adsorption, covalent binding, entrapment, encapsulation etc.) and support materials (e.g. inorganic clays, polymer beads, membranes, nanoparticles etc.) has been proposed and used for the immobilization of enzymes [59, 60]. Immobilized enzymes can be broadly classified

as carrier-bound immobilized enzyme and carrier-free immobilized enzyme (Fig. 1.7).

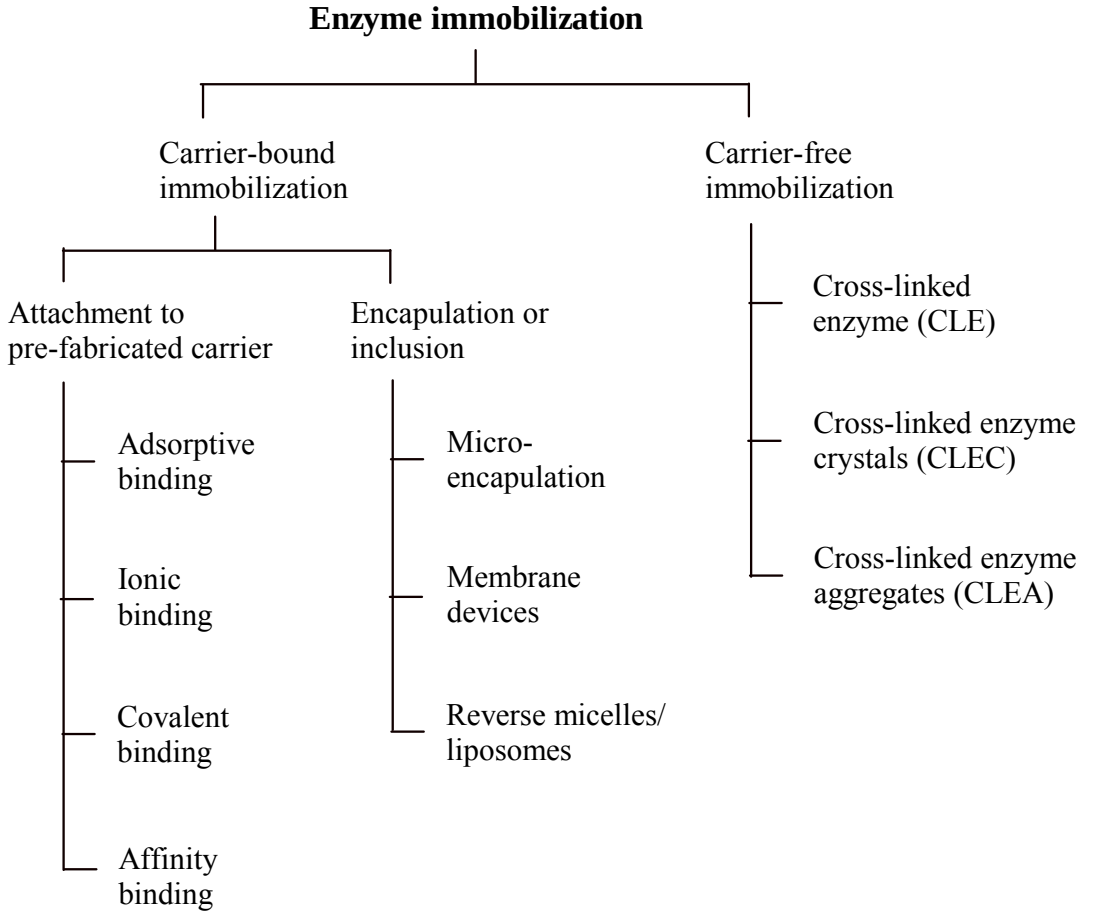

Fig. 1.7: Methods of enzyme immobilization

In carrier-bound immobilized enzyme, the enzyme is immobilized on/inside (non-porous/porous) physical support or carriers. Carrier-bound immobilized enzymes can be obtained by two ways:

- Attachment of an enzyme to the pre-fabricated support by means of hydrophobic interactions and hydrogen bonds (adsorptive binding), electrostatic bonds (ionic binding), covalent binding or affinity binding.
- Encapsulation or inclusion of enzyme in microcapsules, membrane devices (e.g. hollow fibers) or in reverse micelles.

The cross-linking of enzyme molecules by bifunctional reagents (cross-linking agent) results in gelation/solidification of the soluble enzyme without losing their catalytic activity (provided binding does not affect the catalytic site). Owing to their

insoluble nature in both organic and aqueous media, cross-linked enzymes can be used as heterogeneous biocatalysts. Since the molecular weight of the cross-linking agent is negligible, compared with that of the enzyme, the resulting biocatalyst essentially comprises 100% wt of protein. Thus compared to carrier-bound biocatalyst, cross-linked enzymes express high catalytic activity per volume thereby maximizing volumetric productivity and space-time yields. [61].

Depending upon their method of preparation, the cross-liked enzymes can be classified as:

- Cross-linked enzyme (CLE) prepared by direct cross-linking of soluble enzyme
- Cross-linked enzyme crystals (CLEC) prepared by cross-linking of crystalline enzyme and
- Cross-linked enzyme aggregates (CLEAs) prepared by cross-linking of physically aggregated enzyme

In spite of this clear division, the procedure used in many cases requires a combination of two or more methods such as adsorption of the enzyme onto a suitable support followed by intermolecular cross-linking.

1.3.3. Enantioselectivity of an enzyme

When a racemic substrate is subjected to an enzymatic reaction (e.g. hydrolysis), a chiral discrimination occurs due to the difference in the rate of transformation of the two enantiomers. Owing to the three dimensional structure of the active site of the enzyme, one enantiomer fits betters into the active site and is therefore transformed at higher rate than its counterpart. The selectivity of an enzyme towards chiral discrimination of two enantiomers is called as 'enantioselectivity'. Initially the enantioselectivity was expressed in terms of 'stereoselectivity factor' which was defined as ratio of rate of transformation of individual enantiomers [62-64].

For instance, assuming that the rate of transformation of *S*-substrate (k_S) is greatly higher than that of *R*-substrate (k_R) and the transformation proceeds with retention of configuration, *S*-substrate will be selectively transformed into *S*-product and transformation of *R*-substrate will begin after transformation of *S*-substrate. If the reaction is terminated at ~ 50% conversion then, the product formed gets enriched with *S*-enantiomer while the (un-transformed) substrate gets enriched with *R*-

enantiomer. On the other hand, if $k_S \approx k_R$, distinct enantio-enrichment of product and substrate cannot occur [65].

Ideally, the ratio of the rates of transformation of two enantiomers should be infinite so that an enzymatic transformation will automatically stop at 50% conversion − where only one enantiomer of substrate will be transformed into enantiopure product while another enantiomer of substrate remained un-transformed. However, often in practice the ratio of the rates of transformation of two enantiomers is not infinite but measurable. In such cases, the enzymatic transformation needs to be (manually) stopped at certain point where maximum enantio-enrichment of product and unreacted substrate can be achieved.

Later, Chen *et al.* introduced a new dimensionless parameter, 'enantiomeric ratio' to describe the enantioselectivity of irreversible enzymatic resolution reaction [66]. It is an intrinsic property of the enzyme which remains constant through out the reaction. By definition, E can be expressed as ratio of specificity constants i.e. (V_{max}/K_m) of the two enantiomers (Eq. 1.1).

$$E = \frac{(V^R_{max} / K^R_m)}{(V^S_{max} / K^S_m)} \qquad \text{– Eq. 1.1}$$

Where, V^R_{max} and K^R_m are respectively the maximum reaction velocity and Michaelis constant for *R*-enantiomer. V^S_{max} and K^S_m are respectively the maximum reaction velocity and Michaelis constant for *S*-enantiomer.

The measurement of E using Eq. 1.1 needs pure enantiomers of substrate which are often not available. Hence the Eq. 1.1 is not commonly used in practice. Chen *et al.* have also derived useful mathematical expressions (Eq. 1.2, Eq. 1.3 and Eq. 1.4) for experimental determination of enantiomeric ratio [66]. These expressions are based on the dependence of ee_S and ee_S on the extent of conversion. During an irreversible chiral resolution process, the rate of transformation of each enantiomer varies with time, as the relative concentration of the two enantiomers is continuously changing. Hence, the enantiopurity of substrate (expressed as ee_S) and the enantiopurity of product (expressed as ee_P) becomes a function of the extent of conversion.

$$E = \frac{\ln[1 - C(1 + ee_P)]}{\ln[1 - C(1 - ee_P)]} \qquad \text{– Eq. 1.2}$$

$$E = \frac{\ln[(1-C)(1-ee_S)]}{\ln[(1-C)(1+ee_S)]} \quad \text{– Eq. 1.3}$$

$$E = \frac{\ln[(1-ee_S)/(1+ee_S/ee_P)]}{\ln[(1+ee_S)/(1+ee_S/ee_P)]} \quad \text{– Eq. 1.4}$$

Where, C is conversion ratio and, ee_S and ee_P are enantiomeric excess of substrate and that of product respectively. C can be determined by using Eq. 1.5 while ee_S and ee_P can be determined by using Eq. 1.6 and Eq. 1.7 respectively.

$$C = 1 - \left(\frac{c^S_{S(t)} + c^R_{S(t)}}{c^S_{S(0)} + c^R_{S(0)}} \right) \quad \text{– Eq. 1.5}$$

Where, $c^S_{S(t)}$ and $c^R_{S(t)}$ are concentration of *S*-enantiomer and concentration of *R*-enantiomer of substrate respectively at time, t. $c^S_{S(0)}$ and $c^R_{S(0)}$ are concentration of *S*-enantiomer and concentration of *R*-enantiomer of substrate respectively at t = 0.

$$ee_S = \frac{\left| c^S_S - c^R_S \right|}{c^S_S + c^R_S} \quad \text{– Eq. 1.6}$$

$$ee_P = \frac{\left| c^S_P - c^R_P \right|}{c^S_P + c^R_P} \quad \text{– Eq. 1.7}$$

Where, c^S_S and c^R_S are concentration of *S*-enantiomer and *R*-enantiomer of substrate respectively while c^S_P and c^R_P are concentration of *S*-enantiomer and *R*-enantiomer of product respectively.

The interdependence of enantiomeric ratio and enantio-enrichment of product and unreacted substrate is illustrated in Fig. 1.8. Here, three hypothetical biotransformation reactions *viz.* A, B and C having respective E values of 2 (indicating poor enantioselectivity), 20 (indicating good enantioselectivity) and 200 (indicating excellent enantioselectivity) are taken into consideration. The profiles of ee_P and ee_S for A, B and C as a function of extent of conversion were obtained from the 'Selectivity' software. (A free version of software was downloaded from the URL: http://borgc185.kfunigraz.ac.at/index.htm). At 50% conversion, values of ee_S and ee_P for the biotransformation were close to 22 while that for the biotransformation B were close 79 and that for the biotransformation C were close to 97. Thus, higher enantiomeric ratios indicate better enantio-enrichment of substrate and product.

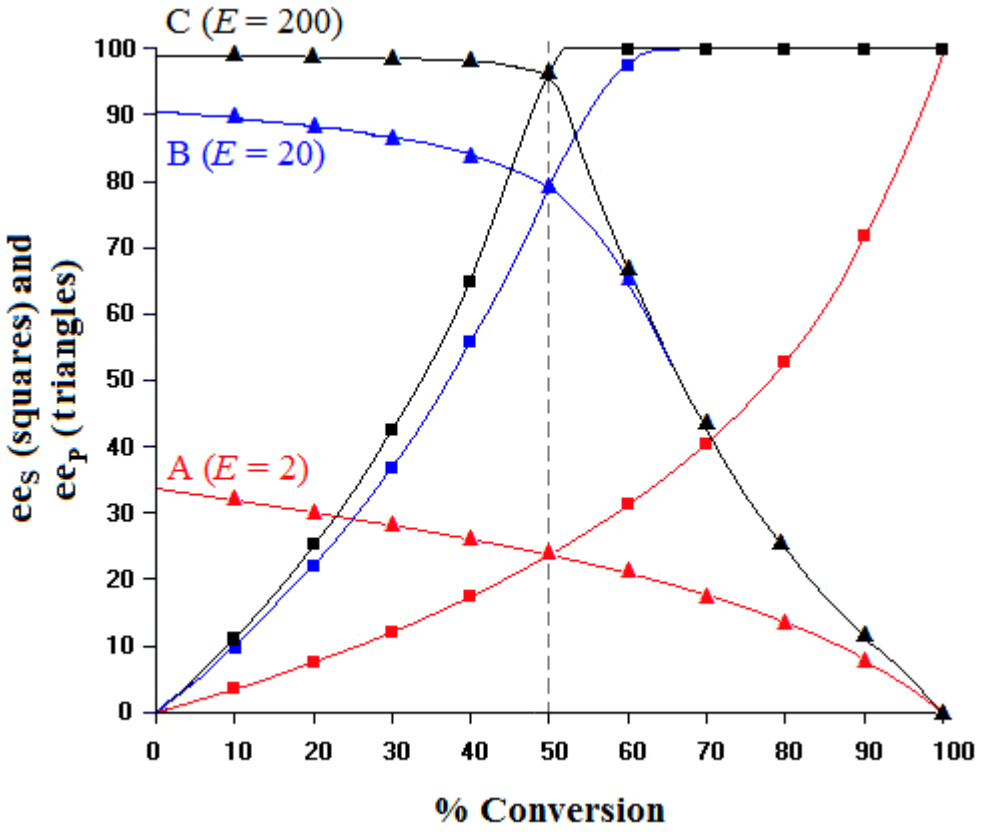

Fig. 1.8: Relationship between ee_S and ee_P as a function of extent of conversion (%) at different enantiomeric ratios

The enantiomeric ratio is the prime parameter for describing the enantioselectivity of an enzyme. As a rule of thumb, *E* below 15 is unacceptable for any practical purpose. *E* in the range of 15 to 30 is regarded as acceptable, that in the range of 30-100 is regarded as good while above 100 is excellent [67].

It must be emphasized that determination of *E* is very sensitive to values of ee_S and ee_P. In general low *E* values can be determined more accurately. In fact, when *E* values are above 200 even a very small variation in ee_S or ee_P (arising from experimental errors in the analytical method) causes a large difference in numerical values of the former [67]. Hence, when experimental value of *E* exceed 200, it is usually represented as >200 instead of the exact value. Furthermore, the accuracy of *E* value estimates based on a single-point evaluation is inherently poor. Hence averaging of *E* values from multiple data points must be performed [68].

1.4. SCOPE OF THE THESIS

The present thesis deals with enantioselective synthesis of commercially important chiral drug intermediates (unnatural amino acids and vicinal diols) using a suitable immobilized biocatalyst.

1.4.1. Unnatural amino acids - critical components of drugs and drug intermediates

Amino acids have always played a crucial role in drug discovery. Further, due to renewed interest in peptides as therapeutics, the amino acid market is growing steadily. This has led to the development of several marketed drugs composed of or derived from amino acids. The annual market of protein-based therapeutics is expected to surpass $50 billion by 2010 [69]. Besides pharmaceuticals, there is great demand for amino acids and amino acids derivatives in foods, agrochemicals and synthetic organic chemistry as a source of chiral materials. According to reports, about 20% of all new drugs launched during 1995-2001 have one or more amino acid residues incorporated into them. Most of these new drugs have an unnatural amino acid as a structural element [70-72].

Unnatural amino acids are non-genetically-coded amino acids that either occur naturally or are chemically synthesized. They are becoming very important tools for modern drug discovery led research. Due to their structural diversity and functional versatility, they are widely used as chiral building blocks and molecular scaffolds in constructing combinatorial libraries. While the total amino acid market is expanding at annual rate of roughly 10-15%, the market for natural amino acids is only growing at an annual rate of about 1-2% − evidently indicative of the increasing demand for unnatural amino acids [70].

Many of these unnatural amino acids are used as drugs or drug intermediates. Unnatural amino acids can be valuable pharmaceuticals. For example, L-DOPA (i.e. L-3,4-dihydroxy phenylalanine) is used in symptomatic treatment of Parkinson's disease, particularly to alleviate trembling, rigidity, and slow movements; D-penicillamine is used for symptomatic treatment of arthritis [71].

Numerous therapeutically relevant compounds with an unnatural amino acid moiety in their structures have been reported. In view of their dual functionality (carboxylic and amino), unnatural amino acids are recognized as highly versatile chiral synthons (drug intermediates) that are widely used to introduce chirality in the

drug molecule. Unnatural amino acids are components of several known drug molecules as well as those being developed. For example, (*R*)-phenylglycine and (*R*)-4-hydroxy-phenylglycine are used in the semisynthetic broad-spectrum antibiotics Ampicillin and Amoxicillin. (*R*)-2-Naphthylalanine is found in peptide drug Nafarelin, a LHRH analogue used for the symptomatic treatment of endometriosis. A very important class of antihypertensive drugs (Benzpril, Enalapril, Lisinopril etc.) contains (*S*)-homophenylalanie [71].

Unnatural amino acids are vital in future peptide related drug discovery. If the use of peptide is associated with side effects arising from the conformational freedom of the flexible peptide, rendering a peptide more rigid would result in the selective peptide interactions with only one receptor, thereby producing fewer side effects. Incorporation of conformationally constrained unnatural amino acids has become a useful strategy in the design and development of selective peptide drugs [72]. Moreover, the possibility of protein engineering as a method of creating improved enzymes has infinitely widened the scope of enantioselective synthesis of diverse unnatural amino acids [73].

1.4.2. Vicinal diols - versatile chiral building blocks

The epoxides as well as their corresponding vicinal diols are highly versatile chiral building blocks used in synthesis of a variety of bioactive compounds, for example: β-3-adrenergic receptor agonists, anti-obesity drugs, N-methyl D-aspartate receptor antagonists, nematocides and anticancer agents [74-77]. In view of their commercial potential, the enantioselective synthesis of these compounds is of great interest in synthetic organic chemistry. In the past few years, different methods have been reported (mainly based on transition metal catalysis) for synthesis of chiral epoxides and vicinal diols. However, the environmental concerns and the regulatory constraints faced in the chemical and pharmaceutical industries have spurred the need of alternative biological methods that can offer cleaner and milder synthetic processes. One of the most promising methods to produce enantiopure vicinal diol involves kinetic resolution of racemic epoxide with epoxide hydrolases [78]. Epoxide hydrolases (EC 3.3.2.3) catalyze the addition of a water molecule to the oxirane ring of epoxides leading to formation of the corresponding 1,2-diols [75]. Epoxide hydrolases are widespread in nature. Recently, they have been obtained from

microbial sources and hence can be produced in bulk quantities as per demand for industrial applications. The enzyme does not require renewable co-factors and is therefore suitable for operation at large scale [79, 80].

Among the several types of biocatalytic reactions, kinetic resolution of racemates is dominant in the majority of applications. Despite their widespread applications, classic kinetic resolutions are impeded by several inherent limitations, the most crucial being – a restriction of the theoretical yield of each enantiomer to 50%. Enantioconvergent strategy is one of the most effective methods to overcome the 50% yield limitation [81].

An enantioconvergent process:

In an enantioconvergent process, two enantiomers of substrate are converted into single enantiomer of product and 100% theoretical yield is possible. As far as epoxide hydrolases-catalyzed reactions are concerned, 'de-racemization' can be achieved by making use of two independent reactions, which transform each of the enantiomers in an enantioconvergent manner. As demonstrated in Scheme 1.1, one enantiomer could be converted into product in an enantioselective way through retention of configuration whereas its antipode is transformed with inversion of configuration to give the same enantiopure vicinal diol.

Scheme 1.1: Principle of enantioconvergent process from racemic epoxides, leading to a theoretical yield of enantiopure diol to 100%

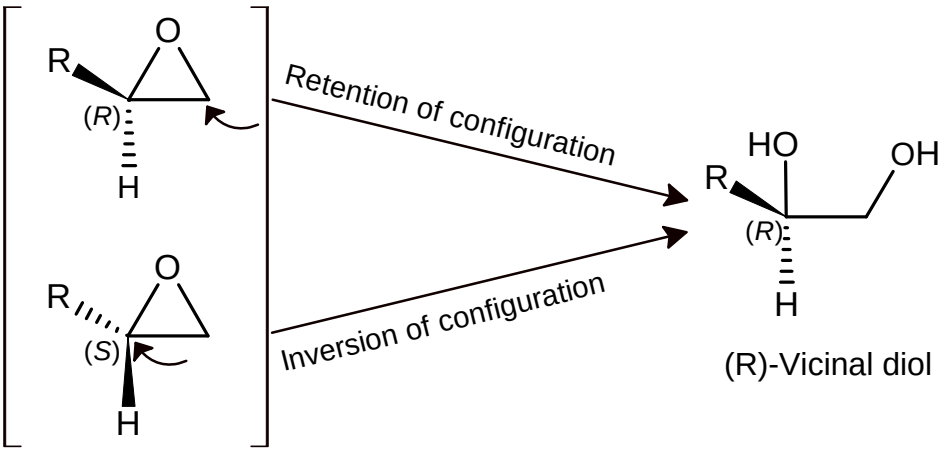

The different approaches to accomplish an enantioconvergent process are:

- Chemo-enzymatic approach;
- Bi-enzymatic approach;
- Mono-enzymatic approach

A 'chemo-enzymatic approach' is based on the consecutive use of an enantio- and regio-selective enzymatic hydrolysis followed by an opposite regio- and stereo-selective chemical hydrolysis of the residual epoxide [82]. The chemo-enzymatic enantioconvergent process finds application in synthesis of (*R*)-*p*-nitro-phenylethane diol (a chiral intermediate of (*R*)-Nifenalol having β-blocker activity). Enzymatic hydrolysis was carried out using *Aspergillus niger* epoxide hydrolase and chemical hydrolysis was carried out using H_2SO_4.

'Bi-enzymatic approach' involves the use of two enantio-complementary epoxide hydrolases having an opposite regioselectivity towards the oxirane ring opening [83]. For example, the sequential use of *Solanum tuberosum* epoxide hydrolase and *Aspergillus niger* epoxide hydrolase enabled the enantioconvergent preparation of the corresponding (*R*)-*p*-chloro-phenylethane diol (a component of NMDA receptor antagonist: Eliprodil).

The most elegant enantioconvergent method reported use of the 'Mono-enzymatic approach'. It is based on the use of only one epoxide hydrolase having a characteristic opposite regioselectivity towards two enantiomers of the same substrate i.e. starting from racemic mixture of epoxide, 100% conversion to a single enantiomer of diol is possible. For example, enantioconvergent production of (*R*)-phenylethane diol is possible using *Solanum tuberosum* epoxide hydrolase [83, 84].

1.5. RESEARCH OBJECTIVES

1.5.1. Enantioselective synthesis of unnatural amino acids [*namely*: phenylglycine (PG), 3,4-dihydroxy phenylalanine (DOPA), homophenylalanine (HPA) and 2-naphthylalanine (NA)] using immobilized enzymes (*viz.* lipases, amidase and aminoacylase).

(*R*)-Phenylglycine is used in the semisynthetic broad-spectrum antibiotics Ampicillin and Amoxicillin. (*S*)-3,4-Dihydroxy phenylalanine is used as a drug in symptomatic treatment of Parkinson's disease, particularly to alleviate trembling, rigidity, and slow movements. A very important class of antihypertensive drugs

(*namely*: Benzapril, Enalapril and Lisinopril) contains (*S*)-homophenylalanie (Scheme 1.2). (*S*)-2-Naphthylalanine is found in peptide drug Nafarelin, a LHRH analogue used for symptomatic treatment of endometriosis. Being components of high selling drugs, all these unnatural amino acid have high commercial potential especially in pharmaceutical and medicinal chemistry.

Scheme 1.2: L-Homophenylalnine as component of antihypertensive drugs (*namely:* benzapril, lisinopril and enalapril) [85, 86]

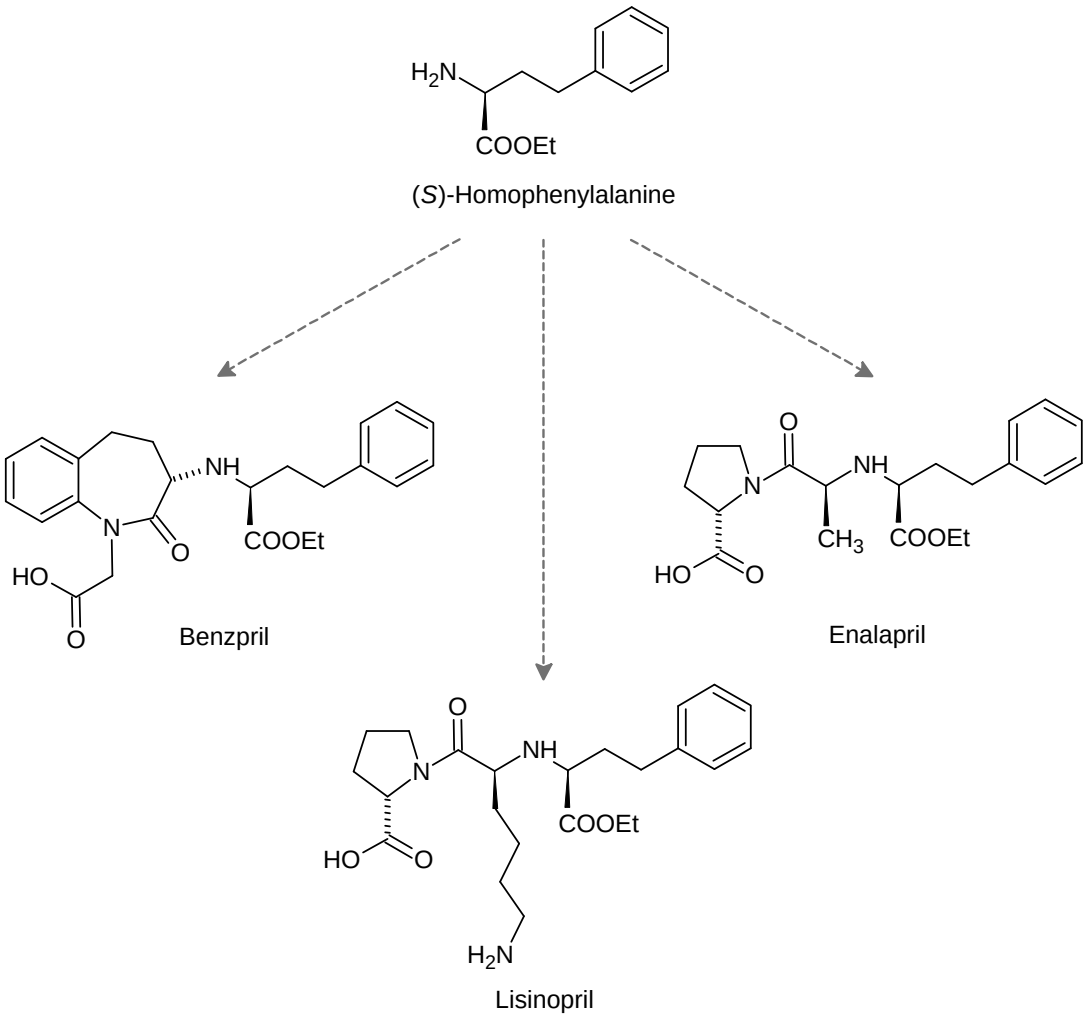

Prior art:

Specific details of previous reports regarding the enantioselective biocatalytic synthesis of phenylglycine, 3,4-dihydroxy phenylalanine, homophenylalanine and 2-naphthylalanine are summarized in Table 1.4, Table 1.5, Table 1.6 and Table 1.7

respectively. Most of the reports mention preliminary work that involves use of soluble enzyme. Detail reports on enantioselective biocatalytic synthesis of unnatural amino acids from the perspective of 'industrial biocatalysis' are scant.

Table 1.4: Reports on the enantioselective biocatalytic synthesis of phenylglycine (PG)

Enzyme	Substrate	Process details
Different lipases	PG-ethyl ester	Kinetic resolution, ester hydrolysis, porcine pancreatic lipase gave maximum enantioselectivity (E = 1.9) [87].
Candida antarctica lipase B (Novozym 435)	PG-esters	Dynamic kinetic resolution, ester hydrolysis, (E = 20, for butyl ester) [88, 89].
Candida antarctica lipase B (Novozym 435)	PG-esters	Kinetic resolution, ester hydrolysis, (E = 43, in ionic liquid) [90, 91].
Penicillin-G acylase	PG	Kinetic resolution, ester synthesis [92].
Rhodococcus cells (nitrile hydratase + amidase)	PG-nitrile	Kinetic resolution, PG-nirile is hydrolyzed to PG-amide (by nitrile hydratase) which was kinetically resolved by amidase [93-96].

Table 1.5: Reports on the enantioselective biocatalytic synthesis of 3,4-dihydroxy phenylalanine (DOPA)

Enzyme	Substrate	Process details
Different lipases	DOPA-ethyl ester	Kinetic resolution, ester hydrolysis, porcine pancreatic lipase gave maximum enantioselectivity (E = 43.2) [87].
Proteases (α-chymotrypsin, subtilisin)	DOPA-ethyl ester	Kinetic resolution in acetonitrile-water medium [97].
α-Chymotrypsin	N-protected DOPA	Transesterification, ester synthesis in organic solvents [98].
Tyrosinase and α-chymotrypsin	Tyrosine ester	Tyrosine ester was converted into DOPA ester by tyrosinase which was subsequently kinetically resolved by α-Chymotrypsin [99].

Table 1.6: Reports on the enantioselective biocatalytic synthesis of homophenylalanine (HPA)

Enzyme	Substrate	Process details
Different lipases	HPA-ethyl ester	Kinetic resolution, ester hydrolysis, *Rhizopus* lipase gave maximum enantioselectivity (E = 5) [87].
Alcalase	N-protected HPA-methyl ester	Kinetic resolution, ester hydrolysis (ee = 98%) [100].
Aminoacylase from (sheep, beef, hog) Kidney	N-acetyl HPA	Kinetic resolution, (ee = 94-99%) [101].
B. licheniforms alcalase	HPA-ethyl ester	Kinetic resolution; reaction medium: organic solvents and ionic liquids; ionic liquids gave better results than organic solvents [102, 103].
B. caldolyticus hydantoinase and *B. kaustophilus* L-N-carbamoylase	5-[2-phenylethyl]-imidazolidine-2,4-dione	Kinetic resolution, (*RS*)-5-[2-phenylethyl]-imidazolidine-2,4-dione is hydrolyzed to (*S*)- 4-phenyl-2-ureidobutanoic acid by hydantoinase which was further transformed into (*S*)-HPA by L-N-carbamoylase [104].
Porcine pancreatic lipase	N-acylated HPA-ethyl ester	Kinetic Resolution, reaction medium: ionic liquids [105].
Different lipases and proteases	N-BOC-protected HPA methyl ester	Ammonolysis reaction wherein protected methyl ester is transformed into amide; *Thermomyces lanuginosus* lipase and *Bacillus licheniformis* protease gave maximum enantioselectivity (E = 15 and >100 respectively) [106].
Aromatic amino acid transaminase	2-oxo-4-phenylbutyric acid	Asymmetric synthesis, (ee >99) [107].
Aminoacylase	HPA-amide, N-acetyl HPA	Kinetic Resolution, (E >200) [108].

Table 1.7: Reports on the enantioselective biocatalytic synthesis of 2-naphthylalanine (NA)

Enzyme	Substrate	Process details
α-Chymotrypsin and subtilisin	N-acetyl NA	Kinetic resolution, subtilisin offered high enantioselectivity than α-chymotrypsin [109].
Immobilized subtilisin	N-acetyl NA	Kinetic resolution, 92% yield of L-NA, subtilisin was immobilized on alumina support [110].
Pronase (a mixture of several proteolytic enzymes obtained from *Streptomyces griseus*)	DL-NA methyl ester	Kinetic resolution, the biotransformation gave optically pure L-NA (ee ≈ 100%) with 87% yield [111].
Thermitase (an alkaline serine protease from *Thermoactinomyces vulgaris*)	N-Boc-NA methyl esters	Kinetic resolution, high yield (> 90%) of L-NA was obtained [112].

1.5.2. Preparative scale enantioselective synthesis of (*R*)-phenylethane diol and (*R*)-*m*-chloro-phenylethane diol, based on a mono-enzymatic enantioconvergent strategy using immobilized *Solanum tuberosum* epoxide hydrolase.

Enantiopure phenylethane diols and their halo-substituted derivatives are useful for the synthesis of pharmaceutically active compounds [113-115]. (*R*)-Phenylethane diol, for example, is component of β-adrenoreceptor agonists (e.g. isoproterenol and its analogues used in treatment of cardiac arrest) [113]. In addition to this, enantiopure phenylethane diol is useful to synthesize (*R*)-1,3-amino alcohol and the latter is a chiral intermediate of (*R*)-norfluoxetine and (*R*)-fluoxetine (pharmaceuticals which are used in the treatment of psychiatric disorders like depression, anxiety and alcoholism) [114]. (*R*)-*m*-chloro-phenylethane diol is a key chiral intermediate for the synthesis of β-3 adrenalin receptor agonists (Scheme 1.3) *namely* SR 58611A or A-9677 (developmental drug compounds having potential to treat anxiety and depressive disorders) [116]. Enantiopure phenylethane diols and their halo-derivatives are also useful to synthesize chiral catalysts [117, 118], macrocyclic polyether–diester ligands [119] and liquid crystals [120].

Scheme 1.3: (*R*)-*m*-Chloro-phenylethane diol as chiral synthon for β-3 adrenalin receptor agonists *namely* SR-58611A, AJ-9677.

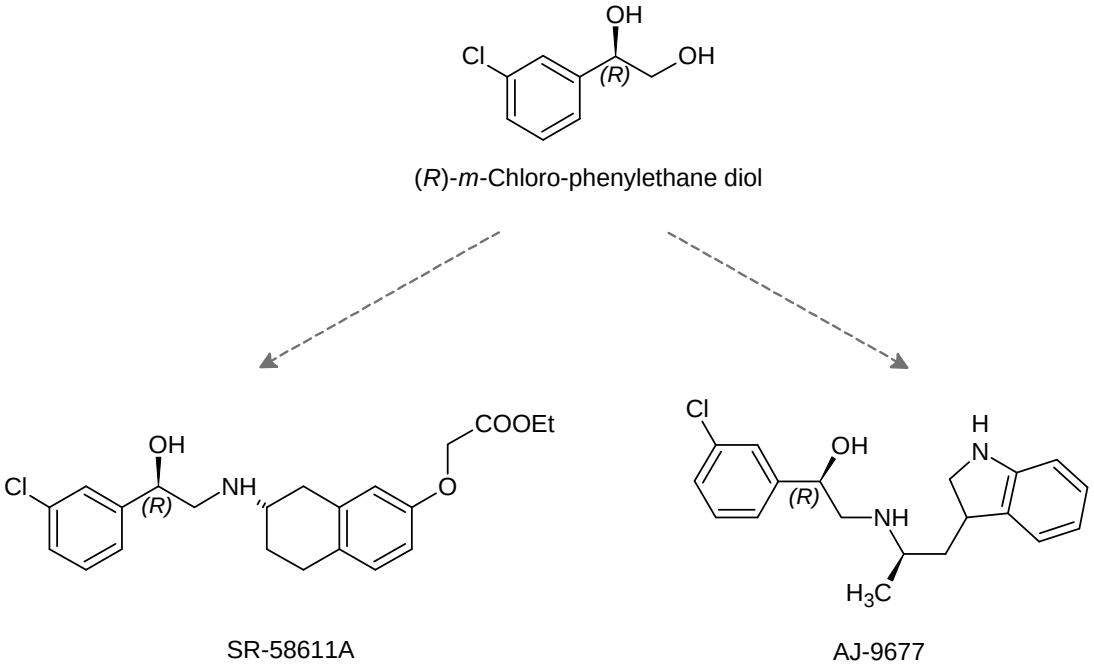

Prior art:

Limitations of substrate solubility and inherent complex nature of the enantioconvergent transformations present serious limitations for use of high substrate concentrations in reactions. This is why enantioconvergent processes are difficult to practice on commercial scale. The maximum reported substrate concentration in process of enantioconvergent production of (*R*)-phenylethane diol is 6 g/L [115] and that of (*R*)-*m*-chloro-phenylethane diol is 10 g/L [116]. In this context, the present work was undertaken to explore the preparative scale enantioconvergent production of (*R*)-phenylethane diol and (*R*)-*m*-chloro-phenylethane diol.

1.6. OUTLINE OF THE THESIS

***Chapter 2**:* **Enantioselective synthesis of unnatural amino acids using covalently immobilized lipase on porous beaded polymers**

Five commercial lipases from different sources were screened for chiral resolution of unnatural amino acid esters. The *Candida rugosa* lipase (CRL) and porcine pancreatic lipase (PPL) were immobilized on epoxy activated functional

polymers. More than 50 functional polymers of different monomer-cross-linking agent compositions were screened for lipase immobilization. The effect of cross-link density and porogen on lipase immobilization was evaluated. The acrylic functional polymers containing allyl glycidyl ether (AGE) monomer units synthesized by using lauryl alcohol as a porogen, gave higher lipase binding and therefore thoroughly analyzed for their catalytic performance, stability and reusability. Under the optimum conditions, AGE-(L)-100 gave 96.64% activity recovery for CRL binding and 74.35% activity recovery for PPL binding. The immobilized CRL and immobilized PPL were employed for the kinetic resolution of unnatural amino acid ethyl esters.

Chapter 3: **Chiral resolution of unnatural amino acid esters using immobilized lipase in membrane bioreactor**

The *Candida rugosa* lipase (CRL) and porcine pancreatic lipase (PPL) were immobilized on poly(urethane methacrylate -co- glycidyl methacrylate)-supported-polypropylene biphasic membrane. A polypropylene membrane was hydrophilized by coating followed by UV curing of a blend of 2-hydroxyethyl methacrylate terminated polyurethane prepolymer and glycidyl methacrylate. This allows formation of a hydrophobic membrane with increased surface hydrophilicity, biocompatibility and stability. Immobilized membranes were treated with 5% glutaraldehyde as a cross-linking agent for post immobilization stabilization of enzyme on membrane. Under the optimum conditions, the biocatalytic membranes retained >90% of initial lipase activity. The biocatalytic membrane was characterized for its catalytic performance, stability and reusability. The immobilized membranes were placed in membrane reactor where enantioselective synthesis of unnatural amino acids was studied.

Chapter 4: **Chiral resolution of unnatural amino acid amides using immobilized resting cells of *Rhodococcus erythropolis* MTCC 1526**

Statistical experimental methodology was used to enhance the production of amidase from *Rhodococcus erythropolis* MTCC 1526. *R. erythropolis* MTCC 1526 was selected through screening of seven strains of *Rhodococcus* species. The Placket–Burman screening experiments suggested that carbon source (sorbitol), nitrogen sources (yeast extract and meat peptone) and amidase inducer (acetamide) are the most influential media components. The concentrations of these four media

components were optimized using face centered design of Response Surface Method (RSM). Use of RSM increased the production of amidase from *R. erythropolis* MTCC 1526 by 6.88 fold. The cells of *R. erythropolis* MTCC 1526 having enhanced amidase activity were immobilized by different entrapment methods. The immobilized cells of *R. erythropolis* MTCC 1526 were used for chiral resolution of unnatural amino acid amides.

Chapter 5: **Use of immobilized *Aspergillus melleus* aminoacylase for enantioselective synthesis of unnatural amino acids**

Macroporous functional polymers containing surface epoxy groups were synthesized for immobilization of *Aspergillus melleus* aminoacylase. The effect of cross-link density of polymer on enzyme immobilization was studied. The novel styrenated acrylic ter-polymers gave maximum aminoacylase activity recovery (75.47%). Immobilized polymers were characterized for pH, temperature and storage stability. Immobilization of aminoacylase on styrenated ter-polymers gave excellent thermal stability to the enzyme. A kinetic model of thermal inactivation was derived to quantify the extent of thermal stability conferred to aminoacylase by immobilization. Immobilized aminoacylase catalyzed enantioselective synthesis of unnatural amino acids was studied.

Chapter 6: **Preparation of cross-linked enzyme aggregates of *Aspergillus melleus* aminoacylase for enantioselective synthesis of unnatural amino acids**

The cross-linked enzyme aggregates (CLEA) of aminoacylase were prepared via co-aggregation of the enzyme with polyethyleneimine (PEI). The PEI-enzyme co-aggregates were stabilized by cross-linking between primary amino groups of the PEI and the primary amino groups of enzyme using glutaraldehyde. The method described gave physically stable CLEAs and no release of enzyme was found upon prolonged storage. The process parameters such as PEI:enzyme ratio, glutaraldehyde concentration and time of glutaraldehyde treatment necessary to form stable CLEA were optimized. Under the optimum conditions, PEI-aminoacylase CLEA expressed 74.90% activity recovery with 81.20% aggregation yield. The thermal inactivation kinetics of soluble enzyme and PEI-aminoacylase CLEA was studied. The results suggest that the co-aggregation gave excellent thermal stability to the enzyme.

Finally, PEI-aminoacylase CLEA were employed for synthesis of enantiopure unnatural amino acids.

Chapter 7: **Preparative scale enantioselective synthesis of vicinal diols using immobilized *Solanum tuberosum* epoxide hydrolase**

The recombinant plasmid (pGEF-*St*EH) containing functional gene of *Solanum tuberosum* epoxide hydrolase was inserted in *Escheria coli* BL21(DE3) strain. The recombinant *E. coli* cells were grown in LB medium at 37^{o}C for about 16 h in a 5L fermenter. The extracellular enzyme was isolated from the fermentation broth. The enzyme was immobilized by multipoint covalent attachment on glyoxyl-agarose support. Immobilized enzyme gave ~ 150 units epoxide hydrolase activity per gram of support. Further, the immobilized enzyme was characterized with respect to pH stability, temperature stability and miscible/immiscible solvent stability. The immobilized epoxide hydrolase was used for enantioselective production of two vicinal diols (*namely*: phenylethane diol and *m*-chloro-phenylethane diol) via hydrolysis of their corresponding epoxides (*namely*: styrene oxide and *m*-chloro-styrene oxide respectively). The effect of incorporation of ionic liquids and organic solvents in aqueous reaction medium on enzymatic hydrolysis of epoxides was studied. The 'Regio-selectivity constants' for enzymatic hydrolysis of styrene oxide and *m*-chloro-styrene oxide were calculated. The preparative scale production of (*R*)-phenylethane diol and (*R*)-*m*-chloro-phenylethane diol (on gram scale) was studied using stirred cell bioreactor. The bioreactor performance was evaluated over 10 repeated cycles for production of each diol.

Chapter 8: **Conclusions**

This chapter recapitulates the significant findings of the present work and delineates the concluding remarks.

REFERENCES

[1] Caner, H.; Groner, E.; Levy, L.; Agranat, I. Trends in the development of chiral drugs. *Drug Discov. Today*, **2004**, *9(3)*, 105-110.

[2] Eichelbaum, M.; Gross, A.S. Stereochemical aspects of drug action and disposition. *Adv. Drug Res.*, **1996**, *28*, 1-64.

[3] Stinson, S.C. Chiral Pharmaceuticals. *Chem. Eng. News*, **2001**, *79(40)*, 79-97.

[4] Sheldon, R.A. Chirotechnology: Designing economic chiral syntheses. *J. Chem. Technol. Biotechnol.*, **1996**, *67*, 1-14.

[5] Nguyen, L.A.; He, H.; Pham-Huy, C. Chiral drugs: An overview. *Int. J. Biomed. Sci.*, **2006**, *2(2)*, 85-100.

[6] McConathy, J.; Owens M.J. Stereochemistry in Drug Action, *J. Clin. Psychiat.*, **2003**, *5(2)*, 70-73.

[7] URL: http://web99.arc.nasa.gov/~astrochm/chirality.jpg

[8] Burke, D.; Henderson, D.J. Chirality: A blueprint for the future. *Brit. J. Anaesth.*, **2002**, *88(4)*, 563-576.

[9] Cahn, R.S.; Ingold, C.K.; Prelog, V. The specification of asymmetric configuration in organic chemistry. *Experienta*, **1956**, *12*, 81-124.

[10] Hutt, A.J. The development of single-isomer molecules: Why and how. *CNS Spectrums*, **2002**, *7*, 14-22.

[11] Asmus, M.J.; Hendeles L. Levalbuterol nebulizer solution: Is it worth five times the cost of Albuterol? *Pharmacotherapy*, **2000**, *20(2)*, 123-129.

[12] Nowak, R. Single-isomer Levalbuterol: A review of the acute data. *Curr. Allergy Asthm. R.*, **2003**, *3*, 172-178.

[13] Drayer, D.E. Pharmacodynamic and pharmacokinetic differences between drug enantiomers in human: an overview. *Clin. Pharmac. Ther.*, **1986**, *40(2)*, 125-133.

[14] Ho, I.I.; Harris, R.A. Mechanism of action of barbiturates. *Ann. Rev. Pharmaco. Toxic.*, **1988**, *37(10)*, 1919-1926.

[15] Katzung, B.G. The nature of drugs, *In*: Basic and Clinical Pharmacology. 9th edt. Lange Medical Books/McGraw Hill, New York, **2004**, pp. 3-5.

[16] Lee, E.J.D.; Williams, K.M. Chirality: Clinical pharmacokinetic and pharmacodynamic considerations. *Clin. Pharmacokinet.*, **1990**, *18(5)*, 339-345.

[17] Echizen, H.; Manz, M.; Eichelbaum, M. Electrophysiologic effects of dextro- and levo- verapamil on sinus node and AV node function in humans. *J. Cardiov. Pharm.*, **1988**, *12*, 543-546.

[18] Satoh, K.; Yanagisawa, T.; Taira, N. Coronary vasodilatator and cardiac effects of optical isomers of verapamil in the dog. *J. Cardiov. Pharm.*, **1980**, *2*, 309-318.

[19] Patocka, J.; Dvorak, A. Biomedical aspects of chiral molecules. *J. Appl. Med.*, **2004**, *2*, 95-100.

[20] Rentsch, K.M. The importance of stereoselective determination of drugs in the clinical laboratory, *J. Biochem. Bioph. Meth.*, **2002**, *54(1-3)*, 1-9.

[21] Olsen, G.D.; Wendel, H.A.; Livermore, J.D.; Leger, R.M. Clinical effects and pharmacokinetics of racemic methadone and its optical isomers. *Clin. Pharmacol. Ther.*, **1977**, *21*, 147-157.

[22] Davies, N.M.; Teng, X.V. Importance of chirality in drug therapy and pharmacy practice, Implication for psychiatry. *Adv. Pharm.*, **2003**, *1(3)*, 242-252.

[23] Stoschitzky, K.; Lindner, W.; Egginger, G.; Brunner, F. Racemic (*R,S*)-propranolol versus half-dosed optically pure (*S*)-propranolol in man at steady state: Hemodynamic effects, plasma concentrations, and influence on thyroid hormone levels. *Clin. Pharmacol Ther.*, **1992**, *51*, 445-453.

[24] Wiersinga, W.M.; Touber, J.L. The influence of β-adrenoceptor blocking agents on plasma thyroxine and triiodothyronine. *J. Clin. Endocr. Metab.*, **1977**, *45*, 293-308.

[25] Drayer, D.E. Pharmacokinetic and pharmacodynamic differences between drug enantiomers in humans: an overview. *Clin. Pharmacol. Ther.*, **1986**, *40*, 125-133.

[26] Landoni, M.F.; Soraci, A. Pharmacology of chiral compounds: 2-Arylpropionic acid derivatives. *Curr. Drug Metabol.*, **2001**, *2(1)*, 37-51.

[27] Waldeck, B. Three-dimensional pharmacology, a subject ranging from ignorance to overstatements. *Pharmacol. Toxicol.*, **2003**, *93(5)*, 203-210.

[28] Powell, J.R.; Ambre, J.J.; Ruo, T.I. The efficacy and toxicity of drug stereoisomers. *In*: Drug stereochemistry. Analytical methods and pharmacology. 1st edt., Wainer, I.W., (*Eds.*) Marcel Dekker Publisher, New York, **1988**, 245-270.

[29] Tucker, G.T. Chiral switches. *Lancet*, **2000**, *355*, 1085-1087.

[30] Food and Drug Administration FDA's policy statement for the development of new stereoisomeric drugs. **1992**, 57 *Fed. Reg*. 22-249.

[31] Committee for Proprietary Medical Products, Working parties on quality, safety and efficacy of medical products. Note for guidance: investigation of chiral active substances. **1993**, III/3501/91.

[32] Patel, R.N. Biocatalytic synthesis of intermediates for the synthesis of chiral drug substances. *Curr. Opin. Biotechnol*., **2001**, *12*, 587-604.

[33] Walshe, J.M. Penicillamine, a new oral therapy for Wilson's disease. *Am. J. Med.*, **1956**, *21*, 487-495.

[34] Sheldon, R.A. Chirotechnology: Industrial Synthesis of optically active compounds. 2nd edt., Marcel Dekker, New York, **1993**.

[35] Thayer, A.M. Interaction yields. *Chem. Eng. News*, **2008**, *86(31)*, 12-20.

[36] Rouhi, A.M. Chirality at Work. *Chem. Eng. News*, **2003**, *5*, 56-57.

[37] Rouhi, A.M. Chiral business. *Chem. Eng. News*, **2003**, *81(18)*, 45-55.

[38] Ager, D.J.; Allen, D.R.; East, M.B.; Fotheringham, I.G.; Laneman, S.A.; Liu, W.G.; Pantaleone, D.P.; Schaad, D.R.; Taylor, P.P. *In:* Handbook of Chiral Chemicals, Ager D.J. (*Ed*.), Marcel Dekker, New York, **1999**, pp. 83.

[39] Collins, A.N.; Sheldrake, G.N.; Crosby, J. Chirality in Industry II. Wiley, New York, **1997**.

[40] Aboun-Enein, H.Y.; Ali, I. Introduction, *In*: Chiral separations by liquid chromatography and related technologies. Aboun-Enein, H.Y.; Ali I. (*Ed*s.), New York, Marcel Dekker, **2003**, pp. 1-20.

[41] Nicoud, R.M.; Fuchs, G.; Adam, P.; Bailly, M.; Kusters, E.; Antia, F.D.; Reuille, R.; Schmid, E. Preparative scale enantioseparation of a chiral epoxide: a comparison of liquid chromatography and simulated moving-bed adsorption technology. *Chirality*, **1993**, *5*, 267-271.

[42] Pais, L.S.; Loureiro, J.M.; Rodrigues, A.E. Chiral separation by SMB chromatography. *Sep. Purif. Technol.*, **2000**, *20*, 67-77.

[43] Vedejs E.; Jure, M. Efficiency in nonenzymatic kinetic resolution. *Angew. Chem. Int. Edt.*, **2005**, *44*, 3974-4001.

[44] Bornscheuer, U.T.; Kazlauskas, R.J. Hydrolases in organic synthesis: regio- and stereoselective biotransformations. Wiley-VCH, Weinheim, Germany, **1999**.

[45] URL: http://www.basf.de/en/produkte/chemikalien/interm/nbd/chipros/ (This website provides a lot of information on products and underlying biocatalytic technologies).

[46] Xie, R.; Chu, L-Y.; Deng, J-G. Membranes and membrane processes for chiral resolution. *Chem. Soc. Rev.*, **2008**, *37*, 1243-1263.

[47] Atwood, J.L.; Davies, J.E.D.; MacNicol, D.D. (*Eds.*), Inclusion Compounds.

Academic Press: London, Oxford, **1984**.

[48] Cheng, X.; Hou, G.-H.; Xie, J.-H.; Zhou, Q.-L. Synthesis and optical resolution of 9,9'-spirobifluorene-1,1'-diol. *Org. Lett.*, **2004**, *6*, 2381-2383.

[49] Vries, T.R.; Wynberg, H.; van Echten, E.; Koek, J.; ten Hoeve, W.; Kellogg, R.M.; Broxterman, Q.B.; Minnaard, A.; Kaptein, B.; van der Sluis, S.; Hulshof, L.A.; Kooistra, J. The family approach to the resolution of racemates. *Angew. Chem. Int. Edt.*, **1998**, *37*, 2349-2354.

[50] Kaptein, B.; van Dooren, T.J.G.M.; Boesten, W.H.J.; Sonke, T.; Duchateau, A.L.L.; Broxterman, Q.B.; Kamphuis, J. Synthesis of 4-sulfur-substituted (2S,3R)-3-phenylserines by enzymatic resolution, Enantiopure precursors for thiamphenicol and florfenicol. *Org. Process Res. Dev.*, **1998**, *2*, 10-17.

[51] Thayer, A.M. Centering on chirality. *Chem. Eng. News*, **2007**, *85(32)*, 11-19.

[52] de Vries, J.G.; de Vries, A.H.M. The power of high-throughput experimentation in homogeneous catalysis research for fine chemicals. *Eur. J. Org. Chem.*, **2003**, 799-811.

[53] Koeller, K.M.; Wong, C.H. Enzymes for chemical synthesis. *Nature*, **2001**, *409*, 232-240.

[54] Carrea, G.; Riva, S. Properties and synthetic applications of enzyme in organic solvents. *Angew Chem. Int. Edt.*, **2000**, *39*, 2226-2254.

[55] Tao, J.; Xu, J-H. Biocatalysis in development of green pharmaceutical processes. *Curr. Opin. Chem. Biol.*, **2009**, *13*, 43-50.

[56] Bornscheuer, U.T. Immobilizing Enzymes: How to create more suitable biocatalysts. *Angew. Chem. Int. Edt.*, **2003**, *42*, 3336-3337.

[57] Chibata, I. Immobilized enzymes research and development. Wiley, New York, **1978**.

[58] Bagi, K.; Simon, L.M.; SzajPni, B. Immobilization and characterization of porcine pancreas lipase. *Enzyme Microb. Technol.*, **1997**, *20*, 531-535.

[59] Mosbach, K. (*Ed*.), Methods in Enzymology. Academic Press, New York, 1976.

[60] Messing, R.A. Immobilized enzymes for industrial reactors. Academic Press, New York, **1975**.

[61] Cao, L.; van Langeny, L.; Sheldon, R.A. Immobilised enzymes: carrier-bound or carrier-free? *Curr. Opin. Biotechnol.*, **2003**, *14*, 387-394.

[62] Balavoine, G.; Moradpour, A.; Kagan, H. B. Preparation of chiral compounds

with high optical purity by irradiation of circularly polarized light, a model reaction for the prebiotic generation of optical activity. *J. Am. Chem. Soc.*, **1974**, *96*, 5152-5158.

[63] Kagan, H.B.; Fiaud, J.C. Kinetic resolution. *Top. Stereochem.*, **1988**, *l8*, 249-330.

[64] Martin, V.S.; Woodard, S.S.; Katsuki, T.; Yamada, Y.; Ikeda, M.; Sharpless, K.B. Kinetic resolution of racemic allylic alcohols by enantioselective epoxidation: A route to substances of absolute enantiomeric purity. *J. Am. Chem. Soc.*, **1981**, *103*, 6237-6240.

[65] Straathof, A.J.J.; Jongejan, J.A. The enantiomeric ratio: origin, determination and prediction. *Enzyme Microb. Technol.*, **1997**, *21*, 559-571.

[66] Chen. C.S.; Fujimoto. Y.; Girdaukas. G.; Sih, C.J. Quantitative analysis of biochemical kinetic resolutions of enantiomers. *J. Am. Chem. Soc.*, **1982**, *104*, 7294-7299.

[67] Faber K. Biotransformations in Organic Chemistry, 2nd edt., Springer, Heidelberg, **1995**, pp. 32-38.

[68] Ottolina, G.; Bovara, R.; Riva, S.; Carrea, G. Activity and selectivity of some hydrolases in enantiomeric solvents. *Biotechnol. Lett.*, **1994**, *16*, 923-928.

[69] Service, R.F. Unnatural amino acid could prove boon for protein therapeutics. *Science*, **2005**, *308*, 44.

[70] Lubec, G.; Rosenthal, G.A. Amino Acids: Chemistry, Biology, and Medicine. ESCOM Science Publishers B.V., Leiden, Netherlands, **1990**.

[71] Ma, J.S. Unnatural amino acids in drug discovery. *Chimica Oggi/Chemistry Today*, June **2003**, 65-68.

[72] Gallos, J.K.; Sarli, V.C.; Massen, Z.S.; Varvogli, A.C.; Papadoyanni, C.Z.; Papaspyrou, S.D.; Argyropoulos, N.G. A new strategy for the stereoselective synthesis of unnatural α-amino acids. *Tetrahedron*, **2005**, *61*, 565-574.

[73] Pojitkov, A.E.; Efremenko, E.N.; Varfolomeev, S.D. Unnatural amino acids in enzymes and proteins. *J. Mol. Catal. B: Enzym.*, **2000**, *10*, 47-55.

[74] Besse, P.; Veschambre, E.N. Chemical and biological synthesis of chiral epoxides. *Tetrahedron*, **1994**, *50*, 8885-8927.

[75] Archelas, A.; Furstoss, R. Synthetic applications of epoxide hydrolases. *Curr. Opin. Chem. Biol.*, **2001**, *5*, 112-119.

[76] Kasai, N.; Suzuki, T.; Furukawa, Y. Chiral C3 epoxides and halohydrins: Their preparation and synthetic application. *J. Mol. Catal. B: Enzym.*, **1998**, *4*, 237-252.

[77] Genzel, Y.; Archelas, A.; Broxterman, Q.B.; Schulze, B.; Furstoss, R. Microbiological transformation: 50. Selection of epoxide hydrolase for enzymatic resolution of 2-, 3-, or 4-pyridyloxirane. *J. Mol. Catal. B: Enzym.*, **2002**, *16*, 217-222.

[78] de Vries, E.J.; Janssen, D.B. Biocatalytic conversion of epoxides. *Curr. Opin. Biotechnol.*, **2003**, *14*, 414-420.

[79] Weijers, C.A.G.M.; de Bont J.A.M. Epoxide hydrolases from yeasts and other sources: Versatile tools in biocatalysis. *J. Mol. Catal. B: Enzym.*, **1999**, *6*, 199-214.

[80] Steinreiber, A.; Faber, K. Microbial epoxide hydrolases for preparative biotransformations. *Curr. Opin. Biotechnol*., **2001**, *12*, 552-558.

[81] Strauss, U.T.; Felfer, U.; Faber, K. Biocatalytic transformation of racemates into chiral building blocks in 100% chemical yield and 100% enantiomeric excess. *Tetrahedron: Asymmetr.*, **1999**, *10*, 107-117.

[82] Pedragosa-Moreau, S.; Morisseau, C.; Baratti, J.C.; Zylber, J.; Archelas, A.; Furstoss, R. Microbial transformations 37. An enantioconvergent synthesis of the β-blocker (*R*)-Nifénalol® using a combined chemoenzymatic approach. *Tetrahedron*, **1997**, *53*, 9707-9714.

[83] Manoj, K.M.; Archelas, A.; Baratti, J.; Furstoss, R. Microbiological transformations. Part 45: A green chemistry preparative scale synthesis of enantiopure building blocks of Eliprodil: elaboration of a high substrate concentration epoxide hydrolase-catalyzed hydrolytic kinetic resolution process. *Tetrahedron*, **2001**, *57*, 695-701.

[84] Archelas, A. Fungal epoxide hydrolases: new tools for the synthesis of enantiopure epoxides and diols. *J. Mol. Catal. B: Enzym.*, **1998**, *5*, 79-85.

[85] Yu, L-T.; Huang, J-L.; Chang, C-Y.; Yang, T-K. Formal synthesis of the ACE inhibitor Benazepril·HCl via an asymmetric Aza-Michael Reaction. *Molecules*, **2006**, *11*, 641-648.

[86] Iwasaki, G.; Kimura, R.; Numao, N.; Kondo, K. A stereoselective synthesis of *N*-[(*S*)-1-ethoxycarbonyl-3-phenylpropyl]-L-alanine derivatives by means of

reductive amination. *Chem. Lett.*, **1988**, *17(10)*, 1691-1694.

[87] Houng, J-Y.; Wu, M-L.; Chen, S-T. Kinetic resolution of amino acid esters catalyzed by lipases. *Chirality*, **1996**, *8*, 418-422.

[88] Wegman, M.A.; Hacking, M.A.P.J.; Rops, J.; Pereira, P.; van Rantwijk, F.; Sheldon, R.A. Dynamic kinetic resolution of phenylglycine esters via lipase-catalysed ammonolysis. *Tetrahedron: Asymmetr.*, **1999**, *10*, 1739-1750.

[89] Du, W.; Zong, M.; Guo, Y.; Liu, D. Improving lipase-catalyzed enantioselective ammonolysis of phenylglycine methyl ester in organic solvent by *in situ* racemization. *Biotechnol. Lett.*, **2003**, *25*, 461-464.

[90] Lou, W-Y.; Zong, M-H.; Liu, Y-Y.; Wang, J-F. Efficient enantioselective hydrolysis of d,l-phenylglycine methyl ester catalyzed by immobilized *Candida antarctica* lipase B in ionic liquid containing systems. *J. Biotechnol.*, **2006**, *125*, 64-74.

[91] Du, W.; Zong, M.; Guo, Y.; Liu, D. Lipase-catalysed enantioselective ammonolysis of phenylglycine methyl ester in organic solvent. *Biotechnol. Appl. Biochem.*, **2003**, *38*, 107-110.

[92] Bossi, A.; Cretich, M.; Righetti, P.G. Production of D-phenylglycine from racemic (D,L)-phenylglycine via isoelectrically-trapped penicillin-G-acylase. *Biotechnol. Bioeng.*, **1998**, *60(4)*, 454-461.

[93] Hensel, M.; Lutz-Wahl, S.; Fischer, L. Stereoselective hydration of (*RS*)-phenylglycine nitrile by new whole cell biocatalysts. *Tetrahedron: Asymmetr.*, **2002**, *13*, 2629-2633.

[94] Wegman, M. A.; Heinemann, U.; Stolz, A.; van Rantwijk, F.; Sheldon, R. A. Stereoretentive nitrile hydratase-catalysed hydration of D-phenylglycine nitrile. *Org. Process Res. Dev.*, **2000**, *4,* 318-322.

[95] Wegman, M.A.; Heinemann, U.; van Rantwijk, F.; Stolz, A.; Sheldon, R.A. Hydrolysis of D,L-phenylglycine nitrile by new bacterial cultures. *J. Mol. Catal. B: Enzym.*, **2001**, *11*, 249-253.

[96] Wang, M-X.; Lin, S-J. Highly efficient and enantioselective synthesis of L-arylglycines and D-arylglycine amides from biotransformations of nitriles. *Tetrahedron Lett.*, **2001**, 42, 6925-6927.

[97] Kise, H.; Tomiuchi, Y. Unusual solvent effect on protease activity and effective optical resolution of amino acids by hydrolytic reactions in organic solvents.

Biotechnol. Lett., **1991**, *13(5)*, 317-322.

[98] Vulfson, E.N.; Ahmed, G.; Gill, I.; Goodenough, P.W.; Kozlov, I.A.; Law, B.A. L-DOPA ester synthesis by α-chymotrypsin in organic solvents. *Biotechnol. Lett.*, **1990**, *12(8)*, 597-602.

[99] Ahmed, G.; Vulfson, E.N. Facile synthesis of L-DOPA esters by the combined use of tyrosinase and α-chymotrypsin. *Biotechnol. Lett.*, **1994**, *16(4)*, 347-372.

[100] Chen, S-T.; Chen, S-Y.; Hsiao, S-C.; Wang, K-T. Kinetic resolution of N-protected amino acid esters in organic solvents catalyzed by a stable industrial alkaline protease. *Biotechnol. Lett.*, **1991**, *13(11)*, 773-778.

[101] Regla, I.; Luna, H.; Pérez, H.I.; Demare, P.; Bustos-Jaimes, I.; Zaldívar, V.; Calcagno, M.L. Enzymatic resolution of N-acetyl-homophenylalanine with mammalian kidney acetone powders. *Tetrahedron: Asymmetr.*, **2004**, *15*, 1285-1288.

[102] Zhao, H.; Luo, R.G.; Malhotra, S.V. Kinetic study on the enzymatic resolution of homophenylalanine ester using ionic liquids. *Biotechnol. Prog.*, **2003**, *19,* 1016-1018.

[103] Zhao, H.; Malhotra, S.V. Enzymatic resolution of amino acid esters using ionic liquid *N*-ethyl pyridinium trifluoroacetate. *Biotechnol. Lett.*, **2002**, *24*, 1257-1260.

[104] Lo, H-H.; Kao, C-H.; Lee, D-S.; Yang, T-K.; Hsu, W-H. Enantioselective synthesis of (*S*)-2-Amino-4-phenylbutanoic acid by the hydantoinase method. *Chirality*, **2003**, *15*, 699-702.

[105] Malhotra, S.V.; Zhao, H. Enantioseparation of the esters of α-N-acetyl amino acids by lipase in ionic liquid. *Chirality*, **2005**, *17*, S240-S242.

[106] López-Serrano, P.; Wegman, M.A.; van Rantwijk, F.; Sheldon, R.A. Enantioselective enzyme catalysed ammoniolysis of amino acid derivatives: Effect of temperature. *Tetrahedron: Asymmetr.*, **2001**, *12*, 235-240.

[107] Fadnavis, N.W.; Seo, S-H.; Seo, J-H.; Kim, B-G. Asymmetric synthesis of nonproteinogenic amino acids with L-amino acid transaminase: synthesis of (2S)-2-amino-4-oxo-4-phenylbutyric and (3E,2S)-2-amino-4-phenylbutenoic acids. *Tetrahedron: Asymmetr.*, **2006**, *17*, 2199-2202.

[108] Youshko, M.I.; van Langen, L.M., Sheldon, R.A., Švedas, V.K. Application of aminoacylase-I to the enantioselective resolution of α-amino acid esters and

amides. *Tetrahedron: Asymmetr.*, **2004**, *15*, 1933-1936.

[109] Pattabiraman, T.N.; Lawson, W. B. Comparative studies of the specificities of α-chymotrypsin and subtilisin BPN', studies with flexible and 'locked' substrates. *Biochem. J.*, **1972**, *126*, 659-665.

[110] Pugniere, M.; Castro, B.; Previero, A. Optical resolution of two isomeric naphthylalanines by immobilized enzymes. *Chirality*, **1991**, *3*, 170-173.

[111] Pugniere, M.; Domergue, N.; Castro, B.; Previero, A. Pronase in amino acid technology: Optical resolution of non-proteinogenic α-amino acids. *Chirality*, **1994**, *6*, 472-478.

[112] Lankiewicz, L.; Kasprzykowski, F.; Grzonka, Z.; Kettmann, U.; Hermann, P. Resolution of racemic amino acids with thermitase. *Bioorg Chem*., **1989**, *17*, 275-280.

[113] Märki, H.P.; Crameri, Y.; Eigenmann, R.; Krasso, A.; Ramuz, H.; Bernauer, K.; Goodman, M.; Melmon, K.L. Optically pure isoproterenol analogues with side chains containing an amide bond: synthesis and biological properties. *Helv. Chim. Acta*, **1988**, *71*, 320-336.

[114] Kumar, P.; Upadhyay, R.K.; Pandey, R.K. Asymmetric dihydroxylation route to (*R*)-isoprenaline, (*R*)-norfluoxetine and (*R*)-fluoxetine. *Tetrahedron: Asymmetr.*, **2004**, *15*, 3955-3959.

[115] Kim, H.S., Lee, O.K. Hwang, S.; Kim, B.J.; Lee, E.Y. Biosynthesis of (*R*)-phenyl-1,2-ethanediol from racemic styrene oxide by using bacterial and marine fish epoxide hydrolases. *Biotechnol. Lett.*, **2008**, *30*, 127-133.

[116] Monterde, M.; Lombard, M.; Archelas, A.; Cronin, A.; Arand, M.; Furstoss, R. Enzymatic transformations Part 58: Enantioconvergent biohydrolysis of styrene oxide derivatives catalysed by the *Solanum tuberosum* epoxide hydrolase. *Tetrahedron: Asymmetr.*, **2004**, *15*, 2801-2805.

[117] Brown, J. M.; Murrer, B.A. The mechanism of asymmetric hydrogenation: chiral bis(dipheny1phosphino)-α-phenylalkane complexes in catalytic and structural studies. *J. Chem. Soc. Perkin Trans*., **1982**, *2*, 489-497.

[118] Virsu, P.; Liljeblad, A.; Kanerva, A.; Kanerva, L.T. Preparation of the enantiomers of 1-phenylethane-1,2-diol. Regio- and enantioselectivity of acylase I and *Candida antarctica* lipases A and B. *Tetrahedron: Asymmetr.*, **2001**, *12*, 2447-2455.

[119] Bradshaw, J.S.; Jolley, S.T.; Izatt, R.M. Preparation of chiral diphenyl substituted polyether-diester compounds. *J. Org. Chem.*, **1982**, *47*, 1229-1232.

[120] Pauluth, D.; Wächtler, E.F. *In*: Chirality in Industry II; Collins, A.N.; Sheldrake, G.N.; Crosby, J. (*Eds.*), John Wiley & Sons: Chichester, **1997**, pp. 280-281.

CHAPTER

2 Enantioselective synthesis of unnatural amino acids using covalently immobilized lipase on porous beaded polymers

2.1. INTRODUCTION

Lipases (triacylglycerol ester hydrolase, EC 3.1.1.3) are important enzymes in biological systems, where they catalyze the hydrolysis of triacylglycerol to glycerol and fatty acids. The enzyme is widely distributed among higher animals, plants and microorganisms in which it plays a key role in lipid metabolism. Besides their natural substrates, lipases are also able to catalyze a wide range of unnatural chemical reactions [1, 2]. Depending on the nature of substrate and reaction conditions, lipases catalyze a wide range of enantio- and regio-selective reactions such as hydrolysis, esterifications, transesterifications, aminolysis and ammoniolysis. Due to their catalytic versatility, lipases have emerged as unique industrial biocatalyst in pharmaceutical, food and flavouring and recently in cosmetics and perfumery industries [3].

Many attempts have been made over the years to improve the catalytic activity and operational stability of industrial enzymes through the use of genetic engineering, immobilization and/or process alterations. Enzyme immobilization is the most commonly used strategy to impart the desirable features of conventional heterogeneous catalysts onto biological catalysts [4]. Besides enhanced stability, immobilization is also known to offer several advantages such as reusability, ease of product separation, greater control over catalysis and process economics. Lipases have been immobilized on various supports either by physical adsorption [5, 6], covalent binding [7-9], ionic interactions or by entrapment [10, 11].

The extent of enzyme stabilization and the operational cost of biocatalytic reaction can be significantly manipulated by selection of appropriate immobilization method and choice of suitable support [10]. Compared to other immobilization methods, covalent immobilization protocols are straightforward, easy to scale-up and generally give higher immobilization yields whereby large quantities of enzyme can be immobilized per unit weight of support. Moreover, the physical properties of polymeric supports (such as surface area, porosity, density of functional groups) can be easily tailored according to specific needs. Hence the covalent immobilization is the preferred method at both laboratory and industrial scale [12].

Polymers having reactive epoxy groups on their surface (commonly known as epoxy activated supports) are of technical interest as they provide almost ideal conditions for stable immobilization of enzymes. Epoxy groups are stable at neutral

pH conditions even in wet conditions enabling the long-term storage of epoxy activated supports (in dry or wet form) before enzyme immobilization. While most of other immobilization protocols may cause great alterations to the protein surface, yielding labile enzyme-support attachments (e.g., in case of cyanogen bromide activated supports) [13, 14], epoxy activated supports are able to form extremely strong linkages (such as secondary amino bonds, ether bonds, thioether bonds by selectively reacting with amino, hydroxy, thiol moieties respectively) with minimal chemical modification of the protein e.g., p*K* values of the new secondary amino groups are very close to those of the pre-existing primary amino ones [15]. More importantly, the interaction of epoxy-groups with different protein groups (amino, hydroxyl or thiol) can readily occur at ambient conditions of pH and temperature. At the end of the immobilization process, epoxy groups can be easily blocked by reaction with different thiol or amine compounds under mild conditions, preventing further uncontrolled reaction between the support and the enzyme that could decrease stability of the latter [12,15].

Derivatization of support surface with various activating agents (such as cyanogen bromide, epichlorohydrin or carbodiimide) and preparation of support by copolymerization of different monomers containing reactive groups (such as glycidyl methacrylate, 2-hydroxyethyl methacrylate) are two commonly used methods for preparation of functional support materials. The latter reduces the number of steps involved in the preparation of functional support and the desired amount of functional groups can be easily altered by adjusting the mole ratio of functional group carrying monomer during the process of polymerization [16].

Glycidyl methacrylate (GMA) and allyl glycidyl ether (AGE) are the most preferred monomers as they can be easily modified into various functional groups for synthesis of epoxy-activated polymers. GMA and AGE are bifunctional molecules containing terminal epoxy groups. Besides the terminal epoxy group, GMA monomer has an acrylic functionality whereas AGE monomer contains an allyl functionality. The allyl/acrylic functionality allows copolymerization with a variety of other vinyl monomers in aqueous and non-aqueous systems and the resulting polymers give a unique combination of epoxy functionality with an acrylic backbone. As polymerization of GMA or AGE proceeds, the epoxy groups on the polymer surface become useful for the introduction of various functional groups, such as amino group

and hydroxyl group [17-21]. Moreover, these copolymers can also be employed for grafting of natural/synthetic polymers as reported in the literature for immobilization of a variety of enzymes like lipase [22, 23], urease [24], polyphenol oxidase [25] and trypsin [26], etc.

The present chapter deals with kinetic resolution of unnatural amino acid esters by immobilized lipase. Initially, different commercial lipases were screened for kinetic resolution of unnatural amino acid esters. Due to their better enantioselectivity, *Candida rugosa* lipase (CRL) and porcine pancreatic lipase (PPL) were selected for further experiments. A series of epoxy activated acrylic copolymer supports (having different monomer–cross-linker–porogen composition) were synthesized by suspension polymerization and were used for CRL and PPL immobilization. The immobilized lipases were evaluated for pH, thermal and storage stability. Finally the immobilized lipases were employed for enantioselective hydrolysis of amino acid esters.

2.2. MATERIALS AND METHODS

2.2.1. Materials

Glycidyl methacrylate (GMA), allyl glycidyl ether (AGE), ethylene glycol dimethacrylate (EGDM) and poly vinyl pyrrolidone (PVP, K-90) were purchased from Sigma-Aldrich, USA. 2,20-azobis(isobutyronitrile) (AIBN), cyclohexanol, hexanol, lauryl alcohol were procured from S.D. Fine Chemicals, India. *Candida rugosa* lipase (CRL), *Pseudomonas cepacia* lipase (PCL) and *Alcaligens* lipase (Lipase 20) were purchased from Europa Chemicals, UK. Porcine pancreatic lipase (PPL) and *Thermomyces languginous* lipase (TLL) were purchased from Sigma Chemicals, USA. Unnatural amino acids *namely* phenylglycine (PG), 3,4-dihydroxy phenylalanine (DOPA), homophenylalanine (HPA), and 2-naphthylalanine (NA); and homophenylalanine ethyl ester (HPA-ester) were purchased from Bachem Chemicals, Switzerland. All other chemicals were of analytical grade from Merck India Ltd.

2.2.2. Synthesis of polymer beads

The porous GMA-EGDM and AGE-EGDM copolymer beads were synthesized by suspension polymerization in a jacketed cylindrical polymerization reactor under conditions amenable to scale-up [27]. The continuous phase comprised

250 mL of a 1% by weight aqueous solution of PVP. The discontinuous organic phase consisted of 21.4 mL of GMA and EGDM or AGE and EGDM along with equimolar quantity of porogen (cyclohexanol or hexanol or lauryl alcohol). 0.2 g of 2,20-azobis(isobutyronitrile), i.e. AIBN was used as initiator. The combined volume of the two liquid phases was chosen such that the height of the liquid was almost equivalent to the inner diameter of the reactor [28].

The agitator was a six bladed Rushton disc turbine capable of radial mixing to prevent ingress and entrapment of air in the droplet, which could otherwise create artefacts due to uncontrolled additional voids/pores. The diameter of the Rushton disc turbine was 0.3 times the reactor diameter. The disc was maintained at a liquid height one-third from the bottom. Stirring was maintained at 300 rpm by using a power compensation DC motor and the temperature was maintained to 70°C under a nitrogen overlay by circulating water through the jacket. Polymerization was allowed to proceed to 100% conversion in about 3h. The polymer beads obtained were filtered, washed thoroughly with water and methanol to remove residual contents of porogen. The polymer beads were dried under vacuum and sieved through 80-100 mesh.

The polymerization reactions involved in the formation of poly(GMA-co-EGDM) and poly(AGE-co-EGDM) are schematically represented in Scheme 2.1(a) and Scheme 2.1(b) respectively. The composition of poly(GMA-co-EGDM) and poly(AGE-co-EGDM) at different cross-link densities (50-200%) is presented in Table 2.1(a) and Table 2.1(b) respectively.

The cross-link density (CLD) of polymer beads is defined as a percentile molar ratio of cross-linking agent to monomer (Eq. 2.1).

$$\text{Cross - link density (\%)} = \frac{\text{Moles of cross - liking agent (EGDM)}}{\text{Moles of monomer (GMA or AGE)}} \times 100 \quad \text{– Eq. 2.1}$$

Polymer beads were coded based on monomer, porogen and CLD. For example, poly(GMA-co-EGDM) synthesized using cyclohexanol as porogen were termed as GMA-(C) polymers. Poly(AGE-co-EGDM) synthesized using cyclohexanol as porogen were termed as AGE-(C) polymers. Poly(AGE-co-EGDM) synthesized using hexanol as porogen were termed as AGE-(H) polymers. Poly(AGE-co-EGDM) synthesized using lauryl alcohol as porogen were termed as AGE-(L) polymers.

Scheme 2.1(a): Synthesis of GMA polymers

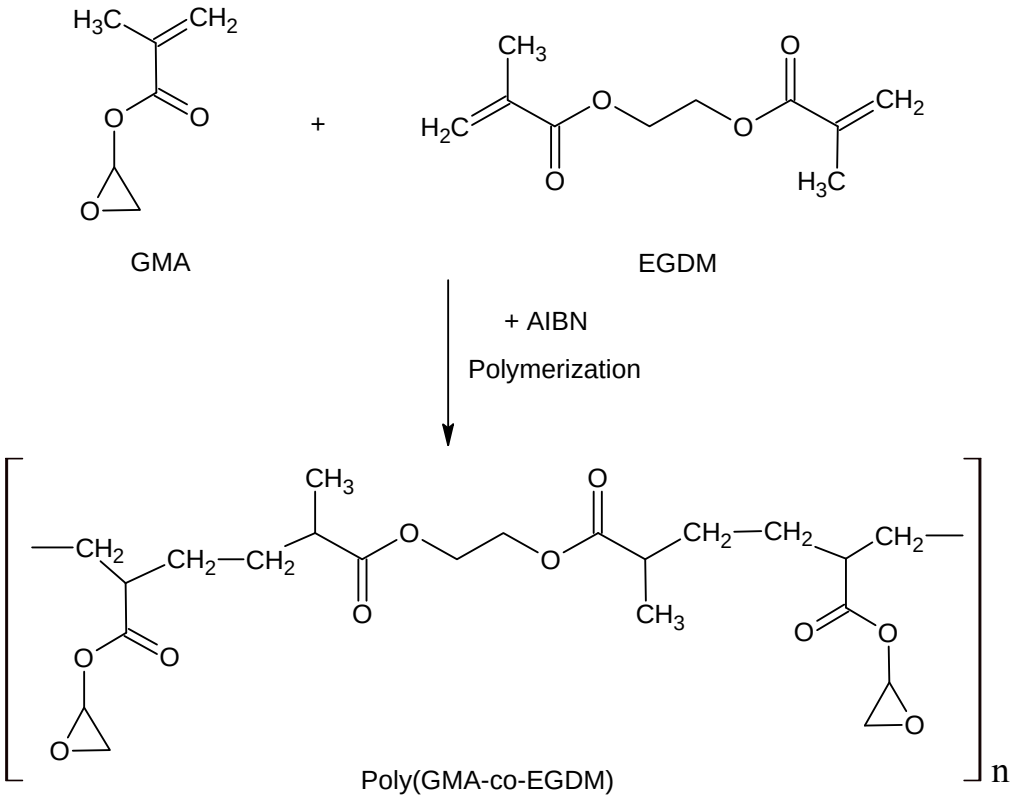

Scheme 2.1(b): Synthesis of AGE polymers

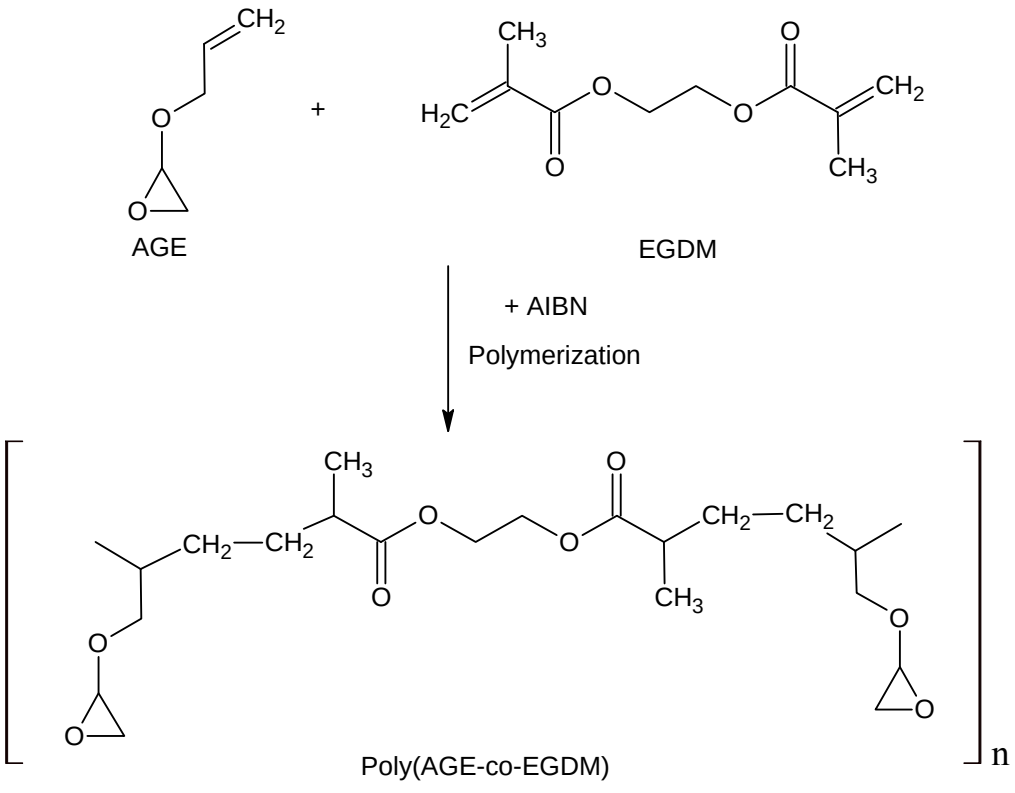

Table 2.1: Composition of poly(GMA-co-EGDM) and poly(AGE-co-EGDM) polymers

(a) Composition of poly(GMA-co-EGDM) beads			
No.	**Cross-link density** (%)	**GMA** (mole)	**EGDM** (mole)
1	50	0.0352	0.0176
2	75	0.0300	0.0225
3	100	0.0249	0.0249
4	150	0.0198	0.0297
5	200	0.0161	0.0322
(b) Composition of poly(AGE-co-EGDM) beads			
No.	**Cross-link density** (%)	**AGE** (mole)	**EGDM** (mole)
6	50	0.0388	0.0194
7	75	0.0312	0.0234
8	100	0.0269	0.0269
9	150	0.0202	0.0303
10	200	0.0168	0.0336

Further, depending on their respective CLDs, GMA-(C) polymers were termed as GMA-(C)-50, GMA-(C)-75, GMA-(C)-100, GMA-(C)-150 and GMA-(C)-200. Similarly, depending on their respective CLDs, AGE-(C) polymers were termed as AGE-(C)-50, AGE-(C)-75, AGE-(C)-100, AGE-(C)-150 and AGE-(C)-200; AGE-(H) polymers were termed as AGE-(H)-50, AGE-(H)-75 … AGE-(H)-200 and AGE-(L) polymers were termed as AGE-(L)-50, AGE-(L)-75 … AGE-(L)-200.

2.2.3. Method of lipase immobilization

To dried polymer beads (1 g), 20 mL of 0.1% Tween-20 solution was added and kept for 3 h with occasional shaking. Tween-20 solution was removed by filtration and wetted polymer beads were washed thoroughly with 0.5 M sodium phosphate buffer (pH 7). In a 100 mL stoppered conical flask, 1 g wetted polymer beads were suspended in 40 mL lipase solution prepared in 0.5 M sodium phosphate buffer (pH 7). The flask was incubated at 30°C at 120 rpm. After 12-18 h, enzyme immobilized polymer beads were separated by filtration and washed thoroughly with 0.05 M sodium phosphate buffer (pH 7). The supernatant and washings were assayed

for protein content. The difference between protein loaded and that remaining unbound indicates quantity of protein bound on the polymer beads. The covalent immobilization of lipase on the epoxy activated support is schematically represented in Scheme 2.2.

Scheme 2.2: Covalent immobilization of lipase on epoxy activated polymer support

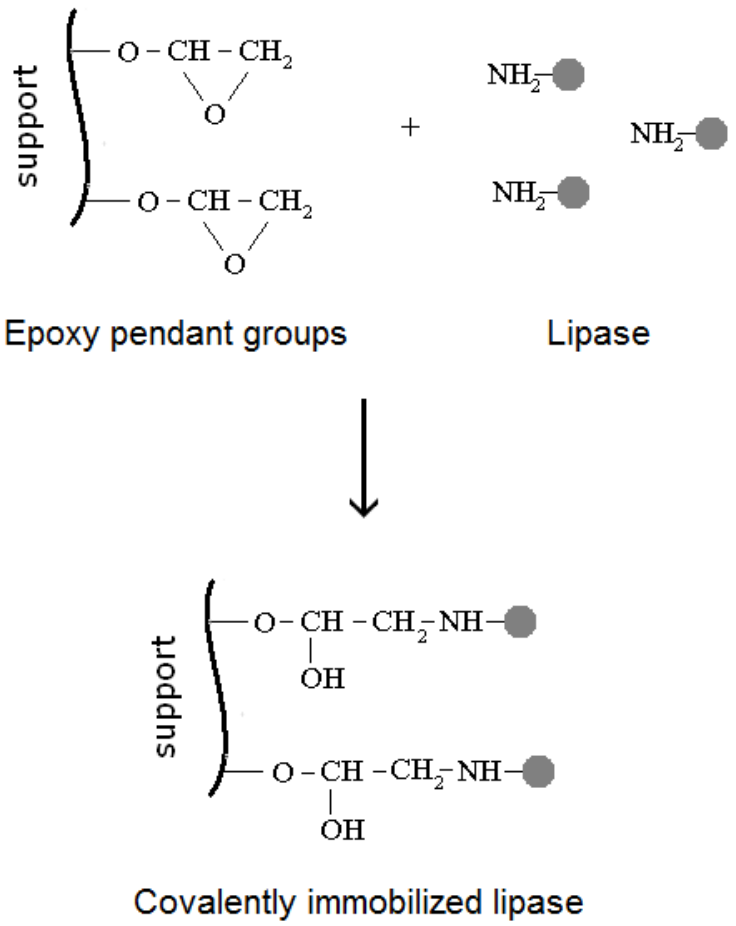

Immobilized polymer beads were treated with 20 mL of 3 M glycine solution (for 12 h at 30°C on an oscillatory shaker) to block the unreacted epoxide groups of the polymer support. Glycine treated immobilized polymer beads were thoroughly washed with 0.05 M sodium phosphate buffer (pH 7) and were subsequently incubated in 20 mL of 5% glutaraldehyde solution (for 3 h at 40°C on an oscillatory shaker) to attain stable enzyme binding onto the support. Glutaraldehyde treated immobilized polymer beads were thoroughly washed with 0.05 M sodium phosphate buffer (pH 7) and analyzed for lipase activity as described in Section 2.2.7(b).

2.2.4. Characterization of immobilized lipase

(a) pH stability

The pH stability of free lipase and immobilized lipase on AGE-(L)-150 polymer beads was studied by incubating the enzyme in buffer solutions of different pH in the range of 4-10 for 30 min at 20°C and then determining the catalytic activity as described in Section 2.2.7(b). The residual activity was calculated as a percentile ratio of the activity of the enzyme after incubation to its initial activity. Residual activities of free and immobilized lipases were plotted against pH.

(b) Temperature stability

The thermal stability of free lipase and immobilized lipase on AGE-(L)-150 polymer beads was evaluated by incubating the enzyme at different temperatures in the range of 20-80°C for 30 min at pH 7 and determining the catalytic activity as described in Section 2.2.7(b). Residual activities of free and immobilized lipases were calculated as mentioned above and plotted against temperature.

(c) Storage stability

The solution of free lipase (prepared in phosphate buffer, pH 7) and immobilized AGE-(L)-150 polymer beads (suspended in phosphate buffer, pH 7) were stored at 4°C. The storage stability was evaluated by determining the lipase activity of free and immobilized lipase at regular time intervals up to 30 days.

(d) Determination of kinetic parameters

The kinetic parameters, K_m and V_{max} of the free and immobilized lipase were determined by measuring initial rates of hydrolysis using *p*-nitro-phenyl palmitate (*p*-NPP) as substrate (1-5 mM) at 30°C. The K_m and V_{max} values for the free and immobilized lipases were calculated from the Lineweaver-Burk plot using Eq. 2.2.

$$v^{-1} = \left(\frac{K_m}{V_{max}}\right) \cdot [S]^{-1} + V_{max}^{-1} \qquad \text{– Eq. 2.2}$$

Where, [*S*] is the concentration of substrate, *v* and V_{max} represents the initial and maximum rate of reaction, respectively. K_m is the Michaelis constant. Eq. 2.2 represents a straight line, slope of which is K_m / V_{max} and Y-intercept is V_{max}^{-1}.

2.2.5. Synthesis and characterization of substrates

(a) Chemical synthesis of rac-amino acid ethyl esters

Rac-amino acid esters were chemically synthesized by esterification of *rac*-amino acids with ethanol in presence of thionyl chloride [29]. Amino acid (1.5 mmol) was suspended in absolute ethanol (20 mL) and cooled to -10°C in an ice-salt bath. Then, 2.5 mmol of thionyl chloride was added dropwise and the reaction mixture kept initially at -10°C for 1 h and then at 40°C for about 24 h. Then the solvent was evaporated to dryness under vacuum using a rotatory evaporator (Buchi Rotapovor® R-124, Switzerland). The solid was then collected and dissolved in the minimum amount of cold water, which was subsequently made alkaline with sodium bicarbonate. The alkaline solution was extracted with ethyl acetate (3×20 mL), dried, and evaporated to dryness (Scheme 2.3). The resultant amino acid ethyl ester was purified by recrystallization using ethyl acetate.

Phenylglycine ethyl ester, 3,4-dihydroxy phenylalanine ethyl ester and 2-naphthylalanine ethyl ester are termed as PG-ester, DOPA-ester and NA-ester respectively.

Scheme 2.3: Chemical synthesis of *rac*-amino acid ethyl ester

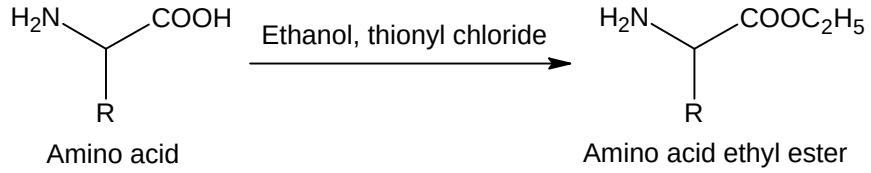

Amino acid — Amino acid ethyl ester

	PG	DOPA	NA
R-	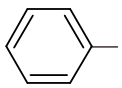	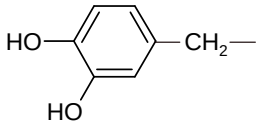	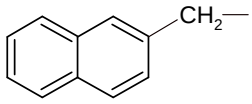

(b) Characterization

(i) Phenylglycine ethyl ester (PG-ester): White solid powder, melting point range 199-201°C; Percent practical yield: 82.2%; Analysis: Calculated for $C_{10}H_{13}NO_2$: C 67.02%, H 7.31%, N 7.82%; Found C 66.88%, H 7.35%, N 7.86%. ^{1}H-NMR (200 MHz, DMSO-d_6): 7.36-7.43 (5H, aromatic *H*), 5.10 (2H, NH_2), 4.82 (1H, Ph-C*H*), 4.02 (2H, COO-CH_2), 1.21 (3H, CH_3).

(ii) 3,4-Dihydroxy phenylalanine ethyl ester (DOPA-ester): white solid powder, melting point range 87-89^{o}C; Percent practical yield: 76.1%; Analysis: Calculated for $C_{11}H_{15}NO_4$: C 58.66%, H 6.71%, N 6.22%; Found C 58.41%, H 6.67%, N 5.56%. ^{1}H-NMR (200 MHz, DMSO-d_6): 6.81-6.96 (3H, aromatic *H*), 5.85 (2H, Ph-O*H*), 5.41 (2H, NH_2), 4.11 (2H, COO-CH_2), 4.01 (1H, Ph-CH$_2$-C*H*), 3.54 (2H, Ph-CH_2), 1.22 (3H, CH_3).

(iii) 2-Naphthylalanine ethyl ester (NA-ester): white solid powder, melting point range 141-143^{o}C; Percent practical yield: 74.6%; Analysis: Calculated for $C_{15}H_{17}NO_2$: C 74.05%, H 7.04%, N 5.74%; Found C 74.1%, H 7.07%, N 5.65%. ^{1}H-NMR (200 MHz, DMSO-d_6): 7.43-8.12 (7H, aromatic *H*), 5.20 (2H, NH_2), 4.16 (2H, COO-CH_2), 4.07 (1H, Naphthyl-CH$_2$-C*H*), 3.65 (2H, Naphthyl-CH_2), 1.20 (3H, CH_3).

2.2.6. Chiral resolution of unnatural amino acid esters using immobilized lipase

The biotransformation reactions were conducted in 25 mL stoppered flasks. Racemic substrate (0.01 g) was suspended or dissolved in 10 mL of 0.05 M phosphate buffer (pH 7). The biotransformation reaction was initiated by adding 0.05 g of immobilized lipase. The flask was incubated on an oscillatory shaker at 30°C at 120 rpm. The samples were periodically withdrawn and analyzed by HPLC.

2.2.7. Analytical methods

(a) Copolymer characterization

(i) Mercury porosimetry

The porosity of polymer beads was determined by mercury intrusion porosimetry with the help of Auto scan 60 mercury porosimeter (Quantachrome, USA) in the range of 0-4000 kg/cm^2.

(ii) Scanning electron microscopy (SEM)

Micrographs were taken on a JEOL-JSM-5200 SEM instrument. Dried polymer beads were mounted on stubs and sputter-coated with gold.

(iii) FT-IR spectroscopy

A Shimadzu 8300-Fourier transform infrared spectrophotometer with a resolution of 1 cm^{-1} in the transmission mode was used to study the infrared

absorption. The polymer beads (2 mg) was milled, mixed with potassium bromide (100 mg), and pressed into a solid disk of 1.2 cm diameter prior to the infra-red measurement.

(b) Enzyme activity assay

(i) Activity assay for CRL

The activities of free and immobilized CRL were analyzed spectrophotometrically measuring the increment in the absorption at 410 nm promoted by the hydrolysis of *p*-nitro-phenyl palmitate (*p*-NPP) [30]. The reaction mixture consisted of 0.1 mL of diluted CRL solution (or 0.05 g of immobilized polymer beads), 1.0 mL of *p*-NPP substrate solution (prepared by dissolving 0.5 g *p*-NPP in 100 mL ethanol) and 1 mL of 0.05 M phosphate buffer (pH 7.0). It was incubated at 37°C under reciprocal agitation at ~ 120 strokes per minute. After 10 min of reaction, agitation was stopped and the reaction was terminated by adding 2.0 mL of 0.5N Na_2CO_3 followed by centrifuging for 10 min (8400×g). The supernatant of 0.50 mL was appropriately diluted with de-ionized water and the absorbance was measured at 410 nm in an UV-visible spectrophotometer (Spectrascan UV-2600, Chemito, India) against an enzyme-blank. The reaction rate was calculated from the slope of the absorbance versus time curve.

One lipase unit (U) of CRL was the amount of enzyme liberating 1.0 μmol *p*-nitro-phenol (*p*-NP) per min under the above assay conditions. The specific activity was defined as the number of lipase units per mg of protein.

(ii) Activity assay for PPL

The hydrolytic activity of free and immobilized PPL was analyzed titrimetrically using olive oil as substrate [31]. The substrate was prepared by mixing 50 ml of olive oil with 50 ml of gum arabic solution (7% w/v). The reaction mixture consisting of 5 mL of substrate emulsion, 2 mL of 0.1 M sodium phosphate buffer (pH 7.0) and 1 mL of diluted PPL solution (or 0.25 mg immobilized polymer beads), was incubated for 15 or 30 min (depending upon the enzyme activity) at 37°C. The reaction was terminated by adding 10 mL of acetone-ethanol solution (1:1). The liberated fatty acid was titrated with 25 mM aqueous NaOH solution using phenolphthalein as an indicator.

One lipase unit (U) of PPL was the amount of enzyme liberating 1.0 μmol of free fatty acids per min under the above assay conditions. The specific activity was defined as the number of lipase units per mg of protein.

(c) Protein estimation

The protein estimation was done by Folin-Lowry method [32] with bovine serum albumin as a standard.

(d) HPLC analysis

All reaction profiles were monitored by HPLC (Thermo Separation Products, Fremont, CA, USA). The quantitative analysis of different amino acids and their esters was carried out using a reverse phase C-18 column (125×4 mm, prepacked column supplemented with a 4×4 mm guard column procured from LiChrospher®, Merck, Darmstadt, Germany) eluted isocratically using acetonitrile-water mobile phase (30:70 v/v, pH adjusted to 3.0 with 50% v/v *o*-phosphoric acid), at a flow rate of 0.6-1.0 mL/min. Peaks were detected using an UV detector at 215 nm. The peak identification was made by comparing the retention times with those of authentic compounds. Peak area was used as a measure to calculate the respective concentration. The reaction conversion was estimated from the ratio of the substrate consumption to its initial concentration. The enantiomeric excess (e.e.) of the product was determined by using a CHIROBIOTIC-T® column (250×4.6 mm prepacked column supplemented with 20×4 mm guard column procured from Astec Inc. USA) eluted isocratically using water-methanol mobile phase (40:60 v/v, pH adjusted to 2.3-2.5 with 50% v/v glacial acetic acid), at a flow rate of 0.6-0.8 mL/min.

(e) Determination of enantiomeric ratio

Enantiomeric ratio (*E*) is the prime parameter for describing the enzyme's enantioselectivity. Enantiomeric ratio was determined by using Eq. 2.3 as described earlier [33].

$$E = \frac{\ln[1 - C(1 + ee_P)]}{\ln[1 - C(1 - ee_P)]} \qquad \text{– Eq. 2.3}$$

Where, *C* is conversion ratio and ee_P is enantiomeric excess of product. *C* and ee_P were calculated by using Eq. 2.4 and Eq. 2.5 respectively.

$$C = 1 - \left(\frac{c^{S}_{S(t)} + c^{R}_{S(t)}}{c^{S}_{S(0)} + c^{R}_{S(0)}} \right) \qquad \text{– Eq. 2.4}$$

Where, $c^{S}_{S(t)}$ and $c^{R}_{S(t)}$ are concentration of *S*-enantiomer and concentration of *R*-enantiomer of substrate respectively at time, t. $c^{S}_{S(0)}$ and $c^{R}_{S(0)}$ are concentration of *S*-enantiomer and concentration of *R*-enantiomer of substrate respectively at t = 0.

$$ee_P = \frac{\left| c^{S}_{P} - c^{R}_{P} \right|}{c^{S}_{P} + c^{R}_{P}} \qquad \text{– Eq. 2.5}$$

Where, c^{S}_{P} is concentration of *S*-enantiomer of product and c^{R}_{P} is concentration of *R*-enantiomer of product.

2.3. RESULTS AND DISCUSSION

More than 50 different acrylic polymer beads of varying composition of monomer, cross-linker and porogen were synthesized. The meso- or macro-porosity of the polymer is prerequisite to achieve better enzyme immobilization. The porosity of polymer greatly depends on its CLD. A low CLD gives hard and non-porous polymer beads (which are not suitable for the enzyme immobilization). On the other hand, high CLD gives highly porous but fragile polymer beads which disintegrate easily even by very low shear forces. Therefore, our preliminary experiments were carried out to establish the optimum range of CLD where an appropriate balance between porosity and mechanical stability of resulting polymer beads is achieved. We observed that, below 50% CLD, the polymer beads were largely microporous while above 200% CLD the polymer beads were macroporous but fragile. The CLD in the range of 50-200% gave optimum results with respect to porosity and mechanical stability and therefore these polymers were selected for the immobilization experiments. Prior to the lipase immobilization experiments, the polymers were thoroughly characterized for their physical properties *viz.* total surface area, pore size and pore size distribution.

2.3.1. Characterization of beaded polymers

(a) Surface area and pore size distribution

The surface area is a key parameter that governs the extent of enzyme binding

on porous particles. Mercury porosimetry provides a good estimate of surface area and pore size distribution. The surface areas for different GMA and AGE polymer beads are given in Table 2.2. In each polymer series, surface area was found to increase with cross-link density. For given cross-link density, the total surface area of GMA-(C) polymers < AGE-(C) polymers < AGE-(H) polymers < AGE-(L) polymers. Thus, AGE-(L) polymers were observed to have maximum surface area.

Table 2.2: Effect of cross-link density on surface area for GMA and AGE polymers

No.	**Cross-link density** (%)	**Surface area** (m^2/g)			
		GMA-(C)-polymers	**AGE-(C)-polymers**	**AGE-(H)-polymers**	**AGE-(L)-polymers**
1	50	85.06	92.03	101.42	110.32
2	75	105.78	122.45	129.49	135.75
3	100	111.69	127.72	139.21	151.93
4	150	141.25	128.98	148.11	168.81
5	200	148.58	139.88	185.23	198.37

The pore size distributions of GMA and AGE polymer series are given in Fig. 2.1. The pore size distribution data revealed that the percent fraction of macro-pores was maximum in AGE-(L) polymers, moderate in AGE-(H) polymers, AGE-(C) polymers and minimum in GMA-(C) polymers.

The polarity of a porogen is one of the crucial factors which decide the porosity of synthetic polymers. In general, during polymerization of acrylic monomers, a non-polar porogen maintains the phase separation for a longer time period and gives macro-porous polymer beads. A polar porogen, on the other hand, causes early precipitation of monomer resulting in less pronounced phase separation that gives micro-porous polymer beads [34, 35].

In the present study, three porogens (*viz.* cyclohexanol, hexanol and lauryl alcohol) were used. The non-polarity (i.e. hydrophobicity) of these porogens is in order of: lauryl alcohol (Log P = 4.31) > hexanol (Log P = 1.8) > cyclohexanol (Log P = 1.27). Owing to its highly non-polar nature, lauryl alcohol introduced highest macro-porosity in the resultant AGE-(L) polymers.

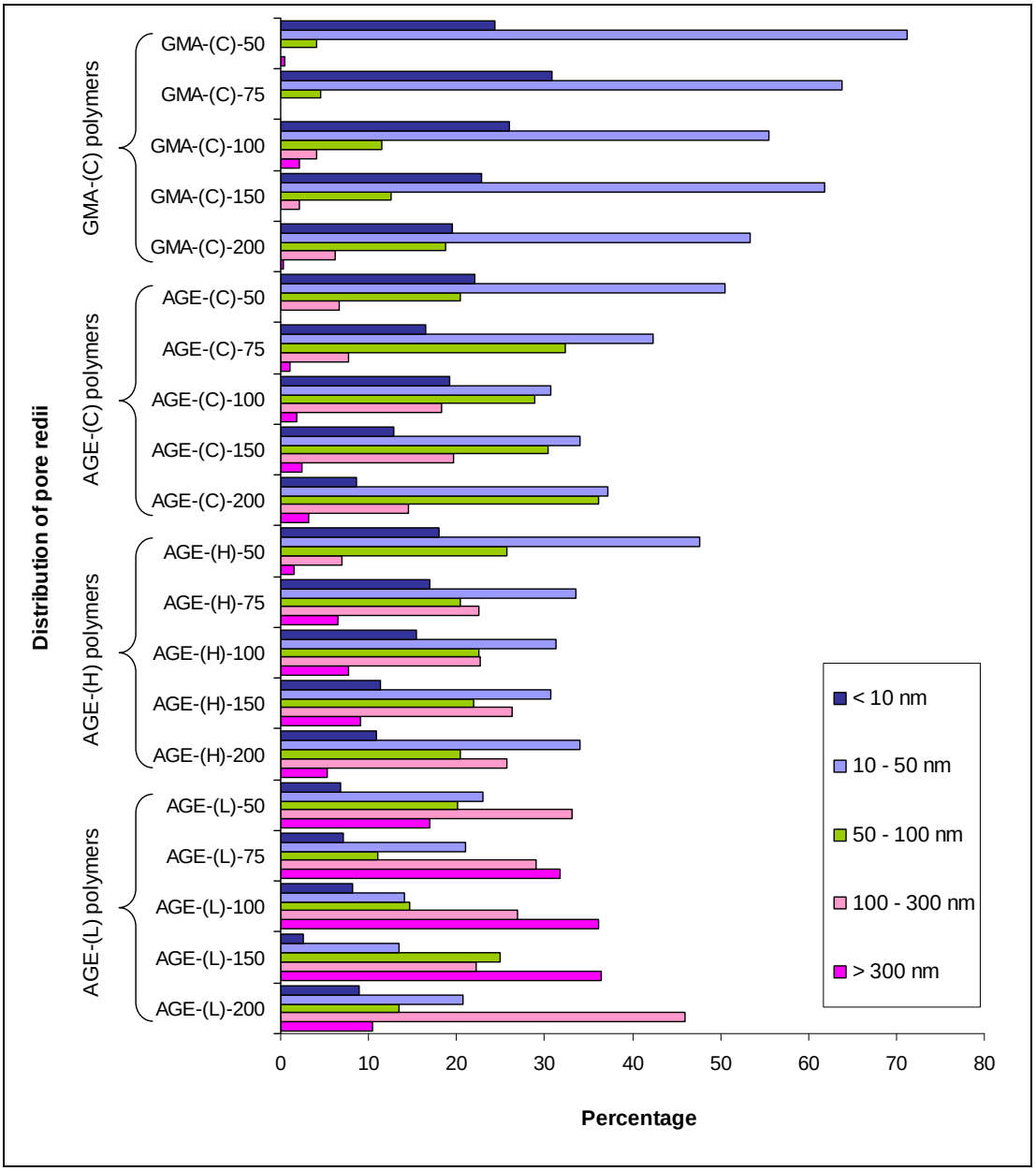

Fig. 2.1: Pore size distribution of GMA-(C), AGE-(C), AGE-(H) and AGE-(L) polymers. [The light and dark blue bars (□, ■) indicate micro-pores, green bar (■) indicates meso-pores, and light and dark pink bars (□, ■) indicate macro-pores; the percent of macro-pores gradually increases from GMA-(C), AGE-(C), AGE-(H) to AGE-(L) polymers.]

(b) Porous surface morphology

The SEM micrographs of GMA-(C)-100 and AGE-(L)-100 are given in Fig. 2.2 which confirm the porous surface morphology and the spherical nature of GMA and AGE polymer beads.

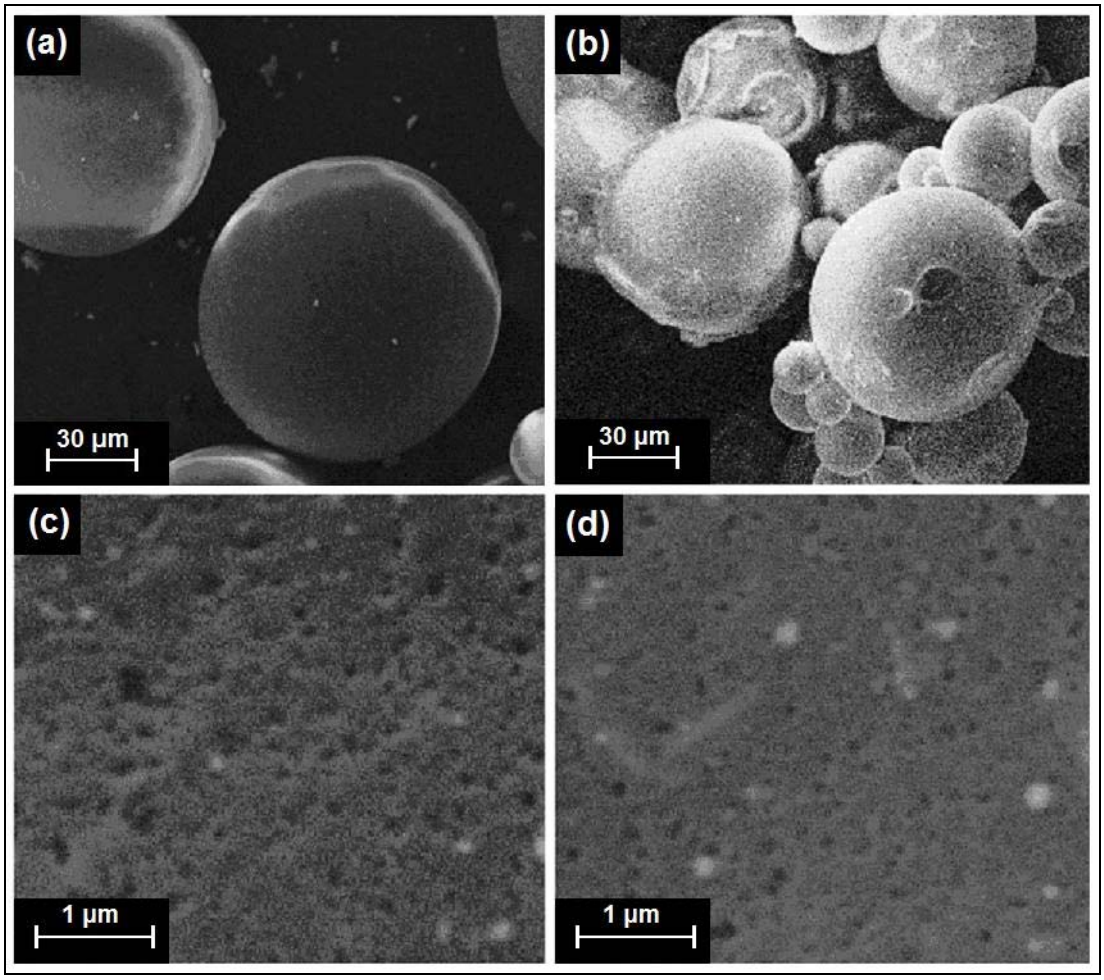

Fig. 2.2: Scanning electron micrographs showing (a) spherical nature and (c) porous surface morphology of GMA-(C)-100 polymer beads; (b) spherical nature and (d) porous surface morphology of AGE-(L)-100 polymer beads. [(a) and (b) are at 500× magnification while (c) and (d) are at 30000× magnification.]

(c) FT-IR spectrum

The IR spectra of GMA and AGE polymers were used to ensure the presence of epoxy groups. The IR spectrum of GMA polymer beads (Fig. 2.3) gave characteristic peaks at 1722 and 1196 cm^{-1} due to C=O of ester group and C–O–C of epoxy group, respectively. The intensity of the band at 1636 cm^{-1} (characteristic band of C=C stretching) was significantly weakened. This ensured the presence of the epoxy groups and consumption of vinyl double bonds. Similarly, the IR spectrum of AGE polymer beads (Fig. 2.4) gave the characteristic peaks at 1731 and 1150 cm^{-1} due to stretching vibrations of C=O of ester and C–O–C of epoxy groups, respectively. The intensity of the band at 1636 cm^{-1} (characteristic band of C=C

stretching) was significantly weakened. This indicated that the epoxy groups are intact and complete consumption of vinyl double bond has occurred.

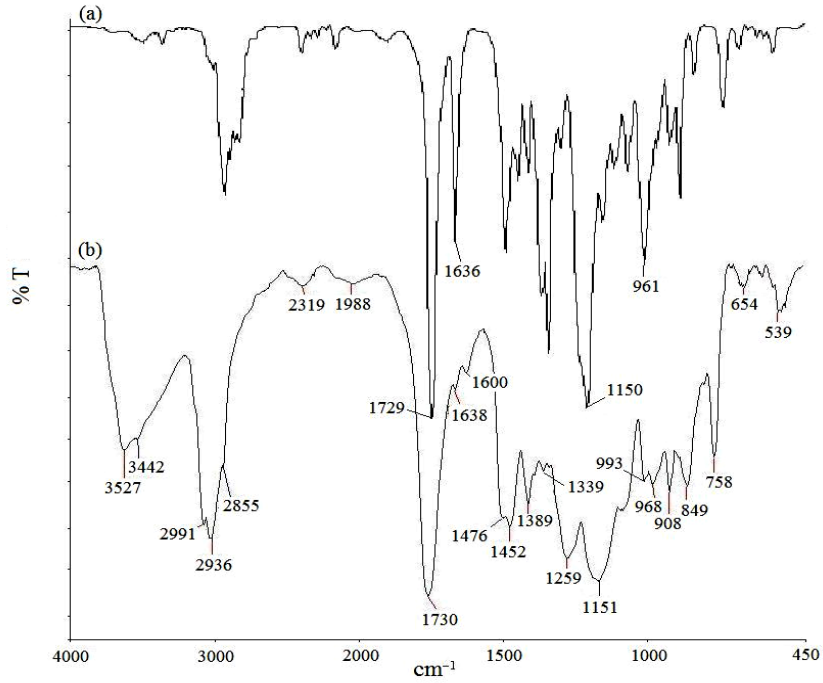

Fig. 2.3: FT-IR spectra of (a) GMA and EGDM mixture before polymerization and (b) after polymerization

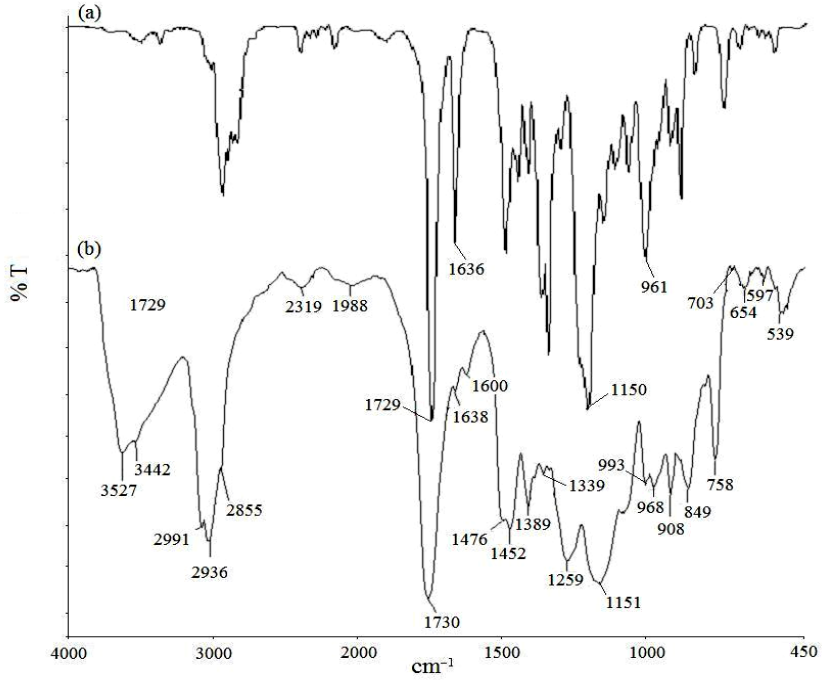

Fig. 2.4: FT-IR spectra of (a) AGE and EGDM mixture before polymerization and (b) after polymerization

2.3.2. Screening of lipases for chiral resolution of unnatural amino acid esters

The enantioselectivity of different lipases are listed in Table 2.3. Among the five lipases screened, CRL gave higher enantioselectivity towards hydrolysis of PG-ester, DOPA-ester and HPA-ester while PPL gave higher enantioselectivity towards hydrolysis of NA-ester. Hence CRL and PPL enzymes were selected for further immobilization experiments.

Table 2.3: Screening of lipase for chiral resolution of unnatural amino acid esters

No.	Lipase [a]	Source	Enantioselectivity, *E*			
			PG	**DOPA**	**HPA**	**NA**
1	AL	Europa Chemicals, UK	8.6	7.6	7.5	11.2
2	CRL	Europa Chemicals, UK	**10.7**	**10.5**	**13.5**	3.3
3	PCL	Europa Chemicals, UK	8.6	6.9	8.3	5.6
4	PPL	Sigma Chemicals, USA	6.4	4.1	3.2	**14.6**
5	TLL	Sigma Chemicals, USA	2.2	3.4	1.3	4.8

[[a] AL: *Alcaligens* lipase; CRL: *Candida rugosa* lipase; PCL: *Pseudomonas cepacia* lipase; PPL: porcine pancreatic lipase; TLL: *Thermomyces languginous* lipase.]

2.3.3. Selection of polymer for lipase immobilization

The efficiency of polymer support to bind and express the lipase activity was calculated in terms of 'activity recovery', which is defined as: the percentile ratio of lipase activity expressed by 1 g of immobilized polymer support to the total lipase activity of free enzyme used for immobilization (Eq. 2.6).

$$\text{Activity recovery } (\%) = \left(\frac{A_{Immo}}{{}^{Total}A_{Free}} \right) \times 100 \qquad \text{– Eq. 2.6}$$

Where, $A_{Immo.}$ is activity of 1 g of immobilized polymer (U/g of support) and ${}^{Total}A_{Free}$ is total activity of free enzyme loaded on 1 g of polymer. ${}^{Total}A_{Free}$ is a product of activity (U/mL) and volume (mL) of free enzyme loaded on 1g of polymer.

AGE polymer beads were found to give better binding and expression of CRL and PPL than GMA polymer beads (Table 2.4 and 2.5). Among different AGE polymers, an increasing trend of activity recovery was observed in order of AGE-(C), AGE-(H) and AGE-(L). AGE-(L) polymers gave maximum activity recovery.

Table 2.4: Selection of polymer support for CRL immobilization

Polymer	**CRL activity** (U/ g of support)	**Protein** (mg/ g of support)	**Specific Activity** ($U\times10^{-2}$/g of support)	**Activity recovery** (%)
Free CRL [a]	0.48 [b]	2.26 [c]	21.37	100.00
GMA-(C) polymers:				
GMA-(C)-50	7.23	46.52	15.55	37.43
GMA-(C)-75	7.73	47.25	16.36	40.01
GMA-(C)-100	8.25	47.37	17.42	42.70
GMA-(C)-150	8.28	47.43	17.46	42.86
GMA-(C)-200	8.40	47.45	17.70	43.48
AGE-(C) polymers:				
AGE-(C)-50	11.14	69.75	15.97	57.66
AGE-(C)-75	11.27	70.47	15.99	58.33
AGE-(C)-100	11.38	70.60	16.12	58.90
AGE-(C)-150	11.53	70.65	16.32	59.68
AGE-(C)-200	11.42	70.67	16.16	59.11
AGE-(H) polymers:				
AGE-(H)-50	12.55	75.19	16.69	64.96
AGE-(H)-75	13.82	73.80	18.73	71.53
AGE-(H)-100	14.03	74.37	18.87	72.62
AGE-(H)-150	14.22	75.56	18.82	73.60
AGE-(H)-200	14.20	75.38	18.84	73.50
AGE-(L) polymers:				
AGE-(L)-50	17.13	87.58	19.56	88.66
AGE-(L)-75	18.08	88.53	20.42	93.58
AGE-(L)-100	18.67	88.53	21.09	96.64
AGE-(L)-150	18.35	86.64	21.18	94.98
AGE-(L)-200	18.21	85.69	21.25	94.25

[[a] Free enzyme solution containing 5mg/mL of commercial CRL enzyme powder (Europa Chemicals, UK); [b] U/mL; [c] mg/mL.]

Table 2.5: Selection of polymer support for PPL immobilization

Polymer	**PPL activity** (U/ g of support)	**Protein** (mg/ g of support)	**Specific Activity** ($U\times10^{-2}$/g of support)	**Activity recovery** (%)
Free PPL [a]	2.14 [b]	0.58 [c]	3.69	100.00
GMA-(C) polymers:				
GMA-(C)-50	27.42	10.20	2.69	32.03
GMA-(C)-75	29.16	10.34	2.82	34.07
GMA-(C)-100	31.90	11.28	2.83	37.27
GMA-(C)-150	26.64	11.02	2.42	31.12
GMA-(C)-200	29.38	11.36	2.59	34.32
AGE-(C) polymers:				
AGE-(C)-50	39.86	16.14	2.47	46.57
AGE-(C)-75	41.60	16.38	2.54	48.60
AGE-(C)-100	40.34	16.72	2.41	47.13
AGE-(C)-150	40.08	16.66	2.41	46.82
AGE-(C)-200	40.18	16.41	2.45	46.94
AGE-(H) polymers:				
AGE-(H)-50	44.70	17.08	2.62	52.22
AGE-(H)-75	43.96	17.12	2.57	51.36
AGE-(H)-100	47.22	17.76	2.66	55.16
AGE-(H)-150	45.48	17.41	2.61	53.13
AGE-(H)-200	45.74	17.44	2.62	53.43
AGE-(L) polymers:				
AGE-(L)-50	49.26	18.62	2.65	57.55
AGE-(L)-75	50.52	18.76	2.69	59.02
AGE-(L)-100	52.78	18.80	2.81	61.66
AGE-(L)-150	52.04	18.74	2.78	60.79
AGE-(L)-200	47.30	18.58	2.55	55.26

[[a] Free enzyme solution containing 2mg/mL of commercial PPL powder (Sigma Chemicals, USA); [b] U/mL; [c] mg/mL.]

The extent of activity recovery can be co-related with the specific surface area and porous nature of the polymer beads. The specific surface area of AGE polymer beads is relatively higher than that of GMA polymer beads. The high specific surface increased the number of surface epoxy groups thereby increasing the binding capacity of the polymer.

Moreover, the mercury porosimetry results showed that the percentage of mesopores (50-100 nm) and macropores (> 100 nm) gradually increases from GMA-(C), AGE-(C), AGE-(H) to AGE-(L) polymer beads. The presence of meso- and/or macroporous morphology in the polymer beads is highly desirable for using them as a support for immobilization of biological macromolecules like enzymes. Macroporous polymer structures primarily facilitate the easy diffusion of globular enzyme molecules inside the pores thereby enhancing the interaction of the latter with the reactive epoxy groups of the polymer. In addition to this, during the assay procedures, macroporous structures effectively reduce the diffusional limitations of substrate as well as product thereby facilitate the catalytic expression of the immobilized enzyme. The reduction in diffusional limitations also assists the rapid biocatalytic reactions by inhibiting substrate or product accumulation within the pores.

Immobilized AGE-(L)-100 gave maximum activity and activity recovery for CRL as well as for PPL. The activity of CRL immobilized on AGE-(L)-100 was 18.67 U/g of support which corresponds to 96.64% activity recovery (Table 2.4). The activity of PPL immobilized on AGE-(L)-100 was 52.78 U/g of support which corresponds to 61.66% activity recovery. Hence, AGE-(L)-100 was selected for further experiments.

The covalent immobilization of lipase on different epoxy activated acrylic supports have been reported by several authors. For example, Bayramoğlu and Arica studied the immobilization of CRL on poly(glycidyl methacrylate–methylmethacrylate) magnetic beads and the maximum activity of immobilized lipase was 935 U/mg of bound protein with 81% activity recovery (determined in terms of olive oil hydrolysis) [36]. Poly(glycidyl methacrylate – hydroxylethyl methacrylate – ethyleneglycol dimethacrylate) were studied for immobilization of CRL and the immobilized support gave activity of 7570 U/g of support with 45% activity recovery (determined in terms of olive oil hydrolysis) [16]. Immobilization of CRL on

poly(methylacrylate – divinyl benzene) gave activity of 997 U/g of support (determined in terms of olive oil hydrolysis) [37]. Xi and Xu studied CRL immobilization on polymer of glycidyl methacrylate – ethylene dimethacrylate – TiO_2 where 0.112 U/g activity (calculated by ketoprofen ester hydrolysis) and 5.8% activity recovery was reported [38]. Immobilization of CRL on poly(methyl methacrylate) polymers gave esterification activity in the range of 0.8-1.0 U/g of support (determined by esterification of oleic acid with butanol) [39]. Kartal *et al.* evaluated the polyvinyl alcohol grafted glycidyl methacrylate polymers for PPL immobilization where 1 g of support expressed 80 U lipase activity (determined by trybutyrin hydrolysis) with 58% activity recovery [40].

Immobilization of lipase on these acrylic supports were performed under different conditions. Moreover, the lipase activity assays were performed using different substrates. Therefore, it is difficult to compare the immobilization results on the basis of activity and activity recovery. However, comparing the protein binding capacities of supports could be a more rational approach. The protein binding capacity of different acrylic polymers was roughly in the range of 10 - 85 mg/g of support [36-40]. The high protein binding capacity of AGE-(L) polymers (~ 88 mg/g for CRL binding) appears to be comparable if not better than that reported earlier.

Immobilization of an enzyme usually results in some loss in its catalytic activity. This could be ascribed to the minor modifications in the three-dimensional structure of enzyme that may lead to the distortion of amino acid(s) residues at the catalytic site. Further the random immobilization often involves embedding of active site of some enzyme molecules thereby preventing expression their catalytic activity. Another possible reason of decreased enzyme activity can be ascribed to the mass transfer limitations of substrate or/and product [41].

2.3.4. Optimization of the lipase immobilization

(a) Cross-linking with glutaraldehyde

The catalytic activity of immobilized lipase (CRL and PPL) was found to decline gradually with time, either due to enzyme leaching or denaturation upon storage or a combination of both. To overcome enzyme leaching and to obtain stable binding of lipase, 5% glutaraldehyde was used to cross-link amino groups of bound enzyme. Our studies indicated that glutaraldehyde treatment for 3 h was optimum.

Glutaraldehyde treatment beyond 3 h resulted in decrease of lipase activity (results not shown). This could be due to excessive cross-linking and consequent conformational changes in the three dimensional structure of enzyme [42].

(b) Optimization of immobilization time

The time required for CRL immobilization on AGE-(L)-100 was optimized. It can be observed from Fig. 2.5 that the CRL activity (U/g of support) and CRL activity recovery (%) of immobilized AGE-(L)-100 attained equilibrium in 12 h. After 12 h CRL activity and CRL activity recovery of immobilized AGE-(L)-100 were found to remain almost constant. Similarly, time required for PPL immobilization on AGE-(L)-100 was optimized. At 18 h, PPL activity (U/g of support) and PPL activity recovery (%) were reached to maximum (Fig. 2.5).

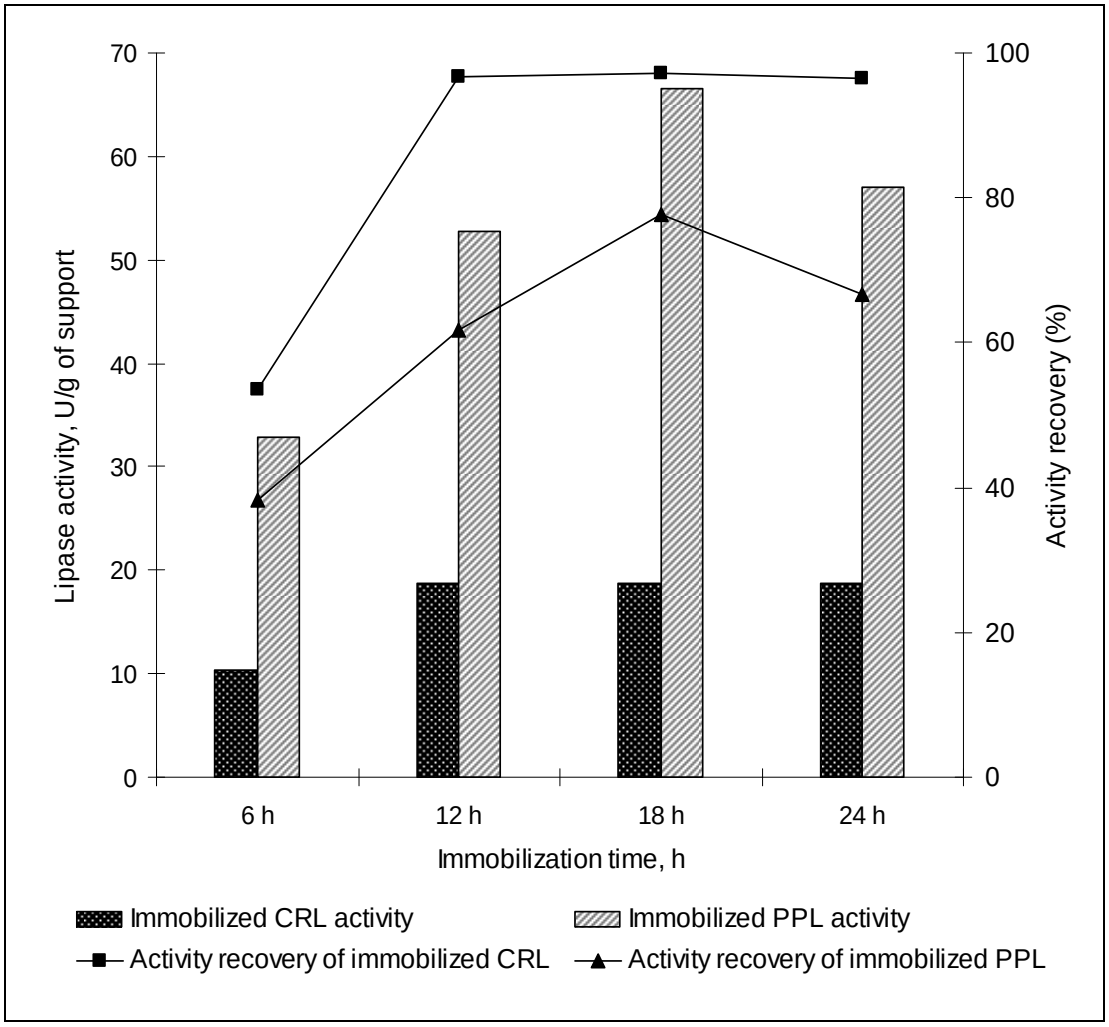

Fig. 2.5: Optimization of time for CRL and PPL immobilization on AGE-(L)-100 polymer beads

(c) Optimization of enzyme loading

AGE-(L)-100 polymer beads were loaded with different concentrations of CRL and the resultant immobilized CRL was analyzed for expression of lipase activity and protein binding. The results are shown in Table 2.6. The CRL activity recovery of immobilized AGE-(L)-100 increased with increase in enzyme loading from 50 to 200 mg/g of polymer support. However, the CRL activity recovery was found to decrease beyond 200 mg. Enzyme loading beyond 200 mg probably might have resulted in embedding of active sites of lipase molecules during the immobilization process by increased stacking and also by increased diffusion limitations.

Likewise, different concentrations of PPL were immobilized on AGE-(L)-100 polymer beads. The activity recovery increased with increase in enzyme loading from 60 to 80 mg/g of polymer support and decreases gradually thereafter (Table 2.7).

Table 2.6: Optimization of CRL loading on AGE-(L)-100 polymer

CRL (mg)	**Activity of free CRL** (U/mL)	**Protein of free CRL** (mg/mL)	**Activity of immobilized CRL** (U/g of support)	**Protein bound** (mg/g of support)	**Activity recovery** (%)
50	0.12	0.565	4.56	22.34	95.60
100	0.25	1.130	9.12	44.76	96.51
150	0.36	1.695	13.62	65.13	93.61
200	0.49	2.260	18.67	88.53	96.64
250	0.59	2.825	19.56	96.14	81.81

Table 2.7: Optimization of PPL loading on AGE-(L)-100 polymer

PPL (mg)	**Activity of free PPL** (U/mL)	**Protein of free PPL** (mg/mL)	**Activity of immobilized PPL** (U/g of support)	**Protein bound** (mg/g of support)	**Activity recovery** (%)
60	1.08	0.43	32.12	15.76	74.35
80	2.12	0.58	56.58	20.01	65.49
100	3.20	0.72	62.37	22.45	48.13
120	4.31	0.87	63.58	22.13	36.79

2.3.5. Stability of immobilized lipase

(a) pH stability

(i) CRL immobilized AGE-(L)-100

The effect of pH on the catalytic activity of free and immobilized CRL was studied over a pH range of 4-12 (Fig. 2.6). Immobilization of lipase on AGE-(L)-100 polymer beads resulted in excellent stabilization of enzyme over a broad pH range. Whereas, the free CRL retained 17.78% and 40.46% residual activity at pH 4 and pH 5 respectively, under identical pH conditions immobilized CRL retained 77.22% and 86.63% residual activity respectively. The free CRL retained 48.56% and 14.80% residual activity at pH 9 and pH 10 while at identical pH conditions immobilized CRL retained 88.64% and 85.09% residual activity respectively. These results indicate that this procedure of immobilization has improved the stability of CRL in the acidic as well as in the alkaline region.

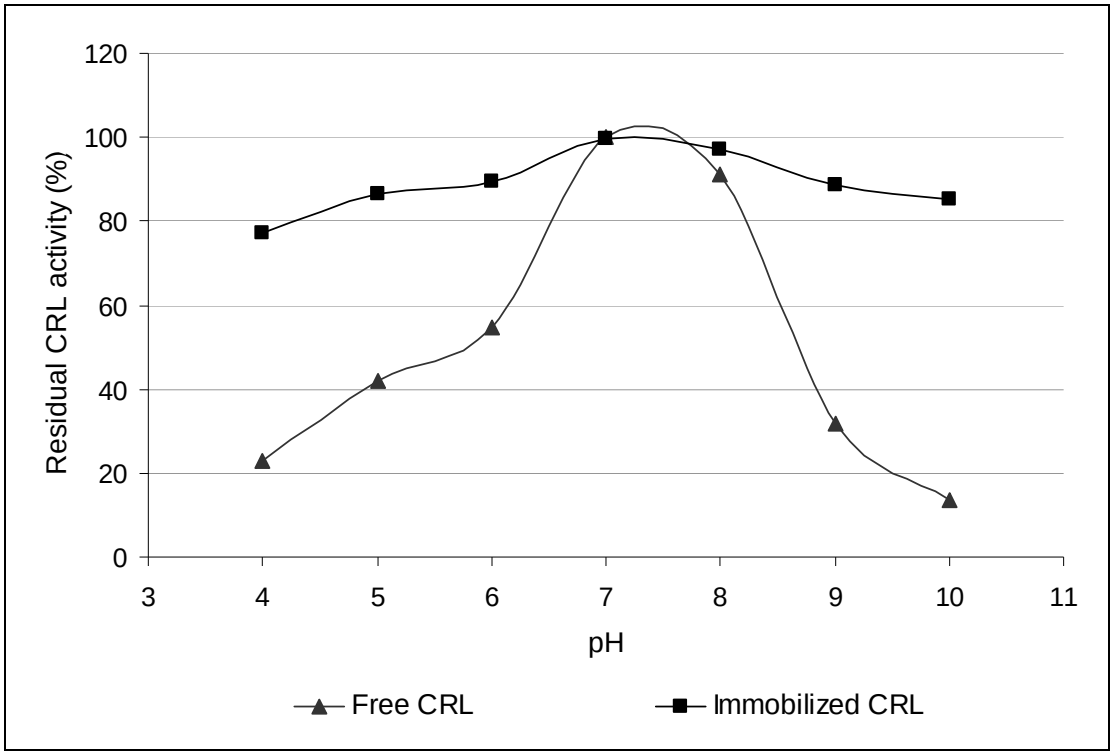

Fig. 2.6: pH stability of immobilized CRL

(ii) PPL immobilized AGE-(L)-100

The effect of pH on the catalytic activity of free and immobilized PPL in pH range of 4-12 is represented in Fig. 2.7. Immobilization of PPL on AGE-(L)-100

polymer beads resulted in moderate stabilization of enzyme over a broader pH range. At pH 4 and 5, the free PPL retained 28.53% and 36.81% residual activity respectively, while at identical pH conditions, immobilized enzyme retained 36.71% and 64.85% residual activity respectively. At pH 9 and pH 10 the free PPL retained 61.60% and 33.60% residual activity, while at identical pH conditions, immobilized enzyme retained 90.24% and 57.71% residual activity respectively. Thus, this procedure of immobilization has improved the stability of PPL in the acidic as well as in the alkaline region.

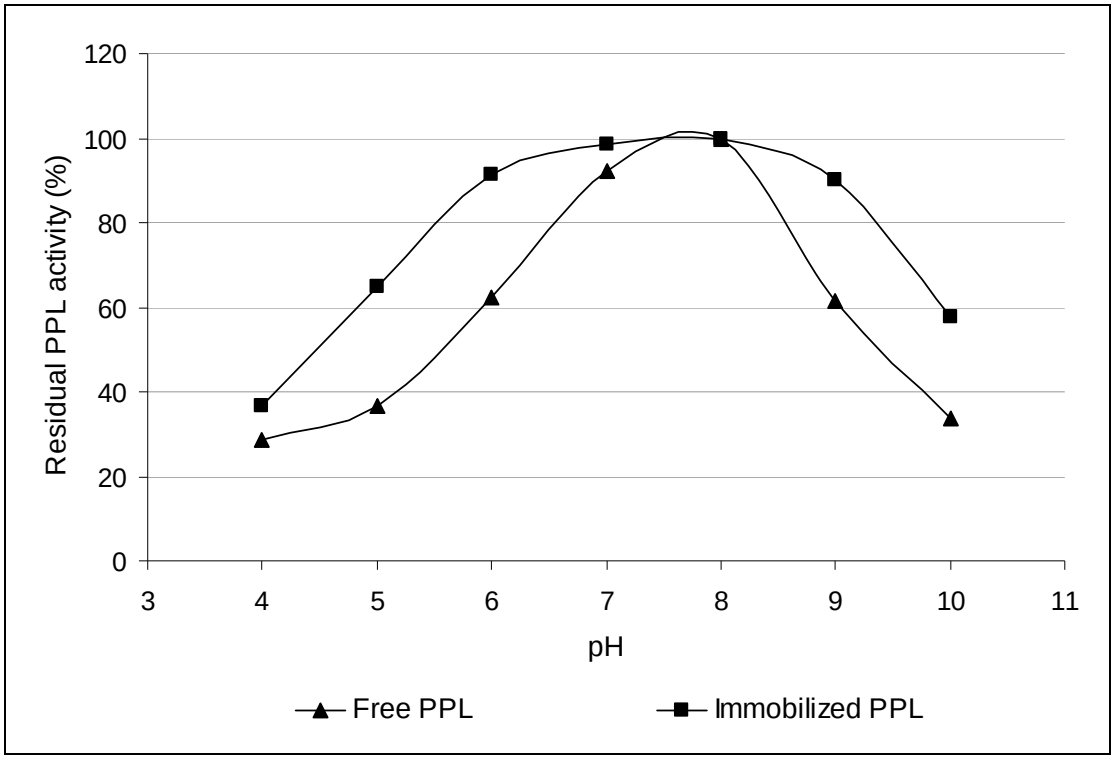

Fig. 2.7: pH stability of immobilized PPL

(b) Temperature stability

(i) CRL immobilized AGE-(L)-100

The stability of free and immobilized CRL was determined by measuring residual enzyme activity as a function of temperature in the range of 20-70°C. The activity profiles of free and immobilized CRL at different temperatures are graphically represented in Fig. 2.8. The immobilization of CRL on AGE-(L)-100 polymer beads has significantly improved the thermal stability of the enzyme. For instance, at 50°C the free enzyme retained only 21.18% residual activity while immobilized enzyme found to retain 100% activity. Similarly at 70°C the free enzyme

retained only 5.41% residual activity while immobilized enzyme was found to retain 58.22% of its initial activity.

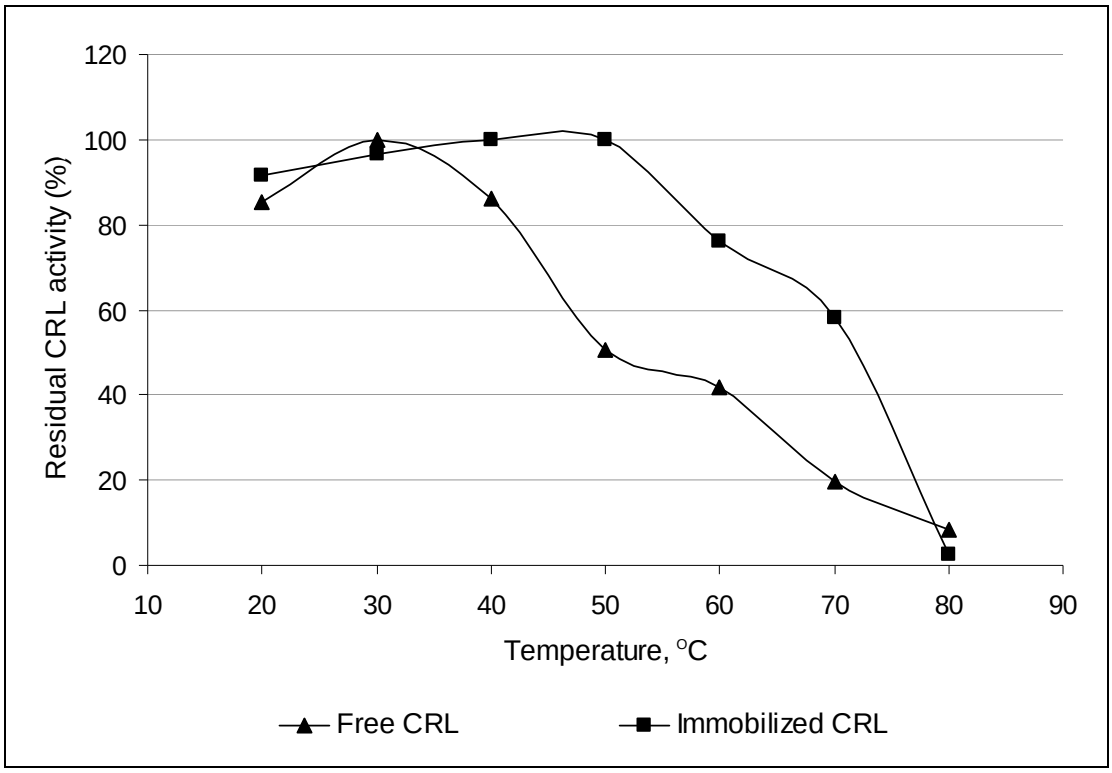

Fig. 2.8: Temperature stability of immobilized CRL

(ii) PPL immobilized AGE-(L)-100

The temperature stability of free and immobilized PPL was studied in the range of 20-70°C (Fig. 2.9). The immobilization of PPL on AGE-(L)-100 polymer beads has improved the thermal stability of the enzyme. For instance, at 50°C the free enzyme retained only 63.17% residual activity while immobilized enzyme retained 95.66% of its initial activity. Likewise, at 70°C the free enzyme retained only 14.42% residual activity while immobilized enzyme was found to retain 37.28% of its initial activity.

Upon increase in temperature, enzyme molecule unfolds which disturbs its active site conformation. Depending upon the severity of the conformational changes, partial or complete loss of catalytic activity (i.e. thermal inactivation) is observed. At elevated temperature, free enzymes unfold easily and readily undergo thermal inactivation. Under the identical condition, immobilized enzymes, because of the additional stabilizing linkages (e.g. enzyme-support covalent linkages in the present

case), maintain their conformation and therefore exhibit improved thermal stability.

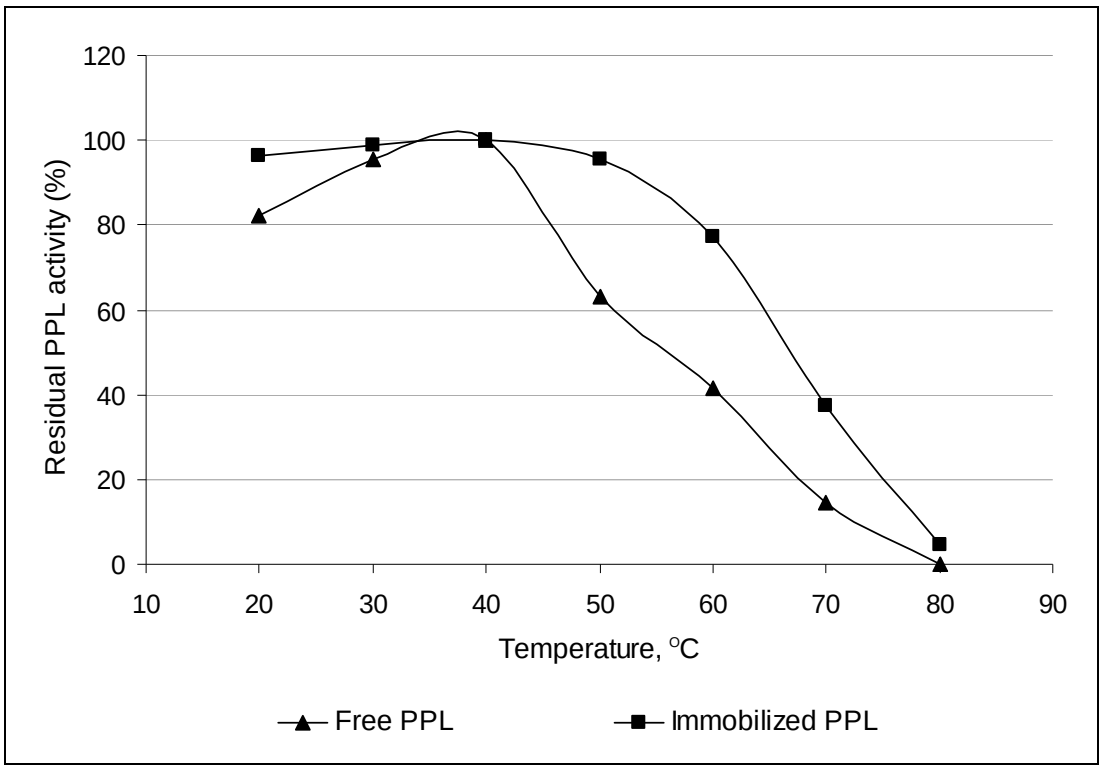

Fig. 2.9: Temperature stability of immobilized PPL

(c) Storage stability

The storage stability of immobilized CRL was determined and compared with that of free CRL. The plot of log residual activity vs. storage time is shown in Fig. 2.10. The linear trend lines were drawn for the activity profiles of free and immobilized CRL. The storage half-life of each lipase preparation was determined from its respective trend line equation. The storage half-life of free CRL was found to be ~ 6 days while that of immobilized CRL was found to be ~ 67 days. Thus, upon immobilization there was significant improvement in the storage stability of the enzyme. Similarly, the storage activity profiles of free and immobilized PPL were studied to calculate their storage half-lives (Fig. 2.10). The storage half-life of immobilized PPL (~ 38 days) was observed to be much higher than that of free PPL (~ 4 days).

Amongst the previous reports on immobilization of CRL and PPL on acrylic supports, few have evaluated the storage stability of immobilized enzyme. The results reported in the literature indicate a significant increase in enzymes's storage stability

upon immobilization. For example, Bayramoğlu and Arica reported 80% increase in the storage stability of immobilized CRL over that of the free enzyme [36]. Immobilization of CRL on poly(glycidyl methacrylate – hydroxylethyl methacrylate – ethyleneglycol dimethacrylate) retained 67% of its initial activity after 12 week storage [16]. Immobilization of PPL on polyvinyl alcohol grafted glycidyl methacrylate polymers retained 50% of initial activity after 22 days storage [40].

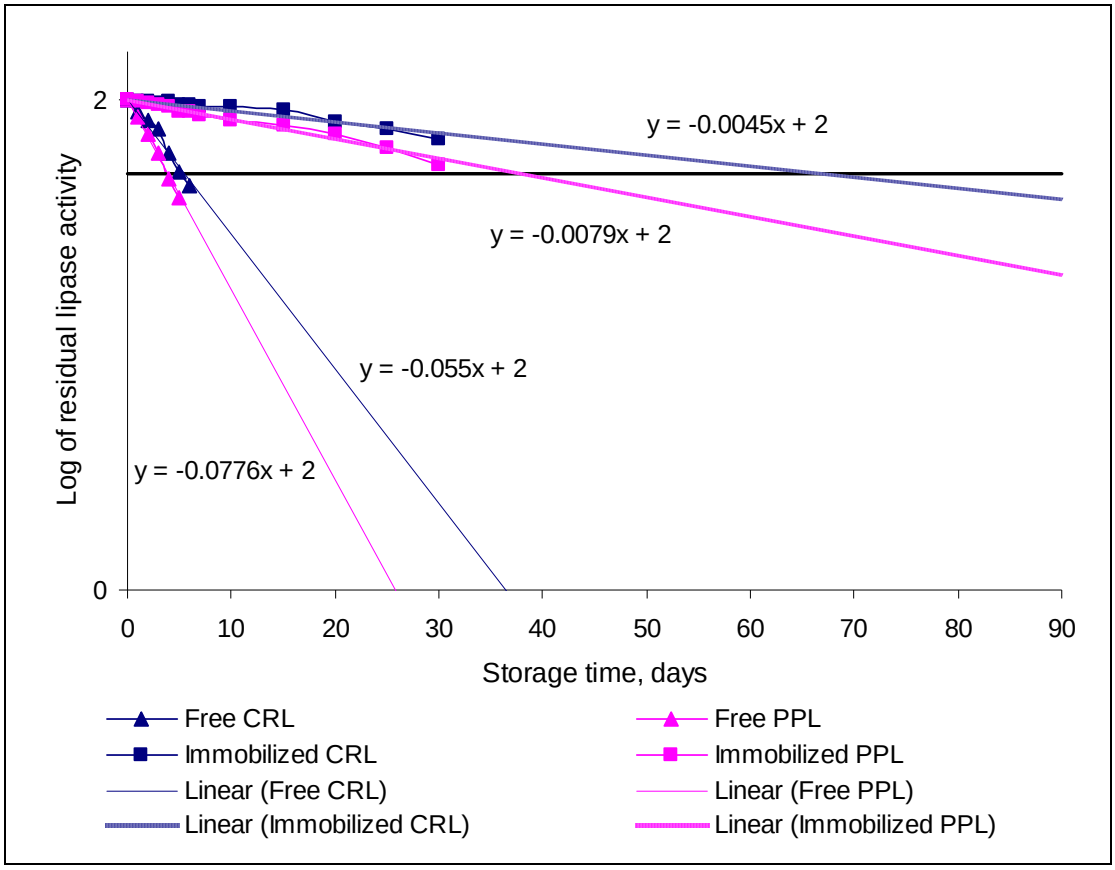

Fig. 2.10: Storage stability of soluble and immobilized lipases [The trend line equations were used to calculate the respective storage half-lives. The horizontal line (—) at log(50) was drawn only for a graphical illustration of the storage half-lives.]

2.3.6. Kinetic behaviour of immobilized CRL

The effect of substrate concentration on the initial rate catalyzed by free and immobilized CRL was studied using *p*-NPP as substrate. Michaelis constant (K_m) and the maximum reaction velocity (V_{max}) of the free and immobilized enzymes were calculated from Lineweaver-Burk plot (Fig. 2.11). The kinetic parameters of free and immobilized CRL are presented in Table 2.8. K_m values for free and immobilized

CRL were 0.60 mM and 1.31 mM respectively. V_{max} values for free and immobilized CRL were 32.79 U/mg and 14.1 U/mg respectively. Thus, immobilized enzyme was observed to have higher K_m and lower V_{max} values than that of free lipase. Similar observations (i.e. increase in K_m and decrease in V_{max} of lipase upon immobilization) have been reported by many authors [30, 36, 41, 43].

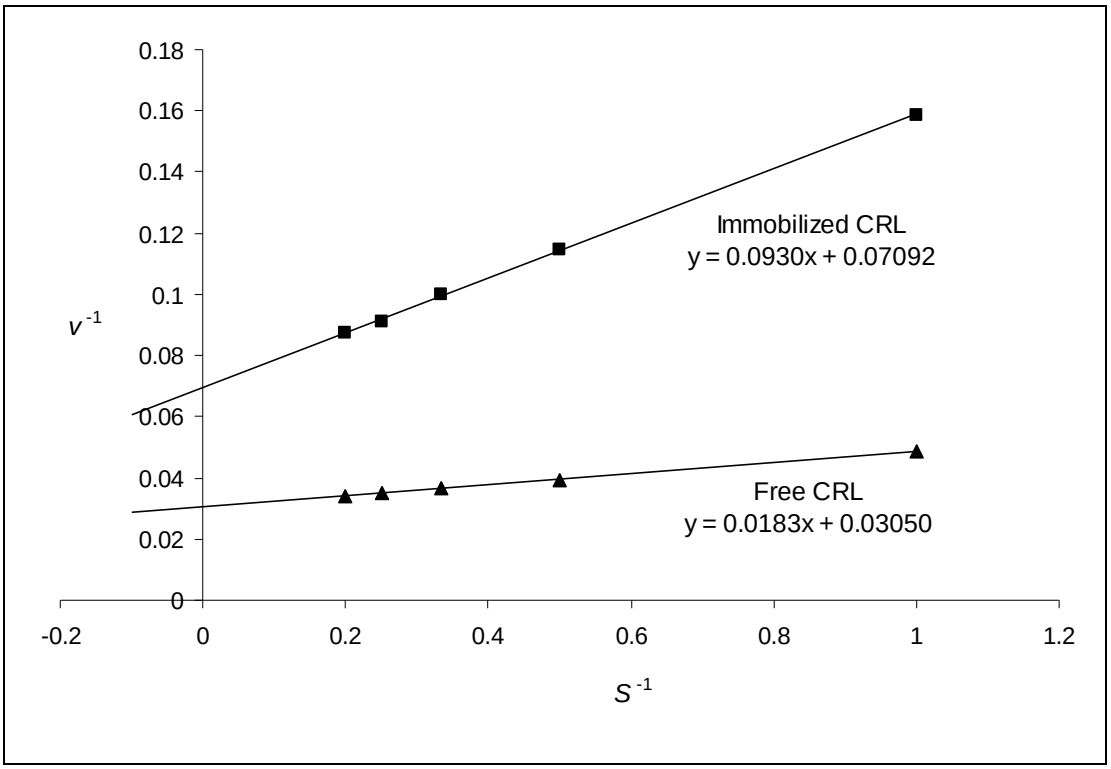

Fig. 2.11: Lineweaver-Burk plots of soluble and immobilized CRL [Y-intercept indicates value of $1/V_{max}$ and the slope indicates value of K_m/V_{max}.]

Table 2.8: Kinetic parameters of free and immobilized CRL

Parameter	**Free CRL**	**Immobilized CRL**
Michaelis constant, K_m (mM)	0.60	1.31 [a]
Maximum reaction velocity, V_{max} (U/mg) [b]	32.79	14.1
Catalytic efficiency, V_{max}/K_m ($min^{-1} \cdot mg^{-1}$)	54.65	10.75
Catalytic constant, k_{cat} (s^{-1})	72.54	159.27
Specificity constant, k_{cat}/K_m ($mM^{-1} \cdot s^{-1}$)	120.91	122.51
Efficiency coefficient, η	–	0.43

[*a* $K_{m,\ app.}$; considering the possibility of interactions of substrate with beaded polymer support, there could be difference in the substrate concentrations in the bulk solution and near the enzyme. This phenomenon is known as 'substrate partition' [44]. Hence, the term 'apparent' is used for the K_m of the immobilized enzyme (which is symbolized as $K_{m,\ app.}$); *b* V_{max} is expressed per mg of protein for the free lipase and per mg of polymer beads for the immobilized lipase.]

The kinetic behaviour of an enzyme can be precisely described using catalytic efficiency (V_{max}/K_m). The catalytic efficiency of immobilized CRL was found to be ~ 5 times lower than that of free CRL. The increase in the K_m and decrease in V_{max} values could be either due to the conformational changes of the enzyme (upon immobilization) resulting in a lesser efficiency of substrate-enzyme complex formation or due to lower accessibility of the substrate to the active site of the immobilized enzyme caused by the increased mass transfer limitations [44, 45].

The catalytic constant (k_{cat}, which is also known as turnover number) was estimated from the V_{max} value using 60 kDa molecular mass of CRL. The k_{cat} values for free CRL and immobilized CRL were 72.54 s^{-1} and 159.27 s^{-1} respectively. The specificity constant (k_{cat}/K_m) of free CRL and immobilized CRL were 120.91 $mM^{-1}\cdot s^{-1}$ and 122.51 $mM^{-1}\cdot s^{-1}$ respectively. Upon immobilization, the catalytic constant increased by ~ 2-fold while the specificity constant remained unchanged.

The efficiency coefficient (η) can be calculated from the ratio of maximum reaction rate of the immobilized enzyme to that of the free enzyme [46] as denoted in Eq. 2.7.

$$\eta = \frac{V_{max\ (Immo.)}}{V_{max\ (Free)}} \qquad \text{– Eq. 2.7}$$

Where, $V_{max\ (Immo.)}$ is the maximum reaction rate of the immobilized enzyme and $V_{max\ (Free)}$ is that of the free enzyme. The η value of immobilized CRL was observed to be 0.43.

2.3.7. Chiral resolution of unnatural amino acid esters

Both CRL and PPL were observed to preferentially hydrolyze the *S*-enantiomer of unnatural amino acid ethyl esters. The chiral resolution of unnatural

amino acid ethyl esters catalyzed by immobilized lipases is represented in Scheme 2.4.

Scheme 2.4: Chiral resolution of unnatural amino acid ethyl esters by immobilized lipases

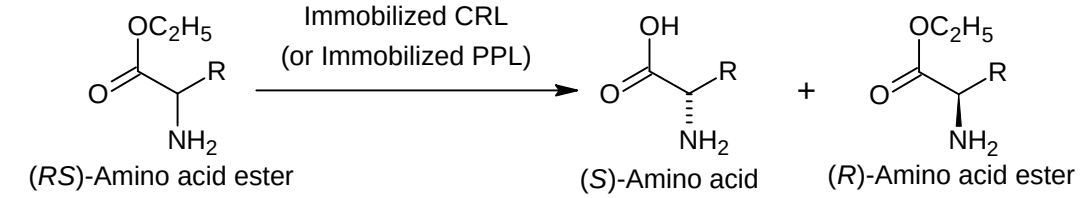

(*RS*)-Amino acid ester (*S*)-Amino acid (*R*)-Amino acid ester

	PG	DOPA	HPA	NA
R-	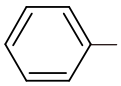	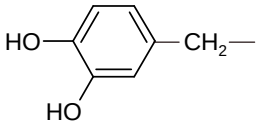	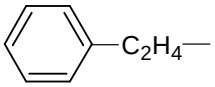	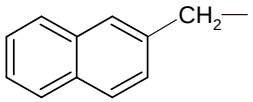

(a) Chiral resolution by immobilized CRL

The results of stereoselective hydrolysis of unnatural amino acid ethyl esters using immobilized CRL are summarized in Table 2.9. The enantioselectivity of immobilized CRL towards hydrolysis of PG-ester, DOPA-ester and HPA-ester was higher (E = 11.9, 9.6 and 15.6 respectively) than that towards hydrolysis of NA-ester (E = 4.3).

Table 2.9: Chiral resolution of ethyl esters of unnatural amino acids using immobilized CRL

Substrate	**Preferred configuration**	**Time** (min)	$\mathbf{ee_p}$ (%)	***C*** (%)	***E***
PG-ester	*S*	30	76.4	38.2	11.9
DOPA-ester	*S*	30	80.1	7.1	9.6
HPA-ester	*S*	30	86.7	11	15.6
NA-ester	*S*	30	59.9	11.6	4.3

(b) Chiral resolution by immobilized PPL

The results of stereoselective hydrolysis of unnatural amino acid ethyl esters using immobilized PPL are summarized in Table 2.10. The enantioselectivity of

immobilized PPL towards hydrolysis of NA-ester (E = 17.9) was higher than that towards hydrolysis of PG-ester, DOPA-ester and HPA-ester (E = 4.6, 4.5 and 4.9 respectively).

Table 2.10: Chiral resolution of ethyl esters of unnatural amino acids using immobilized PPL

Substrate	**Preferred configuration**	**Time** (min)	$\mathbf{ee_p}$ (%)	$\boldsymbol{C}$ (%)	$\boldsymbol{E}$
PG-ester	*S*	30	62.4	9.2	4.6
DOPA-ester	*S*	30	61.5	10.7	4.5
HPA-ester	*S*	30	64.2	8.4	4.9
NA-ester	*S*	30	88.4	10.1	17.9

Several authors have studied enantioselective synthesis of different unnatural amino acids using different enzymes. For example: Hydrolysis of PG-esters using PPL (E = 1.9) is reported by Houng *et al.* [47], that using *Candida antarctica* lipase B (E = 20) is reported by Wegman *et al.* [48] and Du *et al.* [49]. Use of *Candida antarctica* lipase B for enantioselective hydrolysis of PG-methyl esters in presence of ionic liquids is also reported [50, 51]. Enzymatic transformations of DOPA esters e.g. using PPL (DOPA-ester hydrolysis, E = 43.2) [47], using α-chymotrypsin and subtilisin (DOPA-ester hydrolysis, E not determined) [52] and α-chymotrypsin (DOPA-ester synthesis in organic solvents, E not determined) [53] are reported in the literature. Hydrolysis of HPA esters by different lipases has been studied by Houng *et al.* Here among different lipases, *Rhozopus* lipase gave maximum E value i.e. 5 [47]. Besides lipases, alcalase (for hydrolysis of N-protected HPA-methyl ester, E not determined) [54], PPL (for hydrolysis of N-acetylated HPA-ethyl ester, E not determined) [55] and PPL (for hydrolysis of N-protected HPA esters, E not determined) [56] are reported in the literature. To the best of our knowledge, lipase catalyzed enantioselective synthesis of NA ester has not been reported so far. Few proteases *namely* α-chymotrypsin [57], subtilisin [57, 58], thermitase [59] and pronase [60] have been studied so far for synthesis of (*S*)-NA. However, none of these articles reported any data on enantiomeric ratio of the protease used.

2.4. CONCLUSIONS

Epoxy-activated porous polymer beads of allyl glycidyl ether with ethylene glycol dimethacrylate as cross-linking agent and lauryl alcohol as porogen provided an excellent support for lipase immobilization. The immobilization of lipases (CRL and PPL) on AGE-(L)-100 polymer beads resulted in improved pH and temperature stability and extended storage half-life. Among the different lipases screened, CRL exhibited highest enantioselectivity towards hydrolysis of PG-ester, DOPA-ester and HPA-ester (E = 11.9, 9.6 and 15.6 respectively) while PPL exhibited highest enantioselectivity towards hydrolysis of NA-ester (E = 17.9). Both CRL and PPL preferentially hydrolyzed the *S*-enantiomer of unnatural amino acid ethyl esters. The immobilization of lipases (CRL and PPL) on AGE-(L)-100 polymer beads did not alter their enantioselectivity towards hydrolysis of unnatural amino acid ethyl esters.

REFERENCES

[1] Brady, D.; Steenkamp, L.; Skein, E.; Chaplin, J.A.; Reddy, S. Optimization of the enantioselective biocatalytic hydrolysis of naproxen ethyl ester using ChiroCLEC-CR. *Enzyme Microb. Technol.*, **2004**, *34*, 283-291.

[2] Liu, C-H.; Chang, J-S. Lipolytic activity of suspended and membrane immobilized lipase originating from indigenous *Burkholderia sp.* C20. *Bioresource Technol.*, **2008**, *99*, 1616-1622.

[3] Hung, T.C.; Giridhar, R.; Chiou, S.H.; Wu, W.T. Binary immobilization of *Candida rugosa* lipase on chitosan. *J. Mol. Catal. B: Enzym.*, **2003**, *26*, 69-78.

[4] Won, K.; Kim, S.; Kim, K.J.; Park, H.W.; Moon, S.J. Optimization of lipase entrapment in Ca-alginate gel beads. *Process Biochem.*, **2005**, *40*, 2149-2154.

[5] Yujun, W.; Jian, X.; Guangsheng, L.; Youyuan, D. Immobilization of lipase by ultrafiltration and cross-linking onto the polysulfone membrane surface. *Bioresource Technol.*, **2007**, *99*, 2299-2303.

[6] Noureddini, H.; Gao, X.; Philkana, R.S. Immobilized Pseudomonas cepacia lipase for biodiesel fuel production from soybean oil. *Bioresource Technol.*, **2005**, *96*, 769-777.

[7] Amorim, R.V.S.; Melo, E.S.; Carneiro-da-Cunha, M.G.; Ledingham, W.M.; Campos-Takaki, G.M. Chitosan from *Syncephalastrum racemosum* used as a film support for lipase immobilization. *Bioresource Technol.*, **2003**, *89*, 35-39.

[8] Rahman, M.B.A.; Tajudin, S.M.; Hussein, M.Z.; Rahman, R.A.; Salleh, A.B.; Basri, M. Application of natural kaolin as support for the immobilization of lipase from *Candida rugosa* as biocatalyst for effective esterification. *Appl. Clay Science*, **2005**, *29*, 111-116.

[9] Moreno, J-M.; Arroyo, M.; Hernáiz, M-J.; Sinisterra J-V. Covalent immobilization of pure isoenzymes from lipase of *Candida rugosa. Enzyme Microb. Technol.*, **1997**, *21*, 552-558.

[10] Yeşiloğlu, Y. Utilization of bentonite as a support material for immobilization of *Candida rugosa* lipase. *Process Biochem.*, **2005**, *40*, 2155-2159.

[11] Persson, M.; Mladenoska, I.; Wehtje, E.; Adlercreutz, P. Preparation of lipases for use in organic solvents. *Enzyme Microb. Technol.*, **2002**, *31*, 833-841.

[12] Mateo, C.; Abian, O.; Fernandez-Lafuente, R.; Guisan, J.M. Increase in conformational stability of enzymes immobilized on epoxy-activated supports by favoring additional multipoint covalent attachment. *Enzyme Microb. Technol.*, **2000**, *26*, 509-515.

[13] Lasch, J.; Koelsch, R. Enzyme leakage and multipoint covalent attachment of agarose-bound enzyme preparations. *Eur. J. Biochem.*, **1978**, *82*, 181-186.

[14] Kolb, H.J.; Renner, R.; Hepp, K.D.; Weiaa, L.; Wieland, O. Reevaluation of sepharose-insulin as a tool for the study of insulin action. *Proc. Natl. Acad. Sci*., **1975**, *72*, 248-252.

[15] Mateo, C.; Fernandez-Lafuente, G.; Abian, O.; Fernandez-Lafuente, R.; Guisan, J.M. Multifunctional epoxy supports: A new tool to improve the covalent immobilization of proteins, the promotion of physical adsorptions of proteins on the supports before their covalent linkage. *Biomacromolecules*, **2000**, *1*, 739-745.

[16] Bayramoğlu, G.; Kaya, B.; Arica, M.Y. Immobilization of *Candida rugosa* lipase onto spacer-arm attached poly(GMA-HEMA-EGDMA) microspheres. *Food Chem.*, **2005**, *92*, 261-268.

[17] Choi, S.H.; Lee, K.P.; Lee, J.G. Adsorption behavior of urokinase by polypropylene film modified with amino acids as affinity groups. *Microchem. J.*, **2001**, *68*, 205-213.

[18] Choi, S.H.; Nho, Y.C. Adsorption of Co^{2+} and Cs^{1+} by polyethylene membrane with iminodiacetic acid and sulfonic acid modified by radiation-induced graft

copolymerization. *J. Appl. Polym. Sci.*, **1999**, *71*, 999-1006.

[19] Lee, K.P.; Kang, H.J.; Joo, D.L.; Choi, S.H. Adsorption behavior of urokinase by the polypropylene film with amine, hydroxylamine and polyol groups. *Radiat. Phys. Chem.*, **2001**, *60*, 473-482.

[20] Choi, S.H.; Lee, K.P.; Kang H.D. Immobilization of lipase on a polymeric microsphere with an epoxy group prepared by radiation-induced polymerization. *J. Appl. Polym. Sci.*, **2003**, *88*, 1153-1161.

[21] Malmsten, M.; Larsson A. Immobilization of trypsin on porous glycidyl methacrylate beads: effects of polymer hydrophilization. *Colloid. Surf. B.*, **2000**, *18*, 277-284.

[22] Yasuda, M.; Kasahara, H.; Kawahara, K.; Ogino, H.; Ishikawa H. Synthesis of amphiphilic polymer particles for lipase immobilization. *Macromol. Chem., Phys.* **2001**, *202*, 3189-3197.

[23] Vaidya, B.K.; Ingavle, G.C.; Ponrathnam, S.; Kulkarni, B.D.; Nene, S. Immobilization of *Candida rugosa* lipase on poly(allyl glycidyl ether-co-ethylene glycol dimethacrylate) macroporous polymer particles. *Bioresource Technol.*, **2008**, *99*, 3623-3629.

[24] Chellapandian, M.; Krishnan, M.R.V. Chitosan-poly (glycidyl methacrylate) copolymer for immobilization of urease. *Process Biochem.*, **1998**, *33*, 595-600.

[25] Vaidya, B.K.; Karale, A.J.; Suthar, H.K. Ingavle, G.; Pathak, T.S.; Ponrathnam, S.; Nene, S. Immobilization of mushroom polyphenol oxidase on poly(allyl glycidyl ether-co-ethylene glycol dimethacrylate) macroporous beaded copolymers. *React. Funct. Polym.*, **2007**, *67*, 905-915.

[26] Reddy, C.; Reddy, C.R.; Raghunath, K.; Joseph K.T. Immobilization of trypsin on alginic acid-poly(glycidyl methacrylate) graft copolymer. *Biotechnol. Bioeng.*, **1986**, *28*, 609-612.

[27] Leng, D.E.; Quarderer, G.J. Drop dispersion in suspension polymerization. *Chem. Eng. Commun.*, **1982**, *14*, 177-201.

[28] Rajan, C.R.; Mohandas, K.S.; Bahulkar, R.V.; Ponrathnam, S. Indian Patent 184871, **2001**.

[29] Bodanszky, M.; Bodanszky, A. In: The Practice of Peptide Synthesis. Berlin: Springer-Verlag. **1984**.

[30] Tümtürk, H.; Karaca, N.; Demirel, G.; Şahin, F. Preparation and application of

poly(*N*,*N*-dimethylacrylamide-*co*-acrylamide) and poly(*N*-isopropylacrylamide-*co*-acrylamide)/κ-Carrageenan hydrogels for immobilization of lipase. *Int. J. Biol. Macromol.*, **2007**, *40*, 281-285.

[31] Soares, C.M.F.; Santana, M.H.A.; Zanin, G.M.; de Castro, H.F. Covalent coupling method for lipase immobilization on controlled pore silica in the presence of nonenzymatic proteins. *Biotechnol. Prog.*, **2003**, *19*, 803-807.

[32] Lowry, O.H.; Rosebrough, N.J.; Farr, A. L.; Randall, R.J. Protein measurement with the Folin Phenol reagent. *J. Biol. Chem.*, **1951**, *193*, 265-275.

[33] Straathof, A.J.J.; Jongejan, J.A. The enantiomeric ratio: origin, determination and prediction. *Enzyme Microb. Technol.*, **1997**, *21*, 559-571.

[34] Hodge, P.; Sherrington, D.C. Polymer supported reaction in organic synthesis, John Wiley & Sons, New York, **1979**.

[35] Hodge, P. *In*: Hodge P.; Sherrington, D.C. (*Eds.*), Synthesis & separation using fucntional polymers, Wiley & Sons, Chichester, **1988**, pp. 43-122.

[36] Bayramoğlu, G.; Arica, M.Y. Preparation of poly(glycidyl methacrylate–methylmethacrylate) magnetic beads: Application in lipase immobilization. *J. Mol. Catal. B: Enzym.*, **2008**, *55*, 76-83.

[37] Xu, H.; Li, M.; He, B. Immobilization of *Candida cylindracea* lipase on methyl acrylate-divinyl benzene copolymer and its derivatives. *Enzyme Microb. Technol.*, **1995**, *17*, 194-199.

[38] Xi, W-W.; Xu, J-H. Preparation of enantiopure (S)-ketoprofen by immobilized *Candida rugosa* lipase in packed bed reactor. *Process Biochem.*, **2005**, *40*, 2161-2166.

[39] Basri, M.; Zin-Wa-Yunus, W.M.; Yoong, W.S.; Ampon, K.; Abd. Razak, C.N. Salleh, A.B. Immobilization of lipase from *Candida rugosa* on synthetic polymer beads for use in the synthesis of fatty esters. *J. Chem. Tech. Biotechnol.*, **1996**, *66*, 169-173.

[40] Kartal, F.; Akkaya, A.; Kilinc, A. Immobilization of porcine pancreatic lipase on glycidyl methacrylate grafted poly vinyl alcohol. *J. Mol. Catal. B: Enzym.*, **2009**, *57*, 55-61.

[41] Ye, P.; Xu, Z.K.; Wu, J.; Innocent, C.; Seta, P. Nanofibrous membranes containing reactive groups: Electrospinning from poly(acrylonitrile-*co*-maleic acid) for lipase immobilization. *Macromolecules*, **2006**, *39,* 1041-1045.

[42] Roy, J.J.; Abraham, T.E. Strategies in making Cross-Linked Enzyme Crystals. *Chem. Rev.*, **2004**, *104(9)*, 3705-3721.

[43] Yong, Y.; Bai, Y-X.; Li, Y-F.; Lin, L.; Cui, Y-J.; Xia, C-G. Characterization of *Candida rugosa* lipase immobilized onto magnetic microspheres with hydrophilicity. *Process Biochem.*, **2008**, *43*, 1179-1185.

[44] Dordick, J.S. Enzymatic catalysis in monophasic organic solvents. *Enzyme Microb. Technol.*, **1989**, *11,* 194-211.

[45] Pencreaćh, G.; Leullier, M.; Baratti J.C. Properties of free and immobilized lipase from *Pseudomonas cepacia*. *Biotechnol. Bioeng.*, **1997**, *56(20)*, 181-189.

[46] Tischer, W.; Kasche, V. Immobilized enzymes: crystals or carriers? *Trends Biotechnol.*, **1999**, *17*, 326-335.

[47] Houng, J-Y.; Wu, M-L.; Chen, S-T. Kinetic resolution of amino acid esters catalyzed by lipases. *Chirality*, **1996**, *8*, 418-422.

[48] Wegman, M.A.; Hacking, M.A.P.J.; Rops, J.; Pereira, P.; van Rantwijk, F.; Sheldon, R.A. Dynamic kinetic resolution of phenylglycine esters via lipase-catalysed ammonolysis. *Tetrahedron: Asymmetr.*, **1999**, *10*, 1739-1750.

[49] Du, W.; Zong, M.; Guo, Y.; Liu, D. Improving lipase-catalyzed enantioselective ammonolysis of phenylglycine methyl ester in organic solvent by *in situ* racemization. *Biotechnol. Lett.*, **2003**, *25*, 461-464.

[50] Lou, W-Y; Zong, M-H.; Liu, Y-Y.; Wang, J-F. Efficient enantioselective hydrolysis of d,l-phenylglycine methyl ester catalyzed by immobilized *Candida antarctica* lipase B in ionic liquid containing systems. *J. Biotechnol.*, **2006**, *125*, 64-74.

[51] Du, W.; Zong, M.; Guo, Y.; Liu, D. Lipase-catalysed enantioselective ammonolysis of phenylglycine methyl ester in organic solvent. *Biotechnol. Appl. Biochem.*, **2003**, *38*, 107-110.

[52] Kise, H.; Tomiuchi, Y. Unusual solvent effect on protease activity and effective optical resolution of amino acids by hydrolytic reactions in organic solvents. *Biotechnol. Lett.*, **1991**, *13(5)*, 317-322.

[53] Vulfson, E.N.; Ahmed, G.; Gill, I.; Goodenough, P.W.; Kozlov, I.A.; Law, B.A. L-DOPA ester synthesis by α-chymotrypsin in organic solvents. *Biotechnol. Lett.*, **1990**, *12(8)*, 597-602.

[54] Chen, S-T.; Chen, S-Y.; Hsiao, S-C.; Wang, K-T. Kinetic resolution of N-

protected amino acid esters in organic solvents catalyzed by a stable industrial alkaline protease. *Biotechnol. Lett.*, **1991**, *13(11)*, 773-778.

[55] Malhotra, S. V.; Zhao, H. Enantioseparation of the esters of α-N-acetyl amino acids by lipase in ionic liquid. *Chirality*, **2005**, *17*, S240-S242.

[56] López-Serrano, P.; Wegman, M.A.; van Rantwijk, F.; Sheldon, R.A. Enantioselective enzyme catalysed ammoniolysis of amino acid derivatives: Effect of temperature. *Tetrahedron: Asymmetr.*, **2001**, *12*, 235-240.

[57] Pattabiraman, T.N.; Lawson, W.B. Comparative studies of the specificities of α-chymotrypsin and subtilisin BPN', studies with flexible and 'locked' substrates. *Biochem. J.*, **1972**, *126*, 659-665.

[58] Pugniere, M.; Castro, B.; Previero, A. Optical resolution of two isomeric naphthylalanines by immobilized enzymes. *Chirality*, **1991**, *3*, 170-173.

[59] Lankiewicz, L.; Kasprzykowski, F.; Grzonka, Z.; Kettmann, U.; Hermann, P. Resolution of racemic amino acids with thermitase. *Bioorg Chem*., **1989**, *17*, 275-280.

[60] Pugniere, M.; Domergue, N.; Castro, B.; Previero, A. Pronase in amino acid technology: Optical resolution of non-proteinogenic α-amino acids. *Chirality*, **1994**, *6*, 472-478.

CHAPTER

3

Chiral resolution of unnatural amino acid esters using immobilized lipase in membrane bioreactor

3.1. INTRODUCTION

There is a growing interest in immobilization of enzymes on semi-permeable membranes where transport of reaction substrates and products through a catalyst support are studied [1]. Enzyme-immobilized membranes can function both as a catalyst and a means of separation in such enzyme membrane bioreactors (EMB). They offer support to the biocatalysts, control transport of reactant/product and act as a phase barrier for biphasic reactions. On this account they have wide applications in biotechnology [2, 3]. Membrane reactors have numerous advantages such as high enzyme loading, prolonged enzyme activity, high flow rates, ease of scale up and reduction in cost, energy and side products [4, 5].

There are three strategies for immobilization of enzymes on membranes: (i) entrapment of biocatalyst within membrane pores, (ii) gelation of biocatalyst on membrane (iii) bonding of biocatalyst to the membrane by physical adsorption, ionic binding or covalent binding [6]. The first two methods are not commonly practiced as they lead to enzyme leaching. The third is the method of choice and widely used due to a broad choice of membrane materials and better performance in EMB. Non-covalent binding processes are simple but have the disadvantage of weak binding of enzyme. Covalent binding is preferred over physical or ionic binding. However, covalent attachment requires the activation of membrane surface if active groups on the surface are unavailable [7].

Lipases (EC 3.1.1.3) are able to catalyze reactions such as enantio- and regio-selective hydrolysis, esterification, trans-esterification, aminolysis and ammoniolysis. They have become important as versatile biocatalysts for the hydrolytic and synthetic reactions in industrial applications [5]. Lipases have been widely used for biotechnological applications in the dairy industry, oil processing, production of surfactants, and preparation of enantiomerically pure pharmaceuticals. As of today, at least 134 enzyme biotransformation processes have already been developed on an industrial scale of which approximately 25% of the enzymes use lipases [1, 8]. The ability of lipases to act in the presence of aqueous/hydrophobic interfaces has attracted membrane scientists and biotechnologists to synthesize a variety of polymeric membranes as efficient carriers for the lipase immobilization.

A large number of reports are available in literature on use of biphasic EMB for lipase catalyzing reactions ranging from oil hydrolysis to enantioselective

separations. Various membrane materials are reported in the literature [9-13], which can be broadly classified into either hydrophobic or hydrophilic materials. Cellulose, polyamides, PVA/chitosan, zeolites membranes are hydrophilic while polypropylene membranes are hydrophobic. Activation at interface is the characteristic property of lipases, which was first reported by Sarada and Desnuelle [14]. In the absence of interface, lipase has some element of secondary structure (termed as 'lid') covering its active site and making it inaccessible to substrates. However, in the presence of hydrophobic interfaces, the conformational rearrangements occur and lipase is said to be in an 'open state'. As a result, exposure of hydrophobic surfaces and the corresponding functionality of enzyme are observed. Therefore, strongly hydrophobic membranes are widely adopted for lipase immobilization [15]. However, these membranes have poor wettability, thereby causing low contact between enzyme and substrate leading to poor enzyme utilization. On the other hand, hydrophilic membranes can be readily wetted by water and other polar solvents, whereby higher contact between the aqueous and organic phases at the membrane surface is achieved. Therefore, for reasons of economy, hydrophilic membranes are preferred since smaller quantity of enzyme is required [16]. Though hydrophobic surfaces are required to improve lipase activity by interfacial activation, a certain degree of hydrophilicity is essential for high enzyme utilization.

The current trend is to look for new membranes, which have stability, biocompatibility and improved hydrophilicity. One approach to achieving this goal is facile surface modification of membranes in the EMB. Deng *et al.* have reported poly(α-allyl glucoside) modified polypropylene [17], Bayramoglu *et al.* [18] have reported a poly(2-hydroxyethyl methacryl-*co*- 2-methacrylamido phenylalanine) membrane, hybrid membranes based on poly(2-hydroxyethyl methacryl-*co*-ethylene glycol dimethacrylate) filled with clay, and epoxy-derived poly(2-hydroxyethyl methacrylate) membrane are also reported [19, 20]. Polyurethanes (PUs) are one of the industrially important polymers. They possess excellent characteristic in their toughness, abrasion resistance, and flexibility. They have been widely used for making elastomers, foams, coatings [21] or used as biocompatible materials [22]. The block copolymer structure of PU having soft and hard segments results from the polycondensation reaction of the PU precursor formulation. Properties of PU can be tailored by the variation of these soft/hard segments [23].

To the best of our knowledge, poly(urethane methacrylate)-glycidyl methacrylate (PUA-GMA) blend has not been explored in EMB. The idea behind using a PUA-GMA blend is its hydrophilicity and transparency. We synthesized prepolymer (PUA) by a solventless method, which produced no by-products. Bonding of PUA-GMA after coating on PP forms a surface hydrophilized hydrophobic membrane. We employed a flat PP membrane of 0.2 μm pore size (AK30 ENKA) with well-defined and controlled pore matrix for surface modification. Adsorption of lipase on PP membrane is well reported [18], however, PP cannot be easily functionalized. Methods like plasma irradiation or tethering are to be used so that functionalization takes place through grafting [17]. The work strategy involved synthesis of polyurethane (meth)acrylates by conventional isocyanate-polyol condensation reaction followed by creating terminal unsaturation by reaction of 2-hydroxyethyl methacrylate (HEMA) with bound isocyanate linkage. These produced soft segments and hard segments in the prepolymer(s). Once the HEMA terminated prepolymer was formed it was blended with glycidyl methacrylate (GMA) along with a photo-initiator. The formulation was coated on PP membrane as a thin film and exposed to UV irradiation to get a cross-linked structure.

GMA has a pendent epoxy group, which is useful for lipase immobilization. Epoxy-activation is an almost ideal method of immobilization of enzymes at both laboratory as well as industrial scale. Epoxy-activated supports are able to form very stable covalent linkages with different protein groups (amino, thiol, phenolic ones) under very mild experimental conditions (e.g. pH 7.0). Furthermore, these activated supports are very stable during storage in neutral aqueous media, before and during immobilization procedures [24].

Our methodology was solvent less, therefore environmental friendly and cost effective. PUA gives good adhesion to PP surface and helps in forming a three dimensional network with surface epoxy groups. The problem of burying of epoxy groups, a phenomenon often observed while immobilization on polymer beads [25] is obviated. Additionally, the coating on a PP membrane gives an original membrane of higher strength. Photo-polymerization is adopted as it offers a number of advantages over traditional thermal polymerization methods including spatial control of initiation, high polymerization rates, low energy requirements, and increased control over the properties of the resulting materials [26].

In the present chapter, the potential of novel polyurethane methacrylate supported PP membranes has been explored for covalent immobilization of *Candida rugosa* lipase (CRL) and porcine pancreatic lipase (PPL). Immobilized lipase aggregates were cross-linked by treatment with glutaraldehyde for stable binding. Various compositions of membranes were used to study the influence of membrane properties on protein binding and expression of immobilized lipase activity. The biocatalytic membranes were evaluated for pH, thermal stability and storage stability. Esterification of oleic acid was used as a model reaction to examine the performance of this EMB. The immobilized membranes were placed in membrane reactor where chiral resolution of unnatural amino acid esters was studied.

3.2. MATERIALS AND METHODS

3.2.1. Materials

Polytetrahydrofuran (PTHF) of varying molecular weights was procured from Fluka Chemicals Ltd., USA. 2,4-Toluene diisocynate, glycidyl methacrylate, *p*-methoxy phenol, 2-hydroxy ethylmethacrylate, hydroquinone, Irgacure® 184, *p*-nitro-phenyl palmitate (*p*-NPP) and porcine pancreatic lipase (PPL) were purchased from Sigma-Aldrich chemicals, USA. *Candida rugosa* lipase (CRL) was purchased from Europa Chemicals, UK. Unnatural amino acids *namely* phenylglycine (PG), 3,4-dihydroxy phenylalanine (DOPA), homophenylalanine (HPA), and 2-naphthylalanine (NA); and homophenylalanine ethyl ester (HPA-ester) were purchased from Bachem Chemicals, Switzerland.

3.2.2. Preparation of urethane methacrylate membrane

(a) Poly(urethane methacrylate) (PUA) prepolymer synthesis

A 250 mL dry, nitrogen flushed two neck flask equipped with a mechanical stirrer, thermometer, condenser and dropping funnel was charged with 0.4 mol of 2,4-toluene diisocynate (69.66 g), and 0.49 g *p*-methoxy phenol (0.1 mol%). To this, 0.2 mol of polytetrahydrofuran (130 g) was added to it drop wise over the period of 2 h with constant stirring. The reaction was continued for another 2 h and isocyanate content was calculated. The reaction required no additional catalyst, due to the higher reactivity of the NCO groups on the aromatic ring. In the second stage of the condensation process, 0.4 mol of 2-hydroxyethyl methacrylate i.e. HEMA (52.06 g),

stabilized with 0.1 g of hydroquinone, was stepwise added to the NCO terminated prepolymer. Completion of the reaction was monitored by FT-IR by following disappearance of the vibration band at 2270 cm^{-1} attributed to the NCO groups. Total reaction time was typically 19 h. The product was decanted into a plastic bottle and stored in a cold place. This is referred as PUA in ensuing sections. The synthesis of HEMA terminated polyurethane (meth)acrylate is given in Scheme 3.1(a).

Scheme 3.1(a): Synthesis of HEMA terminated polyurethane (meth)acrylate

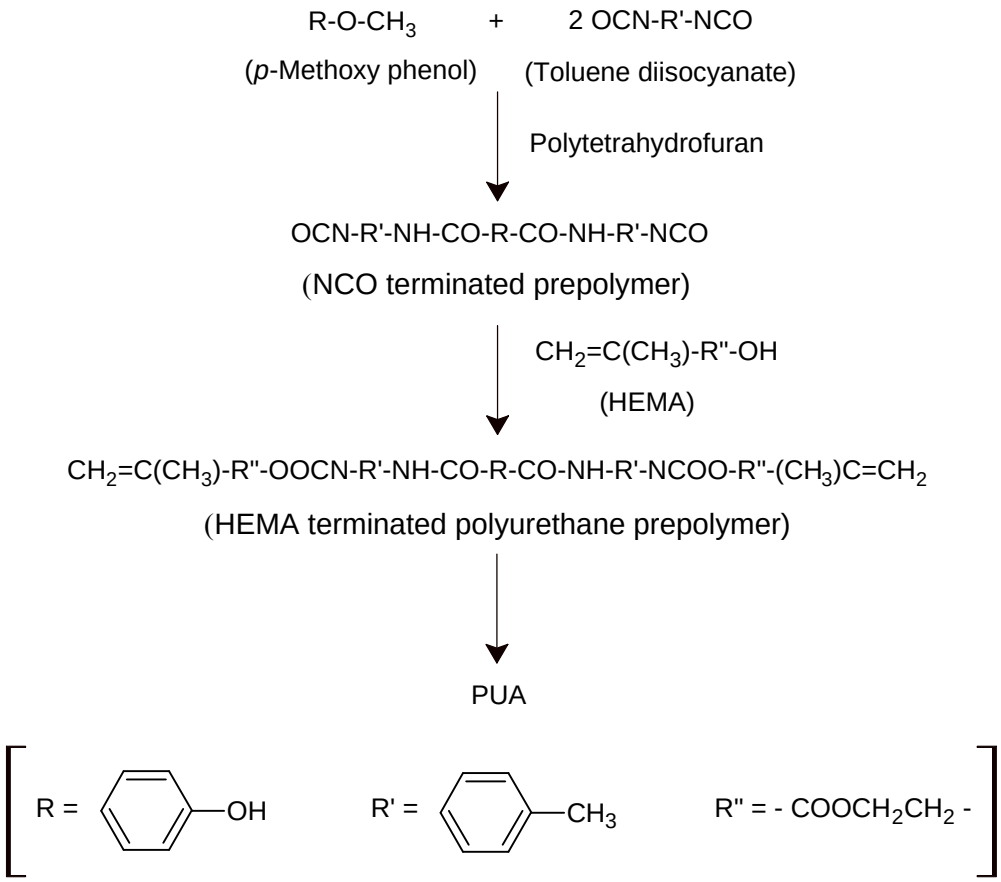

(b) Membrane preparation

A blend of PUA, GMA (20%), cross-linking agent (pentaerythritol tetraacrylate, 5% wt) and Irgacure® 184 (1 mol%) was prepared in a beaker in a clean room with yellow light. This formulation was coated on a AK30 ENKA make 0.2 μm polypropylene (PP) membrane with the help of a bar coater (40 μm). This was termed as PUA-D. Prior to coating, few PP membranes were pre-wetted by isopropanol/methanol (hereafter termed as PUA-I and PUA-M, respectively). After

ensuring uniform coating, the disc was exposed to UV radiation (low pressure mercury lamp: 50 W/cm) for 10 min under nitrogen flow at ambient temperature. The method was standardized by differential photocalorimetric and IR studies. Membranes were washed, heated at 50°C under vacuum and dried to ensure absence of unreacted monomers and cut into small squares (1 cm^2) and flat circular discs (47 mm diameter) which were used for lipase immobilization. The preparation of surface hydrophilized hydrophobic membrane is shown in Scheme 3.1(b).

Scheme 3.1(b): Preparation of surface hydrophilized hydrophobic membrane by blending and copolymerization of HEMA terminated polyurethane pre-polymer and glycidyl methacrylate coated on PP membrane.

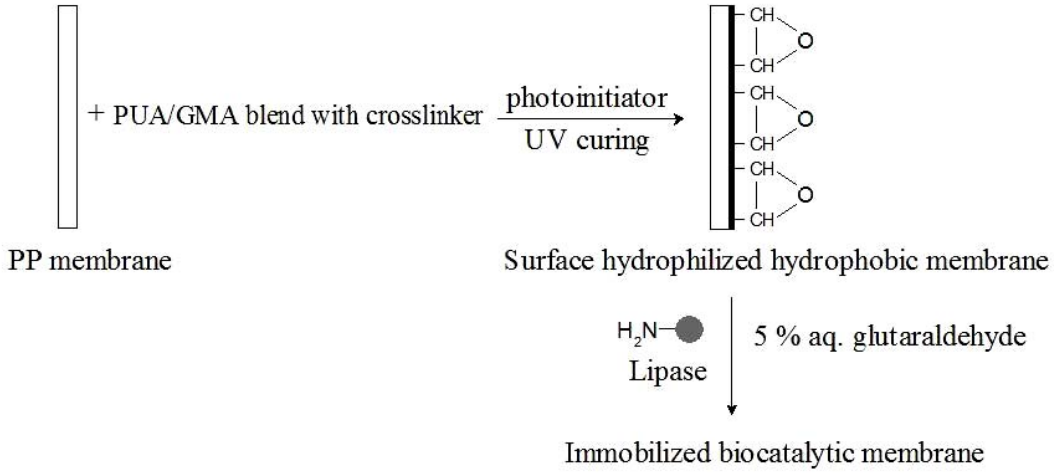

3.2.3. Method of immobilization

Membrane (1 cm^2) was suspended in 20 mL of 0.5 M of sodium phosphate buffer pH 7 containing different concentrations of CRL or PPL and incubated in a rotary shaker at around 120 rpm at 30°C. After 12 h, membrane was separated from enzyme solution and treated with 5% aqueous glutaraldehyde solution at 40°C for 3 h. Membrane was then washed thrice with 10 mL of 0.05 M sodium phosphate buffer (pH 7). The supernatant (residual enzyme solution) and washings were assayed for unbound protein. The biocatalytic membrane was processed for lipase activity as described in Section 3.2.7(a). PUA-D membranes immobilized with CRL and PPL were termed as CRL-PUA-D and PPL-PUA-D respectively. Similarly, PUA-I membranes immobilized with CRL and PPL were termed as CRL-PUA-I and PPL-

PUA-I respectively. The efficiency of immobilized biocatalytic membrane was calculated in terms two parameters, *viz.* 'activity recovery' and 'retention of specific activity' that are defined in Eq. 3.1 and Eq. 3.2 respectively:

$$\text{Activity recovery}\,(\%) = \left(\frac{A_{\text{Membrene}}}{{}^{\text{Total}}A_{\text{Free}}}\right) \times 100 \qquad \text{– Eq. 3.1}$$

Where, $A_{Membrane}$ is immobilized lipase activity expressed by 1 cm^2 of biocatalytic membrane, ${}^{Total}A_{Free}$ is total activity of free lipase. ${}^{Total}A_{Free}$ is a product of activity (U/mL) and volume (mL) of free enzyme loaded on 1 cm^2 of PUA membrane.

Retention of specific activity (%) =

$$\left(\frac{\text{Specific activity of biocatalytic membrane}}{\text{Specific activity of free lipase}}\right) \times 100 \qquad \text{– Eq. 3.2}$$

3.2.4. pH and temperature stability

(a) pH stability

The pH stability of free lipases (CRL or PPL) and immobilized lipases (CRL-PUA-I and PPL-PUA-I) was studied by incubating the enzyme in buffer solutions of different pH in the range of 4-10 for 30 min at 30°C and determining the hydrolytic activity as described in Section 3.2.7(b). The residual activity was calculated as the percentile ratio of the activity of enzyme after incubation to the initial activity. Residual activities of free and immobilized lipases were plotted against pH.

(b) Thermal stability

The thermal stability of free lipase and immobilized lipase on AGE-(L)-150 polymer beads was evaluated by incubating the enzyme at different temperatures in the range of 20-80°C for 30 min at pH 7 and determining the hydrolytic activity as described in Section 3.2.7(b). Residual activities of free and immobilized lipases were calculated as mentioned above and plotted against temperature.

3.2.5. Synthesis and characterization of substrates

(a) Chemical synthesis of rac-amino acid ethyl esters

Rac-amino acid esters were chemically synthesized by esterification of *rac*-amino acids with ethanol in presence of thionyl chloride [27]. The detailed procedure of chemical synthesis of *rac*-amino acid ethyl esters is described earlier in Chapter 2

in Section 2.2.5(a). Phenylglycine ethyl ester, 3,4-dihydroxy phenylalanine ethyl ester and 2-naphthylalanine ethyl ester are termed as PG-ester, DOPA-ester and NA-ester respectively.

3.2.6. Chiral resolution of unnatural amino acid esters using PUA-I membrane

The schematic diagram and the photograph of the membrane bioreactor are shown in Fig. 3.1(a) and Fig. 3.1(b) respectively.

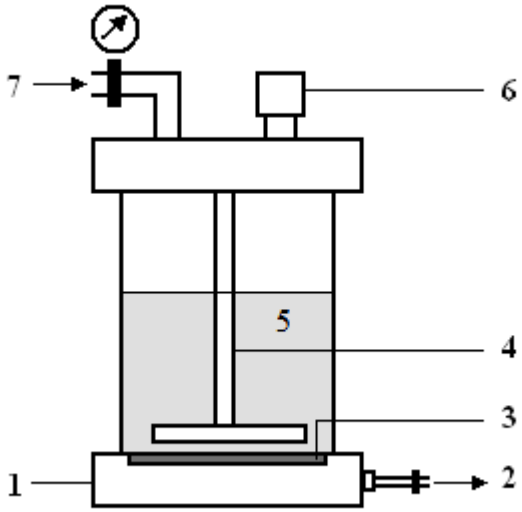

Fig. 3.1(a): Schematic representation of enzyme membrane bioreactor (EMB); 1: membrane support, 2: outlet, 3: biocatalytic membrane, 4: magnetic stirrer, 5: reaction mixture, 6: sample port and 7: pressure gauze.

Fig. 3.1(b): Photograph of the enzyme membrane bioreactor

In laboratory scale Millipore stirred cell (XFUF04701, Millipore Inc. USA), biocatalytic membrane (47mm diameter disc) was placed on the membrane support as shown in Fig. 3.1(a). The reactor was charged with 25 mL solution of *rac*-amino acid ethyl ester (prepared in 50mM phosphate buffer, pH 7). The reactor temperature was maintained at 30°C under constant stirring at 200 rpm. Samples were periodically withdrawn and analyzed by HPLC.

3.2.7. Analytical methods

(a) Membrane characterization

Optimization of pre-polymer synthesis was done using a Shimadzu-8300 Fourier transform infrared spectrophotometer (FT-IR) with a resolution of 1 cm^{-1} in the transmission mode. Estimation of complete curing of surface epoxy groups was done using Reflectance mode ATR (Shimadzu-8300). Flux (mL/min) was estimated by using bubble point apparatus fabricated in NCL-Pune (India). Differential photo-calorimeter (DPC; TA instruments model Q100) was used to optimize the UV curing studies. Hydrophilicity was measured by a contact angle meter, GBX (France), using water as surface wetting liquid. Millimole (mM) of epoxide per cm^2 of modified membrane was estimated titrimetrically using a method of addition of hydrogen halide to epoxy group [28]. The scanning electron micrographs of the dried membrane were obtained by using JEOL-5600 scanning electron microscope, after coating with gold under reduced pressure.

(b) Enzymatic activity assays

(i) Activity assay of free and immobilized CRL

The hydrolytic activity of free and immobilized CRL was analyzed spectrophotometrically using *p*-NPP as substrate [29]. Substrate was prepared fresh by dissolving *p*-NPP (30 mg), 2-propanol (10 mL) and Triton X-100 (0.1 mL) in 100 mL of phosphate buffer (0.05 M, pH 7). Reaction mixture consisted of 0.1 mL diluted lipase, 0.9 mL of *p*-NPP substrate solution and 1 mL of phosphate buffer (0.05 M, pH 7). It was incubated in a water bath at 37°C for 30 min followed by addition of 2 mL 2-propanol. Absorbance was determined at 410 nm (Shimadzu UV absorption Spectrophotometer-160). The unit of enzyme activity unit was defined as the amount of enzyme required to hydrolyze 1 nM *p*-NPP per minute under the described

conditions. Protein estimation of supernatant and washings were determined by the Folin-Lowry method [30].

The hydrolytic activity of immobilized PPL was determined in similar manner as mentioned above using *p*-NPP as substrate. Activity of biocatalytic membrane was expressed in terms of units of lipase activity per unit membrane area (U/cm^2).

(ii) Activity assay of free and immobilized PPL

The hydrolytic activity of free and immobilized PPL was analyzed titrimetrically using olive oil as substrate [31]. The substrate was prepared by mixing 50 mL of olive oil with 50 mL of gum arabic solution (7% w/v). The reaction mixture consisting of 5 mL of substrate emulsion, 2 mL of 0.1 M sodium phosphate buffer (pH 7) and 1 mL of PPL solution, was incubated for 15-30 min at 37°C. The reaction was terminated by adding 10 mL of acetone-ethanol solution (1:1). The liberated fatty acid was titrated with 25 mM aqueous NaOH solution using phenolphthalein as an indicator. One unit (U) of PPL activity was defined as the amount of enzyme that produced 1 μmol of free fatty acids per min under the prescribed assay conditions.

The hydrolytic activity of immobilized PPL was determined in similar manner as mentioned above using olive oil as substrate. Activity of biocatalytic membrane was expressed in terms of units of lipase activity per unit membrane area (U/cm^2).

(iii) Synthetic activity of immobilized enzyme in batch reactor

Synthetic activity of biocatalytic membrane was evaluated by esterification of oleic acid. The reaction set up is shown in Fig. 3.1(a). The 100 mL laboratory scale stirred cell (Millipore) was charged with oleic acid and octanol (0.01M each). The reaction was conducted with constant stirring at 40°C in presence of CRL-PUA-I or PPL-PUA-I biocatalytic membranes (47mm diameter disc). After 1 h, reaction mixture was separated from biocatalytic membrane. To 0.5 mL of reaction mixture, 5.0 mL 1:1 acetone–methanol solution was added and resultant solution was titrated against 50 mM NaOH to determine unreacted oleic acid [32]. The remaining reaction mixture was stored at 30°C and analyzed in similar manner for unreacted oleic acid after 24 h. This was done to check for possible leaching of lipase from membrane into the reaction mixture.

Further, to evaluate operational stability of immobilized lipase (CRL-PUA-I or

PPL-PUA-I) the above reaction was repeated for 10 consecutive runs, using fresh substrate each time. To compare the above results against free enzyme, esterification reaction was carried out in batch mode for 10 h using free lipase. The synthetic activity of free lipase was determined every hour by titrimetric method as described above.

(c) HPLC analysis

All reaction profiles were monitored by HPLC (Thermo Separation Products, Fremont, CA, USA). The quantitative analysis of different amino acids and their esters was carried out using a reverse phase C-18 column (125×4 mm, prepacked column supplemented with a 4×4 mm guard column procured from LiChrospher®, Merck, Darmstadt, Germany) eluted isocratically using acetonitrile-water mobile phase (30:70 v/v, pH adjusted to 3.0 with 50% v/v *o*-phosphoric acid), at a flow rate of 0.6-1.0 mL/min. Peaks were detected using an UV detector at 215 nm. The peak identification was made by comparing the retention times with those of authentic compounds. Peak area was used as a measure to calculate the respective concentration. The reaction conversion was estimated from the ratio of the substrate consumption to its initial concentration. The enantiomeric excess (e.e.) of the product was determined by using a CHIROBIOTIC-T® column (250×4.6 mm prepacked column supplemented with 20×4 mm guard column procured from Astec Inc. USA) eluted isocratically using water-methanol mobile phase (40:60 v/v, pH adjusted to 2.3-2.5 with 50% v/v glacial acetic acid), at a flow rate of 0.6-0.8 mL/min.

(d) Determination of enantiomeric ratio

Enantiomeric ratio (*E*) is the prime parameter for describing the enzyme's enantioselectivity. Enantiomeric ratio was determined by using Eq. 2.3 as described earlier in Chapter 2 in Section 2.2.7(e).

3.3. RESULTS AND DISCUSSION

3.3.1. Membrane characterization

The asymmetric nature of 2,4-toluene diisocynate (TDI) molecule allowed to synthesize pure monoacrylated diisocyanate with only one NCO-group (located in the *para* position) on reaction with the hydroxylacrylate at 60°C (reactivity ratio between

the *ortho* and *para* groups is in the range of 25). Infrared spectroscopy was used to monitor both the synthesis and curing processes. Completion of reaction was confirmed by disappearance of NCO peak at 2270 cm^{-1} [21]. GMA was blended with PUA in suitable amount with a cross-linking agent (5% wt pentaerythritol tetraacrylate) and photoinitiator (Irgacure® 184). This gave fluidity to the formulation for coating on the PP membrane. The coating was done using a bar coater in such a manner that the pores in PP matrix were partially filled by this solution. The film thickness was 60 μm. It was observed that coating and penetration of blend on PP was facilitated due to prior pre-treatment of PP membrane with isopropyl alcohol (IPA)/methanol (MeOH). The photoinitiated cross-linking polymerization of the PUA/GMA coating proceeded very fast upon intense illumination at ambient temperature. Polymerization was optimized by ATR infrared spectroscopy by measuring the disappearance of the acrylate double bond [21]. Irgacure®-184 was chosen because of its high quantum yield. The DPC study revealed that the enthalpy of polymerization was 12.7 kcal/mol/methacrylate bond. This is close to the theoretical value (13.1 kcal/mol/methacrylate bond) [33] which suggests that nearly 100% conversion is possible with this photoinitiator. Surface epoxy content was estimated and found to be 0.147 mM/cm^2 of the membrane. This value is high and indicative of its efficacy in higher enzyme binding.

Enzyme technology employs functionalized membrane surfaces for the immobilization of enzymes, where one of the key issues is the compatibility of membrane for immobilization. Copolymerization of PUA with hydrophilic glycidyl methacrylate on PP support improves the biocompatibility of membrane and also creates a hydrophilic/hydrophobic microenvironment for the immobilized enzyme. Hydrophilicity of modified (PUA-I) and unmodified membranes (PP) was compared. It was found that the unmodified (PP) membrane was hydrophobic (contact angle: 137.3) while modified membrane (PUA-I) was marginally hydrophilic (contact angle: 99.2). Our methodology is effective in that the hydrophilicity is readily introduced into the porous membrane matrix at the required density by selecting the co-monomer ratio in the formulation used for polymer preparation.

Scanning electron micrographs (Fig. 3.2) show the surface morphology of PP and PUA/GMA supported PP membrane, respectively. Commercial PP membrane was very porous and had well defined pore size. This porosity was decreased due to

coating and partial filling of pores by the blend as shown in Fig. 3.2(b). This leads to site availability for covalent attachment of enzyme on the epoxy surface.

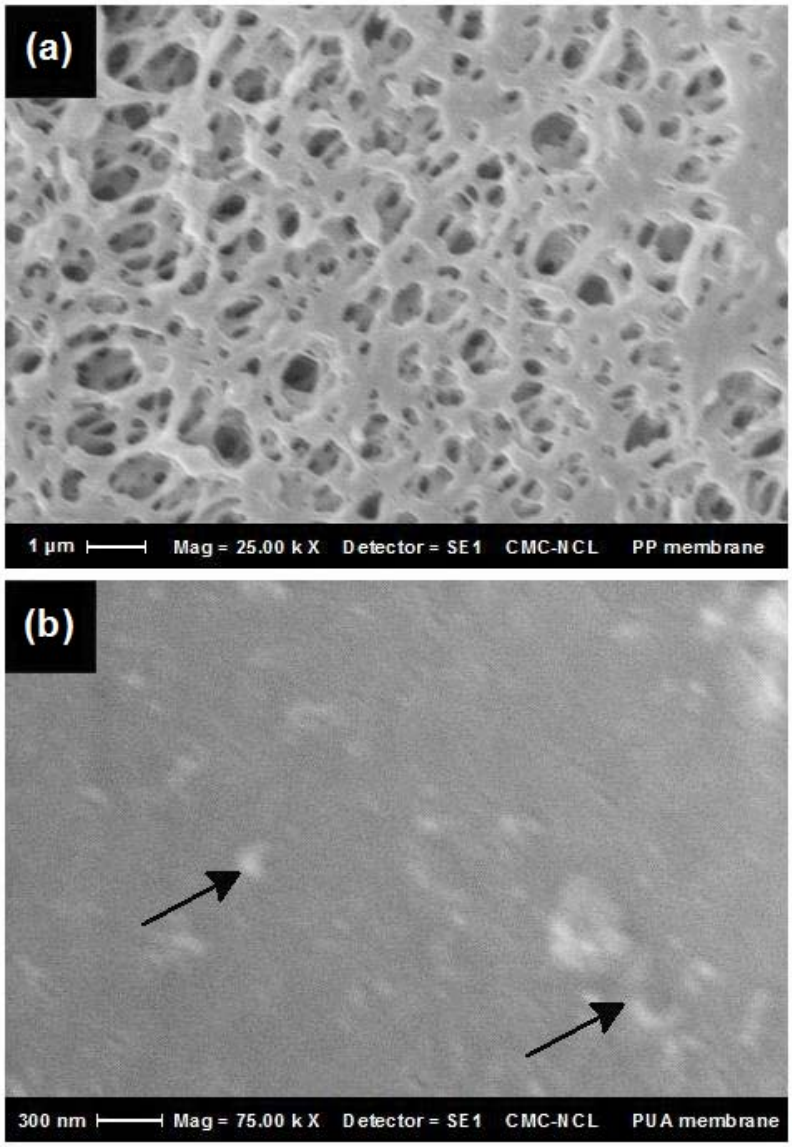

Fig. 3.2: Scanning electron micrographs showing surface morphology of (a) unmodified polypropylene membrane and (b) poly (urethane methacrylate-*co*-glycidyl methacrylate)-*supported*- polypropylene biphasic membrane. In (a), porous open pore structure can be seen which is disappeared in (b), due to partial filling of pores by the coated blend (shown by arrows).

3.3.2. Optimization of the lipase immobilization

(a) Optimization of immobilization time

The time required for immobilization of CRL and PPL was optimized for

PUA-D membranes (Table 3.1 and Table 3.2 respectively). From Table 3.1 values of percent activity recovery and percent retention of specific activity of CRL-PUA-D membrane reached to maximum at 18 h. Their values were 70.31% and 82.03%, respectively. The values of percent activity recovery and percent retention of specific activity of PPL-PUA-D membrane were reached to maximum in 12 h (Table 3.2).

Table 3.1: Optimization of time for CRL immobilization on PUA-D membranes

Time (h)	***p*-NPP activity** [a]	**Protein** [b]	**Specific activity** [c]	**Activity recovery** (%)	**Retention of specific activity** (%)
Free CRL [d]	130.99 [e]	0.14 [f]	935.64	-	-
12	1683.83	2.35	716.52	64.27	76.58
18	1841.94	2.40	767.48	70.31	82.03
24	1768.97	2.38	743.26	67.52	79.44

[[a] U/cm^2 of membrane; [b] mg/cm^2 of membrane; [c] U·mg^{-1}·cm^{-2}; [d] Free enzyme solution containing 2 mg/mL of commercial CRL enzyme powder (procured from Europa Chemicals, UK); [e] U/mL; [f] mg/mL.]

Table 3.2: Optimization of time for PPL immobilization on PUA-D membranes

Time (h)	**Olive oil activity** [a]	**Protein** [b]	**Specific activity** [c]	**Activity recovery** (%)	**Retention of specific activity** (%)
Free PPL [d]	2.16 [e]	0.29 [f]	7.45	-	-
6	22.31	3.88	5.75	51.64	77.20
12	34.75	5.49	6.33	80.44	84.98
18	34.82	5.50	6.33	80.60	85.00

[[a] U/cm^2 of membrane; [b] mg/cm^2 of membrane; [c] U·mg^{-1}·cm^{-2}; [d] Free enzyme solution containing 1 mg/mL of commercial PPL enzyme powder (procured from Sigma Chemicals, USA); [e] U/mL; [f] mg/mL.]

(b) Optimization of enzyme loading

To evaluate the binding capacity, PUA-D membranes were loaded with lipase

of different concentrations and analyzed for expression of lipase activity and protein binding. The results of CRL and PPL loading are given in Table 3.3 and Table 3.4 respectively. In case of CRL immobilization, the lipase activity and bound protein increased with increase in enzyme loading from 2 to 8 mg/cm^2 membrane. However, the specific activity of biocatalytic membrane was found to decrease beyond 4 mg enzyme loading (Table 3.3). Likewise, in case of PPL immobilization, the lipase activity and bound protein increased with increase in enzyme loading from 1 to 4 mg/cm^2 of membrane while the specific activity of biocatalytic membrane was found to decrease beyond 2 mg enzyme loading (Table 3.4). Inadequate expression of enzyme activity may be due to the embedding of active site of lipase during the immobilization process by increased stacking and possible diffusion limitations.

Table 3.3: Optimization of CRL loading on PUA-D membranes

Enzyme loading [a]	***p*-NPP activity** [b]	**Protein** [c]	**Specific activity** [d]	**Activity recovery** (%)	**Retention of specific activity** (%)
2	926.38	1.21	765.60	70.72	81.83
4	1841.94	2.4	767.48	70.31	82.03
6	1959.82	3.81	514.39	49.87	54.98
8	2114.91	4.51	468.94	40.36	50.12

[[a] mg/mL; [b] U/cm^2 of membrane; [c] mg/cm^2 of membrane; [d] U·mg^{-1}·cm^{-2}.]

Table 3.4: Optimization of PPL loading on PUA-D membranes

Enzyme loading [a]	**Olive oil activity** [b]	**Protein** [c]	**Specific activity** [d]	**Activity recovery** (%)	**Retention of specific activity** (%)
1	34.75	5.49	6.33	80.44	84.98
2	69.8	10.84	6.44	80.79	86.45
3	78.94	14.16	5.57	60.91	74.85
4	98.74	19.68	5.02	57.14	67.36

[[a] mg/mL; [b] U/cm^2 of membrane; [c] mg/cm^2 of membrane; [d] U·mg^{-1}·cm^{-2}.]

(c) Immobilization on pre-wetted membranes

Pre-wetted membranes were prepared using methanol and isopropyl alcohol as

prewetting agents. These membranes were found to give higher binding and expression of lipase (both CRL and PPL) than that of dry membrane (Table 3.5 and Table 3.6 respectively). PUA-I gave higher expression of lipase activity than that of PUA-M membranes. CRL-PUA-I gave 90.27% activity recovery and 91.91% retention of specific activity while PPL-PUA-I gave 91.09% activity recovery and 95.8% retention of specific activity. The higher expression of activity by PUA-I is probably due to the channels created by solvents, leading to improved enzyme penetration. IPA was found to be better solvent for prewetting because of its less polar nature and better enzyme compatibility as compared to methanol.

Table 3.5: Effect of prewetting on CRL immobilization on PUA membrane

Membrane	**pNPP activity** [a]	**Protein** [b]	**Specific activity** [c]	**Activity recovery** (%)	**Retention of specific activity** (%)
PUA-D	1841.94	2.4	767.48	70.31	82.03
PUA-M	1974.29	2.52	783.45	75.36	83.73
PUA-I	2364.91	2.75	859.97	90.27	91.91

[[a] U/cm^2 of membrane; [b] mg/cm^2 of membrane; [c] U·mg^{-1}·cm^{-2}.]

Table 3.6: Effect of prewetting on PPL immobilization on PUA membrane

Membrane	**Olive oil activity** [a]	**Protein** [b]	**Specific activity** [c]	**Activity recovery** (%)	**Retention of specific activity** (%)
PUA-D	68.92	10.84	6.36	79.77	85.36
PUA-M	70.08	10.88	6.44	81.11	86.48
PUA-I	78.7	11.03	7.14	91.09	95.80

[[a] U/cm^2 of membrane; [b] mg/cm^2 of membrane; [c] U·mg^{-1}·cm^{-2}.]

In most of the previous reports, immobilization of lipases on different membrane supports was accomplished mainly via either physical adsorption or covalent attachment methods. In general, the membranes capable of binding lipase by physical adsorptive forces have low protein binding capacity i.e. roughly in the range of 0.005 to 0.1 mg/cm^2 [17, 34-43]. On the other hand, functional membranes capable of binding lipase via covalent attachment gave better protein binding capacity i.e. in

the range of 1.5-16 mg/cm^2 [18, 44-46]. Thus, the covalent attachment offers better protein loading on membrane surface than mere physical adsorption.

Several authors studied the covalent immobilization lipase on different modified functional membranes. For example, Bayramoğlu *et al.* have studied the covalent immobilization of CRL on poly(2-hydroxyethyl methacrylate-co-methacrylamido-phenlyalanine) flat-sheet membranes. Under the optimized conditions, the biocatalytic membrane expressed lipase activity of 841 U/g of membrane (corresponding to 78% activity recovery) and showed protein binding of 1.5 mg/cm^2 [18]. Covalent immobilization of CRL on poly(acrylonitrile-co-2-hydroxyethyl methacrylate) flat-sheet membrane is reported by Huang *et al.*. The immobilization showed 40% activity recovery with 16 mg/cm^2 protein binding [44]. Ye *et al.* have studied poly-(acrylonitrile-co-maleic acid) hollow-fiber membrane for covalent immobilization of CRL. Under the optimized conditions, the biocatalytic membrane expressed 15.8 U/mg of specific activity (which correspond to 37% activity recovery) and showed protein binding of 20.2 mg/g [45]. Moreover, the covalent immobilization of PPL on poly(methyl methacrylate-ethylene glycol dimethacrylate) flat-sheet membrane is reported by Pugazhenthi and Kumar. The immobilization resulted in 39% increase in the activity of PPL [46].

In the present study, the PUA-D membrane gave maximum protein binding up to 4.51 mg/cm^2 for CRL and 19.68 mg/cm^2 for PPL (Table 3.3 and Table 3.4 respectively). Compared to the previous reports, PUA-D was found to be a more efficient support for the lipase immobilization. The biocatalytic membranes (CRL-PUA-I and PPL-PUA-I) under optimum conditions, showed very high percent activity recovery (about 90% and 91% respectively). This can be ascribed to increased enzyme stability by immobilization on this hydrophilized-hydrophobic membrane.

3.3.3. Stability of biocatalytic membranes

(a) pH stability

The activity profiles of free and immobilized CRL with respect to pH are shown in Fig. 3.3. In the alkaline pH conditions, e.g. at pH 8 and 9, the free lipase retained 81.1% and 40.3% residual activity while immobilized biocatalytic membrane (CRL-PUA-I) found to retain 94.3% and 82.6% residual activity, respectively.

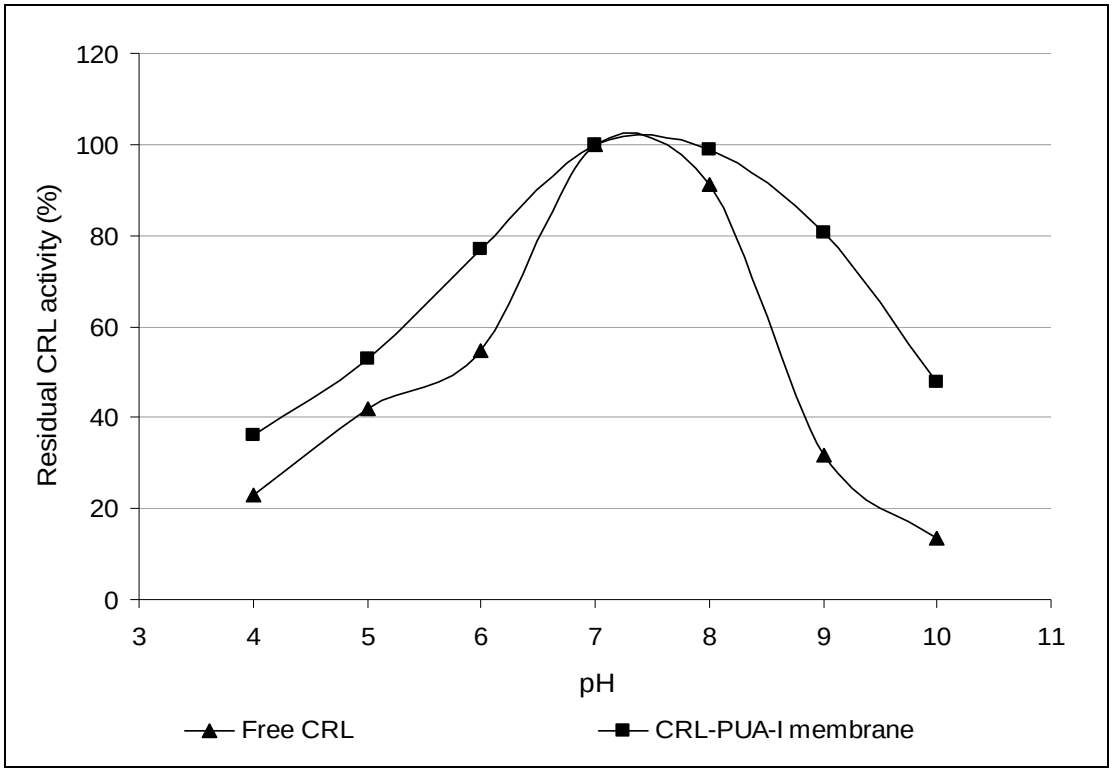

Fig. 3.3: pH stability of CRL-PUA-I membrane

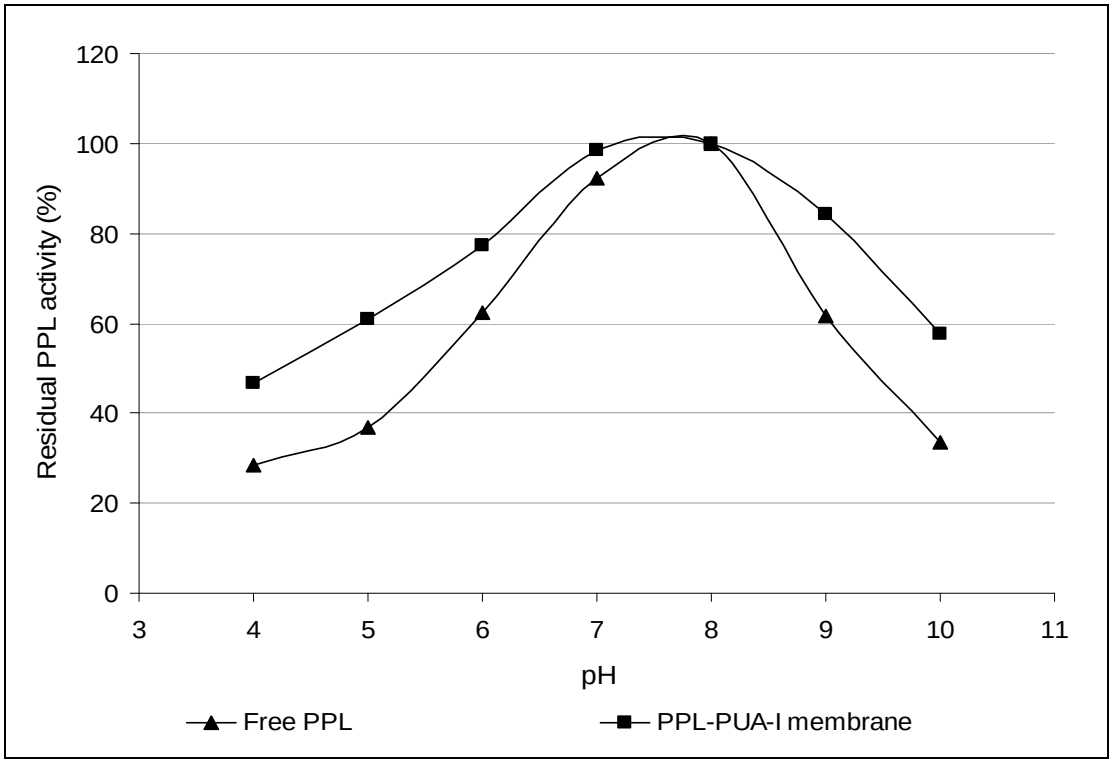

Fig. 3.4: pH stability of PPL-PUA-I membrane

Fig. 3.4 gives the effect of pH on the residual activity of free and immobilized

PPL. In the alkaline pH conditions, e.g. at pH 9 and 10, the free lipase retained 61.6% and 33.6% residual activity whereas, immobilized biocatalytic membrane (PPL-PUA-I) retain 84.24% and 57.71% residual activity, respectively. Fig. 3.3 and Fig. 3.4 indicate that immobilization of CRL and PPL on PUA-I membrane has significantly improved the pH stability of enzymes mainly in the alkaline region.

(b) Temperature stability

The activity profiles of free and immobilized CRL with respect to temperature are given in Fig. 3.5. At 50°C the free enzyme retained only 50.7% residual activity while CRL-PUA-I membrane retained 76.0% of its initial activity. Likewise at 60°C the free enzyme retained 39.1% residual activity while CRL-PUA-I membrane retained 55.5% residual activity.

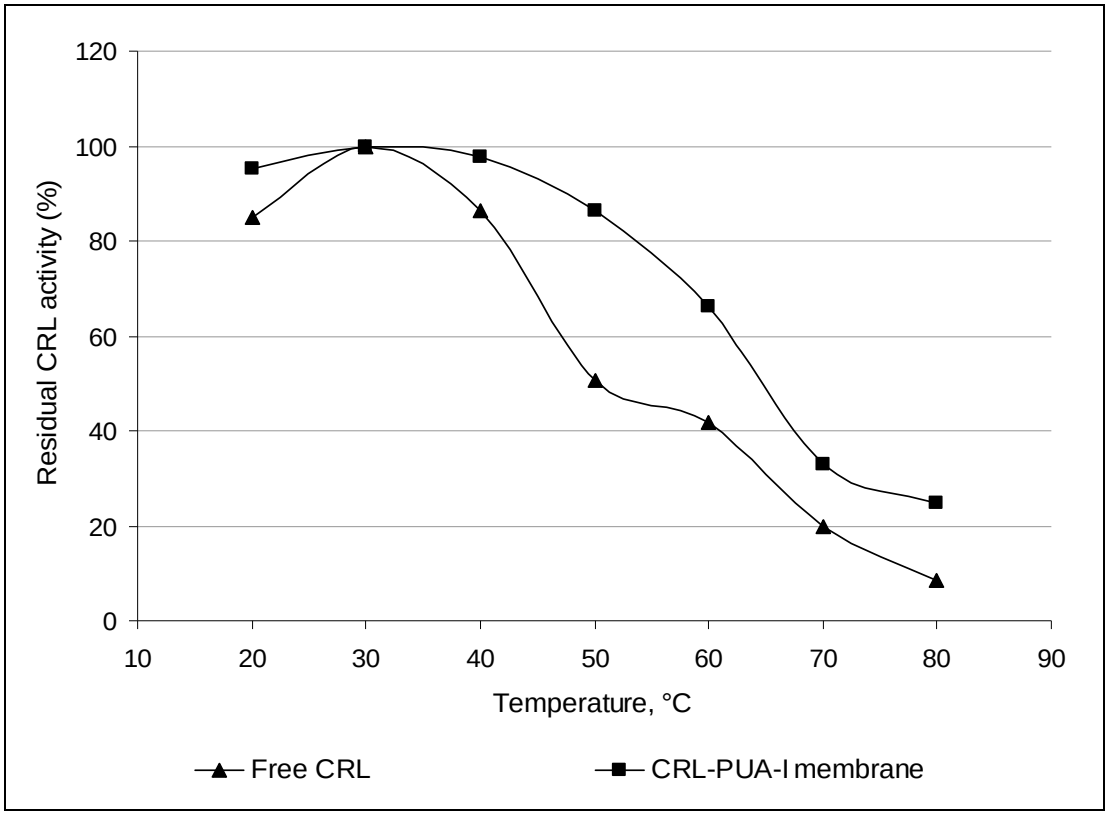

Fig. 3.5: Temperature stability of CRL-PUA-I membrane

The effect of temperature on stability of free and immobilized PPL is given in Fig. 3.6. At 50°C the free enzyme retained only 63.17% residual activity while PPL-PUA-I membrane retained 91.66% of its initial activity. Likewise at 60°C the free enzyme retained 41.40% residual activity while PPL-PUA-I membrane retained

67.25% residual activity. Fig. 3.5 and Fig. 3.6 indicate that this method of lipase immobilization conferred moderate thermal stability to CRL and PPL.

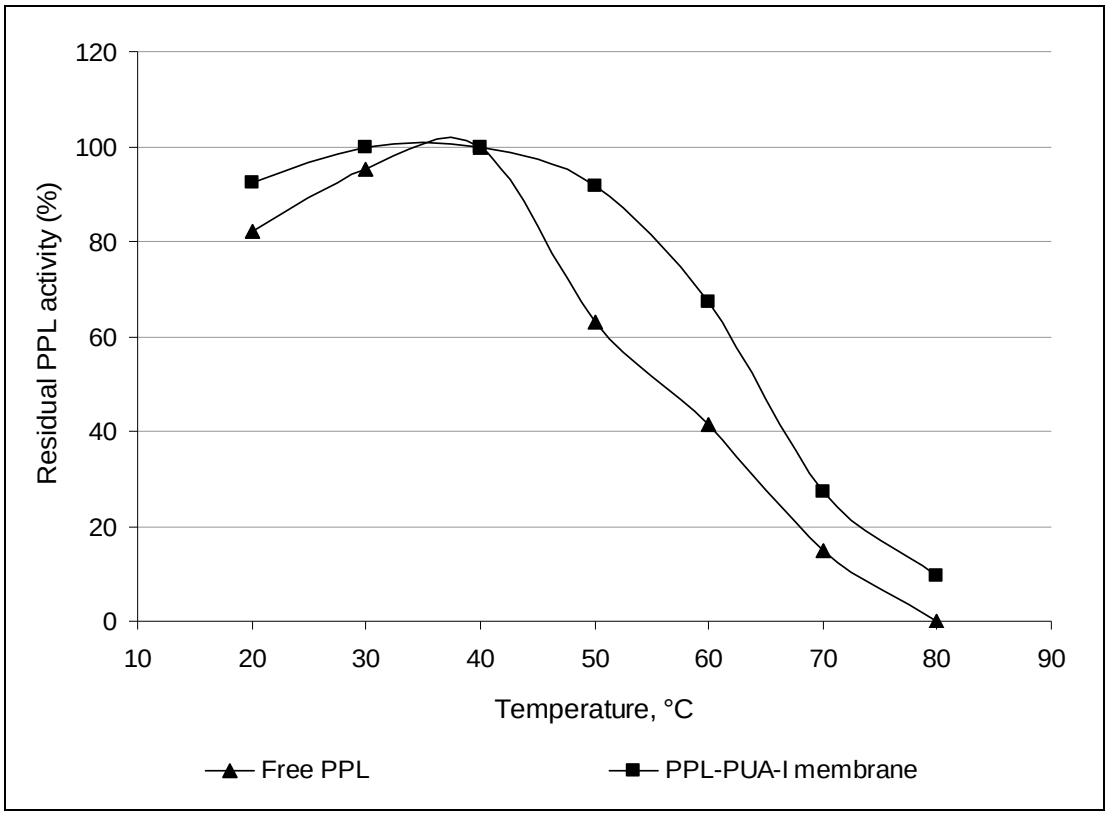

Fig. 3.6: Temperature stability of PPL-PUA-I membrane

Among previous reports, describing the immobilization of CRL and PPL on membrane, few have evaluated the stability of an immobilized enzyme [17, 18, 38, 44, 47]. In general, the previous reports indicate a significant increase in enzyme's stability upon immobilization which has been our observation as well. However, it is difficult to compare present results with results reported earlier since the experimental conditions (such as source of lipase, substrate used, substrate concentration, method of immobilization, storage conditions etc.) vary to a great extent.

3.3.4. Performance of EMB

(a) Synthetic activity and reusability of CRL-PUA-I

The synthetic activity of lipase in organic solvents has shown broad substrate specificity as has been demonstrated with many unnatural substrates [48]. Lipase elicits a major interest in synthetic organic chemistry compared to its hydrolytic activity. It has been observed that lipase with very high hydrolytic activity need not

express a corresponding high degree of synthetic activity and vice versa [49, 50]. Therefore, synthetic activity of lipase was evaluated along with hydrolytic activity.

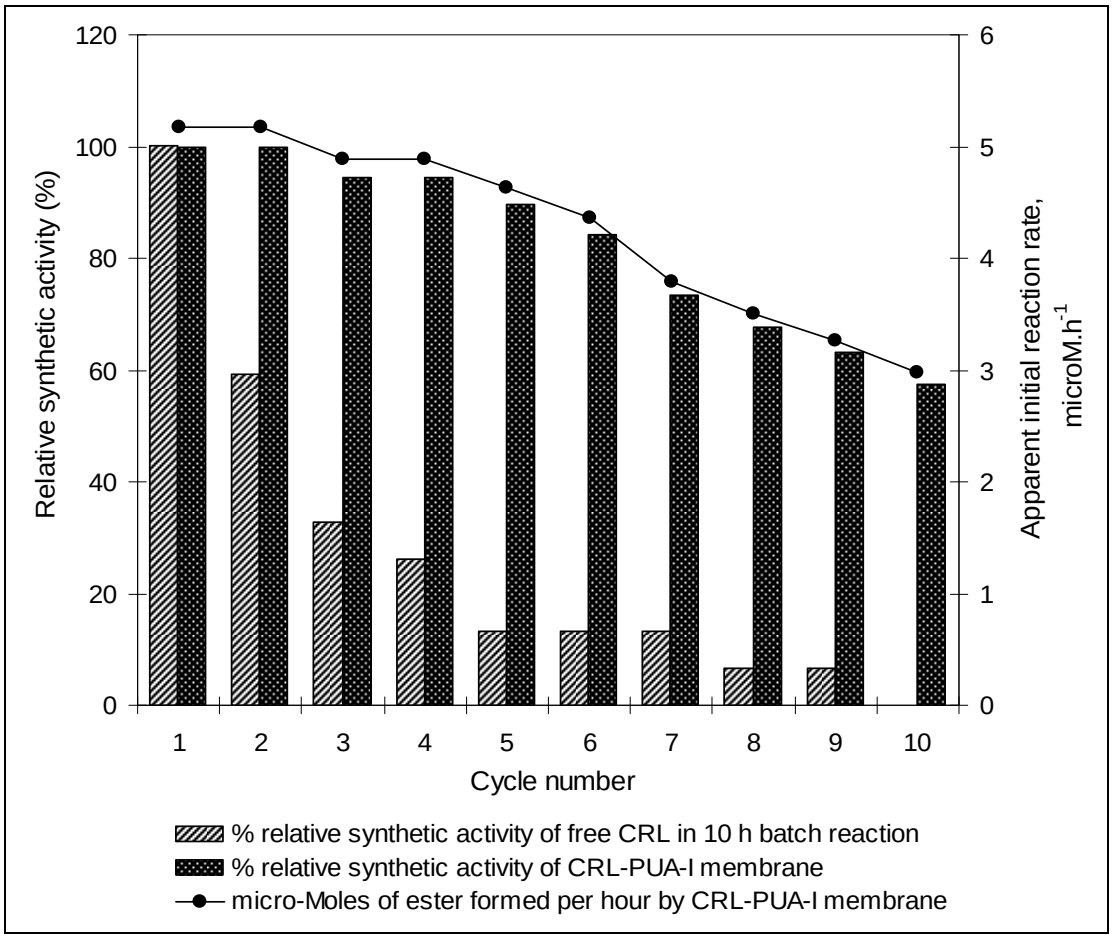

Fig. 3.7: Performance of CRL-PUA-I membrane in oleic acid esterification reaction

Esterification of oleic acid with octanol was studied initially to estimate the synthetic activity of lipases in organic medium. This reaction was repeated for ten consecutively cycles, using fresh substrate each time to evaluate the stability and reusability of immobilized biocatalytic membrane (CRL-PUA-I). Fig. 3.7 shows comparison of synthetic activity of free lipase and immobilized biocatalytic membrane. For the first two esterification cycles the biocatalytic membrane retained almost 100% of synthetic activity; thereafter, a steady reduction in synthetic activity was observed. However, the membrane retained 84.2% and 57.5% of its initial synthetic activity after 5th and 10th consecutive esterification cycle, respectively. Free CRL, on the other hand, retains only 13.1% of its activity after 5 h and loses all its synthetic activity after 10 h.

The simplicity of the EMB provided a useful tool to study biotransformation reactions. The biocatalytic activity of immobilized biocatalyst decreased with time and number of reaction cycles due to enzyme denaturation. Therefore, the initial reaction rate is a crucial parameter, which needs to be determined in order to calculate the residence time of reaction mixture in the EMB. Fig. 3.7 shows the initial velocity of the esterification reaction. The initial reaction rates are expressed for 1 cm^2 biocatalytic membrane in terms of $\mu M \cdot h^{-1} \cdot cm^{-2}$. After ten cycles the initial velocity decreased from 5.17 to 2.97 $\mu M \cdot h^{-1} \cdot cm^{-2}$ with corresponding decrease observed for synthetic activity.

(b) Synthetic activity and reusability of PPL-PUA-I

Fig. 3.8 shows comparison of synthetic activity of free lipase and PPL-PUA-I membrane.

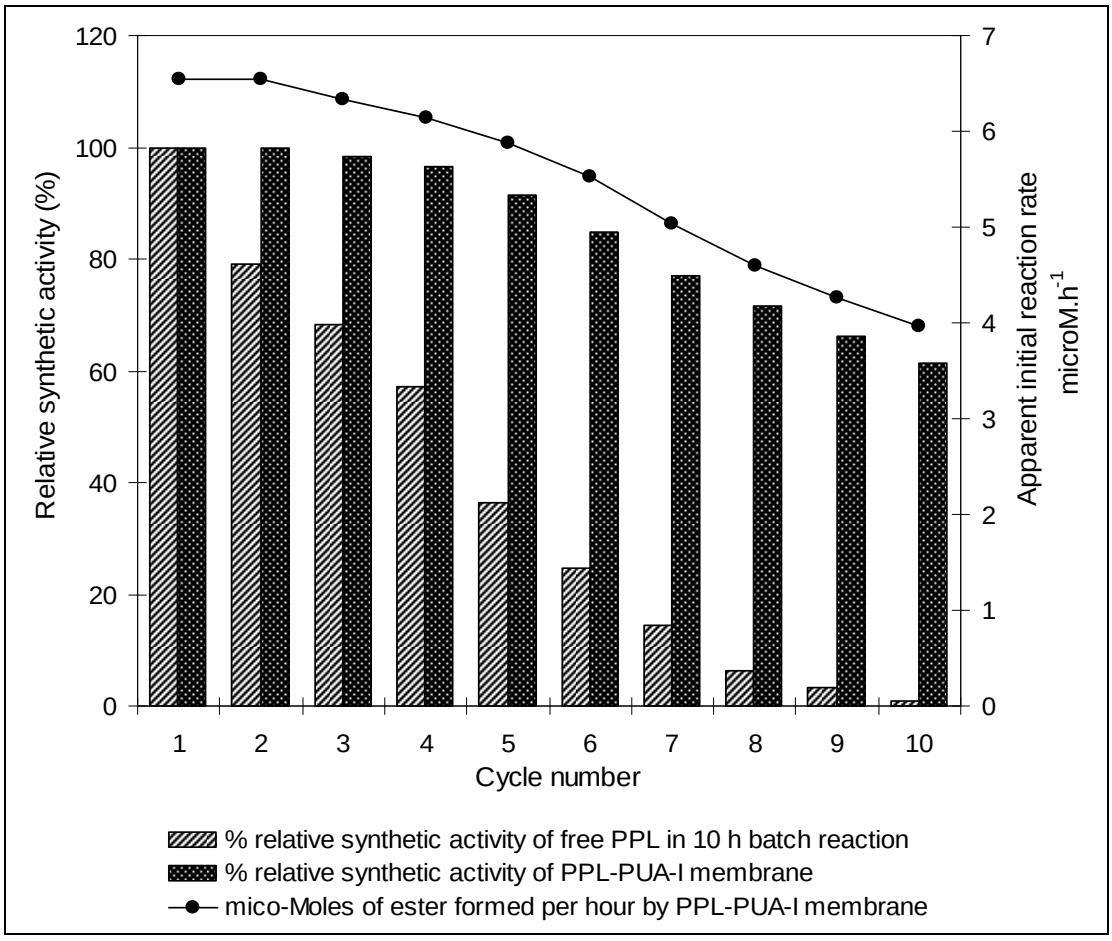

Fig. 3.8: Performance of PPL-PUA-I membrane in oleic acid esterification reaction

For the first two esterification cycles the biocatalytic membrane retained almost 100% of synthetic activity; thereafter, a steady moderate reduction in synthetic activity was observed. However, the membrane retained 91.38% and 61.43% of its initial synthetic activity after 5th and 10th consecutive esterification cycles, respectively. Free PPL, on the other hand, retained only 36.46% and 0.83% of its initial activity after 5 h and 10 h. Fig. 3.8 also shows the initial velocity of the esterification reaction. After ten cycles the initial velocity decreased from 6.55 to 3.96 $\mu M \cdot h^{-1} \cdot cm^{-2}$ with corresponding decrease observed for synthetic activity.

(c) Study of enzyme release from membrane

The remaining reaction mixture after an esterification cycle (catalyzed by CRL-PUA-I membrane) was stored at 20°C for 24 h. The unreacted oileic acid content in the reaction mixture was found to be the same after 24 h. If the lipase would have leached from membrane surface, unreacted oleic acid would have been further reduced in 24 h. The results confirm that CRL binding on PUA-I membrane was irreversible and stable. An identical experiment was conducted for PPL-PUA-I membrane. The unreacted oileic acid content in the reaction mixture was found to be the same after 24 h, indicating here too the PPL binding on PUA-I membrane was irreversible and stable.

3.3.5. Chiral resolution of unnatural amino acid esters

The chiral resolution of unnatural amino acid ethyl esters catalyzed by membrane immobilized lipases is represented in Scheme 3.2.

Scheme 3.2: Chiral resolution of unnatural amino acid ethyl esters by biocatalytic membranes

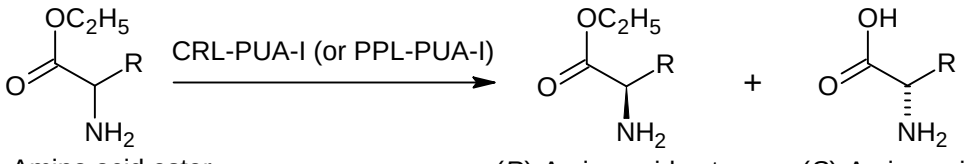

(*RS*)-Amino acid ester (*R*)-Amino acid ester (*S*)-Amino acid

	PG	DOPA	HPA	NA
R-	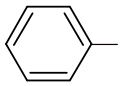	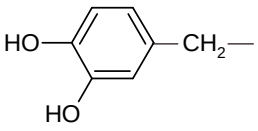	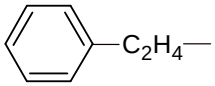	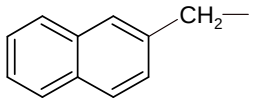

(a) CRL-PUA-I catalyzed chiral resolution of amino acid ethyl esters

The enantioselectivity of an enzyme was determined in terms of enantiomeric ratio (*E*). The results of stereoselective hydrolysis of unnatural amino acid ethyl esters using CRL-PUA-I are summarized in Table 3.7. The enantiomeric ratios of CRL-PUA-I towards hydrolysis of PG-ester, DOPA-ester, HPA-ester were 11.3, 10.3 and 14.4 respectively. CRL-PUA-I showed relatively poor enantioselectivity towards hydrolysis of NA-ester (*E* = 4.7).

Table 3.7: Chiral resolution of ethyl esters of unnatural amino acids using CRL-PUA-I membrane

Substrate	**Preferred configuration**	**Time** (min)	**ee$_p$** (%)	***C*** (%)	***E***
PG-ester	*S*	30	82.4	9.2	11.3
DOPA-ester	*S*	30	81.3	7.1	10.3
HPA-ester	*S*	30	85.7	10.6	14.4
NA-ester	*S*	30	62.7	11.8	4.7

(b) PPL-PUA-I catalyzed chiral resolution of amino acid ethyl esters

The results of stereoselective hydrolysis of unnatural amino acid ethyl esters using PPL-PUA-I are summarized in Table 3.8. The enantiomeric ratios of PPL-PUA-I towards hydrolysis of PG-ester, DOPA-ester, HPA-ester were 6.9, 4.5 and 3.7 respectively. PPL-PUA-I showed relatively higher enantioselectivity towards hydrolysis of NA-ester (*E* = 4.7) than that of PG-ester, DOPA-ester, HPA-ester.

Table 3.8: Chiral resolution of ethyl esters of unnatural amino acids using PPL-PUA-I membrane

Substrate	**Preferred configuration**	**Time** (min)	**ee$_p$** (%)	***C*** (%)	***E***
PG-ester	*S*	30	72.4	12.2	6.9
DOPA-ester	*S*	30	61.5	10.7	4.5
HPA-ester	*S*	30	55.2	9.4	3.7
NA-ester	*S*	30	86.4	11.1	15.2

(c) Reusability of biocatalytic membrane

The reusability of CRL-PUA-I was verified by running the EMB in repetitive batch mode. The hydrolysis of HPA-ester was repeated for five consecutively cycles, using same biocatalytic membrane but fresh substrate each time. Fig. 3.9 shows initial reaction rate and reaction time of five repeated cycles.

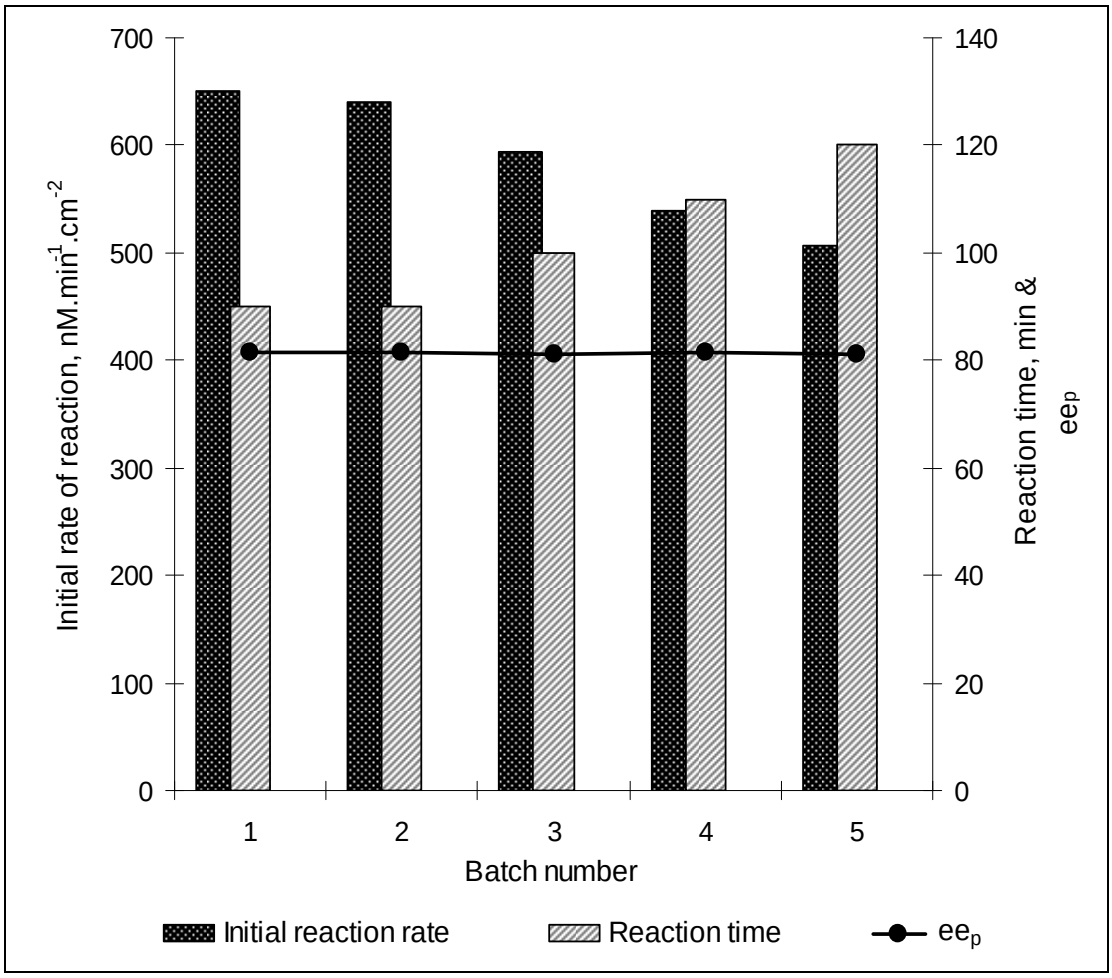

Fig. 3.9: CRL-PUA-I catalyzed hydrolysis of HPA-ester in five repeated cycles

The initial reaction rate is expressed for 1 cm^2 biocatalytic membrane in terms of $nM \cdot min^{-1} \cdot cm^{-2}$. The first cycle proceeded with initial reaction rate of 650.7 $nM \cdot min^{-1} \cdot cm^{-2}$ and ee_p of 81.5% was attained at 90 min. Thereafter the initial reaction rate, in successive cycles, found to decrease gradually from 650.7 to 506.2 $nM \cdot min^{-1} \cdot cm^{-2}$ indicating some loss of enzyme activity during each cycle. In order to maintain the ee_p (>81%) in each successive cycle, the reaction time was accordingly extended. The 5^{th} cycle therefore finished at 120 min.

The results of five repetitive cycles of NA-ester hydrolysis catalyzed by PPL-PUA-I membrane are given in Fig. 3.10. It shows initial reaction rate and reaction time of five repeated cycles. The first cycle proceeded with initial reaction rate of 480.5 $nM \cdot min^{-1} \cdot cm^{-2}$ and ee_p of 83.1% was attained at 120 min. Thereafter the initial reaction rate, in successive cycles, found to decrease gradually from 480.5 to 386.9 $nM \cdot min^{-1} \cdot cm^{-2}$ indicating some loss of enzyme activity during each cycle. In order to maintain ee_p (>83) in each successive cycle, the reaction time was accordingly extended. The 5th cycle therefore finished at 160 min.

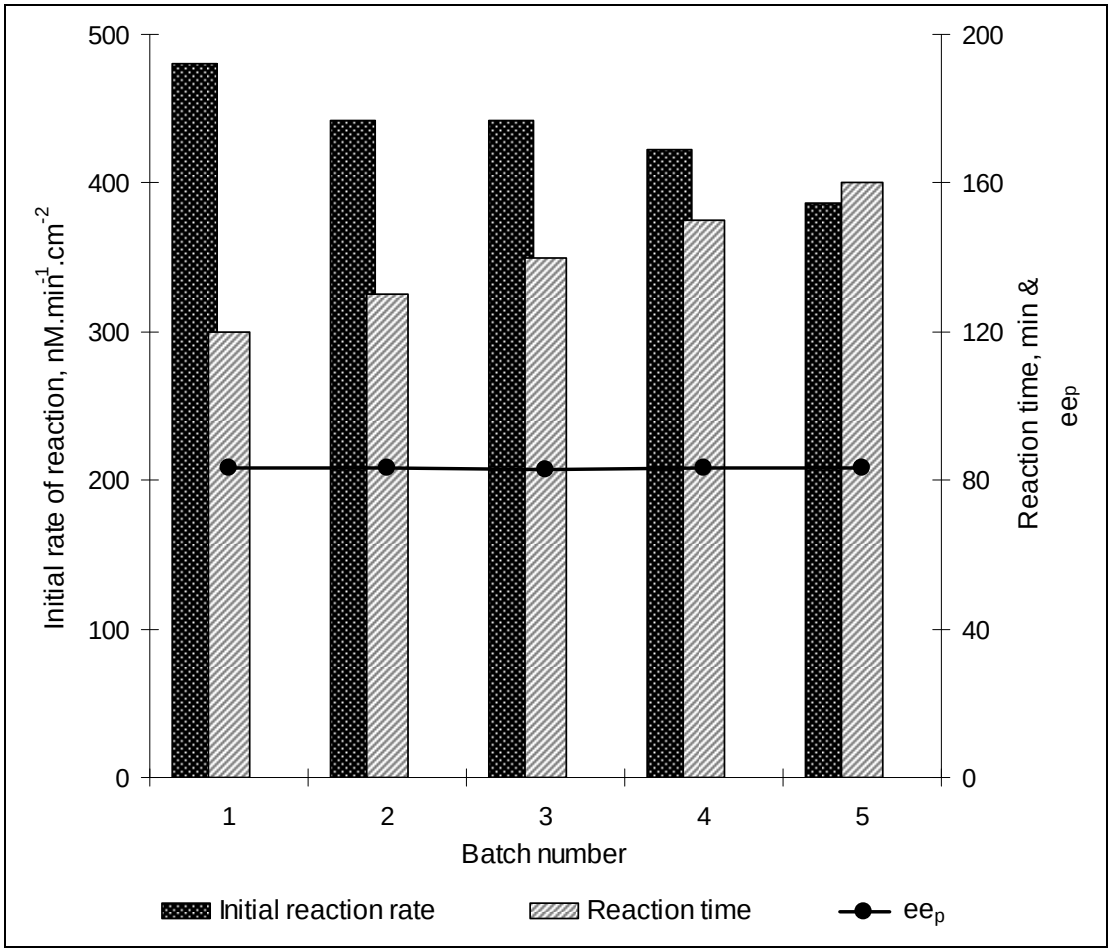

Fig. 3.10: PPL-PUA-I catalyzed hydrolysis of NA-ester in five repeated cycles

Membrane immobilized lipases have been used for a chiral resolution of several drugs and drug intermediates such as ibuprofen [47, 51-53], naproxen [13, 54], 2-(2-fluoro-4-biphenyl) propanoic and (4-isobutylphenyl) propanoic acids [55], *trans*-2-methyl-1-cyclohexanol [56] etc. However, to the best of our knowledge, enantioselective synthesis of PG, DOPA, HPA and NA has not yet been studied using

EMB. The high protein binding capacity, high activity and improved operational stability of CRL-PUA-I and PPL-PUA-I membranes are the promising features of the present study. However, the low enantiomeric ratios ($E < 20$) of immobilized lipases (CRL as well as PPL) towards hydrolysis of different unnatural amino acid ethyl esters suggest a limited utility of these biocatalysts.

3.4. CONCLUSIONS

A blend of polyurethane (meth)acrylate and GMA was coated and cured on a PP membrane to have better surface hydrophilicity, biocompatibility, strength and chemical stability. This membrane has excellent protein binding capacity hence can be used for enzyme immobilization. Under optimum conditions, the biocatalytic membranes (CRL-PUA-I and PPL-PUA-I), showed high activity recovery (about 90% and 91% respectively) and high retention of specific activity (about 92% and 96% respectively). Furthermore these biocatalytic membranes showed better stability over a wider range of pH and temperature than that of free enzyme. CRL-PUA-I showed maximum enantioselectivity towards hydrolysis of PG-ester, DOPA-ester and HPA-ester (E = 11.3, 10.3 and 14.4 respectively) while PPL-PUA-I showed maximum enantioselectivity towards hydrolysis of NA-ester (E = 15.2). Moreover, CRL-PUA-I and PPL-PUA-I exhibited high operational stability during repetitive hydrolytic cycles of HPA-ester and NA-ester respectively.

REFERENCES

[1] Brady, D.; Steenkamp, L.; Skein, E.; Chaplin, J.A.; Reddy S. Optimization of the enantioselective biocatalytic hydrolysis of naproxen ethyl ester using ChiroCLEC-CR. *Enzyme Microb. Technol.*, **2004**, *34*, 283-291.

[2] Balcão, V.M.; Paiva, A.L.; Malcata, F.X. Bioreactors with immobilized lipases: state of the art. *Enzyme Microb. Technol.*, **1996**, *18*, 392-416.

[3] Gekas, V.C. Artificial membranes as carriers for the immobilization of biocatalysts. *Enzyme Microb. Technol.*, **1986**, *8*, 450-60.

[4] Giorno, L.; Drioli, E. Biocatalytic membrane reactors: applications and perspectives. *Trends Biotechnol.*, **2000**, *18*, 339-349.

[5] Hilal, N.; Nigmatullin, R.; Alpatova, A. Immobilization of cross-linked lipase aggregates within microporous polymeric membranes. *J. Membr. Sci.*, **2004**,

238, 131-141.

[6] Magnan, E.; Catarino, I.; Paolucci-Jeanjean, D.; Preziosi-Belloy, L.; Belleville, M.P. Immobilization of lipase on a ceramic membrane: activity and stability. *J. Membr. Sci.*, **2004**, *241*, 161-166.

[7] Yesiloğlu, Y. Utilization of bentonite as a support material for immobilization of *Candida rugosa* lipase. *Process Biochem.*, **2005**, *40*, 2155-2159.

[8] Straathof, A.J.J.; Panke, S.; Schmid, A. The production of fine chemicals by biotransformation. *Curr. Opin. Biotechnol.*, **2002**, *13*, 548-556.

[9] Hilal, N.; Kochkodan, V.; Nigmatullin, R., Goncharuk, V., Al-Khatib, L. Lipase-immobilized biocatalytic membranes for enzymatic esterification: Comparison to various approaches to membrane preparation. *J. Membr. Sci.*, **2006**, *268*, 198-207.

[10] Balcao, V.M.; Vieira, C.; Malcata, F.X. Adsorption of protein from several commercial lipase preparations onto a hollow fiber membrane module. *Biotechnol. Prog.*, **1996**, *12*, 164-172.

[11] Indlekofer, M.; Funke, M.; Claassen, W.; Reuss, M. Continuous enantioselective transesterification in organic solvents: use of suspended lipase preparations in a microfiltration membrane reactor. *Biotechnol. Prog.*, **1995**, *11*, 436-442.

[12] Lozano, P.; Pérez-Marín, A.B.; De Diegoa, T.; Gómez, D.; Paolucci-Jeanjean, D.; Belleville, M.P.; Rios, G.M.; Iborra, J.L. Active membranes coated with immobilized *Candida antarctica* lipase B: Preparation and application for continuous butyl butyrate synthesis in organic media. *J. Membr. Sci.*, **2002**, *201*, 55-64.

[13] Sakaki, K.; Giorno, L.; Drioli, E. Lipase-catalyzed optical resolution of racemic naproxen in biphasic enzyme membrane reactors. *J. Membr. Sci.*, **2001**, *184*, 27-38.

[14] Sarada, L.; Desnuelle, P. Action de la lipase pancreatique sur les esters en emulsion. *Biochim. Biophys. Acta*, **1958**, *30*, 513-521.

[15] Deng, H.T.; Xu, Z. K.; Liu, Z. M.; Wu, J.; Ye, P. Adsorption immobilization of *Candida rugosa* lipases on polypropylene hollow fiber microfiltration membranes modified by hydrophobic polypeptides. *Enzyme Microb. Techol.*, **2004**, *35*, 437-443.

[16] Bouwer, S.T.; Cuperus, F.P.; Derksen, J.T.P.; The performance of enzyme-

membrane reactors with immobilized lipase. *Enzyme Microb. Technol.*, **1997**, *21*, 291-296.

[17] Deng, H.; Xu, Z.; Dai, Z.; Wu, J.; Seta, P. Immobilization of *Candida rugosa* lipase on polypropylene microfiltration membrane modified by glycopolymer: hydrolysis of olive oil in biphasic bioreactor. *Enzyme Microb. Technol.*, **2005**, *36*, 996-1002.

[18] Bayramoğlu, G.; Kacar, Y.; Denizli, A.; Arica, M.Y. Covalent immobilization of lipase onto hydrophobic group incorporated poly(2-hydroxyethyl methacrylate) based hydrophilic membrane matrix. *J. Food. Eng.*, **2002**, *52*, 367-374.

[19] Arica, M.Y. Epoxy-derived pHEMA membrane for use bioactive macromolecules immobilization: covalently bound urease in a continuous model system. *J. Appl. Polym. Sci.*, **2000**, *77*, 2000-2008.

[20] Rios, G.M.; Belleville, M.P.; Paolucci, D.; Sanchez, J. Progress in enzymatic membrane reactors. *J. Membr. Sci*., **2004**, *242*, 189-196.

[21] Hsieh, K.H.; Kuo, C.H.; Dai, C.A.; Chen, W.C.; Peng, T.C.; Ho, G.H. Synthesis and kinetic studies of UV-curable urethane-acrylates. *J. Appl. Polym. Sci.*, **2004**, *91*, 3162-3166.

[22] Huang, L.L.; Lee, P.C.; Chen, L.; Hsieh, K.H. Comparison of epoxides on grafting collagen to polyurethane and their effects on cellular growth. *J. Biomed. Mater. Res.*, **1997**, *39*, 630-636.

[23] Mateo, C.; Ferna´ndez-Lorente, G.; Abian, O.; Ferna´ndez-Lafuente, R.; Guisán, J.M. Multifunctional epoxy supports: A new tool to improve the covalent immobilization of proteins. The promotion of physical adsorptions of proteins on the supports before their covalent linkage. *Biomacromolecules,* **2000**, *1*, 739-745.

[24] Hepurn, C. Polyurethane Elastomers. Applied Science Publishing Ltd, London, **1982**.

[25] Pujari, N.S.; Vishwakarma, A.R.; Pathak, T.S.; Kotha, A.M.; Ponrathnam, S. Functionalized polymer networks: synthesis of microporous polymers by frontal polymerization. *Bull. Mater. Sci.*, **2004**, *27*, 529-535.

[26] Decker, C.; The use of UV irradiation in polymerization. *Polym. Int.*, **1998**, *45*, 133-141.

[27] Bodanszky, M.; Bodanszky, A. *In*: The Practice of Peptide Synthesis. Springer-Verlag, Berlin, **1984**.

[28] Lee, H.; Neville, K. Handbook of Epoxy Resins. McGraw-Hill Book Company, New York, **1967**, pp. 4-5.

[29] Winkler, U.K.; Stuckmann, M. Glycogen, hyaluronate, and some other polysaccharides greatly enhance the formation of exolipase by *Serratia marcescens*. *J. Bacteriol.*, **1979**, *138*, 663-670.

[30] Lowry, O.H.; Roseburgh, N.; Farr, A.L.; Randall, R. Protein measurement with the phenol reagent. *J. Biol. Chem*., **1951**, *193*, 265-275.

[31] Soares, C.M.F.; Santana, M.H.A.; Zanin, G.M.; de Castro, H.F. Covalent coupling method for lipase immobilization on controlled pore silica in the presence of nonenzymatic proteins. *Biotechnol. Prog.*, **2003**, *19*, 803-807.

[32] Yong, Y.P.; Al-Duri, B. Kinetic studies on immobilized lipase esterification of oleic acid and octanol. *J. Chem. Tech. Biotechnol.*, **1996**, *65*, 239-248.

[33] Pamedytyte, V.; Abadie, M.J.M.; Makuska, R. Photopolymerization of *N*,*N*-dimethylaminoethyl methacrylate studied by photocalorimetry. *J. Appl. Polym. Sci.*, **2002**, *86*, 579-588.

[34] Yujun, W.; Jian, X.; Guangsheng, L.; Youyuan, D. Immobilization of lipase by ultrafiltration and cross-linking onto the polysulfone membrane surface. *Bioresource Technol.*, **2008**, *99*, 2299-2303.

[35] Anna, T.H.; Noworyta, A. Catalytic membrane preparation for enzymatic hydrolysis reactions carried out in the membrane phase contactor. *Desalination*, **2002**, *144*, 427-432.

[36] Tsai, S.W.; Shaw, S.S. Selection of hydrophobic membranes in the lipase-catalyzed hydrolysis of olive oil. *J. Membr. Sci.*, **1998**, *146*, 1-8.

[37] Hoq, M.M.; Yamane, T.; Shimidzu, S. Continuous hydrolysis of olive oil by lipase in microporous hydrophobic membrane bioreactor. *J. Am. Oil Chem. Soc.*, **1985**, *62*, 1016-1021.

[38] Hoq, M.M.; Yamane, T.; Shimidzu, S. Continuous hydrolysis of olive oil by lipase in microporous hydrophobic hollow fiber bioreactor. *Agric. Biol. Chem.*, **1985**, *49*, 3171-3178.

[39] Xu, J.; Wang, Y.; Hu, Y.; Luo, G.; Dai, Y. *Candida rugosa* lipase immobilized by a specially designed microstructure in the PVA/PTFE composite membrane.

J. Membr. Sci., **2006**, *281*, 410-416.

[40] Goto, M.; Goto, M.; Nakashio, F.; Yoshizuka, K.; Inoue, K. Hydrolysis of triolein by lipase in a hollow fiber reactor. *J. Membr. Sci.*, **1992**, *74*, 207-211.

[41] Deng, H.T.; Xu, Z.K.; Wu, J.; Ye, P.; Liu, Z.M.; Seta, P. A comparative study on lipase immobilized polypropylene microfiltration membranes modified by sugar-containing polymer and polypeptide. *J. Mol. Catal. B: Enzym.*, **2004**, *28*, 95-100.

[42] Giorno, L.; Molinari, R.; Natoli, M.; Drioli, E. Hydrolysis and regioselective transesterification catalyzed by immobilized lipases in membrane bioreactors. *J. Membr. Sci.*, **1997**, *125*, 177-187.

[43] Rucka, M.; Turkiewicz, B. Ultrafiltration membrane as carriers for lipase immobilization, *Enzyme Microb. Technol.*, **1990**, *12*, 52-55.

[44] Huang, X-J.; Yu, A-G.; Xu, Z-K. Covalent immobilization of lipase from *Candida rugosa* onto poly(acrylonitrile-co-2-hydroxyethyl methacrylate) electrospun fibrous membranes for potential bioreactor application. *Bioresource Technol.*, **2008**, *99*, 5459-5465.

[45] Ye, P.; Xu, Z-K.; Wu, J.; Innocent, C.; Seta, P. Nanofibrous membranes containing reactive groups: Electrospinning from poly(acrylonitrile-co-maleic acid) for lipase immobilization. *Macromolecules*, **2006,** *39,* 1041-1045.

[46] Pugazhenthi, G.; Kumar A. Enzyme membrane reactor for hydrolysis of olive oil using lipase immobilized on modified PMMA composite membrane. *J. Membr. Sci.*, **2004**, *228*, 187-197.

[47] Wang, Y.; Hu, Y.; Xu, J.; Luo, G.; Dai, Y. Immobilization of lipase with a special microstructure in composite hydrophilic CA/hydrophobic PTFE membrane for the chiral separation of racemic ibuprofen. *J. Membr. Sci.*, **2007**, *293*, 133-141.

[48] Zoete, M.C.; van Rantwtjk, F.; Sheldon, R.A. Lipase-catalyzed transformation with unnatural acyl-acceptors. *Catal. Today*, **1994**, *22*, 563-590.

[49] Cardenas, F.; de Castro, M.S.; Sanchez-Montero, J.M.; Sinisterra, J.V.; Valmaseda, M.; Elson, S.W.; Alvarez, E. Novel microbial lipases: catalytic activity in reactions in organic media. *Enzyme Microb. Techol.*, **2001**, *28*, 145-154.

[50] Furutani, T.; Su, R.; Ooshima, H.; Kato, J. Simple screening method for lipase

transesterification in organic solvent. *Enzyme Microb. Technol.*, **1995**, *17*, 1067-1072.

[51] Long, W.S.; Kamaruddin, A.H.; Bhatia, S. Chiral resolution of racemic ibuprofen ester in an enzymatic membrane reactor. *J. Membr. Sci.*, **2005**, *247*, 185-200.

[52] Long, W.S.; Kow, P.C.; Kamaruddin, A.H.; Bhatia, S. Comparison of kinetic resolution between two racemic ibuprofen esters in an enzymic membrane reactor. *Process Biochem.*, **2005**, *40*, 2417-2425.

[53] Long, W.S.; Kamaruddin, A.H.; Bhatia, S. Enzyme kinetics of kinetic resolution of racemic ibuprofen ester using enzymatic membrane reactor. *Chem. Eng. Sci.*, **2005**, *60*, 4957-4970.

[54] Giorno, L.; Li, N.; Drioli, E.; Use of stable emulsion to improve stability, activity, and enantioselectivity of lipase immobilized in a membrane reactor. *Biotechnol. Bioeng.*, **2003**, *84(6)*, 677-685.

[55] Ceynowa, J.; Rauchfleisz, M. High enantioselective resolution of racemic 2-arylpropionic acids in an enzyme membrane reactor. *J. Mol. Catal. B: Enzym.*, **2003**, *23*, 43-51.

[56] Ceynowa, J.; Rauchfleisz, M. Resolution of racemic *trans*-2-methyl-1-cyclohexanol by lipase-catalysed transesterification in a membrane reactor. *J. Mol. Catal. B: Enzym.*, **2001**, *15*, 71-80.

CHAPTER

4 Chiral resolution of unnatural amino acid amides using immobilized resting cells of *Rhodococcus erythropolis* MTCC 1526

4.1. INTRODUCTION

Amidase (acylamide amidohydrolases; EC 3.5.1, 3.5.2) catalyzes the hydrolysis of carboxylic acid amides to free carboxylic acids and ammonium [1]. The enzyme is widely distributed in almost all kingdoms of living world [2]. The exact physiological role of amidase is not yet clearly understood, however in some species amidase (along with nitrile hydratase) is found to be involved in the utilization of nitrogen from nitriles. In recent years, amidase have gained considerable interest in the diverse research fields like chirotechnology, neurobiochemistry and plant physiology [3].

Microbial amidases have emerged as important industrial biocatalyst. For example, amidase catalyzed synthesis of acrylamide and acrylic acid is one of the largest industrial biotransformations in the world [4]. Moreover, a wide range of commercially useful chemicals can be synthesized by using microbial amidases [5-9]. Microbial amidases are abundant in Rhodococci, Nocardia and Arthrobacteria. Rhodococcal amidases exhibit stereoselectivity towards hydrolysis of amides of α-substituted carboxylic acids [1].

Rhodococcal amidase (and nitrile hydratase) in form of whole cell biocatalyst has been studied for synthesis of several commercially important chemicals. For example, amidase from *Rhodococcus erythropolis* NCIMB11540 was used for synthesis of α-hydroxy carboxylic acids [10] and that from *R. erythropolis* ATCC 25544 was used for synthesis of 2,2-dimethylcyclopropane carboxylic acid [11]. Phenylpropionic acid and lysergic acid were synthesized using *Rhodococcus equi* TG328 [12] and *Rhodococcus equi* A4 [13] respectively. Amidase from *R. erythropolis* AJ270 has been extensively studied for synthesis of several useful chemicals such as azetidine-2-carboxylic acids [14], α-substituted phenylacetamides [15], derivatives of 3-arylaziridine-2-carboxamide [16] and (*S*)-ibuprofen [17]. *Rhodococcus erythropolis* MP50 whole-cell amidase has been used for synthesis of enantiopure 2-arylpropionic acids *namely* naproxen [18, 19, 20], ibuprofen [20] and ketoprofen [21]. The amidase (and nitrile hydratase) catalyzed stereoselective transformations are summarized in comprehensive reviews by Fournand and Arnaud [2] and Martínková and Křen [22].

Nitrile hydratase (EC 4.2.1.84) along with amidase can catalyze the unique conversion of nitrile to corresponding enatiopure carboxylic acid. Several α-amino

acids have been synthesized using nitrile hydratase-amidase system. Rhodococcus cells have been thoroughly studied for synthesis of enantiopure natural and unnatural amino acids. For example, Enantioselective synthesis of several α-amino acids is reported by Beard and Page [23]. Wang and Lin reported enantioselective synthesis of L-phenylglycine and other α-amino acids using *Rhodococcus* sp. AJ270 cells [24, 25]. In another report, immobilized *Rhodococcus* sp. (NOVO SP. 361) was used for enantioselective synthesis of D-phenylglycine [26]. Wang *et al.* used whole cell biocatalyst of *Rhodococcus* sp. AJ270 for synthesis of several α-methylamino acids [8]. The synthesis of α-amino acids reported in all these reports involves two sequential steps *viz*. (i) nitrile hydratase catalyzed conversion of α-amino nitrile to α-amino acid amide and (ii) amidase catalyzed conversion of α-amino acid amide to α-amino acid.

In spite of being an elegant system, the two-step bioconversion of α-amino nitrile to α-amino acid incurs serious practical limitation due to the chemical instability of substrates (nitriles). The α-amino nitriles undergo spontaneous degradation into aldehyde and ammonia via a retro-Strecker reaction [27, 28]. This decomposition is difficult to control as it takes place readily even under mild conditions (e.g. pH 7) at which the enzymatic reactions are usually carried out. Using low nitrile concentration (roughly in range of 0.5-1.5 mM) can partially reduce the problem of decomposition, however this decreases the overall yield of product thereby making the reaction unsuitable for large scale conversions [7, 29]. Moreover, nitrile hydratase generally exhibit lower enantioselectivity than amidase [30].

The main objective of present work was to evaluate the usefulness of Rhodococcal amidase for synthesis of enatiopure unnatural amino acids (*namely*: phenylglycine, homophenylalanine and naphthylalanine) from their corresponding amides. Rhodococcal cells contain a large set of enzymes that allow them to carry out large number of bioconversions and degradations. The broad catabolic diversity of rhodococci is primarily related to the presence and mobilisation of large linear plasmids and further amplified due to the presence of multiple homologues of enzymes in catabolic pathways [31]. Therefore it is essential to direct the metabolic pathways of *Rhodococcus* cells towards production of desired enzyme(s). Hence to begin our study we identified and optimized the critical medium components to enhance the production of amidase.

In order to make a fermentative process commercially viable, it is necessary to improve the yield in a cost effective manner. One of the methods for achieving the above objective is selection of appropriate media components and optimal culture conditions. Thus, the optimization of fermentation conditions is generally regarded as a crucial step in the development of a cost-effective fermentation process [32].

The conventional method of medium optimization involves changing one parameter at a time and keeping the others at fixed levels. This method is laborious and time consuming [32]. Furthermore, being linear in nature, the conventional method is incapable of determining interactive effects of operational variables during the fermentation process and therefore, unable to predict the 'true' optimum [33]. The limitations of the one-factor-at-a-time optimization can be eliminated by employing statistical optimization methods. Among the different statistical based approaches, Response Surface Methodology (RSM) has been extensively used for media optimization. RSM is a collection of statistical techniques which uses Design of Experiments (DoE) for building models, evaluating the interactive effects of factors and searching for the optimum conditions. It is a statistically designed experimental protocol in which several factors are simultaneously varied [34]. In biotechnology, the technique has been used for broad range of primary as well as secondary microbial metabolites *viz*. acids [32, 35], enzymes [33, 36], biosurfactants [37, 38], terpenoids [39] etc. However, to the best of our knowledge, such a detailed study has not yet been reported for Rhodoccocal amidase.

Seven *Rhodococcus* strains were screened for amidase production and *Rhodococcus erythropolis* MTCC 1526 was selected for further experiments. The systematic and sequential optimization strategy was adopted to enhance the production of amidase from *R. erythropolis* MTCC 1526. An optimal media composition for production of amidase was achieved in following three steps: (i) Screening of optimum carbon source, nitrogen source and inducer, (ii) Use of a Plackett–Burman experimental design to select the most influential media components (iii) Use of face-centre central composite design (FCCCD) of response surface methodology for optimization of critical media constituents. *R. erythropolis* MTCC 1526 cells with enhanced amidase activity were immobilized by different gel entrapment methods. Cells entrapped in alginate matrix and polyvinyl alcohol matrixes were used for chiral resolution of unnatural amino acid amides.

4.2. MATERIALS AND METHODS

4.2.1. Materials

The seven microbial strains *namely Rhodococcus erythropolis* MTCC 1526, 1548 and *Rhodococcus* spp. MTCC 2574, 2678, 2683, 2794 and 3951 were procured from MTCC-Chandigarh, India. All bacterial growth media components were purchased from Hi-Media, India. Unnatural amino acids *namely* phenylglycine (PG), homophenylalanine (HPA) and 2-naphthylalanine (NA) were purchased from Bachem Chemicals, Switzerland. All other chemicals were of analytical grade procured from S.D. Fine Chemicals, India.

4.2.2. Medium optimization for production of amidase

(a) Strain and cultivation conditions

All *Rhodococcus* strains were maintained on nutrient agar The liquid fermentation medium used for batch culture experiments contained (g/L): glucose (10), yeast extract (3), meat peptone (7.5), Na_2HPO_4 (4.0), KH_2PO_4 (2.0), $MgSO_4.7H_2O$ (0.2), $CaCl_2.2H_2O$ (0.02), ammonium ferric citrate (0.05), acetamide (10mM) and trace mineral solution (1 mL/L) [termed as medium A]. The composition of trace mineral medium was (g/L) H_3BO_3 (0.1), $MnCl_2 \cdot 4H_2O$ (0.1), $ZnSO_4 \cdot H2O$ (0.1), $FeCl_3 \cdot 6H_2O$ (0.1), $CaCl_2 \cdot 2H_2O$ (1), $CuCl_2 \cdot 2H_2O$ (0.05) [10].

(b) Effect of fermentation time for amidase production

Here, the amidase activities (U/g of dry cells) produced by seven *Rhodococcus* strains were studied at regular time intervals (24, 36 and 48 h) in order to determine the effect fermentation time on amidase production.

(c) Selection of optimum nitrogen source, carbon source and inducer

The components containing organic nitrogen (yeast extract and meat peptone) from medium A were replaced by inorganic nitrogen sources (*namely*: urea, ammonium sulphate and ammonium phosphate) at equivalent nitrogen level. To evaluate the optimum carbon source, glucose was replaced by equivalent amount of different carbon sources *namely* glycerol, sucrose, sorbitol and mannitol. Seven inducers (*namely*: acetamide, acetamido-phenol, acetamido-acetophenon, 4-acetamido-benzaldehyde, acetanilide, acrylamide and urea; 10mM each) were

screened to evaluate the enhancement in amidase production. Among seven different inducers, acetamide was found to give maximum amidase production and therefore selected for further experiments.

(d) Amidase activity profile for R. erythropolis MTCC 1526

The cell growth and intracellular amidase activity were simultaneously studied to determine the optimum fermentation time in shake flask fermentation. *Rhodococcus erythropolis* MTCC 1526 were grown on liquid medium containing (g/L) sorbitol (10.12), yeast extract (3), meat peptone (7.5), Na_2HPO_4 (4.0), KH_2PO_4 (2.0), $MgSO_4.7H_2O$ (0.2), $CaCl_2.2H_2O$ (0.02), ammonium ferric citrate (0.05), trace mineral solution (1 mL/L) and acetamide (10 mM) [termed as medium B]. The samples were aseptically removed at regular interval of 6 h up to 48 h and analyzed for optical density (600 nm), amidase activity (500 nm).

(e) Screening of critical media components using a Plackett–Burman design

A total of seven process variables comprising six media components (*namely*: sorbitol, yeast extract, meat peptone, Na_2HPO_4, KH_2PO_4 and acetamide) and one dummy variable were studied in Plackett–Burman screening experiments. Here, experiments were performed at various combinations of 'high' (H) and 'low' (L) values of the process variables and analyzed for their effects on the response of the process [40]. All trials were performed in duplicate and the average of amidase activity (U/ g of dry cells) was used as a response.

(f) Experimental design and data analysis

The concentrations of these four media components (sorbitol, yeast extract, meat peptone and acetamide) were optimized by using Face Centered Design (FCCCD) of RSM [34]. The value of the dependent response was the mean of two replications. The second order polynomial coefficients were calculated and analyzed using the trial version of 'Design Expert' software (Version 6.0, Stat-Ease Inc., USA).

4.2.3. Immobilization of R. erythropolis cells

(a) Agar entrapment of cells

The procedure was carried out according to the method described earlier by

Nilson *et al.* [41]. *R. erythropolis* cells (equivalent to 0.5 g dry weight) were uniformly suspended in 25 mL sterilized agar solution (4% w/v in physiological saline) at 50°C. This agar-cell mixture was added drop-wise under vigorously stirring to pre-warmed 250 mL paraffin oil at 40°C. This mixture was allowed to cool by itself, while stirring continued, and the emulsion slowly solidified. The cell-entrapped agar beads of approximately 2-3 mm thus obtained were washed with distilled water. The resultant biocatalytic matrix was termed as AGA-Re.

(b) Alginate entrapment of cells

The entrapment of cells in alginate was carried out according to the method described earlier by Bettmann and Rehm [42]. *R. erythropolis* cells (equivalent to 0.5 g dry weight) were uniformly suspended in 25 mL sterilized alginate solution (4% w/v in physiological saline). This alginate-cell mixture was extruded drop by drop into a cold sterile 0.2 M $CaCl_2$ solution. Gel beads of approximately 2-3 mm diameter were obtained. The beads were hardened by resuspending into a fresh $CaCl_2$ solution for 2 h with gentle agitation. The resultant biocatalytic matrix was termed as ALG-Re.

(c) Polyurethane entrapment of cells

The procedure was carried out according to the method described earlier by Brànyik *et al.* [43]. *R. erythropolis* cells (equivalent to 0.5 g dry weight) were uniformly suspended in 25 mL physiological saline. 20 g of polyurethane precursor (Hypol 2000) was mixed in cell suspension. The mixture was allowed to polymerize in silicone tube at 25°C. The resulting polyurethane matrix containing cells was cut into uniform cylinders. The beads were thoroughly washed with distilled water. The resultant biocatalytic matrix was termed as PUA-Re.

(d) Polyvinyl alcohol entrapment of cells

The procedure was carried out according to the method described earlier by Chen and Lin [44]. *R. erythropolis* cells (equivalent to 0.5 g dry weight) were uniformly suspended in 25 mL sterile aqueous PVA solution (20% w/v). The resulting mixture was extruded drop by drop into a glass column filled with 500 mL saturated boric acid. The drops polymerized as they passed through the boric acid solution to produce regularly-shaped beads with a diameter of approximately 2-3 mm. The beads

were allowed to remain in the boric acid for 2 h, subsequently suspended into 1M sodium orthophosphate solution (pH 6.5) for 1 h to consolidate hardening. The beads were thoroughly washed with sodium phosphate buffer (0.05M, pH 6.5) and the resultant biocatalytic matrix was termed as PVA-Re.

4.2.4. Synthesis and characterization of substrates

(a) Chemical synthesis of rac-amino acid amides

The chemical synthesis of *rac*-amino acid amide from *rac*-amino acids was done in two steps *viz.* Step 1: Esterification of amino acid and Step 2: Synthesis of amino acid amide from amino acid ester (Scheme 4.1) as described earlier [45].

Scheme 4.1: Chemical synthesis of *rac*-amino acid amides

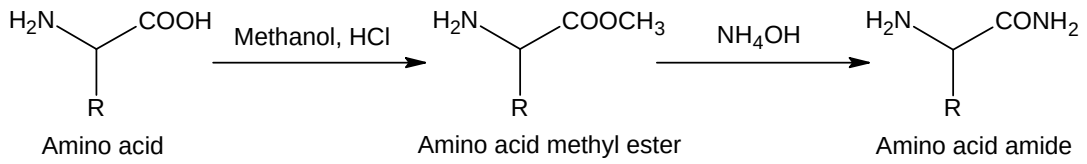

Amino acid | Amino acid methyl ester | Amino acid amide

	PG	HPA	NA
R-	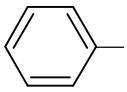	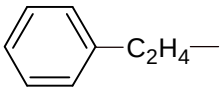	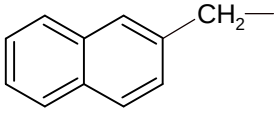

(i) Step 1: Hydrogen chloride was bubbled through a dispersion of amino acid (500 mg) in methanol (50 mL) for 30 minutes and stirred at room temperature for 16-18 hours. The solvent was evaporated using a rotatory evaporator (Buchi Rotapovor® R-124, Switzerland). Then $NaHCO_3$ saturated aqueous solution (50 mL) was added and the mixture was extracted with dichloromethane (3×30 mL). The organic layer was washed with water (50 mL), dried over anhydrous Na_2SO_4 and evaporated to collect amino acid methyl ester.

(ii) Step 2: Amino acid methyl ester (500 mg) was added to saturated aqueous ammonium hydroxide solution (30 mL) and stirred at room temperature for 24 hours. Water (30 mL) was added and the mixture was extracted with dichloromethane (3×30 mL). The organic solvent was evaporated under vacuum using a rotatory evaporator to obtain amino acid amide.

Phenylglycine amide, homophenylalanine amide and 2-naphthylalanine amide are termed as PG-amide, HPA-amide and NA-amide respectively.

(b) Characterization

(i) Phenylglycine amide (PG-amide): White solid powder, Analysis: Calculated for $C_8H_{10}N_2O$: C 63.98%, H 6.71%, N 18.65%; Found C 64.1%, H 6.67%, N 18.56%. ^{1}H-NMR (200 MHz, DMSO-d_6): 7.65-8.01 (5H, aromatic *H*), 7.56 (2H, CONH_2), 5.34 (2H, NH_2), 4.64 (1H, Ph-C*H*).

(ii) Homophenylalanine amide (HPA-amide): white solid powder, Analysis: Calculated for $C_{10}H_{14}N_2O$: C 67.39%, H 7.92%, N 15.72%; Found C 67.32%, H 7.67%, N 15.42%. ^{1}H-NMR (200 MHz, DMSO-d_6): 7.69-7.80 (5H, aromatic *H*), 7.56 (2H, CONH_2), 5.31 (2H, NH_2), 3.31 (1H, Ph-CH_2-CH_2-C*H*), 2.54 (2H, Ph-CH_2), 2.11 (2H, Ph-CH_2-CH_2).

(iii) 2-Naphthylalanine amide (NA-amide): white solid powder, Analysis: Calculated for $C_{13}H_{14}N_2O$: C 72.87%, H 6.59%, N 13.07%; Found C 72.82%, H 6.52%, N 12.92%. ^{1}H-NMR (200 MHz, DMSO-d_6): 7.68-8.21 (7H, aromatic *H*), 7.66 (2H, CONH_2), 5.44 (2H, NH_2), 4.13 (1H, Naphthyl-CH_2-C*H*), 3.64 (2H, Naphthyl-CH_2).

4.2.5. Chiral resolution of unnatural amino acid amides using immobilized cells

The biotransformation reactions were conducted in 25 mL stoppered flasks. The biocatalytic matrix was added in 10 mL solution of substrate (10mM prepared in 50 mM phosphate buffer, pH 7) to initiate the biotransformation reaction. The flask was incubated on oscillatory shaker at 30°C at 120 rpm. The samples were periodically withdrawn and analyzed by HPLC.

4.2.6. Analytical methods

(a) Amidase activity assay

Amidase activity (acyl transfer activity) was determined spectophotometrically at 500 nm as described earlier [9]. The *Rhodococcus* cells were isolated from fermentation medium by centrifugation. Cells were washed twice with 0.1M sodium phosphate buffer (pH 7.2). The washed cells (0.01g wet weight) were suspended in cold sodium phosphate buffer and subjected to ultrasonic treatment for 5 min. The cell debris was removed by centrifugation (15,000 rpm for 10 min). The

supernatant (0.1 mL) was analyzed for amidase activity. The ratio of wet weight to dry weight was determined for each sample and the enzyme activity was expressed in units per gram of dry cells as reported earlier [46]. One unit (U) is defined as amount of enzyme that converts 1.0 μmole of acetamide and hydroxylamine to acethydroxamate and ammonia per minute at pH 7.2 at 37°C. In case of immobilized enzyme, 100 mg freshly prepared biocatalytic matrix was used and the immobilized enzyme activity was expressed in units per gram of matrix.

(b) Characterization of immobilized enzyme

The biocatalytic matrices were characterized by scanning electron microscopy (SEM). Micrographs were taken on a JEOL JSM-5200 SEM instrument.

(c) HPLC analysis

All reaction profiles were monitored by HPLC (Thermo Separation Products, Fremont, CA, USA). The quantitative analysis of different amino acids and their esters was carried out using a reverse phase C-18 column (125×4 mm, prepacked column supplemented with a 4×4 mm guard column procured from LiChrospher®, Merck, Darmstadt, Germany) eluted isocratically using acetonitrile-water mobile phase (30:70 v/v, pH adjusted to 3.0 with 50% v/v *o*-phosphoric acid), at a flow rate of 0.6-1.0 mL/min. Peaks were detected using an UV detector at 215 nm. The peak identification was made by comparing the retention times with those of authentic compounds. Peak area was used as a measure to calculate the respective concentration. The reaction conversion was estimated from the ratio of the substrate consumption to its initial concentration. The enantiomeric excess (e.e.) of the product was determined by using a CHIROBIOTIC-T® column (250×4.6 mm prepacked column supplemented with 20×4 mm guard column procured from Astec Inc. USA) eluted isocratically using water-methanol mobile phase (40:60 v/v, pH adjusted to 2.3-2.5 with 50% v/v glacial acetic acid), at a flow rate of 0.6-0.8 mL/min.

(d) Determination of enantiomeric ratio

Enantiomeric ratio (*E*) is the prime parameter for describing the enzyme's enantioselectivity. Enantiomeric ratio was determined by using Eq. 2.3 as described earlier in Chapter 2 in Section 2.2.7(e).

4.3. RESULTS AND DISCUSSION

4.3.1. Medium optimization for production of amidase

(a) Optimization of fermentation time for amidase production

Amidase production (amidase activity; U/g of dry cells) by seven *Rhodococcus* strains at different time intervals was studied. All *Rhodococcus* strains gave maximum amidase production at 36 h (except MTCC 2794 and MTCC 3951 where maximum amidase production was observed at 24 h). All further fermentations of seven *Rhodococcus* strains were terminated at their respective optimized fermentation time.

(b) Selection of optimum nitrogen source, carbon source and inducer

Use of inorganic nitrogen source resulted in reduced cell density and amidase activity (results not shown) and therefore organic nitrogen sources (yeast extract and meat peptone) were selected for further studies. *R. erythropolis* MTCC 1526 gave maximum amidase activity when grown on sorbitol as carbon source (Table 4.1).

Table 4.1: Effect of carbon source on amidase production

Rhodococcus **Strain**	**Time** (h)	**Amidase activity** (U/g of dry cells)				
		Glucose	**Glycerol**	**Mannitol**	**Sorbitol**	**Sucrose**
MTCC 1526	36	157.85	17.54	19.66	489.14	251.43
MTCC 1548	36	115.40	*Nil*	*Nil*	11.27	136.97
MTCC 2574	36	160.49	0.59	*Nil*	21.83	1.09
MTCC 2678	36	91.38	1.96	21.40	221.38	58.53
MTCC 2683	36	184.82	*Nil*	12.64	30.36	23.26
MTCC 2794	24	284.41	113.15	206.11	359.84	184.04
MTCC 3951	24	212.40	180.35	*Nil*	359.38	*Nil*

Hence *R. erythropolis* MTCC 1526 culture and sorbitol as a carbon source were selected for further studies. The presence of amides in fermentation medium is known to enhance the production of amidase [47]. In present study, seven inducers (*namely*: acetamide, acetamido-phenol, acetamido-acetophenon, 4-acetamido-benzaldehyde, acetanilide, acrylamide, urea) were screened. The amidase activities of *R. erythropolis* MTCC 1526 cells grown on different inducers are given in Fig. 4.1. For comparison, a

control fermentation run (i.e. without adding any inducer) was carried out. Addition of inducer in the fermentation medium was found to increase the production of amidase by *R. erythropolis* MTCC 1526. Among seven inducers, acetamide gave maximum amidase activity (464.23 U/g of dry cells) and therefore selected for further experiments.

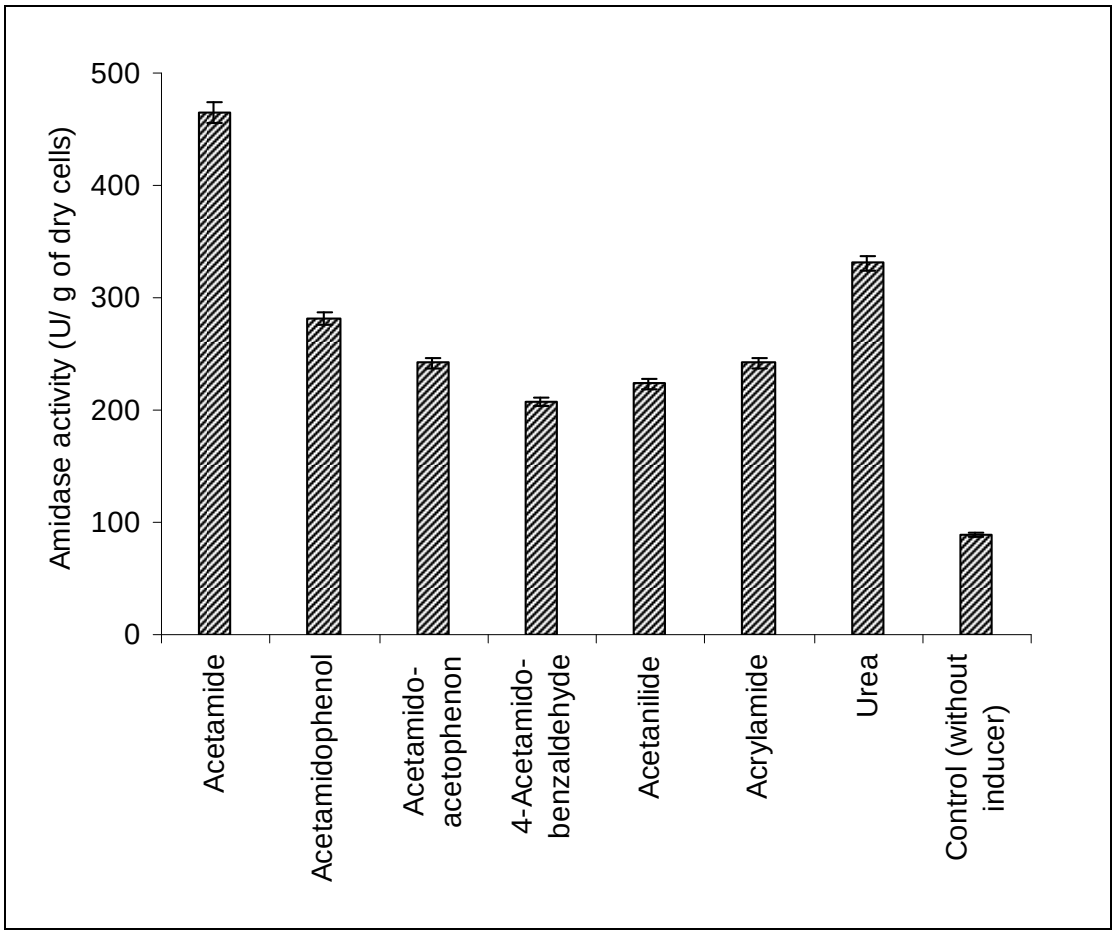

Fig. 4.1: Screening of inducers for amidase production by *R. erythropolis* MTCC 1526 [Medium A + amidase inducer (10mM); incubated for 36 h at 30°C on rotary shaker at 200 rpm]

(c) Amidase activity profile for R. erythropolis MTCC 1526

Cell growth and amidase activity were simultaneously studied with respect to fermentation time and the amidase activity profile was established (Fig. 4.2). During the course of fermentation, maximum amidase activity was found at 36 h and thereafter the activity was found to decline along wilt cell density from 42 h to 48 h. Therefore all further fermentations were terminated at 36 h.

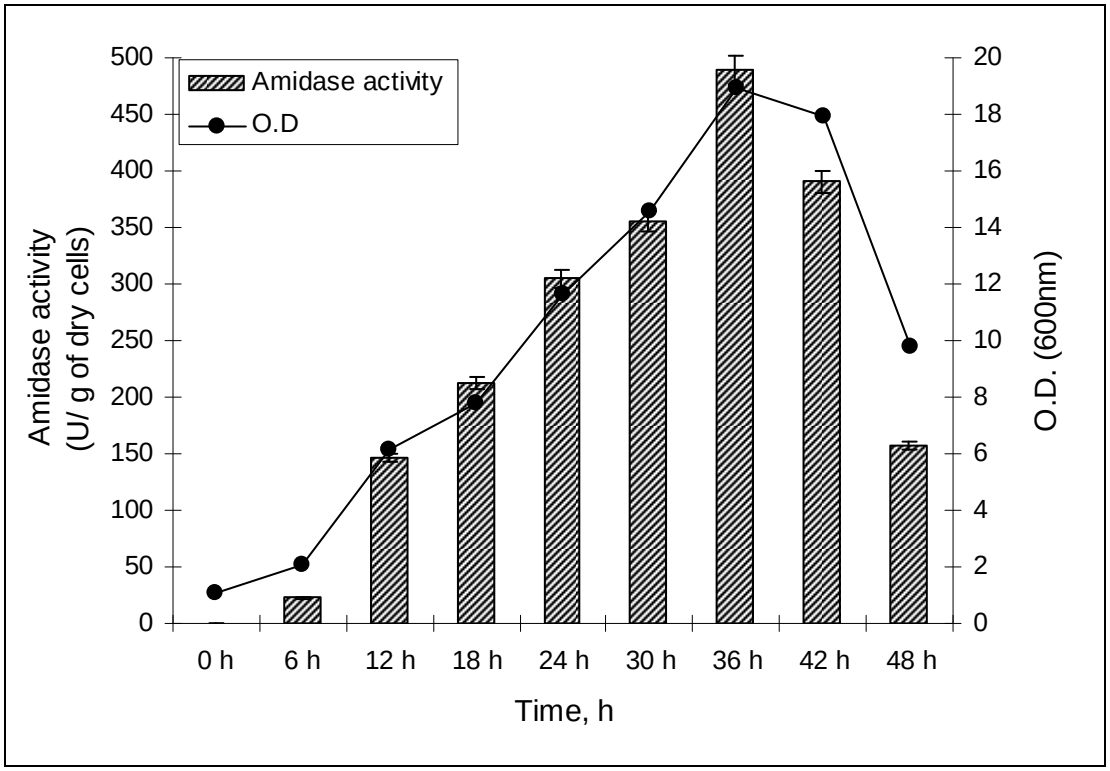

Fig. 4.2: Growth profile and amidase production by *R. erythropolis* MTCC 1526 [Medium B; 30°C at 200 rpm]

(d) Screening of significant media components using a Plackett–Burman design

The Plackett–Burman design served the purpose of ascertaining the critical and influential process variables. Here, seven independent variables were screened in eight combinations organized according to the Plackett–Burman design (Table 4.2).

Table 4.2: Plackett-Burman experimental design [a]

No.	Sorbitol	Yeast Extract	Meat Peptone	Na_2HPO_4	Dummy variable	KH_2PO_4	Aceta-mide	Amidase activity [b]
1	H	H	H	L	H	L	L	358.98
2	L	H	H	H	L	H	L	191.50
3	L	L	H	H	H	L	H	266.81
4	H	L	L	H	H	H	L	191.46
5	L	H	L	L	H	H	H	259.93

Continued…

Table 4.2: *Continued…*

No.	Sorbitol	Yeast Extract	Meat Peptone	Na_2HPO_4	Dummy variable	KH_2PO_4	Aceta-mide	Amidase activity [b]
6	H	L	H	L	L	H	H	417.88
7	H	H	L	H	L	L	H	474.95
8	L	L	L	L	L	L	L	92.57

[[a] H and L represents high level and low level of media component respectively (Sorbitol: H = 10 g/L and L = 1 g/L; Yeast extract: H = 5 g/L and L = 1 g/L; Meat peptone: H = 10 g/L and L = 1 g/L; Na_2HPO_4 : H = 6 g/L and L = 2 g/L; KH_2PO_4 : H = 3 g/L and L = 1 g/L; Acetamide: H = 50 mM and L = 5 mM); [b] Amidase activity is expressed in U/g of dry cells.]

The results of the Plackett–Burman design calculations along with the corresponding variable-specific *F*-scores are summarized in Table 4.3. High value of *F*-score indicates greater significance of input variable. Thus depending on the *F*-score, sorbitol, yeast extract, meat peptone and acetamide were found to be most influential media components. The dummy variable, which is not allocated any value, gives some redundancy required by the statistical procedure. Moreover, incorporation of the dummy variable into an experiment allows an estimation of the variance. The mean square deviation (MSD) of dummy variable was found to be very low compared to that of influential variables.

Table 4.3: Statistical calculations for Plackett-Burman design

Factor	Sorbitol	Yeast Extract	Meat Peptone	Na_2HPO_4	Dummy variable	KH_2PO_4	Aceta-mide
Y_{i+}	1443.3	1285.4	1235.2	1124.7	1077.2	1060.8	1419.6
Y_{i-}	810.8	968.7	1018.9	1129.4	1176.9	1193.3	834.5
ΣY_{i+}-ΣY_{i-}	632.5	316.6	216.3	-4.6	-99.7	-132.5	585.1
MSD	4999.2	12532.6	5845.9	2.7	1243.3	2195.9	42788.0
F-score	40.2	10.1	4.7	0.002	1.0	1.7	34.4

(e) Media optimization by RSM

The design of experiments and respective experimental and predicted values of amidase activities are given in Table 4.4.

Table 4.4: Face centre design matrix of independent variables and their corresponding experimental and predicted values of response

No.	Media components (coded values [a])				Amidase activity [b]	
	Sorbitol	Yeast extract	Meat peptone	Acetamide	Experimental [c]	Predicted
1	-1	-1	-1	-1	789.05	831.48
2	1	-1	-1	-1	688.93	581.69
3	-1	1	-1	-1	679.29	702.27
4	1	1	-1	-1	117.58	195.02
5	-1	-1	1	-1	598.23	540.41
6	1	-1	1	-1	432.29	592.54
7	-1	1	1	-1	330.63	252.40
8	1	1	1	-1	0.9	47.08
9	-1	-1	-1	1	534.28	566.95
10	1	-1	-1	1	112.07	204.05
11	-1	1	-1	1	1162.09	1015.59
12	1	1	-1	1	258.58	395.24
13	-1	-1	1	1	469.37	405.68
14	1	-1	1	1	288.84	344.70
15	-1	1	1	1	509.44	695.53
16	1	1	1	1	405.78	377.10
17	-1	0	0	0	819.96	897.27
18	1	0	0	0	498.98	329.04
19	0	-1	0	0	616.25	585.31

Continued…

Table 4.4: *Continued…*

No.	**Media components** (coded values) [a]				**Amidase activity** [b]	
	Sorbitol	**Yeast extract**	**Meat peptone**	**Acetamide**	**Experimental** [c]	**Predicted**
20	0	1	0	0	550.18	488.49
21	0	0	-1	0	890.21	861.28
22	0	0	1	0	615.77	552.07
23	0	0	0	-1	54.17	47.46
24	0	0	0	1	198.86	112.95
25	0	0	0	0	789.45	783.18
26	0	0	0	0	780.3	783.18
27	0	0	0	0	788.22	783.18
28	0	0	0	0	781.74	783.18
29	0	0	0	0	778.82	783.18
30	0	0	0	0	780.56	783.18

[[a] Real values (in sequence of -1, 0, +1) Sorbitol: 5, 12.5, 20 g/L; Yeast extract: 1, 2.5, 4.0 g/L; Meat peptone 2.5, 6.25, 10 g/L; Acetamide 5, 10, 15 mM ; [b] U/g of dry cells; [c] Values indicate mean of duplicate observations.]

The second order polynomial equation was used to correlate the independent process variables with amidase production. The second order polynomial coefficient for each term of the equation determined through multiple regression analysis using the Design Expert. After regression analysis, the second-order response model was obtained (Eq. 4.1).

Amidase activity (U/g of dry cells) = + 783.18167 - 142.05708 A - 24.20458 B - 77.30292 C + 16.37208 D - 42.50510 A^2 - 61.57 B^2 - 19.13 C^2 - 175.74 D^2 - 64.36 A·B + 75.48 A·C - 28.28 A·D - 39.70 B·C + 144.46 B·D + 32.45 C·D – Eq. 4.1

Where, A: sorbitol, B: yeast extract, C: meat peptone, D: acetamide, and A, C, B^2, D^2, AB, AC, BD were identified as significant terms. Thus the interactive effects between 'sorbitol and yeast extract' (AB); 'sorbitol and meat peptone' (AC); and

'yeast extract and acetamide' (BD) were predominant in the given system. The model significance was analyzed using Analysis of Variance (ANOVA) for the experimental design (Table 4.5). Model F-value was calculated as a ratio of mean square regression and mean square residual. The model F-value of 11.104 implied that the model was significant and there was only a 0.01% chance that a large 'Model F-value' could occur due to noise. The P value was used as a tool to check the significance of each of the coefficients, which, in turn, are necessary to understand the pattern of the mutual interactions between the process variables. Smaller the magnitude of P, more significant is the corresponding coefficient. Values of P less than 0.05 indicate model terms are significant.

Table 4.5: ANOVA analysis of the model

Source	Degree of Freedom	F - Value	Prob > F (P value)
Model significant	14	11.104	< 0.0001
A	1	36.065	< 0.0001
B	1	1.047	0.322
C	1	10.679	0.005
D	1	0.479	0.499
A^2	1	3.690	0.074
B^2	1	7.742	0.014
C^2	1	0.747	0.401
D^2	1	63.084	< 0.0001
AB	1	4.935	0.042
AC	1	6.788	0.019
AD	1	0.952	0.345
BC	1	1.877	0.191
BD	1	24.865	0.0002
CD	1	1.254	0.280

The model fitting values are given in Table 4.6 which indicate model adequacy. A low value of coefficient of variation (21.301%) indicates the very high degree of precision and a good realibility of the experimental values. The fit of the model can also be expressed by coefficient of determination R^2, which was found to

be 0.912, indicating that 91.2% of the variability in the response could be explained by the model. Closer the R^2 value is to 1, the better is the model fit to experimental data and less is the distance between the predicted and the observed values. 'Adeq Precision' measures the signal to noise ratio. A ratio greater than 4 is desirable. Here, a ratio of 11.819 indicates an adequate signal.

Table 4.6: Model fitting values

No.	Model Terms	Values
1	Coefficeint of the variation	21.301
2	R^2	0.912
3	Adj R^2	0.829
4	Adeq Precision	11.819
5	Standard Deviation	115.883

The perturbation plot (Fig. 4.3) indicates that acetamide (D) is the most influential media component where as yeast extract (B) is having least influence on amidase activity. The three-dimensional plots of the statistically significant interactions are shown in Fig. 4.4.

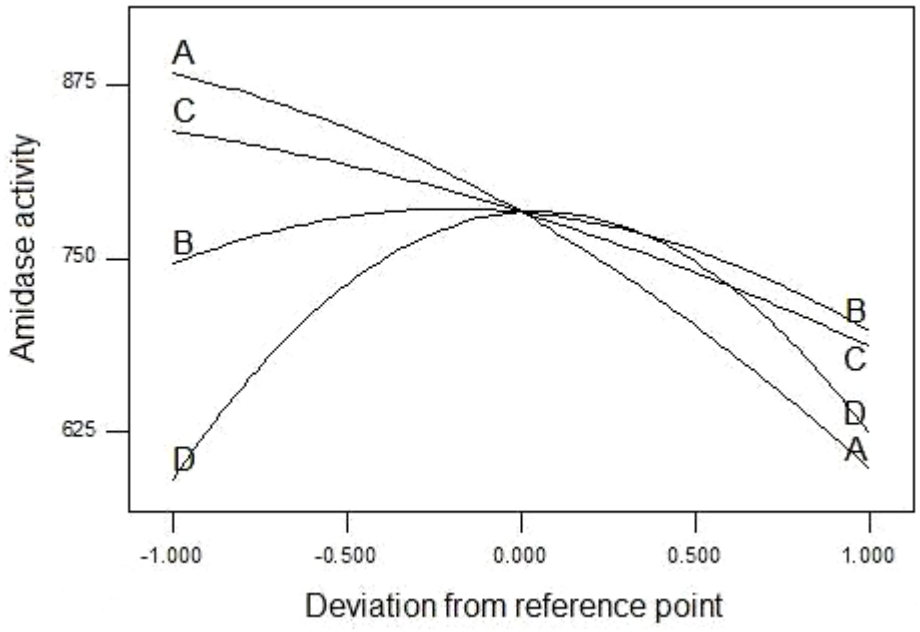

Fig. 4.3: Perturbation plot indicating the relative effect of each media component on amidase activity (U/ g of dry cells) [A: sorbitol, B: yeast extract, C: meat peptone, D: acetamide]

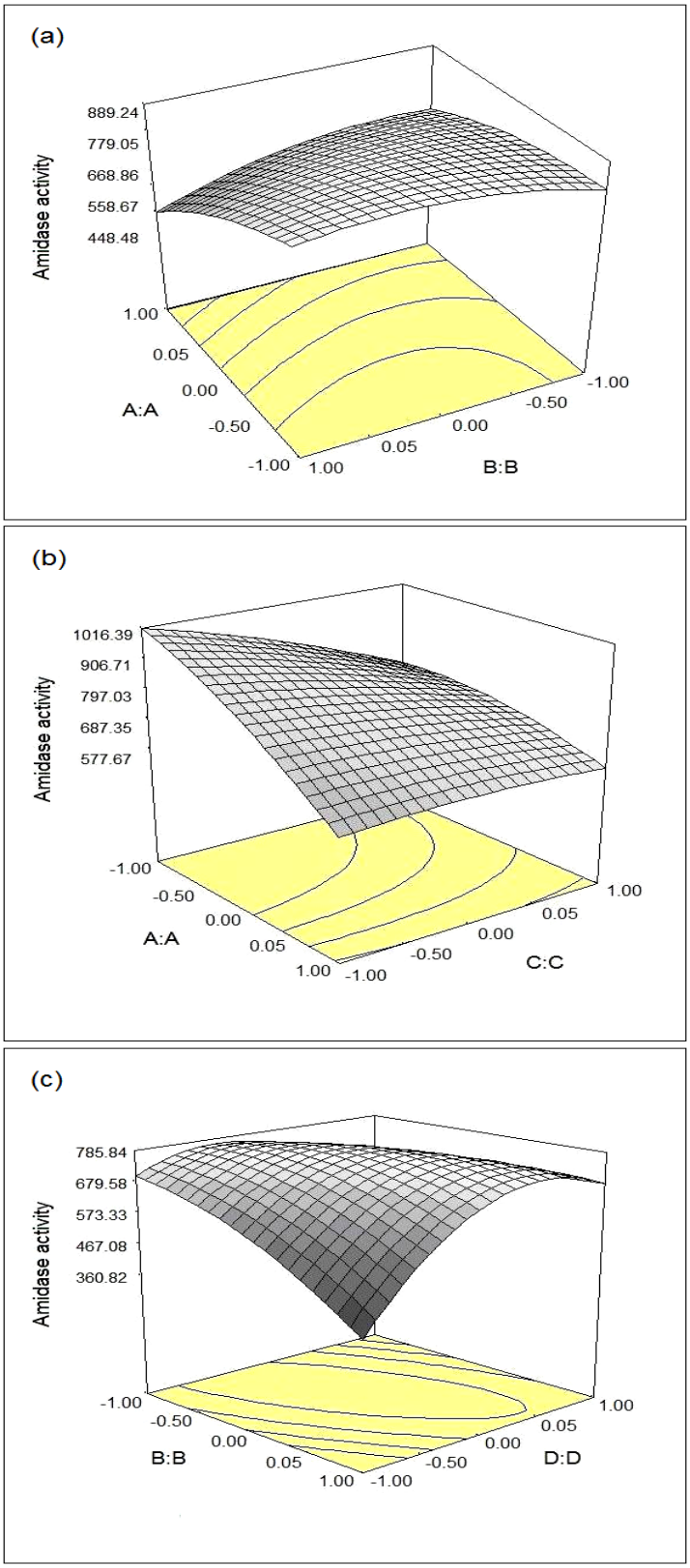

Fig. 4.4: 3-D response surface contour plots for the amidase activity (U/g of dry cells); (a) sorbitol and yeast extract; (b) sorbitol and meat peptone; (c) yeast extract and acetamide. [A: sorbitol, B: yeast extract, C: meat peptone, D: acetamide]

The three dimentional plots were obtained from the pair-wise combination of two independent variables, while keeping the other two variables at their center point levels. From the bump of three-dimensional plot or the central point of its respective contour plot, the optimal composition of medium components can be identified. The contour response plot gives the roles of process variables and their interactive effects.

The three optimum solutions were obtained by substituting levels of the factors into the regression equation (Eq. 4.1). The media composition for these optimal solutions and the corresponding predicted response (amidase activity) are summarized in Table 4.7. The predicted response of three optimal solutions was experimentally verified by conducting actual fermentation runs. In the first optimal solution, the concentrations of four media components were found as: sorbitol (5 g/L), yeast extract (4 g/L), meat peptone (2.5 g/L), acetamide (12.25 mM) [all remaining components are same as mentioned in medium B]. The predicted response of first optimal solution (1069.33 U/g of dry cells) was experimentally verified (1086.57 U/g of dry cells). The close agreement between predicted values and experimental values of amidase activities confirms the significance of the model. The amidase activities before and after optimization were 157.85 U/g of dry cells and 1086.57 U/g of dry cells respectively. Thus, use of RSM has increased the production of amidase from *Rhodococcus erythropolis* MTCC 1526 by 6.88 fold.

Table 4.7: Experimental validation of model predicted values of amidase activity

No.	**Media composition**				**Amidase activity** (U/g dry cells)		**% deviation**
	Sorbitol (g/L)	**Yeast extract** (g/L)	**Meat peptone** (g/L)	**Aceta-mide** (mM)	**Predicted value**	**Observed value**	
1	5.00	4.00	2.50	12.25	1069.33	1086.57	1.61
2	5.00	4.00	2.50	12.40	1069.24	1084.84	1.46
3	5.00	3.88	2.50	11.90	1067.59	1077.73	0.95

The reports on fermentative production of amidase using Rhodococcal strains are scant. Different fermentation media have been used for amidase production. For

example, Rhodococcal cells were grown in mineral medium along with acrylamide as source of carbon and nitrogen for the production of amidase [48]. Webster *et al.* reported a mineral medium with acrylamide or acrylonitrile as a sole source of carbon and nitrogen [49]. Kotlova *et al.* reported a mineral medium with glucose and urea (as carbon and nitrogen sources respectively) for amidase production by *Rhodococcus rhodochrous* M8 [50]. However, no systematic attempt has been made so far to enhance the amidase production by *Rhodococcus sp*. through medium optimization. Rhodococci strains are able to utilize a wide variety of nutrients as well as xenobiotics. In view of the broad catabolic diversity of Rhodococci, many authors have probably used a wide variety of carbon and nitrogen sources for amidase production [51, 52].

4.3.2. Immobilization of R. erythropolis cells

The amidase activities of biocatalytic matrices prepared by different methods are given in Table 4.8. The ALG-Re and PVA-Re matrices expressed higher amidase activity (*viz*. 41.1 and 39.7 U/ g of matrix respectively) than AGA-Re and PUA-Re matrices. This could be due to the higher porosity observed in the ALG-Re and PVA-Re matrices than the other.

Table 4.8: The amidase activity of different biocatalytic matrices

No.	Biocatalytic matrix	Amidase activity (U/g of matrix)
1	AGA-Re	28.4
2	ALG-Re	41.1
3	PUA-Re	16.2
4	PVA-Re	39.7

To confirm this assumption, the surface morphology of matrices was studied by SEM. The scanning electron micrographs presented in Fig. 4.5 show the presence of larger pores (indicated by arrows) on surface of ALG-Re and PVA-Re. Due to their higher activities, ALG-Re and PVA-Re matrices were selected for biocatalytic reactions.

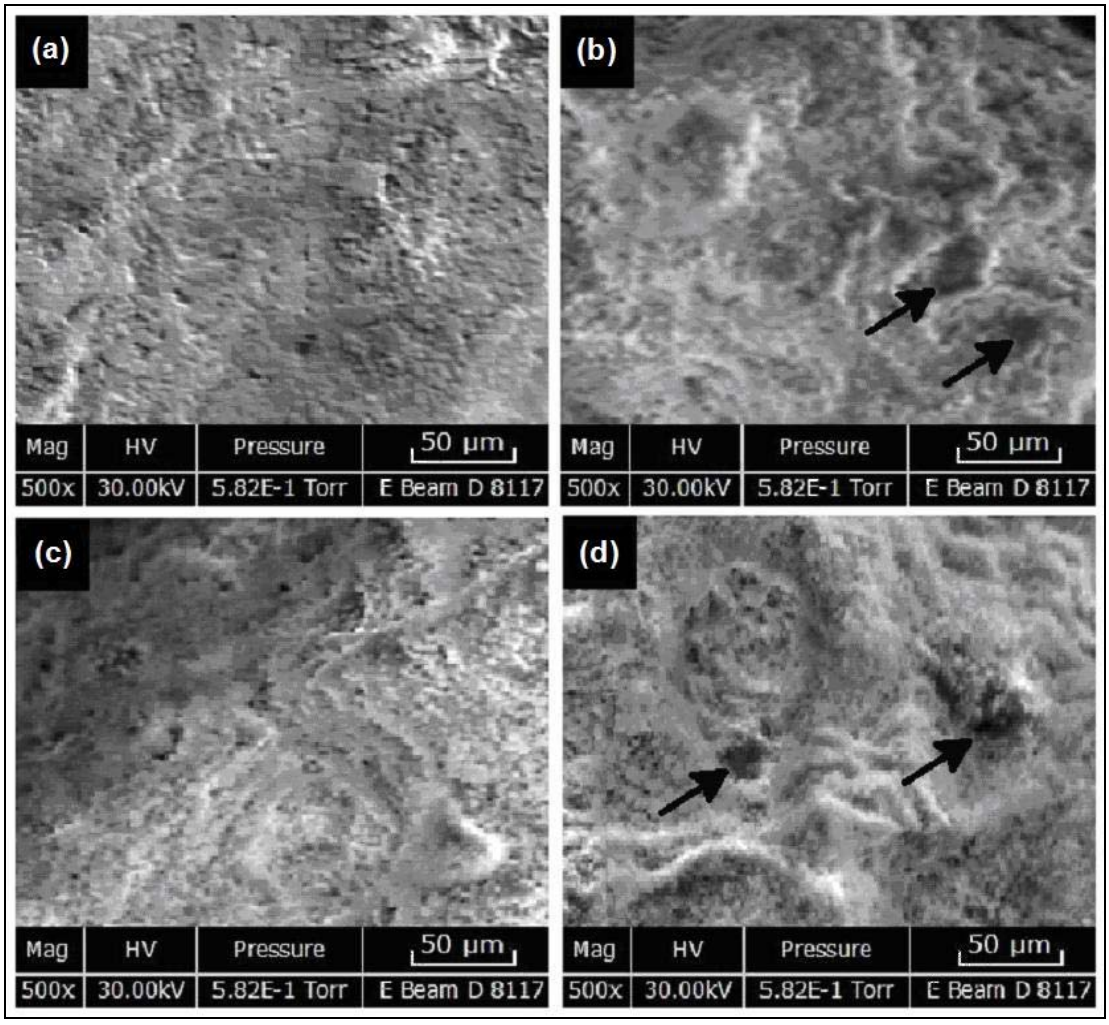

Fig. 4.5: Scanning electron micrographs of biocatalytic matrices: (a) AGA-Re, (b) ALG-Re, (c) PUA-Re and (d) PVA-Re.

Immobilization procedures for immobilization of Rhodococcal cells are reported by many authors. Whole cell immobilization was achieved mainly by entrapment within calcium alginate beads [53, 54], agar and agarose beads [55] and polyacrylamide beads [56]. However, none of the above articles reported any data on amidase activity of the immobilized *Rhodococcus* cells.

4.3.3. Chiral resolution of unnatural amino acid amides using immobilized cells

(a) Stereoselectivity of R. erythropolis amidase

Amidase of *R. erythropolis* MTCC 1526 preferentially hydrolyzed *S*-enantiomer of PG-amide, HPA-amide and NA-amide. The schematic representation of chiral resolution of unnatural amino acid amides catalyzed by amidase of *R. erythropolis* MTCC 1526 is given in Scheme 4.2.

Scheme 4.2: Chiral resolution of unnatural amino acid amides catalyzed by resting cells of *R. erythropolis* MTCC 1526.

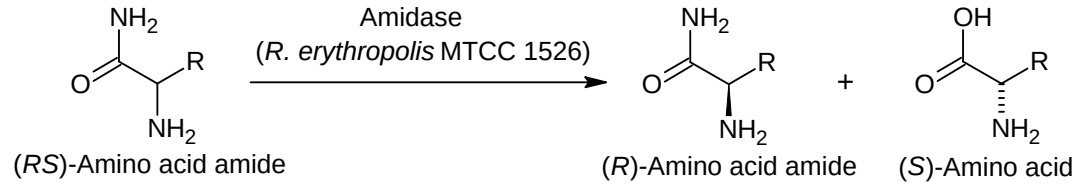

	PG	HPA	NA
R-	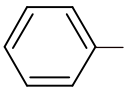	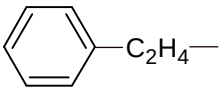	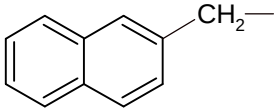

(b) Relative hydrolytic activity

The percent relative hydrolytic activity of two biocatalytic matrices (*namely*: ALG-Re and PVA-Re) towards hydrolysis of amino acid amides was determined (Table 4.9). Both matrices showed similar trend of the relative hydrolytic activity. Both matrices showed maximum hydrolytic activity towards hydrolysis of PG-amide and showed minimum hydrolytic activity towards hydrolysis of NA-amide.

Table 4.9: Relative hydrolytic activity (%) of biocatalytic matrices towards hydrolysis of amino acid amides

Substrate	**Relative hydrolytic activity (%) of biocatalytic matrices towards hydrolysis of amino acid amides**	
	ALG-Re	**PVA-Re**
PG-amide	100	100
HPA-amide	75	74
NA-Amide	64	63

(c) Chiral resolution catalyzed by ALG-Re matrix

The results of stereoselective hydrolysis of unnatural amino acid amides using ALG-Re matrix are summarized in Table 4.10. ALG-Re biocatalytic matrix showed higher enantioselectivity towards hydrolysis of PG-amide and HPA-amide (E = 15.6 and 11.5 respectively) than that of NA-amide (E = 6.2).

Table 4.10: Stereoselective hydrolysis of unnatural amino acid amides using ALG-Re matrix

Substrate	**Preferred configuration**	**Time** (h)	**ee$_p$** (%)	***C*** (%)	***E***
PG-amide	*S*	24	86.1	15.2	15.6
HPA-amide	*S*	32	82.4	11.3	11.5
NA-Amide	*S*	38	71.7	7	6.2

(d) Chiral resolution catalyzed by PVA-Re matrix

The results of stereoselective hydrolysis of unnatural amino acid amides using PVA-Re matrix are summarized in Table 4.11. PVA-Re biocatalytic matrix showed higher enantioselectivity towards hydrolysis of PG-amide and HPA-amide (E = 14.8 and 10.6 respectively) than that of NA-amide (E = 6.1).

Table 4.11: Stereoselective hydrolysis of unnatural amino acid amides using PVA-Re matrix

Substrate	**Preferred configuration**	**Time** (h)	**ee$_p$** (%)	***C*** (%)	***E***
PG-amide	*S*	28	84.5	20.7	14.8
HPA-amide	*S*	38	81.3	10.5	10.6
NA-Amide	*S*	44	70.4	8.3	6.1

(e) Effect of pH and temperature on enantioselectivity of amidase

Previous reports suggest that the enantioselectivity of Rhodococcal amidase towards hydrolysis of carboxylic amides is predominantly affected by change in pH and temperature of the reaction [24-26]. However, we observed no significant effect of pH (in a range of pH 6-8) and temperature (in a range of 20-40°C) on the enantioselectivity of amidase of *R. erythropolis* MTCC 1526 (results not shown).

Data available in the literature indicates high enantioselectivity of amidase from different Rhodococcal strains. For example, Beard and Page studied the enantioselective synthesis of several α-amino acids using whole cells of *Rhodococcus* strain NC1MB 40795. The nitrile hydratase-amidase catalyzed synthesis of L-phenylglycine was obtained with high enantiopurity (ee > 98%). Here, the authors

observed that the nitrile hydratase from of *Rhodococcus* NC1MB 40795 cells was non-enantioselective while amidase exhibited high enantioselectivity [23]. Wang and Lin studied enantioselective synthesis of L-phenylglycine and other α-amino acids using *Rhodococcus* sp. AJ270 cells. The authors investigated the pH dependant enantioselectivity of nitrile hydratase-amidase enzymes. By changing pH from 7.6 to 7.1 the enantiomeric excess of the product (e.g. L-phenylglycine) was greatly increased (from 93% to 99%) [24, 25]. Wegman *et al.* studied the synthesis of L-phenylglycne using whole cells of *Rhodococcus* sp. (NOVO SP 361) in a batch process as well as in a fed-batch process. The authors reported a beneficial effect of lowering the reaction temperature to 5°C on the enantioselectivity of the enzymes. Under the optimum conditions, a fed-batch process gave 94% yield of 99.5% enantiomerically pure L-phenylglycine [26]. In a recent article by Wang *et al.*, synthesis of L-phenylglycine is studied using whole cells of *Rhodococcus* sp. AJ270. The whole cell biocatalyst gave high enantiomeric ratio (E = 94) towards hydrolysis of L-phenylglycine amide [8]. In contrast to these reports, the immobilized *R. erythropolis* MTCC 1526 cells exhibited very poor enantioselectivity towards hydrolysis of unnatural amino acid amides (E < 16).

4.4. CONCLUSIONS

The production of amidase by *Rhodococcus erythropolis* MTCC 1526 was found to depend greatly on four media components (*namely*: sorbitol, yeast extract, meat peptone and acetamide). Using the RSM, it was possible to model individual and interactive effects of media components on amidase production. The validity of the model was confirmed by the close agreement between experimental and predicted values. The media optimization by RSM effectively enhanced the amidase production by 6.88 fold. Among four methods of cell immobilization, entrapment of *R. erythropolis* cells in alginate gel (ALG-Re) and polyvinyl alcohol agar (PVA-Re) gave higher amidase activity. Amidase of *R. erythropolis* MTCC 1526 preferentially hydrolyzed *S*-enantiomer of unnatural amino acid amides. ALG-Re and PVA-Re biocatalytic matrices showed better enantioselectivity towards hydrolysis of PG-amide (E = 15.6 and E = 14.8 respectively) and HPA-amide (E = 11.5 and E = 10.6 respectively). These biocatalytic matrices showed poor enantioselectivity towards hydrolysis of NA-amide (E = 6.2 and E = 6.1 respectively).

REFERENCES

[1] Pertsovich, S.I.; Guranda, D.T.; Podchernyaev, D.A.; Yanenko, A.S.; Švedas, V.K. Aliphatic amidase from *Rhodococcus rhodochrous* M8 is related to the Nitrilase/Cyanide Hydratase Family. *Biochemistry-Moscow*, **2005**, *70(11)*, 1280-1287.

[2] Fournand, D.; Arnaud, A. Aliphatic and enantioselective amidases: from hydrolysis to acyl transfer activity. *J. Appl. Microbiol.*, **2001**, *91*, 381-393.

[3] Kobayashi, M.; Goda, M.; Shimizu, S. The catalytic mechanism of amidase also involves nitrile hydrolysis. *FEBS Lett.*, **1998**, *439*, 325-328.

[4] Nagasawa, T.; Yamada, H. Microbial transformations of nitriles. *Trends Biotechnol.*, **1989**, *7*, 153-158.

[5] Baek, D.H.; Kwon, S.J.; Hong, S.P.; Kwak, M.S.; Lee, M.H.; Song, J.J.; Lee, S.G.; Yoon, K.H.; Sung, M.H. Characterization of a thermostable D-stereospecific alanine amidase from *Brevibacillus borstelensis* BCS-1. *Appl. Environ. Microbiol.*, **2003**, *69(2)*, 980-986.

[6] Yamamoto, K.; Otsubo, K.; Matsuo, A.; Hayashi, T.; Fujimatsu, I.; Komatsu, K.I. Production of *R*-(2)-ketoprofen from an amide compound by *Comamonas acidovorans* KPO-2771-4. *Appl. Environ. Microbiol.*, **1996**, *62(1)*, 152-155.

[7] Stolz, A.; Trott, S.; Binder, M.; Bauer, R.; Hirrlinger, B.; Layh, N.; Knackmuss, H.J. Enantioselective nitrile hydratases and amidases from different bacterial isolates. *J. Mol. Catal. B: Enzym.*, **1998**, *5*, 137-141.

[8] Wang, M.X.; Liu, J.; Wang, D.X.; Zheng, Q.Y. Synthesis of optically active α-methylamino acids and amides through biocatalytic kinetic resolution of amides. *Tetrahedron: Asymmetr.* **2005**, *16*, 2409-2416.

[9] Fournand, D.; Bigey, F.; Arnaud, A. Acyl transfer activity of an amidase from *Rhodococcus* sp. strain R312: Formation of a wide range of hydroxamic acids. *Appl. Environ. Microbiol.*, **1998**, *64(8)*, 2844-2852.

[10] Osprian, I.; Fechter, M.H.; Griengl, H. Biocatalytic hydrolysis of cyanohydrins: an efficient approach to enantiopure α-hydroxy carboxylic acids. *J. Mol. Catal. B: Enzym.*, **2003**, *24/25*, 89-98.

[11] Yeom, S.-J.; Kim, H.-J.; Deok-Kun Oh, D.-K. Enantioselective production of 2,2-dimethylcyclopropane carboxylic acid from 2,2-dimethylcyclopropane carbonitrile using the nitrile hydratase and amidase of *Rhodococcus erythropolis*

ATCC 25544. *Enzyme Microb. Technol.*, **2007**, *41*, 842-848.

[12] Gilligan, T.; Yamada, H.; Nagasawa, T. Production of *S*-(1)-2- phenylpropionic acid from (*R*,*S*)-2-phenylpropionitrile by the combination of nitrile hydratase and stereoselective amidase in *Rhodococcus equi* TG328. *Appl. Microbiol. Biotechnol.*, **1993**, *39*, 720-725.

[13] Martínková , L.; Křen, V.; Cvak, L.; Ovesná ,M.; Přepechalová, I. Hydrolysis of lysergamide to lysergic acid by *Rhodococcus equi* A4. *J. Biotechnol.*, **2000**, *84*, 63-66.

[14] Leng, D.-H.; Wang, D.X.; Pan, J.; Huang, Z.-T.; Wang, M.-X. Highly efficient and enantioselective biotransformations of racemic azetidine-2-carbonitriles and their synthetic applications. *J. Org. Chem.*, **2009**, *74*, 6077-6082.

[15] Wang, M.-X.; Lu, G.; Ji, G.-J.; Huang, Z.-T.; Meth-Cohn, O.; Colby, J. Enantioselective biotransformations of racemic α-substituted phenylacetonitriles and phenylacetamides using *Rhodococcus sp.* AJ270. *Tetrahedron: Asymmetr.*, **2000**, *11*, 1123-1135.

[16] Wang, J.-Y.; Wang, D.X.; Pan, J.; Huang, Z.-T.; Wang M.-X. Nitrile and amide biotransformations for the synthesis of enantiomerically pure 3-arylaziridine-2-carboxamide derivatives and their stereospecific ring-opening reactions. *J. Org. Chem.*, **2007**, *72*, 9391-9394.

[17] Snell, D.; Colby, J. Enantioselective hydrolysis of racemic ibuprofen amide to S-(+)-ibuprofen by *Rhodococcus* AJ270. *Enzyme Microb. Technol.*, **1999**, *24*, 160-163.

[18] Effenberger, F.; Graef, B.W.; Oßwald, S. Enzyme-catalyzed reactions, Part 30: Preparation of (*S*)-naproxen by enantioselective hydrolysis of racemic naproxen amide with resting cells of *Rhodococcus erythropolis* MP50 in organic solvents. *Tetrahedron: Asymmetr.*, **1997**, *8*, 2749-2755.

[19] Layh, N.; Stolz, A.; Böhme, J.; Effenberger, F.; Knackmuss, H.-J. Enantioselective hydrolysis of racemic naproxen nitrile and naproxen amide to *S*-naproxen by new bacterial isolates. *J. Biotechnol.*, **1994**, *33*, 175-182.

[20] Effenberger, F.; Graef, B.W. Chemo- and enantioselective hydrolysis of nitriles and acid amides, respectively, with resting cells of *Rhodococcus* sp. C3II and *Rhodococcus erythropolis* MP50. *J. Bacteriol.*, **1998**, *60*, 165-174.

[21] Layh, N.; Knackmuss, H.-J.; Stolz, A. Enantioselective hydrolysis of ketoprofen

amide by Rhodococcus sp. C3II and *Rhodococcus erythropolis* MP50. *Biotechnol. Lett.*, **1995,** *17(2)*, 187-192.

[22] Martínková, L.; Křen, V. Nitrile- and amide-converting microbial enzymes: Stereo-, Regio- and Chemoselectivity. *Biocatal. Biotransfor.*, **2002**, *20(2)*, 73-93.

[23] Beard, T.M.; Page, M.I. Enantioselective biotransformations using rhodococci. *Anton. van Leeuw.*, **1998**, *74*, 99-106.

[24] Wang, M.-X.; Lin, S.-J. Practical and convenient enzymatic synthesis of enantiopure α-amino acids and amides. *J. Org. Chem.*, **2002**, *67*, 6542-6545.

[25] Wang, M.-X.; Lin, S.-J. Highly efficient and enantioselective synthesis of L-arylglycines and D-arylglycine amides from biotransformations of nitriles. *Tetrahedron Lett.*, **2001**, *42*, 6925-6927.

[26] Wegman, M.A.; Heinemann, U.; Stolz, A.; Rantwijk, F.; Sheldon, R.A. Stereoretentive nitrile hydratase-catalysed hydration of D-phenylglycine nitrile. *Org. Process Res. Dev.*, **2000**, *4,* 318-322.

[27] Osprian, I.; Jarret, C.; Strauss, U.; Kroutil, W.; Orru, R.V.A.; Felfer, U.; Willetts, A.J.; Faber, K. Large-scale preparation of a nitrile-hydrolysing biocatalyst: *Rhodococcus* R 312 (CBS 717.73). *J. Mol. Catal. B: Enzym.*, **1999**, *6*, 555-560.

[28] Macadam, A.M.; Knowles, C.J. The stereospecific bioconversion of α-aminopropionitrile to L-alanine by an immobilised bacterium isolated from soil. *Biotechnol. Lett.*, **1985**, *7*, 865-870.

[29] Bauer, R.; Hirrlinger, B.; Layh, N.; Stolz, A.; Knackmuss, H.-J. Enantioselective hydrolysis of racemic 2-phenylpropionitrile and other (*R,S*)-2 arylpropionitriles by a new bacterial isolate, *Agrobacterium tumefaciens* strain d3. *Appl. Microbiol. Biotechnol.*, **1994**, *42*, 1-7.

[30] Hensel, M.; Lutz-Wahl, S.; Fischer, L. Stereoselective hydration of (*RS*)-phenylglycine nitrile by new whole cell biocatalysts. *Tetrahedron: Asymmetr.*, **2002**, *13*, 2629-2633.

[31] van der Geize R.; Dijkhuizen L. Harnessing the catabolic diversity of rhodococci for environmental and biotechnological applications. *Curr. Opin. Microbiol.*, **2004**, *7*, 255-261.

[32] Lotfy, W.A.; Ghanem, K.M.; El-Helow, E.R. Citric acid production by a novel

Aspergillus niger isolate:II Optimization of process parameters through statistical experimental designs. *Bioresour. Technol.*, **2007**, *98*, 3470-3477.

[33] Tanyildizi, M.S.; Özer, D.; Elibol, M. Optimization of α-amylase production by *Bacillus* sp. using response surface methodology. *Process Biochem.*, **2005**, *40*, 2291-2296.

[34] Plackett, R.L.; Burman, J.P. The design of optimum multifactorial experiments. *Biometrika*, **1946**, *33*, 305-25.

[35] Bustos, G.; Moldes, A.B.; Alonso, J.L.; Vazquez, M. Optimization of D-lactic acid production by *Lactobacillus coryniformis* using response surface methodology. *Food Microbiol.*, **2004**, *21*, 143-148.

[36] Vohra, A.; Satyanarayana, T. Statistical optimization of the medium components by response surface methodology to enhance phytase production by *Pichia anomala*. *Process Biochem.*, **2002**, *37*, 999-1004.

[37] Gu, X.B.; Zheng, Z.M.; Yu, H.Q.; Wang, J.; Liang, F.L.; Liu, R.L. Optimization of medium constituents for a novel lipopeptide production by *Bacillus subtilis* MO-01 by a response surface method. *Process Biochem.*, **2005**, *40*, 3196-3201.

[38] Mutalik, S.R.; Vaidya, B.K.; Joshi, R.M.; Desai, K.M.; Nene, S.N. Use of response surface optimization for the production of biosurfactant from *Rhodococcus* spp. MTCC 2574. *Bioresour. Technol.*, **2008**, *99*, 7875-7880.

[39] Choudhari, S.; Singhal, R. Media optimization for the production of β-carotene by *Blakeslea trispora*: A statistical approach. *Bioresour. Technol.*, **2008**, *99*, 722-730.

[40] Box, G.E.P.; Hunter, W.G.; Hunter, J.S. Statistics for experimenters. Jhon Wiley and Sons, New York, **1978**, pp. 291-334.

[41] Nilson, K.; Birnbaum, S.; Flygare, S.; Linse, L.; Schroder, U.; Jeppsson, U.; Larson, P.O.; Mosbach, K.; Brodelius, P. A general method for the immobilization of cells with preserved viability. *Eur. J. Appl. Microbiol. Biotechnol.*, **1983**, *17*, 319-326.

[42] Bettmann, H.; Rehm, H.J. Degradation of phenol by polymer entrapped microorganisms. *Appl. Microbiol. Biotechnol.*, **1984**, *20*, 285-290.

[43] BránYik, T.; Kuncová, G.; Páca, J. The use of silica gel prepared by sol-gel method and polyurethane foam as microbial carriers in the continuous degradation of phenol. *Appl. Microbiol. Biotechnol.*, **2000**, *54*, 168-172.

[44] Chen, K.C.; Lin, Y. Immobilization of microorganisms with phosphorylated polyvinyl alcohol (PVA) gel. *Enzyme Microb. Technol.*, **1994**, 16, 79-83.

[45] López-Serrano, P.; Wegman, M.A.; Rantwijk, F.; Sheldon, R.A. Enantioselective enzyme catalysed ammoniolysis of amino acid derivatives: Effect of temperature. *Tetrahedron: Asymmetr.*, **2001**, *12*, 235-240.

[46] Prasad, S.S.; Misra, A.; Jangir, V.P.; Awasthi, A.; Raj, J.; Bhalla, T.C. A propionitrile-induced nitrilase of *Rhodococcus* sp. NDB 1165 and its application in nicotinic acid synthesis. *World J. Microbiol. Biotechnol.*, **2007**, *23*, 345-353.

[47] Hughes, J.; Armitage, Y.C.; Symes, K.C. Application of whole cell rhodococcal biocatalysts in acrylic polymer manufacture. *Anton. van Leeuw.*, **1998**, *74*, 107-118.

[48] Nawaz, M.S.; Khan, A.A.; Seng, J.E.; Leakey, J.E.; Siitonen, P.H.; Cerniglia, C.E.; Purification and characterization of an amidase from an acrylamide-degrading *Rhodococcus sp. Appl. Environ. Microbiol.*, **1994**, *60(9)*, 3343-3348.

[49] Webster, N.A.; Ramsden, D.K.; Hughes, J. Comparative characterisation of two *Rhodococcus* species as potential biocatalysts for ammonium acrylate production. *Biotechnol. Lett.*, **2001**, *23*, 95-101.

[50] Kotlova, E.K.; Chestukhina, G.G.; Astaurova, O.B.; Leonova, T.E.; Yanenko, A.S., Debabov, V.G. Isolation and primary characterization of an amidase from *Rhodococcus rhodochrous. Biochemistry (Moscow),* **1999**, *64(4)*, 384-389.

[51] Hirrlinger, B.; Stolz, A.; Knackmuss, H.-J. Purification and properties of an amidase from *Rhodococcus erythropolis* MP50 which enantioselectively hydrolyzes 2-arylpropionamides. *J. Bacteriol.*, **1996**, *178(12)*, 3501-3507.

[52] Gotor, V.; Liz, R.; Testera, A.M. Preparation of N-unsubstituted β-ketoamides by *Rhodococcus rhodochrous* catalysed hydration of β-ketonitriles. *Tetrahedron*, **2004**, *60*, 607-618.

[53] Guo, X.-L.; Deng, G.; Xu, J.; Wang, M.-X. Immobilization of *Rhodococcus sp.* AJ270 in alginate capsules and its application in enantioselective biotransformation of *trans*-2-methyl-3-phenyl-oxiranecarbonitrile and amide. *Enzyme Microb. Technol.*, **2006**, *39*, 1-5.

[54] Nawaz, M.S.; Billedeau, S.M.; Cerniglia, C.E. Influence of selected physical parameters on the biodegradation of acrylamide by immobilized cells of *Rhodococcus* sp. *Biodegradation*, **1998**, *9*, 381-387.

[55] Colby, J.; Snella, D.; Black, G.W. Immobilization of *Rhodococcus* AJ270 and use of entrapped biocatalyst for the production of acrylic acid. *Monatshefte für Chemie/Chemical Monthly*, **2000**, *131*, 655-666.

[56] Kim, B-Y.; Hyun, H-H. Production of acrylamide using immobilized cells of *Rhodococcus rhodochrous* M33. *Biotechnol. Bioprocess Eng*., **2002**, *7*,194-200.

CHAPTER

5

Use of immobilized *Aspergillus melleus* aminoacylase for enantioselective synthesis of unnatural amino acids

5.1. INTRODUCTION

L-Aminoacylase (N-acyl amino acid amidohydrolase or acylase-I; EC 3.5.1.14) catalyzes asymmetric hydrolysis of N-acetyl DL-amino acids to give L-amino acids and unhydrolyzed N-acetyl D-amino acids. Because of their broad substrate specificity and high enantioselectivity, L-aminoacylases have emerged as a potential industrial biocatalyst especially for production of enantiopure L-amino acids from N-acyl derivatives [1]. L-aminoacylases are also capable of hydrolyzing peptide (or amide) and ester derivatives of amino acids in an enantioselective manner to yield enantiopure L-amino acids [2]. Further, this enzyme has been successfully applied to the enantioselective acylation of alcohols [3-5] and amines [6] in organic medium. These findings suggest that the commercial utility of L-aminoacylase is expected to expand in years to come.

L-Aminoacylases are found in a wide variety of plants, animals and microorganisms. The most commonly used L-aminoacylases are those from porcine kidney, *Aspergillus oryzae* and *Aspergillus melleus* [7]. L-Aminoacylases from *Aspergillus* sp. are highly enantioselective, readily available, inexpensive and exhibit broad substrate specificity. Aspergillus L-aminoacylases are therefore intensively utilized for the industrial production of L-amino acids (such as L-alanine, L-methionine, L-phenylalanine etc.) from their N-acyl derivatives [8].

Poor storage and operational stability of Aspergillus L-aminoacylases are major hurdles in the efficient utilization of this enzyme on an industrial scale. Several attempts have been made over the years to improve the catalytic activity and operational stability of industrial enzymes through genetic engineering, immobilization and/or process alterations. Enzyme immobilization is the most commonly used strategy to impart the desirable features of heterogeneous catalysts onto biological catalysts [9]. Besides enhanced stability, immobilization is also known to offer several advantages such as reusability, ease of product separation, greater control over catalysis and improved process economics.

Tosa and his co-workers [10] have effectively immobilized aminoacylase on DEAE-Sephadex to develop an industrial system for the enzymatic resolution of DL-amino acids. Subsequently, aminoacylases were immobilized by different methods e.g. via entrapment [11-16], ionic or physical adsorption on polymers [17-19], adsorption onto ultrafiltration membranes [20-21] and by covalent attachment on

functional supports [22, 23].

The present work is aimed at developing a simple method of covalent immobilization of *Aspergillus melleus* L-aminoacylase on an epoxy activated polymeric support which confers better storage and operational stability to the enzyme, enabling its efficient utilization in synthesis of enantiopure unnatural L-amino acids. The covalent immobilization techniques are straightforward, easy to scale-up and generally give higher binding capacities of enzyme per unit weight of support [24]. The polymers having reactive epoxy groups on their surface (commonly known as epoxy activated supports) are perhaps regarded as ideal supports for enzyme immobilization because of their ability to form strong covalent linkages with amino, hydroxyl and thiol groups present in the enzyme under mild conditions of temperature and pH and without affecting enzyme's tertiary/quaternary structure [25]. More interestingly, the physical properties of polymeric support (such as surface area, porosity, density of functional groups) can be easily tailored according to the specific needs.

The present chapter deals with the use of covalently immobilized *Aspergillus melleus* L-aminoacylase for production of enantiopure unnatural L-amino acids. L-aminoacylase was covalently immobilized on novel styrenated acrylic porous polymer beads. The immobilized enzyme was evaluated for pH, thermal and storage stability. The enantioselectivity of immobilized aminoacylase towards hydrolysis of different amino acid derivatives (amino acid ester, N-acetyl amino acids and amino acid amides) was determined. Finally, immobilized aminoacylase was employed for synthesis of enantiopure L-homophenylalanine via kinetic resolution of homophenylalanine amide in laboratory scale stirred cell.

5.2. MATERIALS AND METHODS

5.2.1. Materials

Styrene, glycidyl methacrylate (GMA), divinyl benzene (DVB) and poly vinyl pyrrolidone (PVP, K-90) were purchased from Sigma-Aldrich, USA. 2,20-azobis(isobutyronitrile) (AIBN) and cyclohexanol, were procured from S.D. Fine Chemicals, India. L-Aminoacylase and N-acetyl L-methionine were purchased from Fluka Chemicals, USA. Unnatural amino acids *namely* phenylglycine (PG), homophenylalanine (HPA) and 2-naphthylalanine (NA); and homophenylalanine

ethyl ester were purchased from Bachem Chemicals, Switzerland. All other chemicals were of analytical grade from Merck India Ltd.

5.2.2. Synthesis of polymer beads

Styrene-GMA-DVB ter-polymer (abbreviated as SGDV polymer) with different cross-link density (CLD) were synthesized. The cross-link density of polymer beads is defined as a percentile molar ratio of cross-linking agent to monomer. The polymerization reactions involved in the formation of poly(styrene-GMA-DVB) is schematically represented in Scheme 5.1.

Scheme 5.1: Synthesis of SGDV ter-polymers

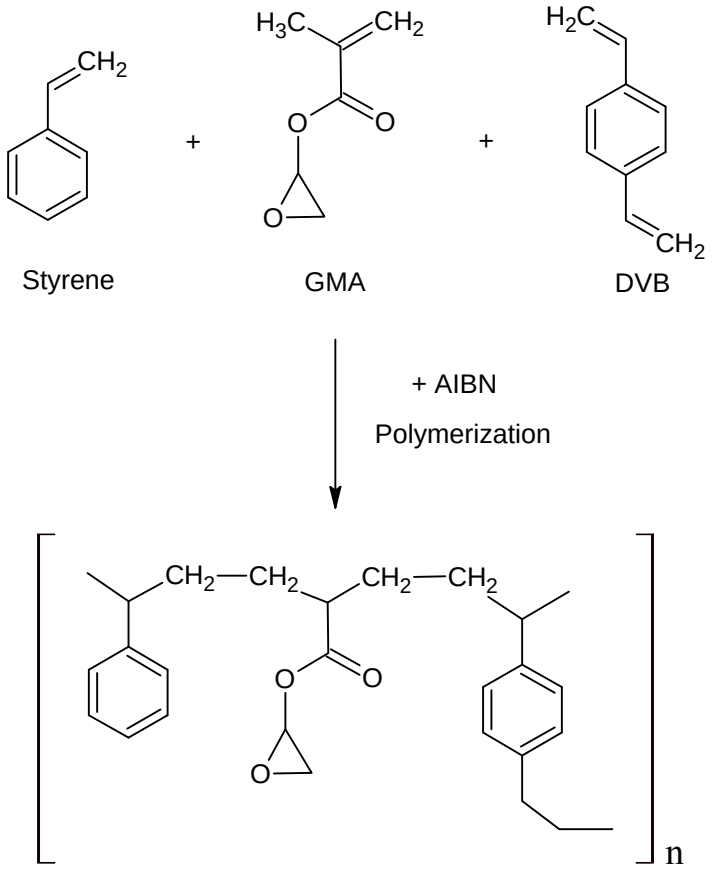

All polymerizations were conducted in a jacketed cylindrical reactor at 70ºC under nitrogen blanket using six bladed Rushton turbines. In the synthesis of SGDV polymer with 25% cross-link density, the continuous phase comprised of 1% by

weight aqueous solution of PVP. The cyclohexanol (discontinuous organic phase) consisted of 3.21 mL styrene, 3.82 mL GMA, 1.99 mL DVB and 0.2 g AIBN. The discontinuous organic phase was introduced into the aqueous phase under stirring at 300 rpm and a constant temperature of 70^{o}C. The polymerization time was 6 hours. The ter-polymer beads obtained were filtered, washed thoroughly with water and methanol, dried under vacuum and sieved through 80-100 mesh. Depending on the CLD, SGDV polymers were termed as SGDV-25, SGDV-50, SGDV-75, SGDV-100, SGDV-150. The composition of different SGDV polymer beads is given in Table 5.1.

Table 5.1: Composition of poly(styrene-GMA-DVB) polymer beads

Polymer	**Styrene**		**GMA**		**DVB**	
	mL	Mole	mL	Mole	mL	Mole
SGDV-25	3.21	0.0280	3.82	0.0280	1.99	0.0139
SGDV-50	2.60	0.0225	3.12	0.0225	3.31	0.0230
SGDV-75	2.21	0.0192	2.63	0.0192	4.13	0.0289
SGDV-100	1.91	0.0166	2.28	0.0166	4.77	0.0334
SGDV-150	1.51	0.0131	1.804	0.0131	5.64	0.0394

5.2.3. Method of aminoacylase immobilization

To dried polymer beads (0.5 g), 10 mL of methanol solution was added in a stoppered conical flask (50 mL capacity) and kept for 1 h with occasional shaking. Methanol was removed by filtration and wetted polymer beads were washed thoroughly with 0.05 M sodium phosphate buffer (pH 8). The wetted polymer beads were suspended in aminoacylase solution prepared in 0.05 M sodium phosphate buffer (pH 8) in a stoppered conical flask (50 mL capacity). Flask was incubated at 30°C at 120 rpm. After 12-18 h immobilized polymer beads were separated by filtration and washed thoroughly with 0.05 M sodium phosphate buffer (pH 8). The supernatant and washings were assayed for protein content. The difference between protein loaded and that remaining unbound indicates quantity of protein bound on the polymer beads.

Immobilized polymer beads were treated with 20 mL of 3 M glycine solution (for 12 h at 30°C on an oscillatory shaker) to block the unreacted epoxide groups of the polymer support. Glycine treated immobilized polymer beads were thoroughly

washed with 0.05 M sodium phosphate buffer (pH 8) and were subsequently incubated in 20 mL of 5% glutaraldehyde solution (for 3 h at 40°C on an oscillatory shaker) to attain stable enzyme binding onto the support. Glutaraldehyde treated immobilized polymer beads were thoroughly washed with 0.05 M sodium phosphate buffer (pH 8) and analyzed for aminoacylase activity as described in Section 5.2.7(b).

5.2.4. Characterization of immobilized aminoacylase

(a) pH stability

The pH stability of free aminoacylase and immobilized aminoacylase on SGDV polymer beads was studied by incubating the enzyme at 20°C in buffers of varying pH in the range of 4-10 for 30 min and then determining the catalytic activity as described in Section 5.2.7(b). Residual activities were calculated as the ratio of the activity of immobilized enzyme after incubation to the activity at the optimum reaction pH.

(b) Temperature stability

The thermal stability of free aminoacylase and immobilized aminoacylase on SGDV polymer beads was tested by incubating the enzyme at varying temperatures in the range of 30-80°C for 30 min (at pH 8) and determining the activity at its optimum reaction temperature. Relative activities were calculated as mentioned above and plotted against temperature.

(c) Kinetic modeling of thermal deactivation of aminoacylase

(i) Thermal deactivation

The thermal deactivation of and free and immobilized aminoacylase were studied at different temperatures between 30°C and 70°C in a shaking water bath (Julabo Ltd.). The samples were withdrawn at regular time interval, rapidly cooled to 37°C and immediately analyzed for residual aminoacylase activity.

(ii) Mathematical modeling

Assuming that *Aspergillus melleus* aminoacylase is not a group of isoenzymes, the deactivation process of the enzyme can proceed through one or several first-order reactions leading to a partially active protein or completely deactivated protein.

Aggregation of deactivated molecules is thought to be a final step after the loss of the activity and this is the only process that can involve higher-order reactions. The kinetic models tested to fit experimental data are shown in Table 5.2.

Table 5.2: Kinetic models tested for the thermal deactivation of *A. melleus* aminoacylase

Model	Deactivation mechanism	Kinetic equation
I	$Enz \xrightarrow{K_1} Enz_1^* \xrightarrow{K_2} Enz_2^*$	$a = \left(1 + \beta_1^* \frac{K_1}{K_2 - K_1} - \beta_2^* \frac{K_2}{K_2 - K_1}\right) \cdot e^{-K_1 t} - \frac{K_1}{K_2 - K_1}(\beta_1^* - \beta_2^*) e^{-K_2 t} + \beta_2^*$
II	$Enz \xrightarrow{K_1} Enz^* \xrightarrow{K_2} Enz^D$	$a = e^{-K_1 t} + \beta_1^* \frac{K_1}{K_2 - K_1}(e^{-K_2 t} - e^{-K_1 t})$
III	$Enz \xrightarrow{K_1} Enz^*$	$a = (1 - \beta^*) e^{-K_1 t} + \beta^*$
IV	$Enz \xrightarrow{K_1} Enz^D$	$a = e^{-K_1 t}$

[*Enz*: Enzyme at time 0; *Enz**: Partially deactivated enzyme; Enz^D: Completely deactivated protein; K_1, K_2: Kinetic constants of thermal deactivation (min^{-1}); *a*: Residual enzyme activity (dimensionless); β_1^*, β_2^* : Activity ratios (dimensionless) between enzyme species; *t*: Time.]

The selection of the aforementioned four models should be enough to fit all the possible kinetic behaviours of the aminoacylase during the deactivation: first-order trend, biphasic behaviour, grace-period tendency to the eventual deactivation [26, 27]. Model I and model II illustrate two consecutive reactions of deactivation with two thermal deactivation kinetic constants, K_1 and K_2. In model I, the enzyme moiety, *Enz* undergoes some deactivation to yield partially deactivated enzyme moiety, Enz_1^* which subsequently undergoes deactivation to yield second partially deactivated enzyme moiety, Enz_2^*. In model II, the enzyme moiety, *Enz* undergoes some deactivation to yield partially deactivated enzyme moiety, Enz^* which undergoes complete deactivation to yield totally deactivated protein, Enz^D. Model III and model IV represent single step deactivation process involving single thermal deactivation kinetic constant, K_1. In model III, the enzyme moiety, *Enz* undergoes

some deactivation to yield partially deactivated enzyme moiety, Enz^* while in model IV, the enzyme moiety, *Enz* undergoes complete deactivation to yield totally deactivated protein, Enz^D.

The parameters of kinetic models were determined using MATLAB code for least square method. For selection of a correct kinetic model, restriction in the parameters was introduced by using the Arrhenius equation in the calculation process. Temperature was used as a variable and the kinetic parameters were developed following the Arrhenius equation.

Statistical and the physical criteria were used for selection of the appropriate kinetic model. The statistical criteria included the goodness of the fit obtained which was assessed by the correlation coefficient (cc) and relative residual sum of squares (RRSSq). The closeness of cc to 1 and lower values of RRSSq are the indicative of better model fit. The physical criteria stipulated that parameters at a given temperature must not be negative and that the activating energy of kinetic constants must be positive [26].

(d) Storage stability

The solution of free aminoacylase (prepared in phosphate buffer, pH 8) and immobilized polymer beads (suspended in phosphate buffer, pH 8) were stored at 4°C. The storage stability was evaluated by determining the enzyme activity of free and immobilized aminoacylase at regular time intervals up to 30 days.

(e) Determination of kinetic constants

The kinetic parameters, K_m and V_{max} of the free and immobilized aminoacylase were determined by measuring initial rates of hydrolysis using as substrate N-acetyl L-methionine (20-100 mM) at 30°C. The K_m and V_{max} values for the free and immobilized aminoacylases were calculated from the Lineweaver-Burk plot using Eq. 5.1.

$$v^{-1} = \left(\frac{K_m}{V_{max}} \right) \cdot [S]^{-1} + V_{max}^{-1} \qquad \text{– Eq. 5.1}$$

Where, [*S*] is the concentration of substrate, *v* and V_{max} represents the initial and maximum rate of reaction, respectively. K_m is the Michaelis constant. Eq. 5.1 represents a straight line slope of which is K_m / V_{max} and Y-intercept is V_{max}^{-1}.

5.2.5. Synthesis and characterization of substrates

(a) Chemical synthesis of rac-amino acid ethyl esters

Rac-amino acid esters were chemically synthesized by esterification of *rac*-amino acids with ethanol in presence of thionyl chloride [28]. The detailed procedure of chemical synthesis of *rac*-amino acid ethyl esters is described earlier in Chapter 2 in Section 2.2.5(a). Phenylglycine ethyl ester and 2-naphthylalanine ethyl ester are termed as PG-ester and NA-ester respectively.

(b) Chemical synthesis of rac-N-acetyl amino acids

N-acetylation of *rac*-amino acids was carried out by standard acetylation procedure (Scheme 5.2) as described by Regla *et al.* [29]. One gram of amino acid was suspended in 10 mL cold water. The temperature of solution was maintained between 0-5°C using ice-bath. At the same temperature, 0.2 g of NaOH was and 1 g of acetic anhydride were added slowly under constant stirring. The pH of resultant reaction mixture was maintained at 11.0-11.5 by adding 50% NaOH. The reaction mixture was allowed to react for 1 h under slow constant stirring (0-5°C, pH 11.0-11.5) and then acidified to pH 2 with 10M HCl. The acidified reaction mixture was allowed to react for 1 h under slow constant stirring at 0-5°C. N-acetyl amino acid precipitate was collected by filtration and washed with minimum quantity of cold water. N-acetyl Phenylglycine, N-acetyl homophenylalanine and N-acetyl 2-naphthylalanine are termed as N-acetyl-PG, N-acetyl-HPA and N-acetyl-NA respectively.

Scheme 5.2: Chemical synthesis of *rac*-N-acetyl amino acids

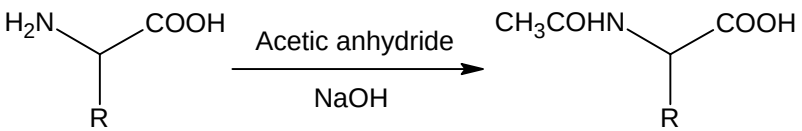

Amino acid → N-acetyl amino acid

	PG	HPA	NA
R-	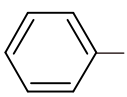	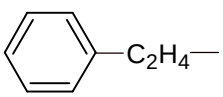	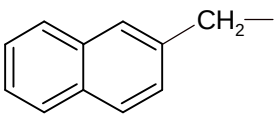

(c) Characterization of rac-N-acetyl amino acids

(i) N-acetyl Phenylglycine (N-acetyl-PG): White solid powder, Analysis: Calculated for $C_{10}H_{11}NO_3$: C 62.17%, H 5.74%, N 7.25%; Found C 62.18%, H 5.73%, N 7.26%. ^{1}H-NMR (200 MHz, DMSO-d_6): 11.87 (1H, COO*H*), 8.34 (1H, N*H*), 8.03-8.45 (5H, aromatic *H*), 5.95 (1H, Ph-C*H*), 2.18 (3H, CH_3).

(ii) N-acetyl Homophenylalanine (N-acetyl-HPA): white solid powder, Analysis: Calculated for $C_{12}H_{15}NO_3$: C 65.14%, H 6.83%, N 6.33%; Found C 65.14%, H 6.82%, N 6.35%. ^{1}H-NMR (200 MHz, DMSO-d_6): 11.92 (1H, COO*H*), 8.23 (1H, N*H*), 7.91-8.42 (5H, aromatic *H*), 4.67 (1H, Ph-CH_2-CH_2-C*H*), 2.54 (2H, Ph-CH_2), 2.07 (2H, Ph-CH_2-CH_2), 1.81 (3H, CH_3).

(iii) N-acetyl 2-Naphthylalanine (N-acetyl-NA): white solid powder, Analysis: Calculated for $C_{15}H_{15}NO_3$: C 70.02%, H 5.88%, N 5.44%; Found C 70.05%, H 5.86%, N 5.45%. ^{1}H-NMR (200 MHz, DMSO-d_6): 12.13 (1H, COO*H*), 8.46 (1H, N*H*), 7.78-8.31 (7H, aromatic *H*), 4.57 (1H, Naphthyl-CH_2-C*H*), 3.12 (2H, Naphthyl-CH_2), 1.92 (3H, CH_3).

(d) Chemical synthesis of rac-amino acid amides

Rac-amino acid amides were synthesized from *rac*-amino acids by the method described by López-Serrano *et al.* [30]. The detailed procedure of chemical synthesis of *rac*-amino acid amides is described in Chapter 4 in Section 4.2.4(a). Phenylglycine amide, homophenylalanine amide and 2-naphthylalanine amide are termed as PG-amide, HPA-amide and NA-amide respectively.

5.2.6. Immobilized aminoacylase catalyzed chiral resolution

(a) General method of chiral resolution

The biotransformation reactions were conducted in 25 mL stoppered flasks. Racemic substrate (0.01 g) was suspended or dissolved in 10 mL phosphate buffer (50mM phosphate buffer, pH 8). Co^{+2} ions act as cofactor for aminoacylase enzyme therefore $CoCl_2$ (1.19 mg) was added in the reaction mixture. The biotransformation reaction was initiated by adding 0.05 g of immobilized aminoacylase. The flask was incubated on an oscillatory shaker at 30°C at 120 rpm. The samples were periodically withdrawn and analyzed by HPLC.

(b) Biocatalytic synthesis of (S)-homophenylalanine in stirred cell

(i) General procedure for synthesis of (S)-homophenylalanine in stirred cell

The schematic diagram and the photograph of the stirred cell bioreactor are shown in Fig. 5.1(a) and Fig. 5.1(b) respectively.

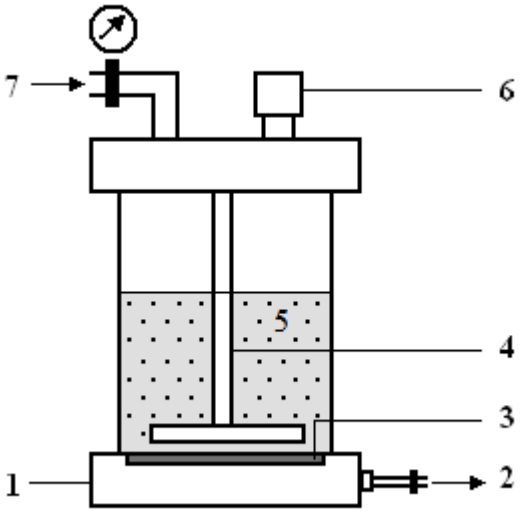

Fig. 5.1(a): Schematic representation of stirred cell bioreactor; 1: membrane support, 2: outlet, 3: macroporous filtration fabric cloth, 4: magnetic stirrer, 5: reaction mixture containing immobilized aminoacylase, 6: sample port and 7: pressure gauze.

Fig. 5.1(b): Photograph of the stirred cell bioreactor

In laboratory scale Millipore stirred cell (XFUF04701, Millipore Inc. USA), macroporous filtration fabric cloth (47mm diameter) was placed on the membrane

support as shown in Fig. 5.1(a). The reactor was charged with 0.1 g of *rac*-HPA-amide and 25 mL of 50 mM phosphate buffer (pH 7) containing 2.98 mg of $CoCl_2$. The biotransformation reaction was initiated by addition of 0.1 g of immobilized aminoacylase. The reactor temperature was maintained at 30°C and constant stirring speed was maintained at 200 rpm. The samples were periodically withdrawn and analyzed by HPLC.

After about 45% of conversion, the reaction was stopped by separating the reaction mixture. The reactor was thoroughly washed twice with phosphate buffer (50mM, pH 7.0) to ensure the complete removal of product and unreacted substrate. The washings and reaction mixture were collected together and the pH of the resultant solution was adjusted to 9 with aqueous 2 M NaOH solution. The unreacted substrate i.e. (*R*)-HPA-amide was extracted with dichloromethane (3×15 mL). The remaining aqueous solution was acidified (to pH 6.3) with 2M HCl solution and maintained at 0-2^{o}C. After ~ 2 h, the precipitate of (*S*)-HPA was collected, washed with cold acidified water (for 3 times) and dried at 60^{o}C under vacuum.

(ii) Evaluation of catalytic performance

The catalytic performance of immobilized aminoacylase was determined in the repetitive cycles of hydrolysis of *rac*-HPA-amide in the stirred cell bioreactor using same biocatalyst and fresh substrate in each cycle.

5.2.7. Analytical Methods

(a) Ter-polymer characterization

(i) Mercury porosimetry

The porosity of polymer beads was determined by mercury intrusion porosimetry with the help of Auto scan 60 mercury porosimeter (Quantachrome, USA) in the range of 0-4000 kg/cm^2.

(ii) Scanning electron microscopy

Surface morphology of the SGDV polymer beads was observed using scanning electron microscopy (SEM). Dried polymer beads were mounted on stubs and sputter-coated with gold. Micrographs were taken on a JEOL-JSM-5200 SEM instrument.

(b) Aminoacylase activity assay

The activity of aminoacylase was measured using the standard hydrolytic assay of N-acetyl L-methionine as described earlier [4]. The detailed assay procedure is as follows: To 1 mL of aminoacylase solution (prepared in 50 mM phosphate buffer, pH 8), 1 mL of 50 mM of $CoCl_2$ solution was added. The temperature of this solution was maintained at 37°C. To this, 1 mL of 100 mM N-acetyl-L-methionine solution was added and incubated at 37°C for 30 min. From this, 1 mL reaction mixture was removed and transferred to stoppered glass test tube and boiled in a boiling water bath for 3 min. The boiled solution was cooled and 2 mL of 2% (w/v) ninhydrin colour reagent and 0.1 mL of 1.6% (w/v) stannous chloride solution ($SnCl_2$) was added to it. The resultant mixture was boiled for 20 min. After cooling 10 mL n-propanol was added, vortexed and the absorbance was determined at 570 nm. One unit (U) is defined as amount of aminoacylase necessary to liberate 1 μmol of L-methionine per hour at 37°C at pH 8.

The activity of immobilized enzyme was determined according to procedure as described above using 0.1 g of immobilized SGDV polymer beads. The activity of immobilized enzyme is expressed in terms of aminoacylase units per g of immobilized SGDV polymer beads.

(c) Protein estimation

The protein estimation was done by Folin-Lowry method [31] wherein bovine serum albumin was used as a standard.

(d) HPLC analysis

All reaction profiles were monitored by HPLC (Thermo Separation Products, Fremont, CA, USA). The quantitative analysis of different amino acids and their esters was carried out using a reverse phase C-18 column (125×4 mm, prepacked column supplemented with a 4×4 mm guard column procured from LiChrospher®, Merck, Darmstadt, Germany) eluted isocratically using acetonitrile-water mobile phase (30:70 v/v, pH adjusted to 3.0 with 50% v/v *o*-phosphoric acid), at a flow rate of 0.6-1.0 mL/min. Peaks were detected using an UV detector at 215 nm. The peak identification was made by comparing the retention times with those of authentic compounds. Peak area was used as a measure to calculate the respective

concentration. The reaction conversion was estimated from the ratio of the substrate consumption to its initial concentration. The enantiomeric excess (e.e.) of the product was determined by using a CHIROBIOTIC-T® column (250×4.6 mm prepacked column supplemented with 20×4 mm guard column procured from Astec Inc. USA) eluted isocratically using water-methanol mobile phase (40:60 v/v, pH adjusted to 2.3-2.5 with 50% v/v glacial acetic acid), at a flow rate of 0.6-0.8 mL/min.

(e) Determination of enantiomeric ratio

Enantiomeric ratio (*E*) is the prime parameter for describing the enzyme's enantioselectivity. Enantiomeric ratio was determined by using Eq. 2.3 as described earlier in Chapter 2 in Section 2.2.7(e).

5.3. RESULTS AND DISCUSSION

5.3.1. Characterization of beaded polymers

(a) Surface area and pore size distribution

Mercury porosimetry provides a good estimate of surface area and pore size distribution. The surface areas for SGDV polymer beads are given in Table 5.3. The increase in CLD from 25 to 100% resulted in increase in pore volume and surface area. However further increase in CLD beyond 100% resulted in decrease in pore volume and surface area.

Table 5.3: Surface area of SGDV polymer beads

Polymer	**CLD** (%)	**Pore volume** (cm^3/g)	**Surface area** (m^2/g)
SGDV-25	25	0.76	90.17
SGDV-50	50	0.80	101.49
SGDV-75	75	1.00	132.32
SGDV-100	100	1.62	148.40
SGDV-150	150	1.23	131.12

The pore size distribution of SGDV polymer beads is given in Table 5.4. The increase in CLD from 25 to 75% resulted in increase in percentage of macropores (pore radii > 100). Increase in CLD beyond 75 resulted in decrease in percentage of macropores. The maximum percentage of macropores was observed in SGDV-75.

Table 5.4: Pore volume distribution in SGDV polymer beads

Polymer	**Distribution in pore radii** (vol%; radius in nm)				
	< 10	**10-50**	**50-100**	**100-300**	**> 300**
SGDV-25	25.95	60.57	11.2	2.08	0.19
SGDV-50	14.08	66.25	17.28	1.01	1.35
SGDV-75	19.50	50.16	21.82	6.22	2.28
SGDV-100	28.91	53.97	12.05	3.64	1.34
SGDV-150	25.88	48.91	20.71	2.79	1.67

(b) Porous surface morphology

The SEM micrographs of SGDV-75 are given in Fig. 5.2. The spherical nature and porous surface morphology of SGDV SGDV-75 were confirmed by the SEM micrographs.

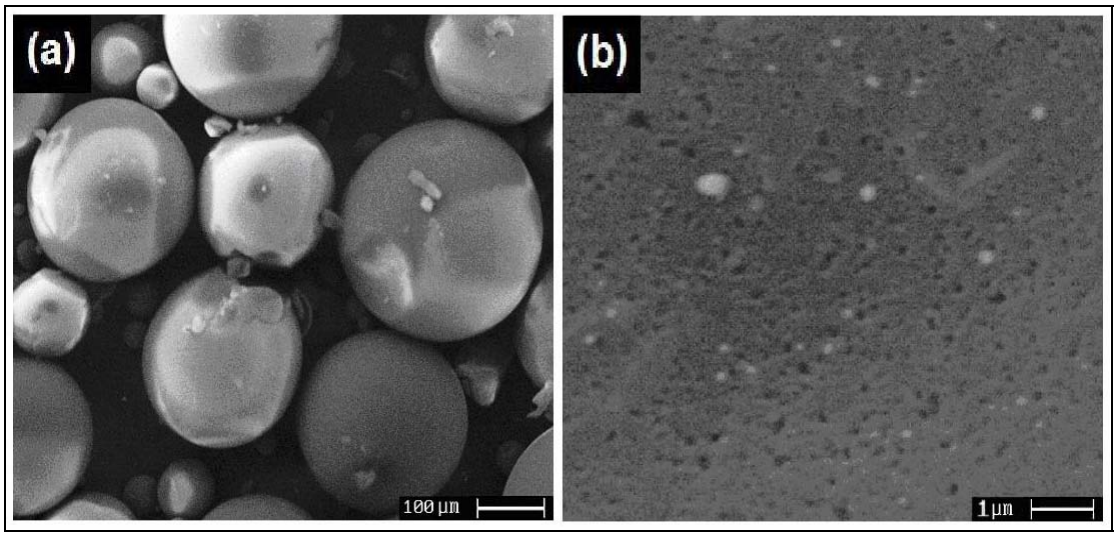

Fig. 5.2: Scanning electron micrographs showing (a) spherical nature of SGDV-75 (250×); (b) porous surface morphology of SGDV-75 (30000×).

5.3.2. Selection of polymer for aminoacylase immobilization

The efficiency of polymer beads to immobilize aminoacylase was calculated in terms of 'activity recovery', which is defined as: the percentile ratio of aminoacylase activity expressed by 1 g of immobilized polymer beads to the total aminoacylase activity of free enzyme used for immobilization (Eq. 5.2).

$$\text{Activity recovery } (\%) = \left(\frac{A_{\text{Immo}}}{{}^{\text{Total}}A_{\text{Free}}} \right) \times 100 \qquad \text{– Eq. 5.2}$$

Where, $A_{Immo.}$ is activity of 1 g of immobilized polymer (U/g of support) and ${}^{Total}A_{Free}$ is total activity of free enzyme loaded on 1 g of polymer. ${}^{Total}A_{Free}$ is a product of activity (U/mL) and volume (mL) of free enzyme loaded on 1g of polymer.

Among five SGDV polymer beads screened for aminoacylase immobilization, SGDV-75 polymer beads gave maximum activity recovery (76.86%, Table 5.5). Therefore, SGDV-75 was selected for further experiments. The maximum activity recovery of immobilized SGDV-75 can be attributed to the macroporous nature of the polymer beads.

Table 5.5: Selection of SGDV polymer for aminoacylase immobilization

Polymer	**Aminoacylase activity** (U/g of support)	**Protein bound** (mg/g of support)	**Specific activity** (U/mg of protein)	**Activity recovery** (%)
Free aminoacylase	5.40 *a*	2.31 *b*	2.34	100.00
SGDV-25	50.98	37.73	1.35	47.20
SGDV-50	73.96	39.38	1.88	68.48
SGDV-75	83.02	39.51	2.10	76.87
SGDV-100	74.45	39.55	1.88	68.94
SGDV-150	78.56	39.47	1.99	72.74

[*a* Units/mL; *b* mg/mL.]

Upon enzyme immobilization, a decrease in enzyme activity has been commonly observed. This is due to the minor modification in the enzyme three-dimensional structure that may lead to the distortion of amino acid(s) residues involved in the catalysis. Further the random immobilization often involves embedding of active sites of a few enzyme molecules making them unable to express their catalytic activity. Another possible reason of decreased enzyme activity can be ascribed to the mass transfer limitations of substrate or/and product [32].

5.3.3. Optimization of immobilization process

(a) Optimization of immobilization time

The time required for aminoacylase immobilization on SGDV-75 was optimized. It can be observed from Fig. 5.3 that aminoacylase activity (U/g of support) and activity recovery (%) of immobilized SGDV-75 attained equilibrium in 12 h. After 12 h aminoacylase activity and activity recovery of immobilized SGDV-75 were found to remain almost constant.

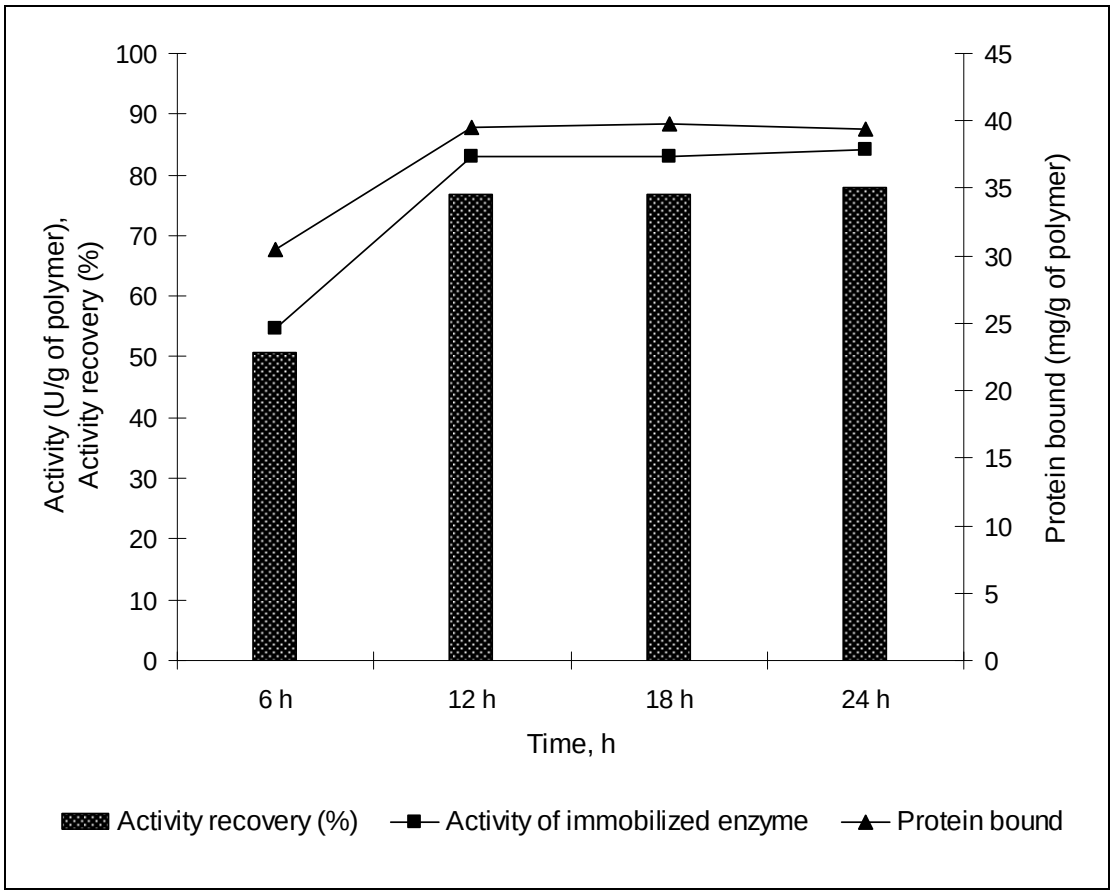

Fig. 5.3: Optimization of time for aminoacylase immobilization on SGDV ter-polymers

(b) Optimization of enzyme loading

SGDV-75 polymer beads were loaded with different concentrations of aminoacylase and the resultant immobilized enzyme was analyzed for aminoacylase activity and protein binding. The results are shown in Table 5.6. The activity recovery of immobilized SGDV remained almost constant in enzyme loading from 40 to 100 mg/g of polymer beads. However, beyond enzyme loading of 100 mg/g a sudden

decrease in the activity recovery was observed. Enzyme loading beyond 100 mg probably might have resulted in embedding of active sites of aminoacylase molecules during the immobilization process by increased stacking and also by increased diffusion limitations.

Table 5.6: Optimization of aminoacylase loading on SGDV polymer beads

Amino-acylase (mg)	**Activity of free enzyme** (U/mL)	**Protein of free enzyme** (mg/mL)	**Activity of immobilized enzyme** (U/g of support)	**Protein bound** (mg/g of support)	**Activity recovery** (%)
40	72.01	30.81	55.43	27.15	76.98
60	108.22	46.22	83.02	39.51	76.71
80	144.14	61.6	110.26	52.11	76.50
100	180.25	77.00	136.04	67.23	75.47
120	216.37	92.41	143.32	79.73	66.24

Among different methods, entrapment and physical adsorption methods have been extensively employed for immobilization of aminoacylase enzyme. Reports on entrapment of aminoacylase within calcium alginate beads [11], chitosan coated calcium alginate beads [12], polyethyleneimine stabilized calcium alginate beads [13], acrylamide gel lattice [14], κ-carrageenan gel [15], gelatine [16] etc. are available in the literature. In addition, many articles on physical adsorption of the enzyme onto different acrylic polymeric supports [17-19] and binding onto ultrafiltration membranes [20, 21] are reported. However, reports on covalent immobilization of aminoacylase are scant. Bódalo *et al.* described the immobilization of L-aminoacylase on porous glass beads [22, 23]. Here, the covalent attachment of enzyme on glass support was carried out by aminoaryle method [33]. One gram of immobilized enzyme expressed 4710 U of aminoacylase activity (determined by N-acetyl DL-valine as substrate) and immobilized ~16 mg of protein.

5.3.4. Stability of immobilized aminoacylase

(a) pH stability

The effect of pH on the catalytic activity of free and immobilized

aminoacylase was studied in the pH range of 4-10 (Fig. 5.4). Immobilization of enzyme on SGDV-75 polymer beads resulted in stabilization of enzyme over a broader pH range. The free aminoacylase retained 11.71% and 30.43% residual activity at pH 4 and pH 5 respectively whereas for the same pH conditions immobilized aminoacylase retained 53.04% and 66.03% residual activity, respectively. The free aminoacylase retained 48.56% and 14.79% residual activity at pH 9 and pH 10 whereas at same pH conditions immobilized aminoacylase retained 89.09% and 73.42% residual activity, respectively. These results indicate that the described immobilization procedure has improved the stability of aminoacylase in the acidic as well as in the alkaline region.

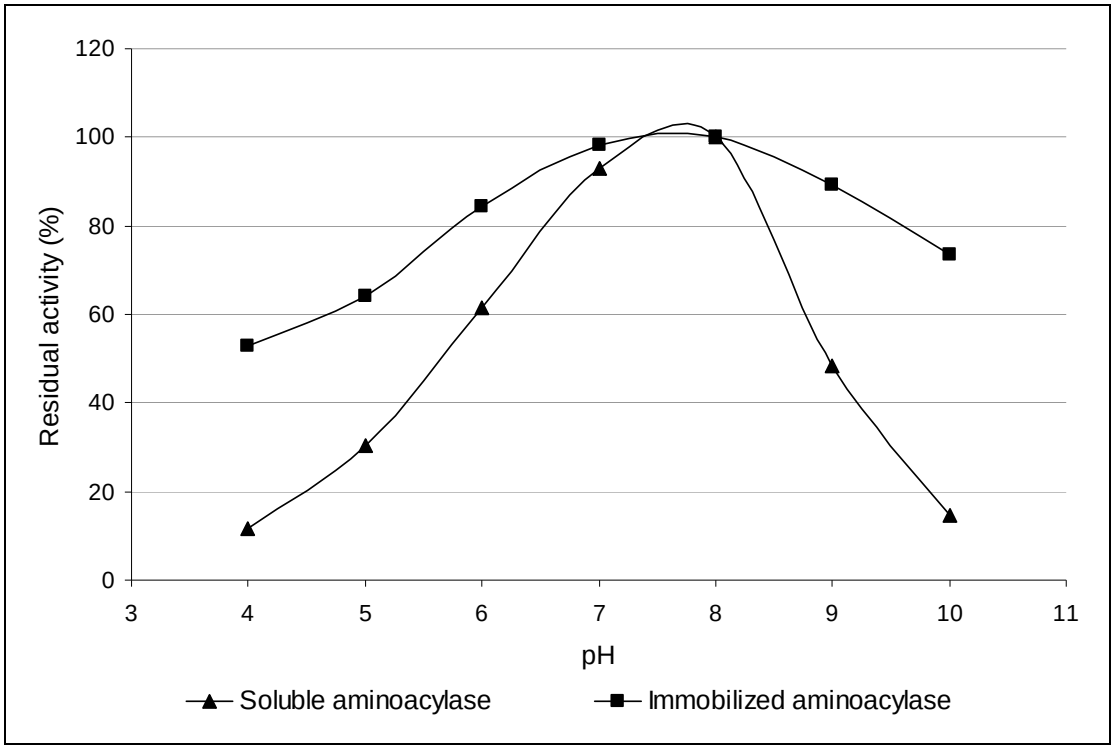

Fig. 5.4: pH stability of immobilized aminoacylase

(b) Temperature stability

The activity profiles of free and immobilized aminoacylase at different temperatures are graphically represented in Fig. 5.5. The stability of free and immobilized aminoacylase was determined by measuring residual enzyme activity as a function of temperature in the range of 30-80°C. The immobilization of enzyme on SGDV-75 polymer beads has significantly improved the thermal stability of the

enzyme. For instance, at 50°C the free aminoacylase retained only 66.42% residual activity while immobilized enzyme found to retain 98.67% activity. Similarly at 70°C the free enzyme retained only 4.75% residual activity while immobilized enzyme was found to retain 93.35% of its initial activity.

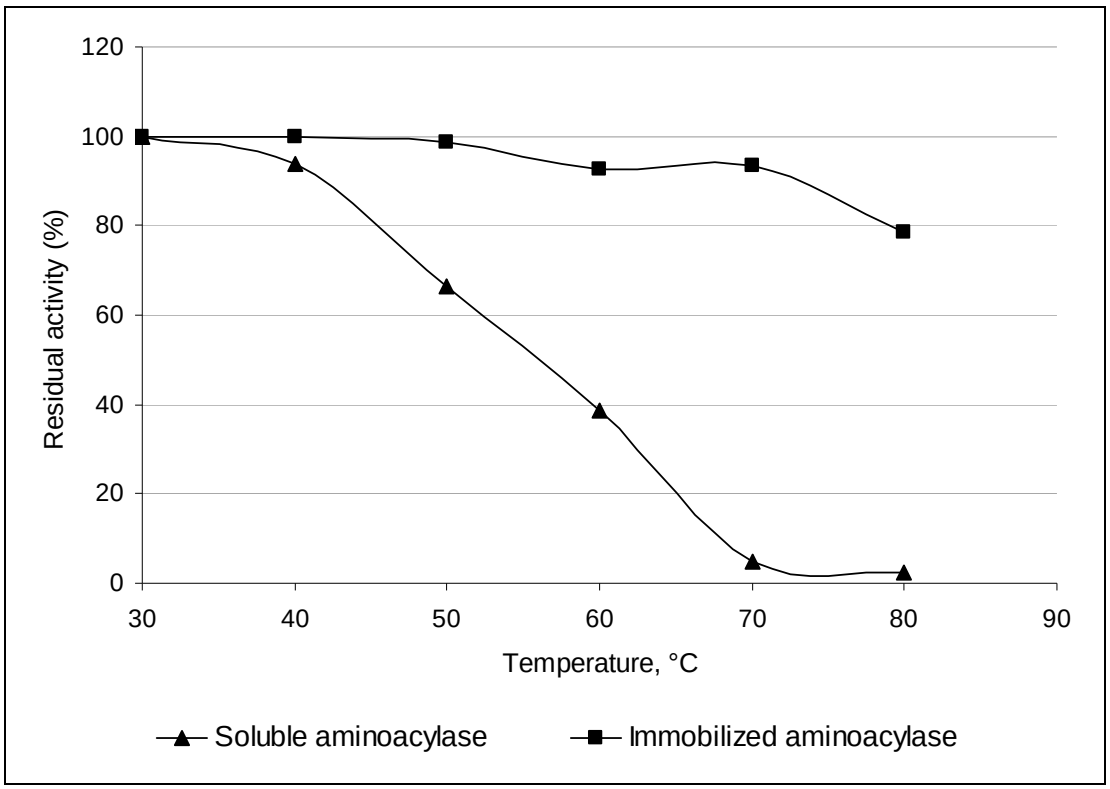

Fig. 5.5: Temperature stability of immobilized aminoacylase

(c) Kinetic modelling for thermal deactivation

The thermal deactivation of free and immobilized aminoacylase are presented in Fig. 5.6(a) and Fig. 5.6(b) respectively. The parameters of kinetic models were determined using MATLAB code for least square method. Selected kinetic models and their parameter values for the thermal deactivation of free aminoacylase are given in Table 5.7. Model I gave best fit for thermal deactivation of soluble aminoacylase at 30°C and 40°C. Model III gave best fit for thermal deactivation of soluble aminoacylase at 50°C and 60°C. Model IV gave best fit for thermal deactivation of soluble aminoacylase at 70°C and 80°C. Similarly, selected kinetic models and their parameter values for the thermal deactivation of immobilized aminoacylase are given in Table 5.8. Model I gave best fit for thermal deactivation of soluble aminoacylase at 30°C to 60°C. Model IV gave best fit for thermal deactivation of soluble

aminoacylase at 70°C and 80°C. The high cc and least RRSSq. values for each model (given in Table 5.7 for soluble enzyme and Table 5.8 for immobilized enzyme) indicate the closeness of experimental values and model predicted values and thus confirm the statistical relevance of the model adequacy.

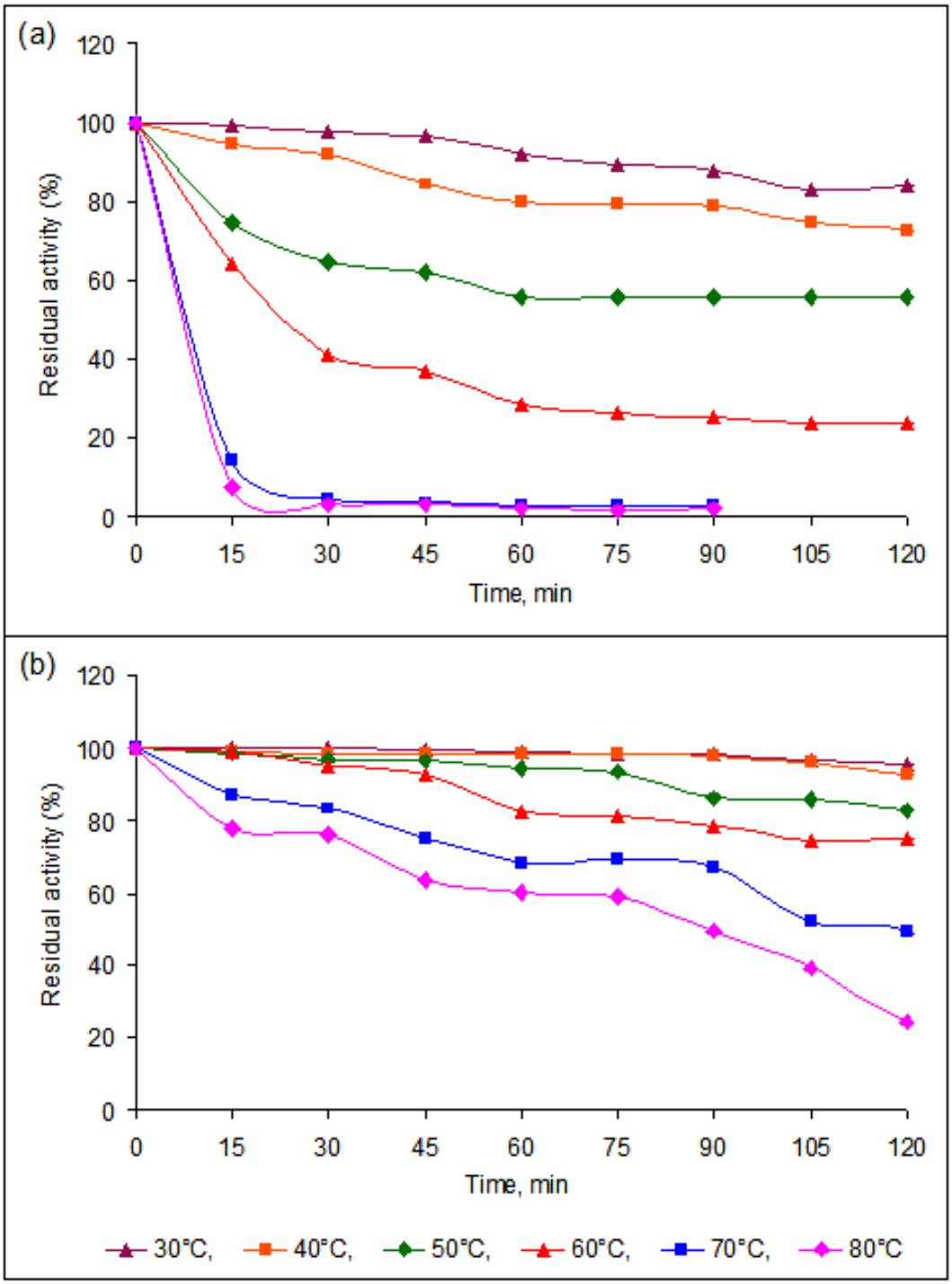

Fig. 5.6: Thermal deactivation of (a) soluble aminoacylase and (b) immobilized aminoacylase in temperature range of 30-80°C

Table 5.7: Selected kinetic models and their parameter values for the thermal deactivation of free aminoacylase

Temperature	Model	Model fitting values [a]	Parameter values
30°C, 40°C	I	cc = 0.997; RRSSq. = 3.16×10^{-4}	$K_1 = \exp[8.22 - (3348.55/ T)]$ $K_2 = \exp[8.80 - (2966.06/ T)$ $\beta_1^* = \exp[2.13 - (671.05/ T)]$ $\beta_2^* = \exp[13.82 - 5035.91/ T)]$
50°C, 60°C	III	cc = 0.988; RRSSq. = 2.76×10^{-3}	$K_1 = \exp[4.3 - (975.71/ T)]$ $\beta^* = \exp[13.12 - (4157.96/ T)]$
70°C, 80°C	IV	cc = 0.986; RRSSq. = 4.41×10^{-3}	$K_1 = \exp[2.41 - (1099.42/ T)]$

[[a] cc: correlation coefficient; RRSSq: relative residual sum of squares. RRSSq. = $[\sum(a_e - a_c)^2/\sum a_e^2]\cdot100$ where, a_e is experimental residual enzyme activity and a_c is calculated residual enzyme activity (calculated using selected kinetic model).]

Table 5.8: Selected kinetic models and their parameter values for the thermal deactivation of immobilized aminoacylase

Temperature	Model	Model fitting values [a]	Parameter values
30°C, 40°C	I	cc = 0.991; RRSSq. = 6.93×10^{-4}	$K_1 = \exp[11.74 - (4458.57/ T)]$ $K_2 = \exp[-0.34 - (634.91/ T)]$ $\beta_1^* = \exp[-0.33 + (108.03/ T)]$ $\beta_2^* = \exp[4.14 - (2059.70/ T)]$
50°C, 60°C	I	cc = 0.986; RRSSq. = 2.62×10^{-3}	$K_1 = \exp[5.09 - 2546.21/ T)]$ $K_2 = \exp[15.29 - 5356.09/ T)]$ $\beta_1^* = \exp[-0.80 + 254.62/ T)]$ $\beta_2^* = \exp[23.79 - 8660.94/ T)]$
70°C, 80°C	IV	cc = 0.982; RRSSq. = 5.41×10^{-3}	$K_1 = \exp[4.43 - (2279.46/ T)]$

[[a] cc: correlation coefficient; RRSSq: relative residual sum of squares.]

The quantitative estimate of thermal stabilization of enzyme upon immobilization can be obtained by the comparison of kinetic constants (K) and activity ratios (β^*) for the given temperature. The comparison of kinetic constants and activity ratios of soluble and immobilized aminoacylase in the range of 30°C to 80°C is given in Table 5.9. For the given temperature, the values of kinetic constants (K) of immobilized enzyme were found consistently lesser than that of soluble enzyme. This indicates the rate of thermal deactivation for immobilized enzyme was lesser than that of soluble enzyme. Moreover, for the given temperature, the values of activity ratios (β^*) of immobilized enzyme were found consistently higher than that of soluble enzyme. Higher β^* values of immobilized enzyme than that of soluble enzyme are also indicative of thermal stabilization of enzyme [26, 27].

Table 5.9: Comparison of kinetic constants (K) and activity ratios (β^*)

Temp.	Enzyme	Model	K_1	K_2	β_1^*	β_2^*
30°C	Soluble enzyme	I	0.0015	0.1043	0.9702	0.0015
	Immobilize enzyme	I	0.0010	0.0864	1.0410	0.0022
40°C	Soluble enzyme	I	0.0034	0.2145	0.8244	0.0054
	Immobilize enzyme	I	0.0032	0.0032	1.0142	0.0064
50°C	Soluble enzyme	III	0.0500	–	0.5500	–
	Immobilize enzyme	I	0.0016	0.0519	0.9581	0.0090
60°C	Soluble enzyme	III	0.0400	–	0.2200	–
	Immobilize enzyme	I	0.0028	0.1634	0.9073	0.0061
70°C	Soluble enzyme	IV	0.1600	–	–	–
	Immobilize enzyme	IV	0.0061	–	–	–
80°C	Soluble enzyme	IV	0.1900	–	–	–
	Immobilize enzyme	IV	0.0094	–	–	–

(d) Storage stability

The storage stability of immobilized aminoacylase was determined and compared with that of free aminoacylase. The plot of log residual activity vs. storage time is shown in Fig. 5.7. The linear trend lines were drawn to the activity profiles of free and immobilized aminoacylase. The storage half-life of each enzyme preparation

was determined from its respective trend line equation. The storage half-life of free aminoacylase was found to be ~ 1 day while that of immobilized aminoacylase was found to be ~ 54 days. Thus upon immobilization, the storage stability of aminoacylase was found to increase dramatically.

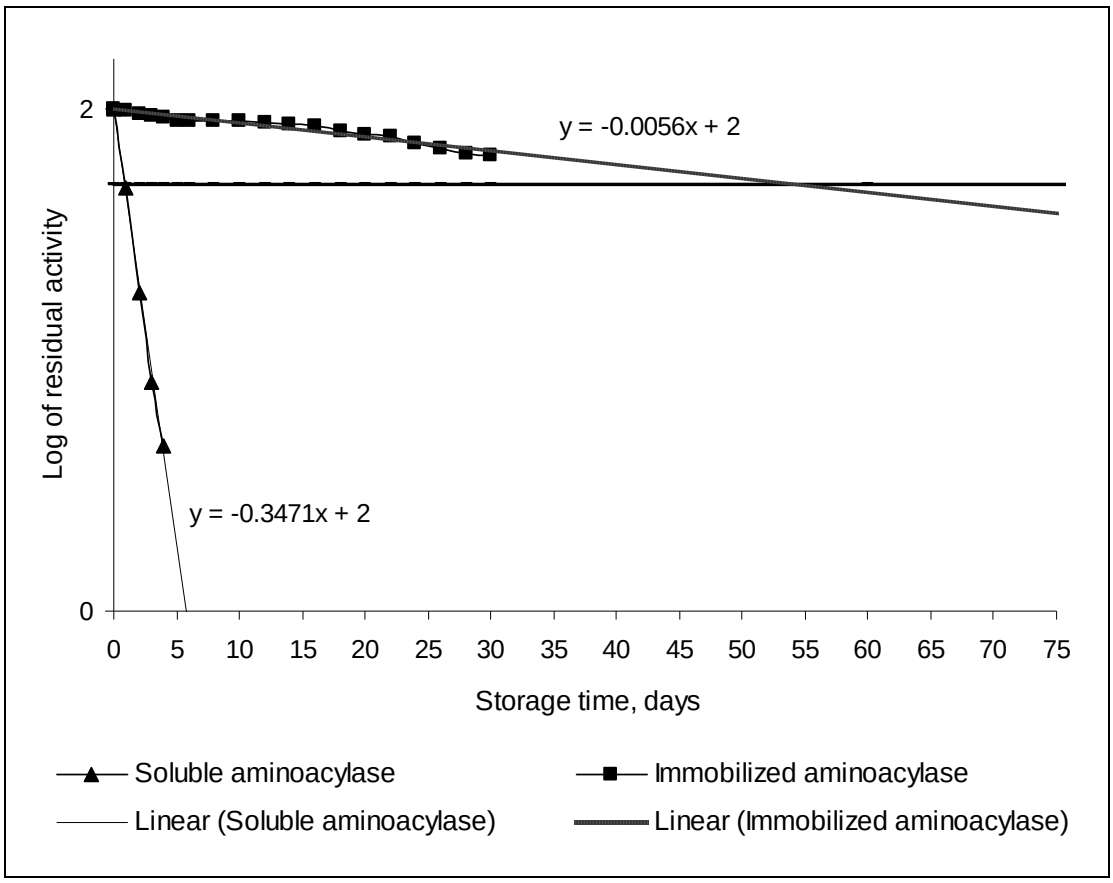

Fig. 5.7: Storage stability of immobilized aminoacylase [The trend line equations were used to calculate the respective storage half-lives. The horizontal line (─) at log(50) was drawn only for a graphical illustration of the storage half-lives.]

5.3.5. Kinetic behaviour of free and immobilized aminoacylase

The effect of substrate concentration on the initial rate catalyzed by free and immobilized aminoacylase was studied using N-acetyl L-methionine as substrate. Michaelis constant (K_m) and the maximum reaction velocity (V_{max}) of the free and immobilized enzymes were calculated from Lineweaver-Burk plot. The kinetic parameters of free and immobilized aminoacylase are presented in Table 5.10. K_m values for free and immobilized enzyme were 0.7 mM and 1.51 mM respectively. V_{max} values for free and immobilized enzyme were 61.70 U/mg and 12.44 U/mg

respectively. Thus, immobilized enzyme was observed to have higher K_m and lower V_{max} values than that of free aminoacylase. The kinetic behaviour of an enzyme can be precisely described using catalytic efficiency (V_{max}/K_m). The catalytic efficiency of immobilized aminoacylase was found to be ~ 10 times lower than that of free aminoacylase. The increase in the K_m and decrease in V_{max} values could be either due to the conformational changes of the enzyme (upon immobilization) resulting in a lesser efficiency of substrate-enzyme complex formation or due to lower accessibility of the substrate to the active site of the immobilized enzyme caused by the increased mass transfer limitations [34, 35].

Table 5.10: Kinetic parameters of free and immobilized aminoacylase

Parameter	**Free aminoacylase**	**Immobilized aminoacylase**
Michaelis constant, K_m (mM)	0.7	1.51 [a]
Maximum reaction velocity, V_{max} (U/mg) [b]	61.70	12.44
Catalytic efficiency, V_{max}/K_m ($min^{-1} \cdot mg^{-1}$)	88.14	8.24
Catalytic constant, k_{cat} (s^{-1})	152.19	228.21
Specificity constant, k_{cat}/K_m ($mM^{-1} \cdot s^{-1}$)	217.42	151.13
Efficiency coefficient, η	–	0.2

[[a] $K_{m,\ app.}$; considering the possibility of interactions of substrate with beaded polymer support, there could be difference in the substrate concentrations in the bulk solution and near the enzyme. This phenomenon is known as 'substrate partition' [35]. Hence, the term 'apparent' is used for the K_m of the immobilized enzyme and symbolized as $K_{m,\ app.}$; [b] V_{max} is expressed per mg of protein for the free aminoacylase and per mg of polymer beads for the immobilized aminoacylase.]

The catalytic constant (k_{cat}, which is also known as turnover number) was estimated from the V_{max} value using 74 kDa molecular mass of *A. melleus* L-aminoacylase. The k_{cat} values of free and immobilized aminoacylase were 152.19 s^{-1} and 228.21 s^{-1} respectively. The specificity constant (k_{cat}/K_m) of free and immobilized aminoacylase were 217.42 $mM^{-1} \cdot s^{-1}$ and 151.13 $mM^{-1} \cdot s^{-1}$ respectively. The efficiency coefficient (η) can be calculated from the maximum reaction rates of the immobilized

enzyme over that of the free enzyme. The η value of immobilized aminoacylase was observed to be 0.20. The very low η value suggests the occurrence of predominant mass-transfer limitations [36].

5.3.6. Immobilized aminoacylase catalyzed chiral resolutions

Aminoacylases exhibit broad substrate specificity. They have ability to hydrolyze wide spectrum of amino acid derivatives (such as amino acid esters, N-acetyl amino acids, amino acid amides) in enantioselective manner. Hence aminoacylases are perhaps the most versatile and potent biocatalyst for synthesis of enantiopure amino acids.

(a) Chiral resolution of amino acid esters

Immobilized aminoacylase preferentially hydrolyzed the *S*-enantiomer of unnatural amino acid ethyl esters. Chiral resolution of amino acid esters catalyzed by immobilized aminoacylase is represented in Scheme 5.3.

Scheme 5.3: Chiral resolution of amino acid esters catalyzed by immobilized aminoacylase

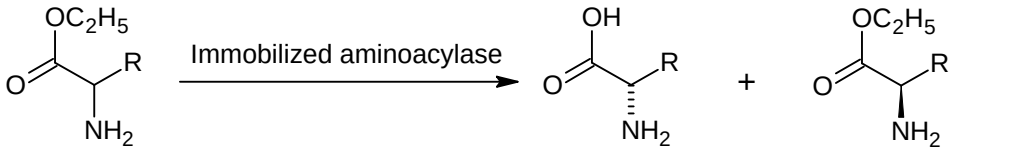

(*RS*)-Amino acid ester (*S*)-Amino acid (*R*)-Amino acid ester

	PG	HPA	NA
R-	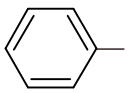	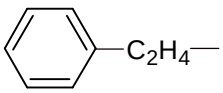	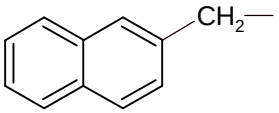

The results of stereoselective hydrolysis of unnatural amino acid ethyl esters using immobilized aminoacylase are summarized in Table 5.11. The enantiomeric ratios of immobilized aminoacylase towards hydrolysis of PG-ester, HPA-ester and NA-ester were 5.8, 14.2, 7.9 respectively.

Table 5.11: Chiral resolution of amino acids ethyl esters catalyzed by immobilized aminoacylase

Substrate	**Preferred configuration**	**Time** (min)	**ee$_p$** (%)	***C*** (%)	***E***
PG-ester	*S*	120	56.2	47.5	5.8
HPA-ester	*S*	120	84.8	15.8	14.2
NA-ester	*S*	120	75.2	13.7	7.9

(b) Chiral resolution of N-acetyl amino acids

As represented in the Scheme 5.4, immobilized aminoacylase was observed to hydrolyze preferentially the *S*-enantiomer of N-acetyl amino acids.

Scheme 5.4: Chiral resolution of N-acetyl amino acids catalyzed by immobilized aminoacylase

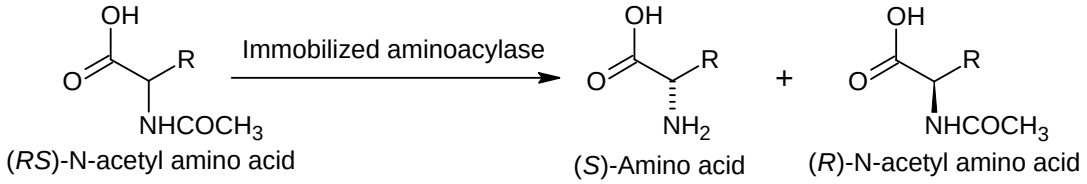

	PG	HPA	NA
R-	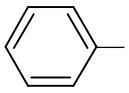	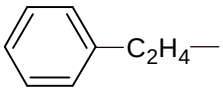	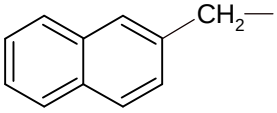

The results of stereoselective hydrolysis of N-acetyl amino acids using immobilized aminoacylase are summarized in Table 5.12.

Table 5.12: Chiral resolution of N-acetyl amino acids catalyzed by immobilized aminoacylase

Substrate	**Preferred configuration**	**Time** (min)	**ee$_p$** (%)	***C*** (%)	***E***
N-acetyl-PG	*S*	120	91.5	45.1	51.0
N-acetyl-HPA	*S*	120	93.2	42.3	58.2
N-acetyl-NA	*S*	120	87	34.3	22.5

The immobilized enzyme exhibited higher enantioselectivity towards hydrolysis of N-acetyl-PG and N-acetyl-HPA as indicated from the higher *E* values (51.0 and 58.2 respectively) than that towards hydrolysis of N-acetyl-NA (*E* = 22.5).

(c) Chiral resolution of amino acid amides

As represented in the Scheme 5.5, immobilized aminoacylase observed to hydrolyze preferentially the *S*-enantiomer of amino acid amides.

Scheme 5.5: Chiral resolution of amino acid amides catalyzed by immobilized aminoacylase

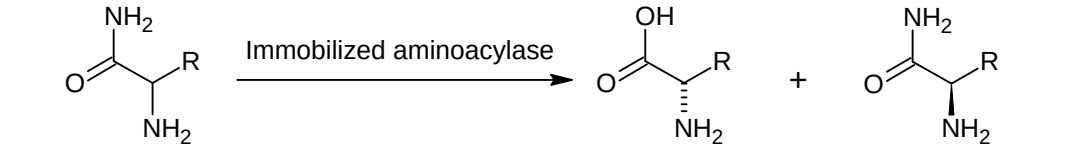

(*RS*)-Amino acid amide (*S*)-Amino acid (*R*)-Amino acid amide

	PG	HPA	NA
R-	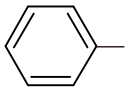	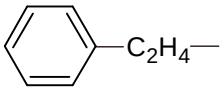	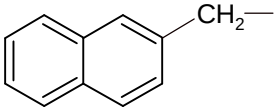

The results of stereoselective hydrolysis of amino acid amides using immobilized aminoacylase are summarized in Table 5.13. The *E* values of hydrolysis of PG-amide and HPA-amide were >200 and that of hydrolysis of 2-NA- amide was >100 indicating the remarkable enantioselectivity of immobilized aminoacylase towards these hydrolytic reactions.

Table 5.13: Chiral resolution of amino acid amides catalyzed by immobilized aminoacylase

Substrate	**Preferred configuration**	**Time** (min)	**ee$_p$** (%)	***C*** (%)	***E***
PG-amide	*S*	120	97.6	45.2	>200
HPA-amide	*S*	120	97.3	47.6	>200
NA-amide	*S*	120	96.0	46.1	125.7

To summarize, enantiomeric ratios of the immobilized enzyme were high ($E \approx$ 125 to 200) towards hydrolysis of amides, moderate ($E \approx$ 22 to 59) towards hydrolysis of N-acetyl derivatives and poor ($E < 15$) towards the hydrolysis of amino acid esters. Youshko *et al.* reported similar observations i.e. authors reported higher enantiomeric ratios of *A. melleus* L-aminoacylase towards hydrolysis of PG-amide and HPA-amide (i.e. $E > 200$) than that towards hydrolysis of N-acetyl-PG and N-acetyl-HPA ($E = 96$ and 70 respectively) [37].

The literature survey on aminoacylase catalyzed enantioselective synthesis of different amino acids from N-acetyl amino acids is summarized in Table 5.14. Most of the previous efforts deal with aminoacylase catalyzed enantioselective hydrolysis of *rac*-N-acetyl amino acid. This process has also been successfully commercialized for the industrial production of enantiopure amino acids [37]. The present study, however, indicates that aminoacylase has higher enantioselectivity towards hydrolysis of amides than that towards hydrolysis of N-acetyl derivatives of unnatural amino acids. Thus, the enantioselective production of these unnatural amino acids via aminoacylase catalyzed hydrolysis of *rac*-amino acid amides appears to be an attractive alternative.

Table 5.14: Literature on aminoacylase catalyzed synthesis of enantiopure amino acids

Amino acid	**Substrate**	**Source of L-aminoacylase**	**Reference**
L-Alanine	N-acetyl DL-alanine	*Pseudomonas* sp.	[15, 38, 39]
L-Methionine	N-acetyl DL-methionine	*Aspergillus oryzae*	[16, 18, 40]
		Porcine kidney	[17]
L-Valine	N-acetyl DL-methionine	Hog kidney	[22]
L-Phenylalanine	N-acetyl DL-phenylalanine	Porcine kidney	[13, 20]
L-Alanine and L-phenylalanine	*Rac*-N-acetyl and N-formyl derivatives	Porcine kidney and *Aspergillus* sp.	[41]
L-Methionine and L-phenylalanine	*Rac*-N-acetyl derivatives of amino acids	*Aspergillus oryzae*	[42]

Continued…

Table 5.14: *Continued…*

Amino acid	Substrate	Source of L-aminoacylase	Reference
L-Valine and L-phenylalanine	*Rac*-N-acetyl derivatives of amino acids	Porcine kidney	[43]
L-4-Fluoro-glutamic acid	*Rac*-N-acetyl derivatives of amino acid	Porcine kidney and *Aspergillus* sp.	[44]
Different L-amino acids	*Rac*-N-acetyl derivatives of amino acid	Porcine kidney and *Aspergillus* sp.	[45]
Different L-amino acids	*Rac*-N-acetyl derivatives of amino acid	*Aspergillus melleus*	[37]
Different L-amino acids	*Rac*-N-acetyl and N-chloroacetyl amino acids	Porcine kidney and *Aspergillus* sp.	[1]
L-Butyrine	N-acetyl-DL-butyrine	Porcine kidney	[21, 46]
Aromatic β-amino acids	*Rac*-N-chloroacetyl derivatives	Porcine kidney	[47]

5.3.7. Reusability of immobilized aminoacylase in hydrolysis of rac-HPA-amide

The initial reaction rate of three repeated cycles of hydrolysis of *rac*-HPA-amide was studied in stirred cell bioreactor. The first cycle proceeded with initial reaction rate of 3.9 $M \cdot min^{-1} \cdot g^{-1}$. However, the initial reaction rate found to decrease sharply in second (2.82 $M \cdot min^{-1} \cdot g^{-1}$) and third (1.9 $M \cdot min^{-1} \cdot g^{-1}$) repetitive cycles. Thus about 2-fold reduction in the rate of reaction was observed indicating the inadequate reusability of the immobilized enzyme. The high stirring speed could possibly be responsible for the mechanical attrition of immobilized polymer beads which might have released enzyme from the polymeric support. Hence in order to overcome this problem, the reactor was operated at slower speed (100 rpm). This however reduced the initial rate of reaction by 3.6 folds.

5.4. CONCLUSIONS

The immobilization of L-aminoacylase on epoxy-activated porous polymer beads of styrene-glycidyl methacrylate-divinyl benzene ter-polymers has significantly improved the stability of aminoacylase with respect to pH, temperature and storage.

Enantiomeric ratios of the immobilized enzyme were high ($E \approx 125$ to 200) towards hydrolysis of amides, moderate ($E \approx 22$ to 59) towards hydrolysis of N-acetyl derivatives and poor ($E < 15$) towards the hydrolysis of amino acid esters. Thus, the production of enantiopure amino acids via aminoacylase catalyzed hydrolysis of *rac*-amino acid amides appears to be an attractive alternative. However the operational stability of immobilized aminoacylase found to be inadequate for reuse of the enzyme in a repetitive batch mode.

REFERENCES

[1] Chenault, H.K.; Jürgen Dahmer, J.; Whitesides, G.M. Kinetic resolution of unnatural and rarely occurring amino acids: Enantioselective hydrolysis of N-acyl amino acids catalyzed by acylase. *J. Am. Chem. Soc.*, **1989**, *III*, 6354-6364.

[2] Youshko, M.I.; van Langen, L.M.; Sheldon, R.A.; Švedas, V.K. Application of aminoacylase I to the enantioselective resolution of α-amino acid esters and amides. *Tetrahedron: Asymmetr.*, **2004**, *15*, 1933-1936.

[3] Faraldos, J.; Arroyo, E.; Herradón, B. Biocatalysis in organic synthesis. 9. Highly enantioselective kinetic resolution of secondary alcohols catalyzed by acylase. *Synlett.*, **1997**, 367-370.

[4] Bakker, M.; Spruijt, A.S.; van Rantwijk, F.; Sheldon, R.A. Highly enantioselective aminoacylase-catalyzed transesterification of secondary alcohols. *Tetrahedron: Asymmetr.*, **2000**, *11*, 1801-1808.

[5] Liljeblad, A.; Aksela, R.; Kanerva, L.T. Use of enantio-, chemo- and regioselectivity of acylase I. Resolution of polycarboxylic acid esters. *Tetrahedron: Asymmetr.*, **2001**, *12*, 2059-2066.

[6] Youshko, M.I.; van Rantwijk, F.; Sheldon, R.A. Enantioselective acylation of chiral amines catalyzed by aminoacylase I. *Tetrahedron: Asymmetr.*, **2001**, *12*, 3267-3271.

[7] Sato, T.; Tosa, T. Optical resolution of racemic amino acids by aminoacylase. *Bioprocess Technol.*, **1993**, *16*, 3-14.

[8] Espenson, J.H. Chemical Kinetics and Reaction Mechanisms. McGraw-Hill, New York, **1981**.

[9] Won, K.; Kim, S.; Kim, K. J.; Park, H.W.; Moon, S. J. Optimization of lipase entrapment in Ca-alginate gel beads. *Process Biochem.*, **2005**, *40*, 2149-2154.

[10] Tosa, T.; Mori, T.; Fuse, N.; Chibata, I. Studies on continuous enzyme reactions. I. Screening of carriers for preparation of water-insoluble aminoacylase. *Enzymologia*, **1966**, *31*, 214-218.

[11] Bódalo, A.; Bastida, J.; Gómez, J.L.; Gómez, E.; Alcaraz, I.; Asanza, M.L. Stabilization studies of L-aminoacylase-producing *Pseudomonas* sp. BA2 immobilized in calcium alginate gel. *Enzyme Microb. Technol.*, **1997**, *21*, 64-69.

[12] Lee, K.H.; Lee, P.M.; Siaw, Y.S. Studies of L-phenylalanine production by immobilized aminoacylase in stabilized calcium alginate beads. *J. Chem. Technol. Biotechnol.*, **1992**, *54*, 375-82.

[13] Lee, P.M.; Lee, K.H.; Siaw, Y.S. Immobilization of aminoacylase in polyetheleneimine stabilized calcium alginate beads for L-phenylalanine production. *Biomaterials, Artificial Cells and Immobilization Biotechnology*, **1993**, *21(4)*, 563-570.

[14] Mori, T.; Sato, T.; Tosa, T.; Chibata, I. Studies on immobilized enzymes. X. Preparation and properties of aminoacylase entrapped into acrylamide gel lattice. *Enzymologia*, **1972**, *43*, 213-216.

[15] Bódalo-Santoyo, A.; Rodríguez, J.B.; Gómez-Carrasco, J.L.; Gómez, E.G.; Rojo, I.A.; Asanza-Teruel, M.L. Production of optically pure L-alanine by immobilized *Pseudomonas* sp. BA2 cells. *J. Chem. Technol. Biotechnol.*, **1998**, *73*, 197-202.

[16] Yuan, Y.-J.;_ Wang, S.-H.; Song, Z.-X.; Gao, R.-C. Production of L-methionine by immobilized pellets of *Aspergillus oryzae* in a packed bed reactor. *J. Chem. Technol. Biotechnol.*, **2002**, *77*, 602-606.

[17] Maxim, S.; Fondor, A.; Bunia, I. Optical resolution of D,L-acetylmethionine with immobilized aminoacylase on acrylic supports. *J. Mol. Catal.*, **1992**, *72*, 351-359.

[18] He, B.; Li, M.; Wang, D. Studies on aminoacylase from *Aspergiuus oryzae* immobilized on polyacrylate copolymer. *React. Polym.*, **1992**, *17*, 341-346.

[19] Wang, D.; Li, M.; He, B. Immobilization of aminoacylase from *Aspergillus oryzae* on synthetic modified polyacrylamides. *Biotechnol. Appl. Biochem.*, **1992**, *16(2)*, 115-124.

[20] Bódalo, A.; Gómez, J.L.; Gómez, E.; Bastida, J.; Máximo, M.F.; Montiel, M.C. Ultrafiltration membrane reactors for enzymatic resolution of amino acids:

design model and optimization. *Enzyme Microb. Technol.*, **2001**, *28*, 355-361.

[21] Bódalo, A.; Gómez, J.L.; Gómez, E.; Máximo, M.F.; Montiel, M.C. Study of L-aminoacylase deactivation in an ultrafiltration membrane reactor. *Enzyme Microb. Technol.*, **2004**, *35*, 261-266.

[22] Bódalo-Santoyo, A., Gómez-Carrasco, J.L.; Gómez-Gómez, E.; Bastida-Rodriquez, J.; Máximo-Martín, M.F.; Hidalgo-Montesinos A.M. Production of optically pure L-valine in fluidized and packed bed reactors with immobilized L-aminoacylase. *J. Chem. Technol. Biotechnol.*, **1999**, *74*, 403-408.

[23] Bódalo, A.; Gómez, J.L.; Gómez, E.; Bastida, J.; León, G.; Máximo, M.F.; Hidalgo, A.M. Influence of pore size on covalent immobilization of L-aminoacylase on porous glass supports. *Anales de Química, Int. Edt.*, **1998**, *94*, 78-83.

[24] Mateo, C.; Abian, O.; Fernandez-Lafuente, R.; Guisan, J.M. Increase in conformational stability of enzymes immobilized on epoxy-activated supports by favoring additional multipoint covalent attachment. *Enzyme Microb. Technol.*, **2000**, *26*, 509-515.

[25] Mateo, C.; Fernandez–Lafuente, G.; Abian, O.; Fernandez-Lafuente, R.; Guisan, J.M. Multifunctional epoxy supports: A new tool to improve the covalent immobilization of proteins, the promotion of physical adsorptions of proteins on the supports before their covalent linkage. *Biomacromolecules*, **2000**, *1*, 739-745.

[26] Ladero, M.; Ferrero, R.; Vian, A.; Santos, A.; Garcia-Ochoa, F. Kinetic modelling of the thermal and pH inactivation of a thermostable β-galactosidase from *Thermus* sp. strain T2. *Enzyme Microb. Technol.*, **2005**, *37*, 505-513.

[27] Ladero, M.; Ruiz, G.; Pessela, B.C.C.; Vian, A.; Santos, A.; Garcia-Ochoa, F. Thermal and pH inactivation of an immobilized thermostable β-galactosidase from *Thermus* sp. strain T2: Comparison to the free enzyme. *Biochem. Eng. J.*, **2006**, *31*, 14-24.

[28] Bodanszky, M.; Bodanszky, A. In: The Practice of Peptide Synthesis. Berlin: Springer-Verlag. **1984**.

[29] Regla, I.; Luna, H.; Herminia, I.; Pérez, H.I.; Demare, P.; Bustos-Jaimes, I.; Zaldívar, V.; Calcagno, M.L. Enzymatic resolution of N-acetyl-homophenylalanine with mammalian kidney acetone powders. *Tetrahedron:*

Asymmetr., **2004**, *15*, 1285-1288.

[30] López-Serrano, P.; Wegman, M.A.; Rantwijk, F.; Sheldon, R.A. Enantioselective enzyme catalysed ammoniolysis of amino acid derivatives: Effect of temperature. *Tetrahedron: Asymmetr.*, **2001**, *12*, 235-240.

[31] Lowry, O.H.; Rosebrough, N.J.; Farr, A.L.; Randall, R. J. Protein measurement with the Folin Phenol reagent. *J. Biol. Chem.*, **1951**, *193*, 265-275.

[32] Ye, P.; Xu, Z.K.; Wu, J.; Innocent, C.; Seta, P. Nanofibrous membranes containing reactive groups: Electrospinning from poly(acrylonitrile-*co*-maleic acid) for lipase immobilization. *Macromolecules*, **2006**, *39,* 1041-1045.

[33] Weetall, H.H. Covalent coupling methods for inorganic supports. *In:* Methods in Enzymology, Mosbach K. (*Ed*.), Vol. 44, Academic Press, New York, **1996**, pp. 134-148.

[34] Pencreaćh, G.; Leullier, M.; Baratti, J.C. Properties of free and immobilized lipase from *Pseudomonas cepacia*. *Biotechnol. Bioeng.*, **1997**, *56(20)*, 181-189.

[35] Dordick, J.S. Enzymatic catalysis in monophasic organic solvents. *Enzyme Microb. Technol.*, **1989**, *11,* 194-211.

[36] Tischer, W.; Kasche, V. Immobilized enzymes: crystals or carriers? *Trends Biotechnol.*, **1999**, *17*, 326-335.

[37] Youshko, M.I.; van Langen, L.M.; Sheldon, R.A.; Švedas, V.K. Application of aminoacylase I to the enantioselective resolution of α-amino acid esters and amides. *Tetrahedron: Asymmetr.*, **2004**, *15*, 1933-1936.

[38] Bódalo-Santoyo, A.; Bastida-Rodriquez, J.; Gómez-Carrasco, J.L.; Gómez-Gómez, E.; Alcaraz Rojo, I.; Asanza Teruel, M.L. Immobilization of *Pseudomonas* sp. BA2 by entrapment in calcium alginate and its application for the production of L-alanine. *Enzyme Microb. Technol.*, **1996**, *19*, 176-180.

[39] Bódalo, A.; Bastida, J.; Gómez, J.L.; Gómez, E.; Alcaraz, I.; Asanza, M.L. Stabilization studies of L-aminoacylase-producing *Pseudomonas* sp. BA2 immobilized in calcium alginate gel. *Enzyme Microb. Technol.*, **1997**, *21*, 64-69.

[40] Li, M.-Q.; Wang, D.-B.; Zhou, J.-Y.; He, B.-L. Studies on immobilization of aminoacylase from *Aspergillus oryzae* on macroporous carriers. *Science in China (Scientia Sinica), Series B*., **1993**, *36(7)*, 778-784.

[41] Simons, C.; van Leeuwen, J.G.E.; Stemmer, R.; Arends I.W.C.E.; Maschmeyer, T.; Sheldon, R.A.; Hanefeld, U. Enzyme-catalysed deprotection

of *N*-acetyl and *N*-formyl amino acids. *J. Mol. Catal. B: Enzym.*, **2008**, *54*, 67-71.

[42] Li, M.; Wang, D.; Zhou, J.; He, B. Studies on the immobilization of aminoacylase (from *Aspergillus oryzae*) with polymer carriers. *Lizi Jiaohuan Yu Xifu/Ion Exchange and Adsorption*, **1993**, *9(3)*, 199-203.

[43] Bódalo, A.; Gómez, E.; Gómez, J.L.; Bastida, J.; León, G.; Máximo, M.F.; Hidalgo, A.M.; Montiel, M.C. Kinetic calculations in the enzymatic resolution of DL-amino acids. *Enzyme Microb. Technol.*, **1999**, *24*, 381-387.

[44] Kokuryo, Y.; Nakatani, T.; Kobayashi, K.; Tamura, Y.; Kawada, K.; Ohtani, M. Practical synthesis of L-erythro- and L.threo-4.Fluoroglutamic acids using aminoacylase. *Tetrahedron: Asymmetr*., **1996**, *7(12)*, 3545-3551.

[45] Bommarius, A.S.; Drauz, K.; Klenk, H.; Wandrey, C. Operational stability of enzymes: Acylase-catalyzed resolution of N-acetyl amino acids to enantiomerically pure L-amino acids. *Annals of the New York Academy of Sciences*, **1992**, *672*, 126-136.

[46] Bódalo, A.; Gómez, J.L.; Gómez, E.; Máximo, M.F.; Montiel, M.C. Kinetics of the L-aminoacylase-catalyzed resolution of N-acetyl-DL-butyrine. *J. Chem. Technol. Biotechnol.*, **2002**, *77*, 552-558.

[47] Gröger, H.; Trauthwein, H.; Buchholz, S.; Drauz, K.; Sacherer, C.; Godfrin, S.; Werner, H. The first aminoacylase-catalyzed enantioselective synthesis of aromatic β-amino acids. *Org. Biomol. Chem.*, **2004**, *2*, 1977-1978.

CHAPTER

6

Preparation of cross-linked enzyme aggregates of *Aspergillus melleus* aminoacylase for enantioselective synthesis of unnatural amino acids

6.1. INTRODUCTION

The development of stable and robust biocatalysts for industrial use is currently the subject of great research interest [1]. Cross-linked enzyme technology in the past couple of decades, has emerged as an attractive tool for enhancing the stability of enzymes [2-7]. The cross-linking of enzymes by means of bifunctional cross-liking agents results in formation of stable heterogeneous biocatalyst which offers distinct benefits over conventionally immobilized enzyme. Immobilized enzymes are 'carrier-bound biocatalysts' and the presence of a large proportion of non-catalytic carrier (about 90-99% of total mass) causes dilution of their volumetric activity. On the other hand, the cross-linked enzymes are referred as 'carrier-free biocatalysts' and express very high catalytic activity per unit volume thereby maximizing volumetric productivity and space-time yields [8-10].

The cross-linked carrier-free biocatalyst can be obtained by either of following three approaches *namely*: (i) direct cross-linking of free enzyme which gives cross-linked enzymes (CLE); (ii) cross-linking of crystalline enzyme which yields cross-linked enzyme crystals (CLEC) and (iii) cross-linking of physically aggregated enzyme which yields cross-linked enzyme aggregates (CLEA) [11].

More often than not, direct cross-linking of enzyme molecules (CLE) suffer from several disadvantages such as low activity retention, poor reproducibility, poor mechanical stability and difficulty in handling the gelatinous CLE. The cross-linking of enzyme in crystalline form (CLEC) was found to give better results in terms of activity retention and mechanical stability and therefore has been successfully commercialized [12-17]. However, the need for highly pure enzyme and development of crystallization protocols (which are often expensive, laborious and time consuming) have discouraged further growth of the CLEC methodology.

To overcome the above drawbacks of CLE and CLEC, a novel strategy called cross-linked enzyme aggregates (CLEA) was developed by Cao *et al.* in 2000 [18]. The synthesis of CLEA involves the precipitation of the enzyme (not necessarily in its pure form) followed by chemical cross-linking of the resulting enzyme aggregates. Precipitation and aggregation are generally induced by the addition of precipitant (salts, organic solvents, non-ionic polymers or acids) to aqueous solutions of proteins. These physical aggregates are supramolecular structures held together by non-covalent bonding and redissolve when precipitant is removed. Cross-linking of these

aggregates produces CLEA which remain insoluble in absence of precipitant [8].

The reactive functional groups (mainly amino groups of lysine) present on the surface of an enzyme (termed as external functional groups) can participate in the process of cross-linking. Thus, cross-linking efficiency of an enzyme depends principally on the number of external amino groups. Enzymes having sufficient external amino groups can be effectively cross-linked leading to formation of stable CLEA. Enzymes having low number of surface reactive amino groups suffer from inadequate cross-linking leading to formation of mechanically fragile CLEA. This often causes leaching of enzyme in the reaction medium during the biocatalysis [19].

Wilson *et al.* have demonstrated that the co-precipitation of enzyme with ionic polymers (having a large number of primary amino groups such as polyethyleneimine) prior to cross-linking can improve the cross-linking efficiency [6]. The co-precipitation of enzyme with ionic polymers allows the extension of polymer branches (having terminal amino groups) closer to some of the embedded amino groups of enzyme favouring cross-linking between them [19, 20]. Thus, besides surface reactive groups, a few embedded reactive groups (which are otherwise not accessible during conventional cross-linking procedures) can also be utilized in formation of stable cross-links. Moreover, the co-precipitation of enzyme with ionic polymers such as polyethyleneimine (PEI) is known to exert excellent stabilizing effects on enzyme by altering the microenvironment of enzyme molecules [21].

The present chapter explores the feasibility of the PEI induced co-aggregation technique for making CLEA of *Aspergillus melleus* aminoacylase. L-Aminoacylase (N-acyl amino acid amidohydrolase or acylase-I; EC 3.5.1.14) catalyzes asymmetric hydrolysis of N-acetyl DL-amino acids to give L-amino acids and unhydrolyzed N-acetyl D-amino acids. L-Aminoacylases are found in various sources such as plants, animals and microorganisms. The most commonly used L-aminoacylases are those from porcine kidney, *Aspergillus oryzae*, and *Aspergillus melleus* [22]. L-Aminoacylases from *Aspergillus* sp. are highly enantioselective, readily available, inexpensive and exhibit broad substrate specificity. *Aspergillus* L-aminoacylases are therefore extensively used for the industrial production of L-amino acids (such as L-alanine, L-methionine, L-phenylalanine etc.) from their N-acyl derivatives [23].

CLEA of L-aminoacylase were prepared via co-precipitating the enzyme with PEI and cross-linking the enzyme-PEI co-aggregates by glutaraldehyde. The critical

process parameters (*namely*: enzyme:PEI ratio, glutaraldehyde concentration and cross-linking time) were optimized. The systematic characterization of aminoacylase-PEI CLEA was done with respect to their physical properties (particle size, porosity etc.) and catalytic behaviour (storage, pH and temperature stability). The thermal deactivation of free enzyme and CLEA was studied using Arrhenius plots. Finally, CLEA were employed for synthesis of enantiopure unnatural amino acids.

6.2. MATERIALS AND METHODS

6.2.1. Materials

L-Aminoacylase and N-acetyl L-methionine were purchased from Fluka Chemicals, USA. Polyethyleneimine (PEI) was purchased from Sigma-Aldrich, USA. Unnatural amino acids *namely* phenylglycine (PG), homophenylalanine (HPA) and 2-naphthylalanine (NA); and homophenylalanine ethyl ester (HPA-ester) were purchased from Bachem Chemicals, Switzerland. All other chemicals were of analytical grade and purchased from Merck India Ltd.

6.2.2. Synthesis of cross-linked enzyme aggregates (CLEA)

All experiments were performed at least in triplicate and the results are presented as their mean value. Standard deviation of results never exceeded 5%.

(a) Co-aggregation of aminoacylase with PEI

Cross-linked enzyme aggregates (CLEA) of *A. melleus* aminoacylase were prepared by co-aggregation of the enzyme with polyethyleneimine (PEI). To 25 mL solution of PEI (750 KDa, 25 mg/mL) 25 mL of aminoacylase (25 mg/mL) solution was added under agitation. The mixture was left under gentle stirring for 10 min. After 10 min, 2.0 mL of glutaraldehyde solution (25% v/v) was added to cross-link the enzyme precipitate and the mixture was kept under stirring for 1 h. Then the volume was doubled by adding 100 mM sodium bicarbonate buffer (pH 10) and a total amount of 75 mg of sodium borohydride powder was added to reduce the Schiff's bases formed. After 15 min, an additional 75 mg of sodium borohydride powder was added and allowed to react for 15 min. The resultant precipitate of aminoacylase-PEI CLEA was repeatedly washed with sodium phosphate buffer (100 mM, pH 7) and centrifuged at 12,000 rpm for 15 min. Finally the CLEA were dried at

50°C for 24 hours using vacuum oven to remove residual moisture.

(b) Optimization of process parameters

Optimization of different process parameters (such as enzyme-PEI ratio, glutaraldehyde concentration and cross-linking time) was done on the basis of two parameters: *namely* activity recovery (Eq. 6.1) and aggregation yield (Eq. 6.2) as described earlier [19].

$$\text{Activity recovery}\,(\%) = \left(\frac{A_{CLEA}}{A_{Free} \times V_{Free}}\right) \times 100 \qquad \text{– Eq. 6.1}$$

$$\text{Aggregation yield}\,(\%) = \left[100 - \left(\frac{A_{Residual} \times V_{Residual}}{A_{Free} \times V_{Free}}\right)\right] \times 100 \qquad \text{– Eq. 6.2}$$

Where, A_{CLEA} is activity (U) expressed by CLEA; A_{Free} is activity (U/mL) of free enzyme; V_{Free} is volume (mL) of free enzyme used to synthesize CLEA; $A_{Residual}$ is activity (U/mL) of residual enzyme solution and $V_{Residual}$ is volume (mL) of residual enzyme solution after formation of CLEA.

6.2.3. Characterization of cross-linked enzyme aggregates

(a) Study of the enzyme release from the aggregates

The storage stability of aminoacylase-PEI CLEA was evaluated in terms of the enzyme release from the aggregates as described earlier [19]. To determine the covalent attachment of enzyme subunits, different aggregates were boiled (at about 95°C) in 2 volumes of 2% sodium dodecyl sulfate (SDS). Thereby, any non-covalently attached enzyme molecule in the aggregate was released in the medium. Then, the supernatants were subjected to SDS-polyacrylamide gel electrophoresis (SDS-PAGE) and the gel (stained with either Coomassie blue or silver staining) was analyzed by densitometry.

(b) Storage stability of aminoacylase-PEI CLEA

The free aminoacylase and aminoacylase-PEI CLEA were incubated at 4°C. The activity of free enzyme and CLEA were determined at regular time intervals up to 168 h. The storage stability was evaluated by plotting activity profiles of both enzyme preparations against storage time.

(c) pH stability of aminoacylase-PEI CLEA

The pH stability of free aminoacylase and aminoacylase-PEI CLEA was studied by incubating the enzyme in buffers of different pH in the range of 4-12 at 20°C for 30 min and then determining the catalytic activity as described in Section 6.2.6(a). Residual activities were calculated as the percentile ratio of the activity of enzyme after incubation to the activity of enzyme at the optimum reaction pH.

(d) Temperature stability of aminoacylase-PEI CLEA

The effect of temperature on stability of free aminoacylase and aminoacylase-PEI CLEA was evaluated by incubating the enzyme at varying temperatures in the range of 20-90°C (at pH 8) and determining the activity at its optimum reaction temperature. Residual activities were calculated and plotted against temperature. Residual activities were calculated as the percentile ratio of the activity of enzyme after incubation to the activity enzyme at the optimum temperature.

(e) Kinetics of thermal deactivation of aminoacylase before and after cross-linking

Kinetics of thermal deactivation of free aminoacylase and aminoacylase-PEI CLEA were studied at different temperatures between 30°C and 70°C in a shaking water bath (Julabo Ltd.). The samples were withdrawn at regular time interval, rapidly cooled to 37°C and immediately analyzed for residual aminoacylase activity. The thermal deactivation rate constant (k_d) was determined from the Arrhenius equation (Eq. 6.3) [24].

$$\ln k_d = \ln A - \left(\frac{E_d}{\mathrm{RT}}\right) \qquad \text{– Eq. 6.3}$$

Where, E_d is the deactivation energy, A is percent residual activity, R is the universal gas constant (8.314×10^{-3} kJ kmol^{-1} K^{-1}) and T is temperature in Kelvin.

Natural logarithm of percent residual activities at different temperatures were plotted against time and the slope of lines indicates the values of deactivation rate constant k_d at the respective temperatures [25]. Half-life of CLEA and free aminoacylase for each temperature was calculated from their respective trend line equations. Arrhenius plot (a graph of ln k_d versus 1/T) was obtained, slope of which indicates the deactivation energy (E_d). The difference in the deactivation energies (ΔE_d) of free enzyme and CLEA was calculated to quantify the thermal stabilization.

6.2.4. Synthesis and characterization of substrates

(a) Chemical synthesis of rac-amino acid ethyl esters

Rac-amino acid esters were chemically synthesized by esterification of *rac*-amino acids with ethanol in presence of thionyl chloride [26]. The detailed procedure of chemical synthesis of *rac*-amino acid ethyl esters is described earlier in Chapter 2 in Section 2.2.5(a). Phenylglycine ethyl ester and 2-naphthylalanine ethyl ester are termed as PG-ester and NA-ester respectively.

(b) Chemical synthesis of rac-N-acetyl amino acids

N-acetylation of *rac*-amino acids was carried out by standard acetylation procedure as described by Regla *et al.* [27]. The detailed procedure of chemical synthesis of *rac*- N-acetyl amino acids is described earlier in Chapter 5 in Section 5.2.5(b). N-acetyl Phenylglycine, N-acetyl homophenylalanine and N-acetyl 2-naphthylalanine are termed as N-acetyl-PG, N-acetyl-HPA and N-acetyl-NA respectively.

(c) Chemical synthesis of rac-amino acid amides

Rac-amino acid amides were synthesized from *rac*-amino acids by the method described by López-Serrano *et al.* [28]. The detailed procedure of chemical synthesis of *rac*-amino acid amides is described earlier in Chapter 4 in Section 4.2.4(a). Phenylglycine amide, homophenylalanine amide and 2-naphthylalanine amide are termed as PG-amide, HPA-amide and NA-amide respectively.

6.2.5. Aminoacylase-PEI catalyzed chiral resolutions

(a) General method of chiral resolution

The biotransformation reactions were conducted in 25 mL stoppered flasks. Racemic substrate (0.01 g) was suspended or dissolved in 10 mL phosphate buffer (50mM phosphate buffer, pH 8). Co^{+2} ions act as cofactor for aminoacylase enzyme therefore $CoCl_2$ (1.19 mg) was added in the reaction mixture. The biotransformation reaction was initiated by adding 0.05 g of aminoacylase-PEI CLEA. The flask was incubated on oscillatory shaker at 30°C at 120 rpm. The samples were periodically withdrawn and analyzed by HPLC.

(b) Biocatalytic synthesis of (*S*)*-homophenylalanine in stirred cell*

(i) General procedure for synthesis of (*S*)*-homophenylalanine in stirred cell*

Reaction was carried out in a laboratory scale Millipore stirred cell (XFUF04701, Millipore Inc. USA; Fig. 6.1).

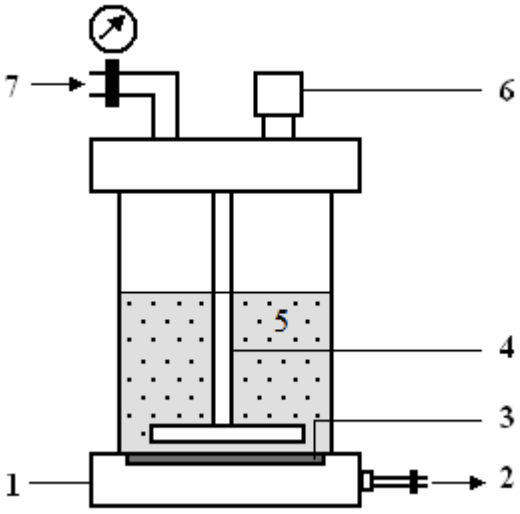

Fig. 6.1(a): Schematic representation of stirred cell bioreactor; 1: membrane support, 2: outlet, 3: macroporous filtration fabric cloth, 4: magnetic stirrer, 5: reaction mixture containing CLEA, 6: sample port and 7: pressure gauze.

Fig. 6.1(b): Photograph of the stirred cell bioreactor

A macroporous filtration fabric cloth (47 mm diameter) was placed on the membrane support. The reactor was charged with 0.1 g of *rac*-HPA-amide and 25 mL

of 50 mM of phosphate buffer (pH 7) containing 2.98 mg of $CoCl_2$. The biotransformation reaction was initiated by addition of 0.1 g of aminoacylase-PEI CLEA. The temperature within the stirred cell was maintained at 30°C under constant stirring at 200 rpm. The samples were periodically withdrawn and analyzed by HPLC.

After about 45% conversion, the reaction was stopped by separating the reaction mixture. The reactor was thoroughly washed twice with phosphate buffer (50mM, pH 7.0) to ensure the complete removal of product and unreacted substrate. The washings and reaction mixture were collected together and the pH of the resultant solution was adjusted to 9 with aqueous 2 M NaOH solution. The unreacted substrate i.e. (*R*)-HPA-amide was extracted with dichloromethane (3×15 mL). The remaining aqueous solution was acidified (to pH 6.3) with 2M HCl solution and maintained at 0-2^{o}C. After ~ 2 h, the precipitate of (*S*)-HPA was collected, washed thrice with cold acidified water and dried at 60^{o}C under vacuum.

(ii) Optimization of catalytic performance

Effect of biocatalyst loading, diffusional limitations and temperature on the rate of reaction was investigated in order to optimize the catalytic performance of the reactor.

6.2.6. Analytical Methods

(a) Aminoacylase activity assay

The activity of aminoacylase was measured using the standard hydrolytic assay of N-acetyl L-methionine as described earlier [29]. The detailed assay procedure is as follows: To 1 mL of aminoacylase solution (prepared in 50 mM phosphate buffer, pH 8), 1 mL of 50 mM of $CoCl_2$ solution was added. The temperature of this solution was maintained at 37°C. To this, 1 mL of 100 mM N-acetyl L-methionine solution was added and incubated at 37°C for 30 min. From this, 1 mL reaction mixture was removed and transferred to stoppered glass test tube and boiled in boiling water bath for 3 min. The boiled solution was cooled and 2 mL of 2% (w/v) ninhydrin colour reagent and 0.1 mL of 1.6% (w/v) stannous chloride solution ($SnCl_2$) was added to it. The resultant mixture was boiled for 20 min. After cooling 10 mL n-propanol was added, vortexed and the absorbance was determined at 570 nm. One unit (U) is defined as amount of aminoacylase necessary to liberate 1

μmol of L-methionine per hour at 37°C at pH 8.

The activity of aminoacylase-PEI CLEA was determined according to procedure described above using 0.1 g of CLEA. The activity of CLEA is expressed in terms of aminoacylase units per g of CLEA.

(b) Characterization of physical properties of aminoacylase-PEI CLEA

(i) Pore size and pore volume

The pore size and pore volume of CLEA were determined by mercury intrusion porosimetry using Auto-scan 60 Mercury Porosimeter (Quantachrome, USA) in the range of 0-4000 kg/cm2.

(ii) Scanning electron microscopy

The surface morphology of biocatalytic matrices was studied by scanning electron microscopy (SEM). Micrographs were taken on a JEOL JSM-5200 SEM instrument.

(c) HPLC analysis

All reaction profiles were monitored by HPLC (Thermo Separation Products, Fremont, CA, USA). The quantitative analysis of different amino acids and their esters was carried out using a reverse phase C-18 column (125×4 mm, prepacked column supplemented with a 4×4 mm guard column procured from LiChrospher®, Merck, Darmstadt, Germany) eluted isocratically using acetonitrile-water mobile phase (30:70 v/v, pH adjusted to 3.0 with 50% v/v *o*-phosphoric acid), at a flow rate of 0.6-1.0 mL/min. Peaks were detected using an UV detector at 215 nm. The peak identification was made by comparing the retention times with those of authentic compounds. Peak area was used as a measure to calculate the respective concentration. The reaction conversion was estimated from the ratio of the substrate consumption to its initial concentration. The enantiomeric excess (e.e.) of the product was determined by using a CHIROBIOTIC-T® column (250×4.6 mm prepacked column supplemented with 20×4 mm guard column procured from Astec Inc. USA) eluted isocratically using water-methanol mobile phase (40:60 v/v, pH adjusted to 2.3-2.5 with 50% v/v glacial acetic acid), at a flow rate of 0.6-0.8 mL/min.

(d) Determination of enantiomeric ratio

Enantiomeric ratio (*E*) is the prime parameter for describing the enzyme's enantioselectivity. Enantiomeric ratio was determined by using Eq. 2.3 as described earlier in Chapter 2 in Section 2.2.7(e).

6.3. RESULTS AND DISCUSSION

6.3.1. Optimization of process parameters

The 'extent of cross-linking' is the key parameter which decides the extent of cross-linked enzyme activity (calculated in terms of activity recovery) and the extent of enzyme aggregation (calculated in terms of aggregation yield). Hence the 'extent of cross-linking' in CLEA should be critically controlled. Adequate cross-linking is essential to form stable enzyme aggregates. However, excessive cross-linking results in enzyme inactivation and reduction in porosity which ultimately adversely affects the activity recovery. To summarize, up to the optimum point, the activity recovery and the aggregation yield increase with 'extent of cross-linking'. However, additional cross-linking leads to decrease in the activity recovery. The aggregation yield may increase or remain constant beyond the optimum. The 'extent of cross-linking' in the present study was controlled by optimizing three process variables *namely* relative concentration of enzyme and PEI, concentration of glutaraldehyde and cross-linking time (i.e. time of glutaraldehyde treatment).

(a) Effect of enzyme:PEI ratio

To evaluate the effect of enzyme-PEI ratio, aminoacylase and PEI solutions (25 mg/mL each) were mixed in different concentrations (1:3, 1:2, 1:1, 2:1 and 3:1) and the resultant CLEA were analyzed for the activity recovery and aggregation yield as described in Section 6.2.2(b). Table 6.1 gives the effect of enzyme:PEI ratio. Among the different enzyme-PEI ratios studied, 1:1 enzyme to PEI ratio was found to be optimum and gave maximum for activity recovery (50.42%) and therefore 1:1 enzyme to PEI ratio was used in all further experiments.

(b) Effect of glutaraldehyde concentration

Different concentrations of glutaraldehyde (100 to 600 mM) were used to determine the optimum quantity required for stable cross-linking of aminoacylase and

PEI. The activity recovery and aggregation yield of CLEA were found to increase initially with increase in glutaraldehyde concentration from 100-500 mM (Table 6.2). Further increase in glutaraldehyde concentration above 500 mM resulted in slight decrease in yield with no significant change in the aggregation yield. The slight decrease in the activity recovery could be due to over cross-linking of enzyme molecules making them catalytically inactive. Glutaraldehyde concentration of 500 mM gave maximum activity recovery (61.38%) and aggregation yield (74.88%) and hence used in all further experiments.

Table 6.1: Effect of enzyme:PEI ratio

Enzyme:PEI ratio	**Activity recovery** (%)	**Aggregation yield** (%)
1:3	23.36	68.01
1:2	33.17	62.68
1:1	50.42	60.48
2:1	44.00	42.88
3:1	37.54	34.67

Table 6.2: Effect of glutaraldehyde (GLA) concentration

GLA (mM)	**Activity recovery** (%)	**Aggregation yield** (%)
100	50.94	60.80
200	55.86	63.36
300	58.06	68.08
400	60.06	70.24
500	61.38	74.88
600	56.97	74.77

(c) Effect of cross-linking time

The cross-linking time was studied from 1 h to 48 h for stable cross-linking of PEI-enzyme aggregates (Table 6.3). The increase in cross-linking time resulted in significant increase in the activity recovery of CLEA. The cross-linking reached to optimum within 24 h where maximum activity recovery (74.90%) and aggregation yield (81.20%) were obtained. Beyond 24 h, there was moderate decrease in the activity recovery with negligible change in the aggregation yield.

Table 6.3: Effect of cross-linking time

Cross-linking time (h)	**Activity recovery** (%)	**Aggregation yield** (%)
1	45.06	51.24
6	61.06	74.24
12	69.58	79.88
24	74.90	81.20
36	74.52	81.64
48	70.97	82.36

6.3.2. Characterization of aminoacylase-PEI CLEA

(a) Study of the enzyme release from the aggregates

The aminoacylase-PEI CLEA were boiled with SDS and mercaptoethanol as described in Section 6.2.3(a). The supernatant was analyzed by SDS-PAGE. The SDS-PAGE was run in duplicate and one gel was stained with Coomassie blue while the second gel was stained with silver stain (Fig 6.2(a) and Fig. 6.2(b) respectively).

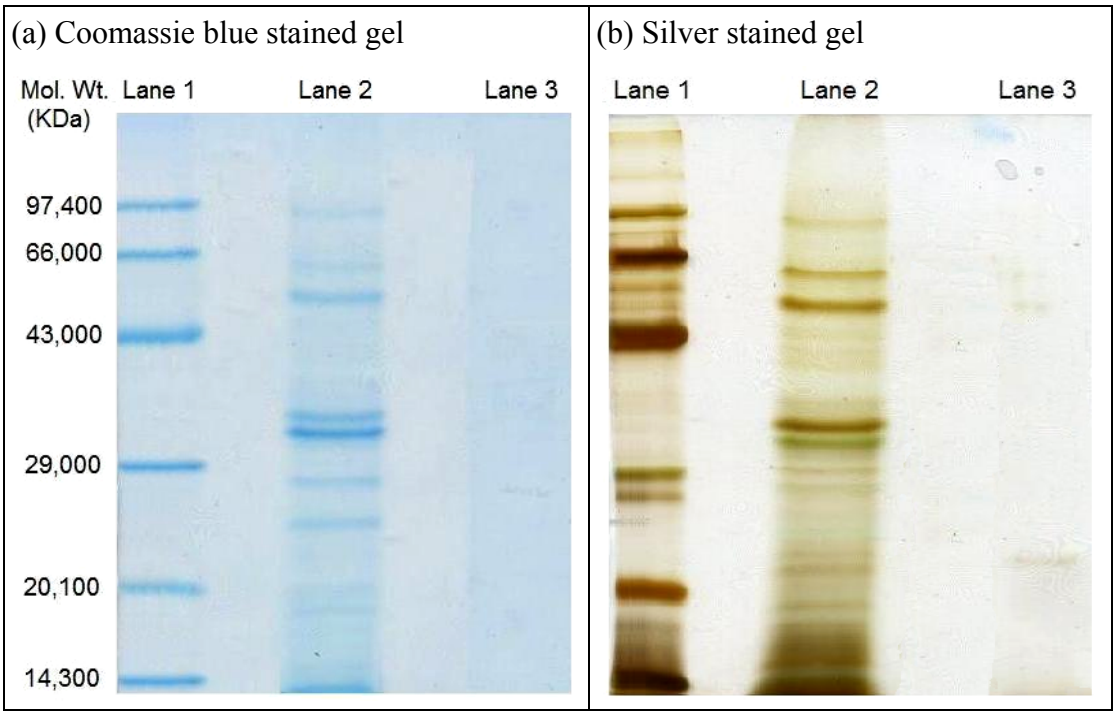

Fig. 6.2: Study of enzyme release from aminoacylase-PEI CLEA; (a) Coomassie blue stained SDS-PAGE gel and (b) Silver stained SDS-PAGE gel; sample sequence in both (a) and (b): molecular weight markers (Lane 1), free aminoacylase (Lane 2), aminoacylase-PEI CLEA (Lane 3).

No protein band was observed in the sample of aminoacylase-PEI CLEA (Lane 3 of Fig. 6.2(a) and Fig. 6.2(b) indicating no release of enzyme from CLEA thereby confirming the stable and effective binding of enzyme molecules. Further, SDS-PAGE results also confirm that *Aspergillus melleus* aminoacylase is dimer and each subunit is having molecular weight approximating to 37 kDa as mentioned in the literature [30].

(b) Storage stability of aminoacylase-PEI CLEA

The storage stability of aminoacylase-PEI CLEA was determined and compared with free aminoacylase. The plot of log residual activity vs. storage time is shown in Fig. 6.3. The linear trend lines were drawn to the activity profiles of free aminoacylase and aminoacylase-PEI CLEA. The storage half-life of each enzyme preparation was determined from its respective trend line equation. The storage half-life of free aminoacylase at 4°C was found to be ~ 1 day while that of CLEA was found to be ~ 40 days. Thus, there was significant increase in storage stability upon cross-linking of enzyme with PEI.

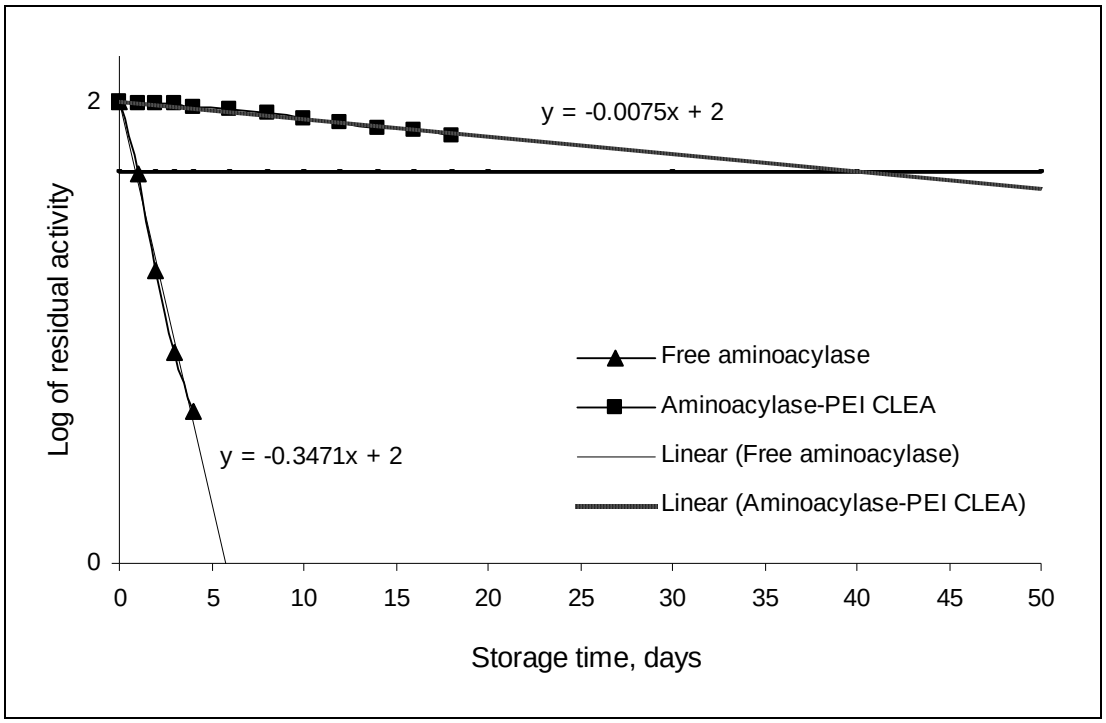

Fig. 6.3: Storage stability of aminoacylase-PEI CLEA [The trend line equations were used to calculate the respective storage half-lives. The horizontal line (─) at log(50) was drawn only for a graphical illustration of the storage half-lives.]

(c) Scanning electron microscopy

The scanning electron micrographs of aminoacylase-PEI CLEA are given in Fig. 6.4. The SEM of aminoacylase-PEI CLEA shows the cross-linked structure of enzyme and PEI. The SEM also indicates the highly porous structure of aggregate which would be very useful in minimizing the diffusional limitations during biocatalysis.

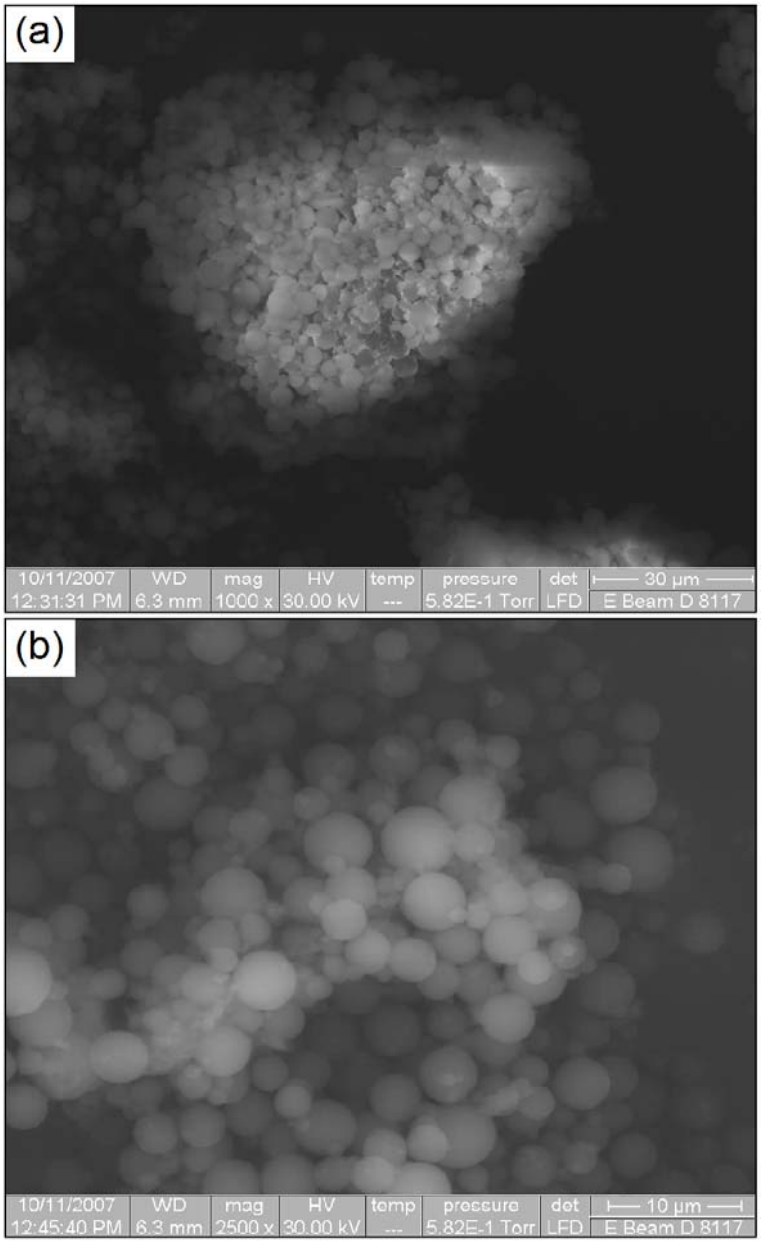

Fig. 6.4: Scanning electron micrographs of aminoacylase-PEI CLEA showing (a) individual CLEA particle observed at lower magnification (1000×); (b) macroporous nature of CLEA observed at higher magnification (2500×).

(d) Physical properties

The physical properties of aminoacylase-PEI CLEA are summarized in Table 6.4. The values of pore surface area and pore volume as determined by mercury porosimetry were 66 ± 0.5 m^2/g and 0.5 ± 0.01 cm^3/g respectively. The average particle size of aminoacylase-PEI CLEA as estimated from SEM data was 50 ± 10 µm.

Table 6.4: Physical characterization of aminoacylase-PEI CLEA

No.	Physical property	Value
1	Pore surface area	66 ± 0.5 m^2/g
2	Pore volume	0.5 ± 0.01 cm^3/g
3	Particle size	50 ± 10 µm

(e) pH stability of aminoacylase-PEI CLEA

Effect of pH on the residual activity of aminoacylase for free enzyme and aminoacylase-PEI CLEA was studied for the pH range of 4 to 12 (Fig. 6.5).

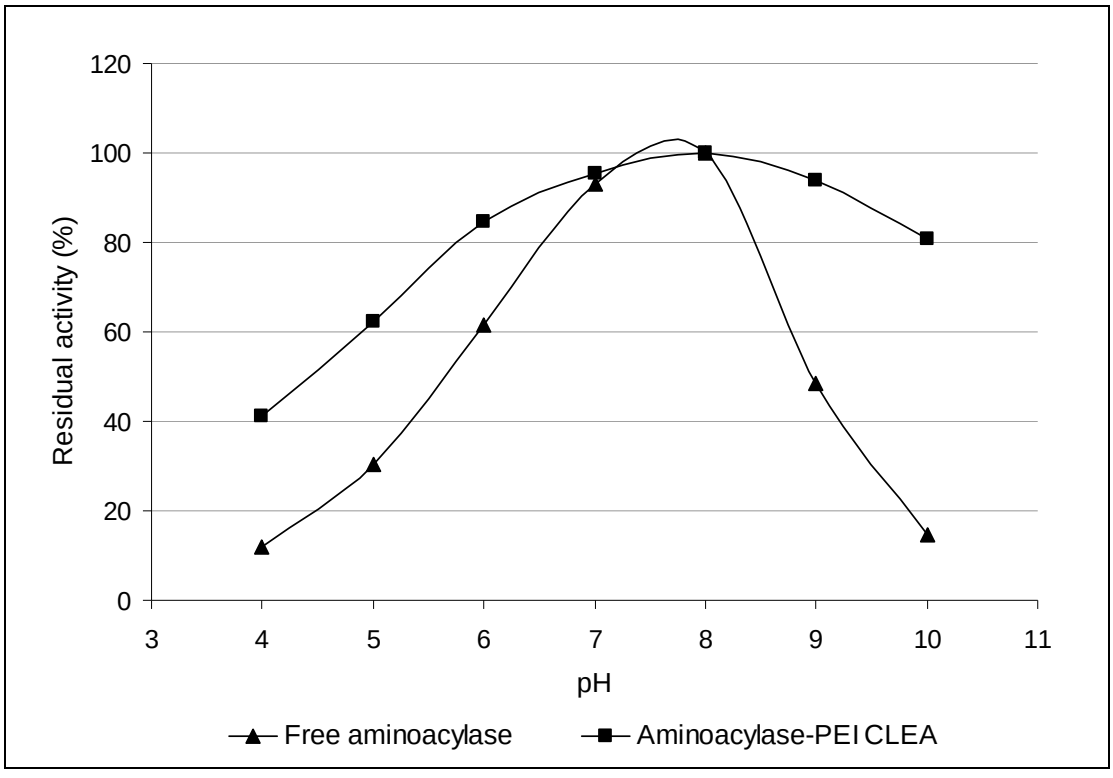

Fig. 6.5: pH stability of aminoacylase-PEI CLEA

Cross-linking of aminoacylase resulted in moderate stabilization of the enzyme over a broader pH range. The free aminoacylase retained 84.89% and 60.15% residual activity at pH 9 and pH 10 whereas; at same pH conditions aminoacylase-PEI CLEA retained 94.01% and 80.73% residual activity respectively. This indicated that the cross-linking of aminoacylase with PEI has improved the stability of enzyme to a moderate extent.

(f) Temperature stability of aminoacylase-PEI CLEA

Stability of free aminoacylase and aminoacylase-PEI CLEA were determined by measuring residual enzyme activity as function of temperature in the range of 20°C to 90°C. The activity profiles of free aminoacylase and aminoacylase-PEI CLEA at different temperature are represented in Fig. 6.6. At 50°C the free enzyme retained only 66.42% residual activity while aminoacylase-PEI CLEA 98.56% of its initial activity. Similarly at 70°C the free enzyme retained only 4.75% residual activity while aminoacylase-PEI CLEA was found to retain 76.63% of its initial activity. Thus, the cross-linking of aminoacylase with PEI was observed to confer excellent thermal stability to the enzyme.

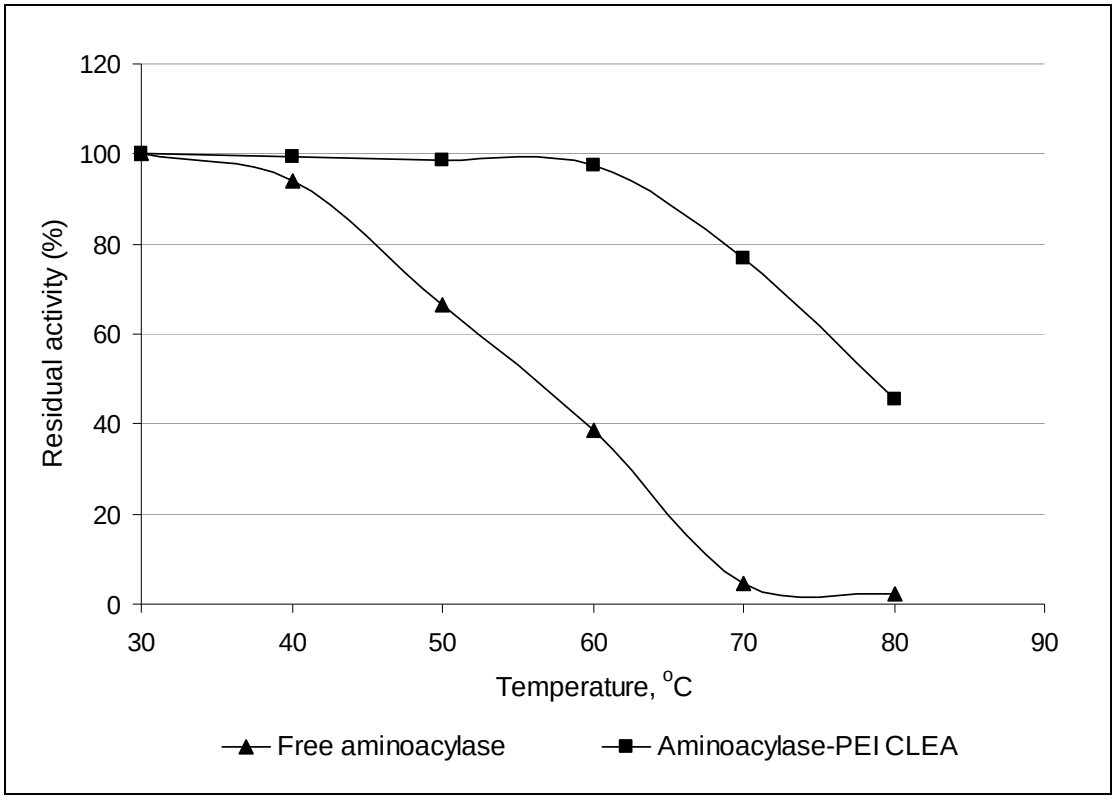

Fig. 6.6: Temperature stability of aminoacylase-PEI CLEA

(g) Kinetics of thermal deactivation of aminoacylase before and after cross-linking

The temperature dependant activity profiles of free aminoacylase and CLEA are presented in Fig. 6.7(a) and Fig. 6.7(b) respectively.

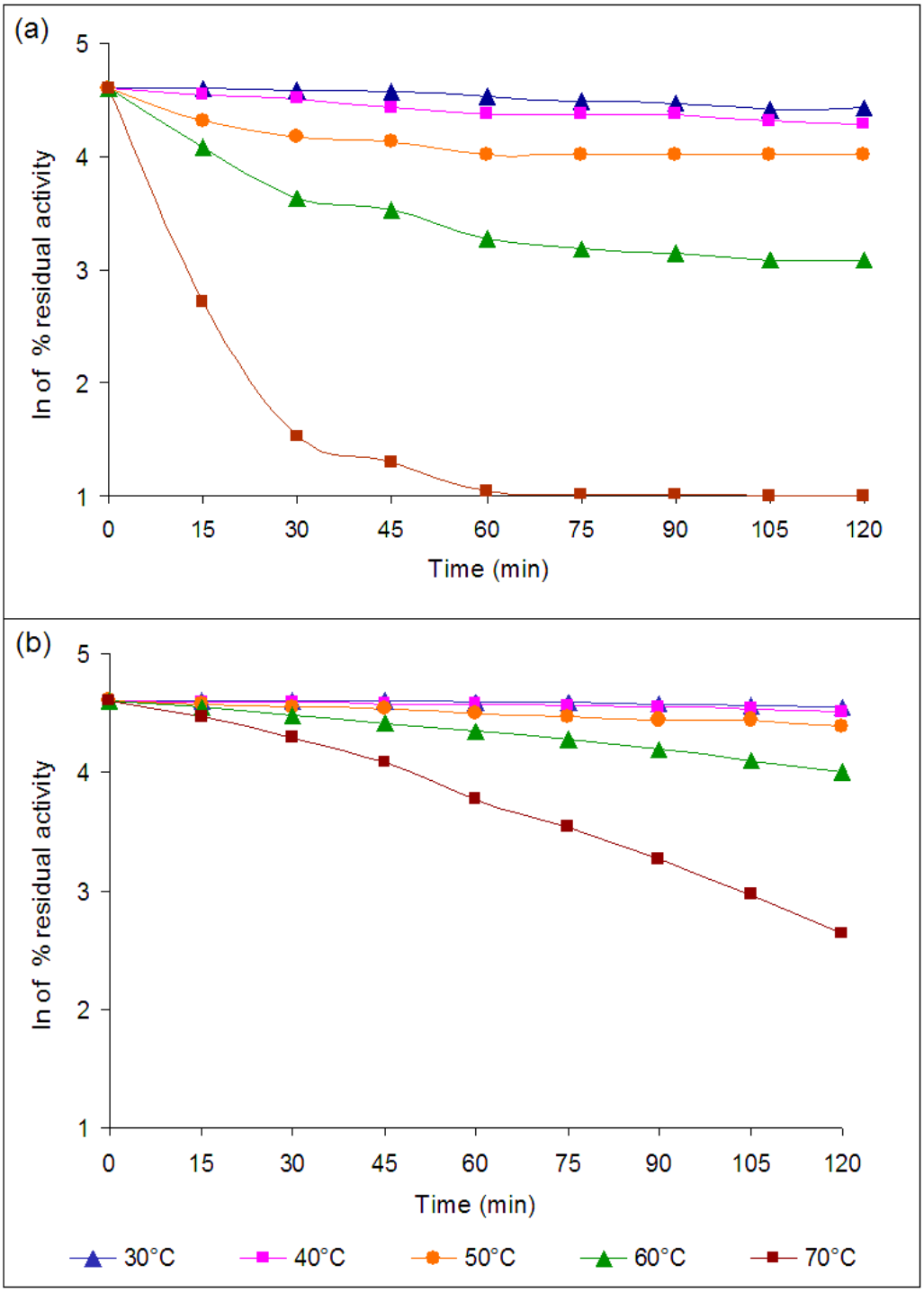

Fig. 6.7: Thermal deactivation of (a) free aminoacylase and (b) aminoacylase-PEI CLEA in temperature range of 30-70°C

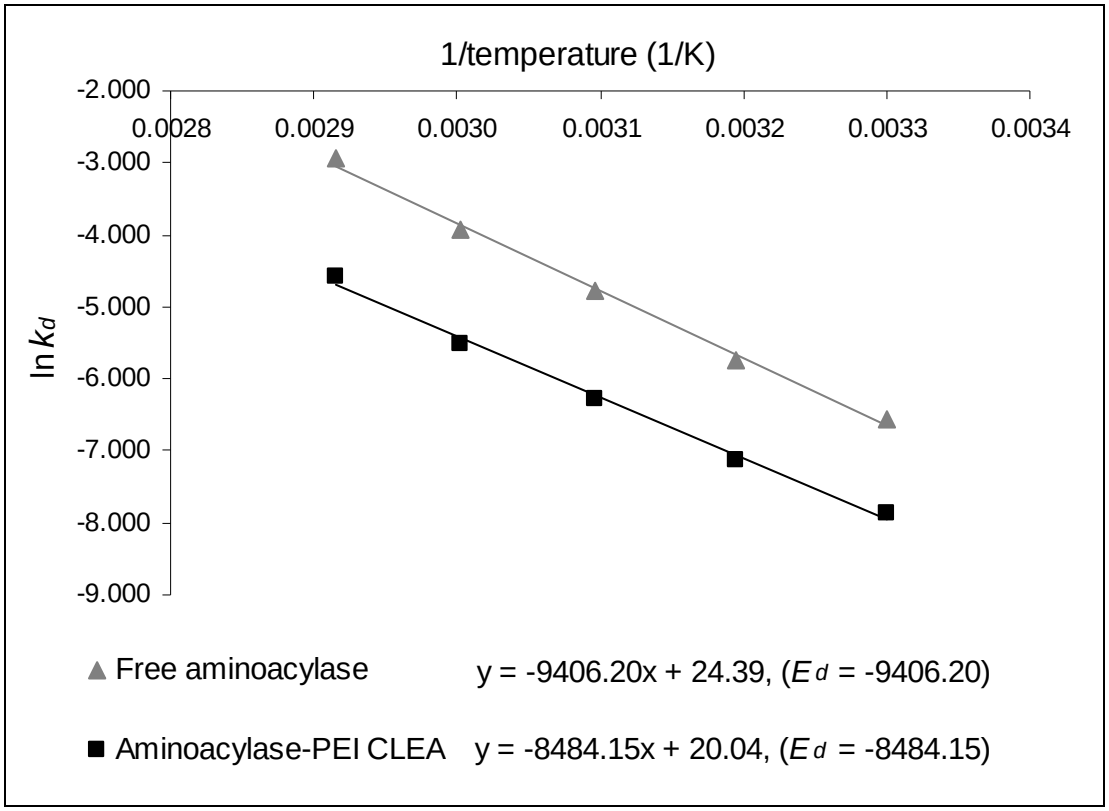

Fig. 6.8: Arrhenius plot for free aminoacylase and aminoacylase-PEI CLEA

Table 6.5: Thermal deactivation coefficient (k_d) and Half-life ($t_{1/2}$) of free enzyme and aminoacylase-PEI CLEA

Temperature (°C)	k_d (min^{-1})		$t_{1/2}$ (min)		**Fold increase in $t_{1/2}$**
	Free enzyme	CLEA	Free enzyme	CLEA	
30	-0.00141	-0.00038	496.45	1842.11	3.71
40	-0.00319	-0.00081	219.43	864.19	3.94
50	-0.00840	-0.00189	83.33	370.37	4.44
60	-0.01979	-0.00404	35.37	173.26	4.90
70	-0.05262	-0.01015	13.30	68.96	5.18
Average fold increase in the half life over the range of 30-70°C					4.43

The half life ($t_{1/2}$) and deactivation rate constants (k_d) of free aminoacylase and CLEA are given in Table 6.5. On an average, upon cross-linking, there was 4.43 fold increase in the half life of enzyme. This could be ascribed to "optimal" cross-linking of enzyme-PEI molecules which has maintained the active conformation of enzyme

for a longer time at elevated temperatures. These results are significantly in favour of employing CLEA in the biotransformation reactions at elevated temperatures. Co-aggregation followed by cross-linking leads to formation of a large number of stabilizing linkages which maintain the catalytically active conformation of the enzyme even at elevated temperatures hence often confer better thermal stability to the enzyme than conventional immobilization procedures [6].

The PEI induced co-aggregation technique for making CLEA is a largely unexplored field. By this technique, CLEA of only few enzymes (*namely*: penicillin-G acylase [6], glutaryl acylase [19], *Alcaligenes* sp. lipase and *Candida antarctica* B lipase [20], and *Pseudomonas fluorescens* nitrilase [32]) have been prepared. Wilson *et al.* employed this co-aggregation technique for making CLEA of Penicillin-G acylase to enhance the stability of enzyme in organic medium. The CLEA prepared with the co-aggregation technique showed increased stability (~25 fold higher) than the CLEA prepared by conventional method [6]. López-Gallego *et al.* prepared the CLEA of glutaryl acylase using the PEI induced co-aggregation technique. It has been demonstrated that the use of PEI prevented the release of enzyme molecules from the aggregate. These CLEA showed enhanced thermal and storage stability [19]. The co-aggregation method has also been used to prepare stable CLEA of lipase. The nature of the polymers co-aggregated with the lipases was found to alter the catalytic properties (i.e. specificity and enantioselectivity) of the enzyme [20]. Mateo *et al.* prepared the co-aggregates of the nitrilases with high molecular weight PEI. Here, PEI induced co-aggregation technique increased the oxygen-resistance of nitrilase than free enzyme and conventionally cross-liked enzyme [32].

The *in vitro* stability of enzymes remains a critical issue in the field of biocatalysis. Both storage and operational stabilities affect the usefulness of enzyme-based products [33]. The reports in the literature clearly indicate that facile cross-linking of enzyme via PEI-induced co-aggregation method greatly improves the storage as well as operational stability of an enzyme. The present study has also demonstrated the significant improvement in the thermal and storage stability of the aminoacylase enzyme upon co-aggregation with PEI. The improved stability of aminoacylase-PEI CLEA can be explained by the fact that the co-precipitation of enzyme with ionic polymers such as PEI alters the microenvironment of enzyme

molecules which exerts excellent stabilizing effects on enzyme [21]. Furthermore, in aminoacylase-PEI CLEA, the enzyme molecules are held together by multipoint enzyme-polymer linkages that possibly help in preserving the active-site conformation of enzyme under stress conditions [34, 35].

6.3.3. Aminoacylase-PEI CLEA catalyzed chiral resolutions

Aminoacylases exhibit broad substrate specificity. They have the ability to hydrolyze a wide spectrum of amino acid derivatives (such as amino acid esters, N-acetyl amino acids, amino acid amides) in enantioselective manner. Hence aminoacylases are perhaps the most versatile and potent biocatalyst for synthesis of enantiopure amino acids.

(a) Chiral resolution of amino acid esters

Aminoacylase-PEI CLEA were observed to preferentially hydrolyze the *S*-enantiomer of unnatural amino acid ethyl esters. Chiral resolution of amino acid esters catalyzed by aminoacylase-PEI CLEA is represented in Scheme 6.1.

Scheme 6.1: Chiral resolution of amino acid esters catalyzed by aminoacylase-PEI CLEA

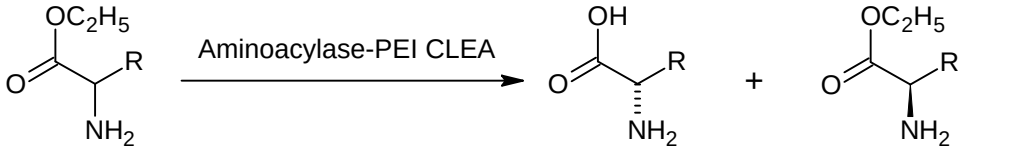

(*RS*)-Amino acid ester (*S*)-Amino acid (*R*)-Amino acid ester

	PG	HPA	NA
R-	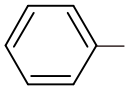	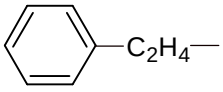	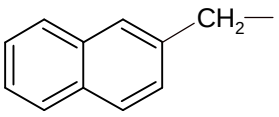

The results of stereoselective hydrolysis of unnatural amino acid ethyl esters using aminoacylase-PEI CLEA are summarized in Table 6.6. The enantiomeric ratios of CLEA towards hydrolysis of PG-ester, HPA-ester and NA-ester were 6.5, 14.1 and 8.1 respectively.

Table 6.6: Chiral resolution of amino acids ethyl esters catalyzed by aminoacylase-PEI CLEA

Substrate	**Preferred configuration**	**Time** (min)	**ee$_p$** (%)	***C*** (%)	***E***
PG-ester	*S*	60	64.7	35.2	6.5
HPA-ester	*S*	60	82.4	27.9	14.1
NA-ester	*S*	60	67	41.7	8.1

(b) Chiral resolution of N-acetyl amino acids

As represented in the Scheme 6.2, aminoacylase-PEI CLEA were observed to hydrolyze preferentially the *S*-enantiomer of N-acetyl amino acids. The results of stereoselective hydrolysis of N-acetyl amino acids using aminoacylase-PEI CLEA are summarized in Table 6.7. CLEA exhibited higher enantioselectivity towards hydrolysis of N-acetyl-PG and N-acetyl-HPA as indicated from the higher *E* values (54.3 and 60.0 respectively) than that towards hydrolysis of N-acetyl-NA (*E* = 22.6).

Scheme 6.2: Chiral resolution of N-acetyl amino acids catalyzed by aminoacylase-PEI CLEA

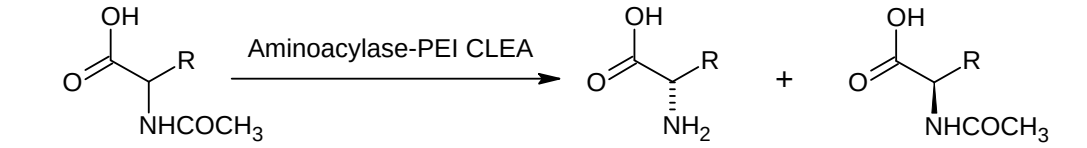

(*RS*)-N-acetyl amino acid (*S*)-Amino acid (*R*)-N-acetyl amino acid

	PG	HPA	NA
R-	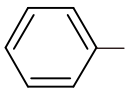	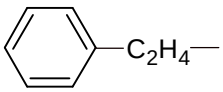	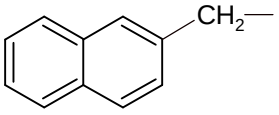

Table 6.7: Chiral resolution of N-acetyl amino acids catalyzed by aminoacylase-PEI CLEA

Substrate	**Preferred configuration**	**Time** (min)	**ee$_p$** (%)	***C*** (%)	***E***
N-acetyl-PG	*S*	60	92.5	43.3	54.3
N-acetyl-HPA	*S*	60	93.5	41.8	60.0
N-acetyl-NA	*S*	60	87.4	32.9	22.6

(c) Chiral resolution of amino acid amides

As represented in the Scheme 6.3, aminoacylase-PEI CLEA were observed to preferentially hydrolyze the *S*-enantiomer of amino acid amides. The results of stereoselective hydrolysis of amino acid amides using aminoacylase-PEI CLEA are summarized in Table 6.8. The *E* values of hydrolysis of PG-amide and HPA-amide were >200 and that of hydrolysis of 2-NA- amide was >100 indicating the remarkable enantioselectivity of CLEA towards these hydrolytic reactions.

Scheme 6.3: Chiral resolution of amino acid amides catalyzed by aminoacylase-PEI CLEA

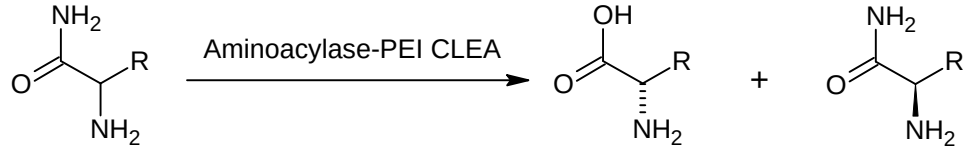

(*RS*)-Amino acid amide (*S*)-Amino acid (*R*)-Amino acid amide

	PG	HPA	NA
R-	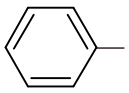	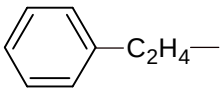	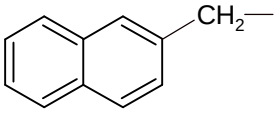

Table 6.8: Chiral resolution of amino acid amides catalyzed by aminoacylase-PEI CLEA

Substrate	**Preferred configuration**	**Time** (min)	**ee$_p$** (%)	***C*** (%)	***E***
PG-amide	*S*	60	98.5	44.2	>200
HPA-amide	*S*	60	98.2	41.6	>200
NA-amide	*S*	60	96.4	43.9	124.4

The process of co-aggregation/cross-linking occasionally alters the catalytic properties (such as specificity, enantioselectivity etc.) of an enzyme. For instance, Wilson *et al.* have reported drastic changes in the enantioselectivity of lipases upon formation of CLEA by PEI-induced co-aggregation technique [20]. The extent of change in the catalytic properties of enzyme greatly depends on the nature of polymer, nature of enzyme (mono- or multi-meric) and type of protein-polymer interactions. Considering the possibility of enantioselectivity modulation, we compared the

enantiomeric ratios of free aminoacylase with that of aminoacylase-PEI CLEA towards hydrolysis of unnatural amino acid amides. For the given amide substrate, no significant difference in the enantiomeric ratio of free enzyme and that of aminoacylase-PEI CLEA was observed.

To summarize, enantiomeric ratios of the aminoacylase-PEI CLEA were high ($E \approx 124$ to 200) towards hydrolysis of amides, moderate ($E \approx 23$ to 60) towards hydrolysis of N-acetyl derivatives and poor ($E < 15$) towards the hydrolysis of amino acid esters. Youshko *et al.* reported similar observations i.e. authors reported higher enantiomeric ratios of *A. melleus* L-aminoacylase towards hydrolysis of PG-amide and HPA-amide (i.e. $E > 200$) than that towards hydrolysis of N-acetyl-PG and N-acetyl-HPA ($E = 96$ and 70 respectively) [36].

L-Aminoacylase catalyzed enantioselective synthesis of different amino acids is discussed in detail in Chapter 5. As mentioned earlier, most of the previous efforts deal with aminoacylase catalyzed enantioselective hydrolysis of *rac*-N-acetyl amino acid. This process has also been successfully commercialized for the industrial production of enantiopure amino acids [36]. The present study, however, indicates that aminoacylase has higher enantioselectivity towards hydrolysis of amides than that towards hydrolysis of N-acetyl derivatives of unnatural amino acids. Thus, the enantioselective production of these unnatural amino acids via aminoacylase catalyzed hydrolysis of *rac*-amino acid amides appears to be an attractive alternative.

6.3.4. Optimization of catalytic performance

(a) Effect of biocatalyst loading

The effect of catalyst loading per batch as described in Section 6.2.5(b) was studied in the range of 0.05-0.15 g of aminoacylase-PEI CLEA. Increase in biocatalyst loading from 0.05-0.1g resulted in proportional increase in the rate of hydrolysis of HPA-amide from 4.11 $\mu M \cdot min^{-1} \cdot mg^{-1}$ to 19.04 $\mu M \cdot min^{-1} \cdot mg^{-1}$ (Fig. 6.9). However, increase in the catalyst loading beyond 0.1 g did not have any significant effect on rate of conversion. This reflects enzyme saturation at concentration of 0.1 g per batch. Therefore 0.1 g of aminoacylase-PEI CLEA was used in further experiments.

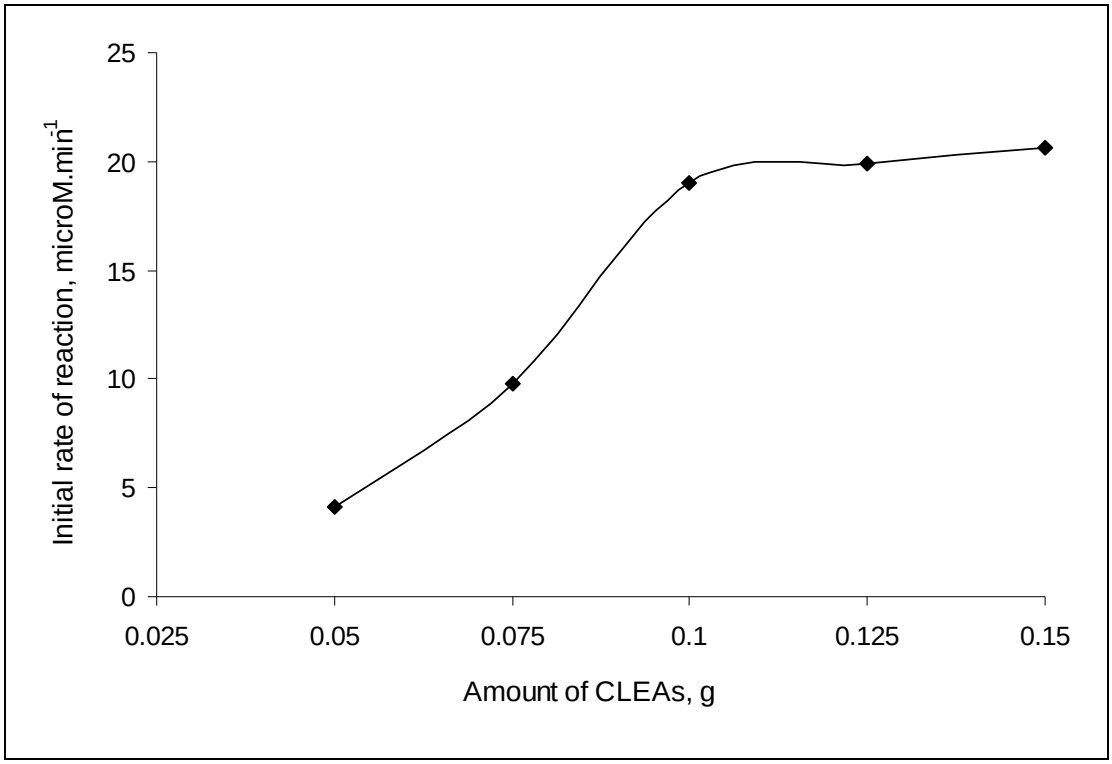

Fig. 6.9: Effect of catalyst loading on hydrolysis of *rac*-HPA-amide

(b) Effect of diffusional limitations

The reaction kinetics of heterogeneous biocatalysts is greatly affected by the diffusional resistance to the transport of substrate molecules from the bulk solution to the enzyme active site where the actual reaction takes place. The resistance to the transport of substrate through boundary layer solvent covering the solid biocatalyst is called as 'external diffusional limitations' while the resistance to the transport of substrate inside the matrix of heterogeneous biocatalysts towards the enzyme active site is called as 'internal diffusional limitations' [37].

In order to ensure the maximum possible conversion rates, it is very important to overcome the external and internal diffusional limitations. The external diffusional limitations can be overcome by rapid agitation. The effect of the speed of agitation was studied at 50, 100, 150, 200 and 250 rpm. The rate of reaction increased with increasing speeds from 50 to 200 rpm. Beyond 200 rpm, there was only a marginal increase in the reaction rate (Fig. 6.10). The results suggest that presence of the external diffusional limitations largely below agitation speed of 200 rpm. Therefore the reactor was run at 200 rpm speed in all further experiments.

The assessment of internal diffusional limitations is a relatively difficult task.

Here, reaction rates in a series of hydrolytic reactions catalyzed by CLEA, containing increasing amount of enzyme are determined. The linear relationship between rate of reaction and the amount of enzyme present in immobilized enzyme (or in cross-lined aggregates) is generally interpreted as absence of internal diffusion limitations [37]. However, CLEA having increasing amount of enzyme are difficult to prepare and therefore in the present work no attempt was made to evaluate the occurrence of internal diffusion. Nevertheless, in view of large pore volume (0.5 ± 0.01 cm^3/g, refer Table 6.4) of CLEA, the internal diffusional limitations are supposed to be at minimal possible levels.

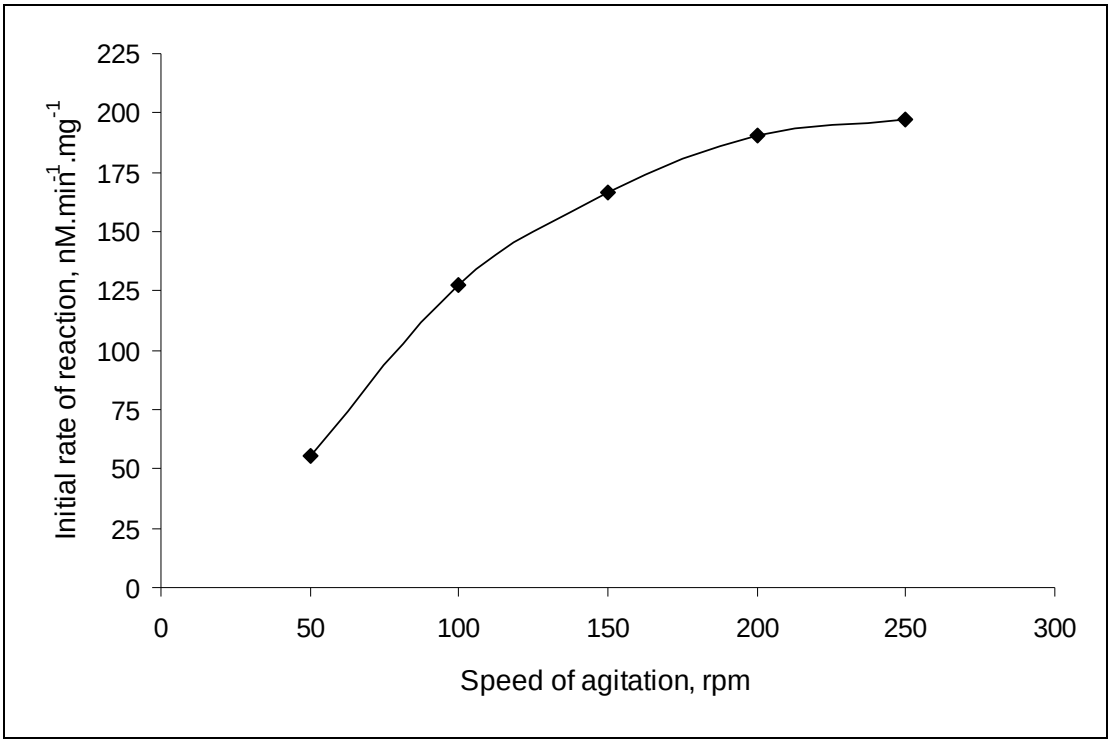

Fig. 6.10: Effect of speed of agitation on hydrolysis of *rac*-HPA-amide

(c) Effect of temperature

Rate of reaction is dependent on temperature. However, at times higher temperature may adversely affect the enantioselectivity of the enzyme [38]. Hence, the asymmetric biocatalytic reaction is generally run at '*so called* optimum' temperature where the rate of reaction and enantioselectivity are at suboptimal.

The effect of temperature on rate of reaction and enantioselectivity was studied in the range of 20-60°C (Fig. 6.11). The initial rate increased with an increase in temperature from 20-60°C. However the progressive rise in temperature from 20-

60°C has severely reduced the enantioselectivity of enzyme. At 20°C (as well as at 30°C) the *E* value was observed to be >200 whereas at 60°C the *E* value fell down to 76. Hence, in order to maintain maximum enantioselectivity and moderate rate of reaction all further experiments were carried out at 30°C.

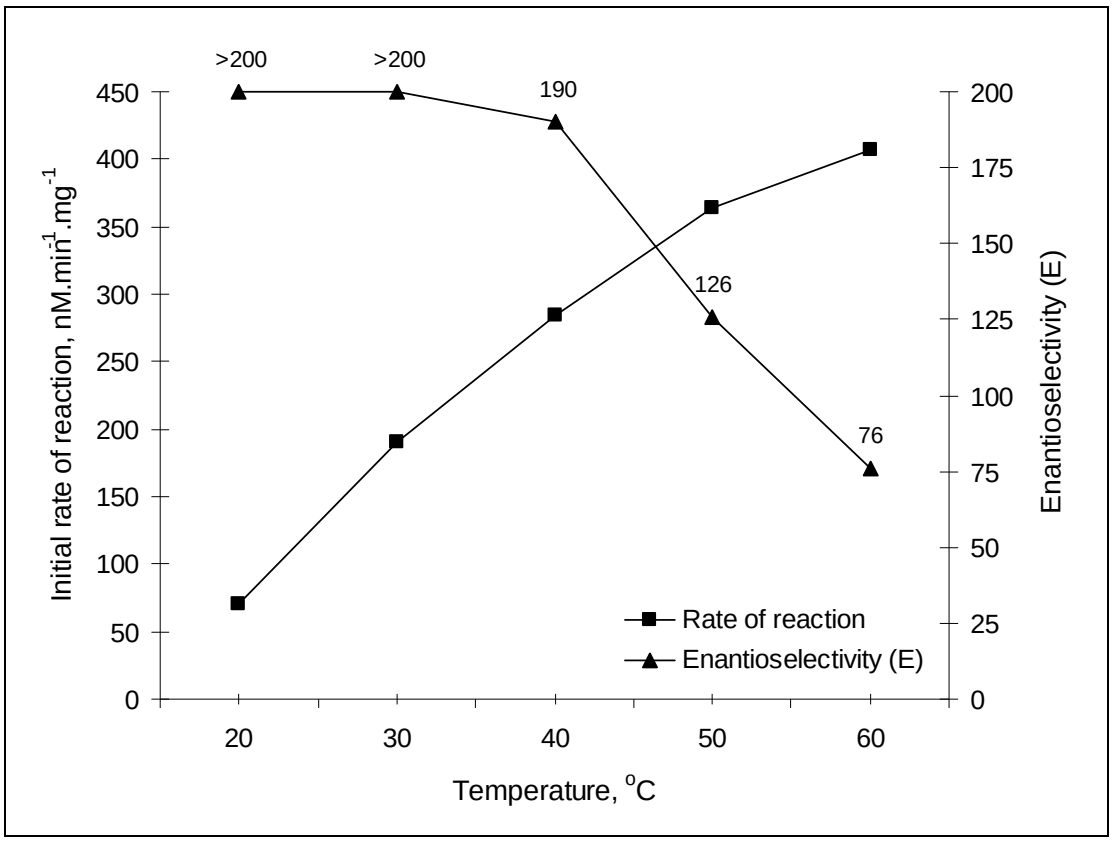

Fig. 6.11: Effect of temperature on hydrolysis of *rac*-HPA-amide

6.3.5. Synthesis of (S)-homophenylalanine in repetitive batch mode

The initial reaction rate and reaction time of five repeated cycles of hydrolysis of *rac*-HPA-amide are summarized in Fig. 6.12. The first cycle proceeded with initial reaction rate of 190.43 $nM \cdot min^{-1} \cdot mg^{-1}$ and maximum ee_p (98.5%) was attained at 70 min. Thereafter the initial reaction rate, in successive cycles, found to decrease steadily from 190.43 to 157.16 $nM \cdot min^{-1} \cdot mg^{-1}$ indicating some loss of enzyme activity during each cycle. To attain equal ee_p (>98%) in successive cycles, the reaction time was accordingly extended. The 5^{th} cycle therefore finished at 140 min. From five repeated cycles, 213.9 mg of *S*-HPA (which corresponds to 85% yield) was obtained with cumulative ee_p of 98.3% (Table 6.9).

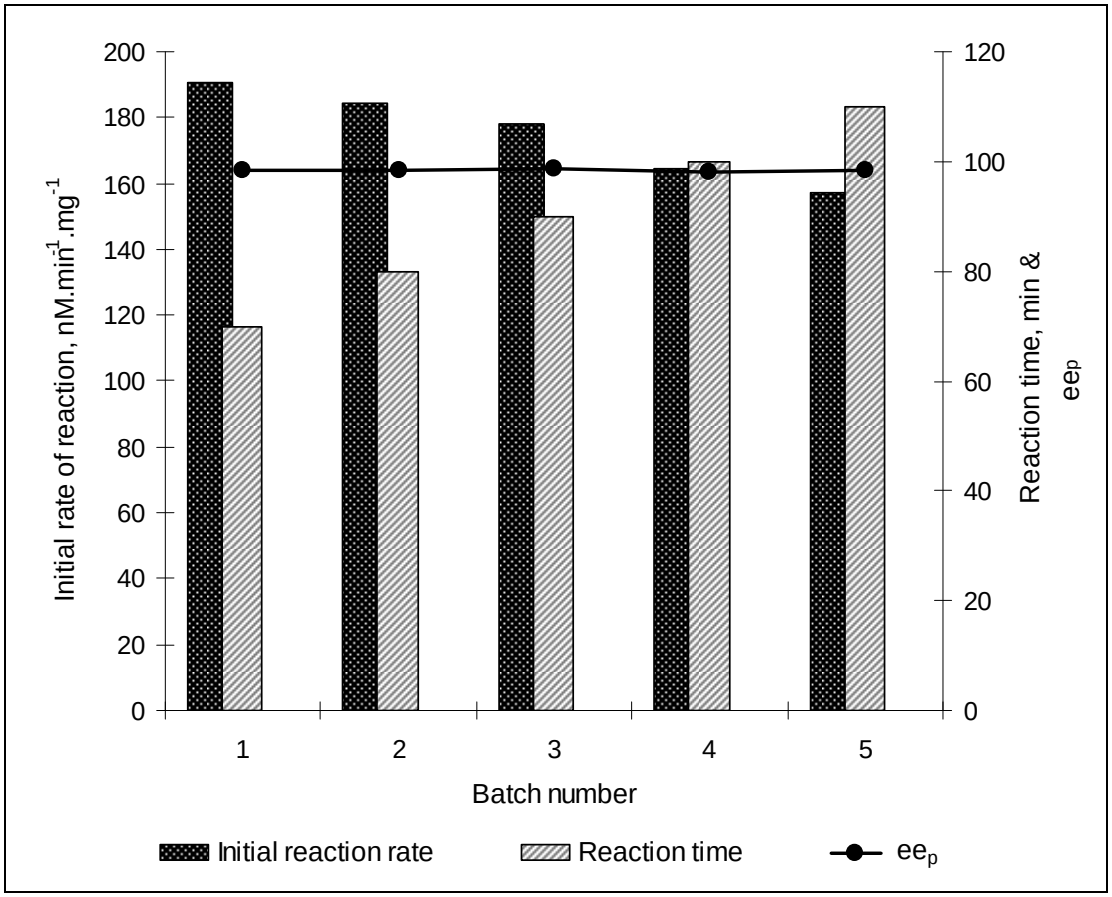

Fig. 6.12: Performance of stirred cell reactor in repetitive batch mode

Table 6.9: Summary of five repetitive batches of hydrolysis of *rac*-HPA-amide

Batch no.	**ee$_p$** (%)	***C*** (%)	***E***	**Yield of *rac*-HPA** (mg)	**% Yield**
1	98.5	44.3	>200	42.6	84.7
2	98.0	45.4	>200	43.7	86.9
3	98.6	44.1	>200	43.0	85.5
4	98.2	44.3	>200	42.4	84.3
5	98.3	44.0	>200	42.2	83.9
Total	98.3	-	-	213.9	85.0

6.4. CONCLUSIONS

In this work, we have demonstrated that co-aggregation of aminoacylase with an aminated polymer (e.g. PEI) facilitates formation of physically stable CLEA. The method described yields stable cross-linking and no release of enzyme was found upon storage. The cross-linking significantly improved the stability of aminoacylase

with respect to pH, temperature and storage. Aminoacylase-PEI CLEA were able to hydrolyze different amino acid derivatives (*namely*: amino acid esters, N-acetyl amino acids and amino acid amides) in an enantioselective manner. The enantioselectivity however, was dependent on the type of amino acid derivative. The enantioselectivity of CLEA was remarkably high towards hydrolysis of amides, moderate towards hydrolysis of N-acetyl derivatives and poor towards the hydrolysis of amino acid esters. Aminoacylase-PEI CLEA exhibited high operational stability in repetitive cycles of *rac*-HPA amide hydrolysis. Aminoacylase-PEI CLEA catalyzed hydrolysis of *rac*-amino acid amides gave best results for biocatalytic production of the given enantiopure amino acids.

REFERENCES

[1] Wong, C-H.; Whitesides, G.M. Enzymes in Synthetic Organic Chemistry. Pergamon: Tarryton, New York, **1994**.

[2] Xu, K.; Klibanov, A.M. pH control of the catalytic activity of cross-linked enzyme crystals in organic solvents. *J. Am. Chem. Soc.*, **1996**, *118(41)*, 9815-9819.

[3] Wang, Y-F.; Yakovlevsky, K.; Zhang, B.; Margolin A.L. Cross-Linked Crystals of subtilisin: versatile catalyst for organic synthesis. *J. Org. Chem.*, **1997**, *62*, 3488-3495.

[4] Tyagi, R.; Batra, R.; Gupta, M. Amorphous enzyme aggregates: stability toward heat and aqueous-organic co-solvent mixtures. *Enzyme Microb. Technol.*, **1999**, *24*, 348-354.

[5] Cao, L.; van Langen, F.; van Rantwijk, F.; Sheldon, R.A. Cross-linked aggregates of penicillin acylase: robust catalysts for the synthesis of β-lactam antibiotics. *J. Mol. Catal. B: Enzym.*, **2001**, *11*, 665-670.

[6] Wilson, L.; Illanes, A.; Abian, O.; Pessela, B.; Fernández-Lafuente, R.; Guisán, J.M. Co-aggregation of penicillin G acylase and polyionic polymers: a simple methodology to prepare enzyme biocatalysts stable in organic media. *Biomacromolecules*, **2004**, *5(3)*, 852-857.

[7] Roy, J.J.; Abraham, T.E. Preparation and characterization of cross-linked enzyme crystals of laccase. *J. Mol. Catal. B: Enzym.*, **2006**, *38*, 31-36.

[8] Schoevaart, R.; Wolbers, M.W.; Golubovic, M.; Ottens, M.; Kieboom, A.P.G.;

van Rantwijk, F.; van der Wielen, L.A.M.; Sheldon, R.A. Preparation, optimization, and structures of Cross-Linked Enzyme Aggregates (CLEAs). *Biotechnol. Bioeng.*, **2004**, *87*, 754-761.

[9] Roy, J.J.; Abraham, T.E. Strategies in making cross-linked enzyme crystals. *Chem. Rev.* **2004**, *104(9)*, 3705-3721.

[10] Sheldon, R.A.; Schoevaart, R.; van Langen, L.M. Cross-linked enzyme aggregates (CLEAs): A novel and versatile method for enzyme immobilization. *Biocatal. Biotransfor.*, **2005**; *23(3/4)*, 141-147.

[11] Cao, L.; van Langeny, L.; Sheldon, R.A. Immobilised enzymes: carrier-bound or carrier-free? *Curr. Opin. Biotechnol.*, **2003**, *14*, 387-394.

[12] Margolin, A.L. Novel crystalline catalysts. *Trends Biotechnol.*, **1996**, *14*, 223-230.

[13] Lalonde, J. Practical catalysis with enzyme crystals. *Chem-tech.*, **1997**, *27(2)*, 38-45.

[14] Häring, D.; Schreier, P. Cross-linked enzyme crystals. *Curr. Opin. Biotechnol.*, **1999**, *3*, 35-38.

[15] Margolin, A.L; Navia, M.A. Protein crystals as novel catalytic materials. *Angew. Chem. Int. Edt.*, **2001**, *40*, 2204-2222.

[16] St. Clair, N.L.; Navia, M.A. Cross-linked enzyme crystals as robust biocatalysts. *J. Am. Chem. Soc.*, **1992**, *114*, 7314–7316.

[17] Persichetti, R.A.; St. Clair, N.L.; James, P.; Griffith, J.P.; Navia, M.A.; Margolin, A.L. Cross-Linked Enzyme Crystals (CLECs) of thermolysin in the synthesis of peptides. *J. Am. Chem. Soc.*, **1995**, *117*, 2732-2737.

[18] Cao, L.Q.; van Rantwijk, F.; Sheldon, R.A. Cross-linked enzyme aggregates: A simple and effective method for the immobilization of penicillin acylase. *Org. Lett.*, **2000**, *2*, 1361-1364.

[19] López-Gallego, F.; Betancor, L.; Hidalgo, A.; Alonso, N.; Fernández-Lafuente, R.; Guisán J.M. Co-aggregation of enzymes and polyethyleneimine: A simple method to prepare stable and immobilized derivatives of glutaryl acylase. *Biomacromolecules*, **2005**, *6*, 1839-1842.

[20] Wilson, L.; Fernández-Lorente, G.F.; Fernández-Lafuente, R.F.; Illanes, A.; Guisán, J.M.; Polomo, J.M. CLEAs of lipases and poly-ionic polymers: A simple way of preparing stable biocatalysts with improved properties. *Enzyme*

Microb. Technol., **2006**, *39*, 750-755.

[21] Andersson, M.M.; Hatti-Kaul, R. Protein stabilising effect of polyethyleneimine. *J. Biotechnol.*, **1999**; *72*, 21-31.

[22] Bakker, M.; Spruijt, A.S.; van de Velde, F.; van Rantwijk, F.; Sheldon, R.A. Enantioselective transesterification of secondary alcohols mediated by aminoacylases from *Aspergillus* species. *J. Mol. Catal. B: Enzym.*, **2001**, *11*, 373-376.

[23] Sato, T.; Tosa, T. Optical resolution of racemic amino acids by aminoacylase. *Bioprocess Technol.*, **1993**, *16*, 3-14.

[24] Espenson, J.H. Chemical Kinetics and Reaction Mechanisms. McGraw-Hill, New York, **1981**.

[25] Gouda, M.D., Singh, S.A., Rao, A.G.A., Thakur, M.S., Karanth, N.G. Thermal inactivation of glucose oxidase. *J. Biol. Chem.*, **2003**, *278*, 24324-24333.

[26] Bodanszky, M.; Bodanszky, A. In: The Practice of Peptide Synthesis. Springer-Verlag, Berlin, **1984**.

[27] Regla, I.; Luna, H.; Herminia, I.; Pérez, H.I.; Demare, P.; Bustos-Jaimes, I.; Zaldívar, V.; Calcagno, M.L. Enzymatic resolution of N-acetyl-homophenylalanine with mammalian kidney acetone powders. *Tetrahedron: Asymmetr.*, **2004**, *15*, 1285-1288.

[28] López-Serrano, P.; Wegman, M.A.; Rantwijk, F.; Sheldon, R.A. Enantioselective enzyme catalysed ammoniolysis of amino acid derivatives: Effect of temperature. *Tetrahedron: Asymmetr.*, **2001**, *12*, 235-240.

[29] Bakker, M.; Spruijt, A.S.; van Rantwijk, F.; Sheldon, R.A. Highly enantioselective aminoacylase-catalyzed transesterification of secondary alcohols. *Tetrahedron: Asymmetr.*, **2000**, *11*, 1801-1808.

[30] Moira, L.; Bode, M.L.; van Rantwijk, F.; Sheldon, R. A. Crude aminoacylase from *Aspergillus* sp. is a mixture of hydrolases. *Biotechnol. Bioeng.*, **2003**, *84(6)*, 710-713.

[31] Grim, M.D.; *In:* Kirst H.A.; Yeh, W-K.; Zmijewski, M.J. (*Eds.*), Enzyme Technologies for Pharmaceutical and Biotechnological Applications. Marcel Dekker Inc., New York, **2001**, pp. 209-226.

[32] Mateo, C. Fernandes, B.; van Rantwijk, F.; Stolz, A.; Sheldon, R.A. Stabilisation of oxygen-labile nitrilases via co-aggregation with

poly(ethyleneimine). *J. Mol. Catal. B: Enzym.*, **2006**, *38*, 154-157.

[33] Ó'Fágáin, C. Enzyme stabilization-recent experimental progress. *Enzyme Microb. Technol.*, **2003**, *33*, 137-149.

[34] Govardhan, C.P. Crosslinking of enzymes for improved stability and performance. *Curr. Opin. Biotech.*, **1999**, *10*, 331-335.

[35] Fernandez-Lafuente, R.; Rosell, C.M.; Caanan-Haden, L.; Rodes, L.; Guisan, J.M. Facile synthesis of artificial enzyme nano-environments via solid-phase chemistry of immobilized derivatives: Dramatic stabilization of penicillin acylase versus organic solvents. *Enzyme Microb. Technol.*, **1999**, *24*, 96-103.

[36] Youshko, M.I.; van Langen, L.M.; Sheldon, R.A.; Švedas, V.K. Application of aminoacylase I to the enantioselective resolution of α-amino acid esters and amides. *Tetrahedron: Asymmetr.*, **2004**, *15*, 1933-1936.

[37] Engasser, J.-M., Horvath, C. Diffusion and kinetics with immobilized enzymes, *In*: Wingard, L. B.; Katchalski-Katzir, E.; Goldstein, L. (*Eds.*), Applied Biochemistry and Bioengineering: Immobilized enzymes principles. *Vol. 4*, Academic Press, London, **1976**, pp. 128-216.

[38] Phillips, R.S. Temperature modulation of the stereochemistry of enzymatic catalysis: Prospects for exploitation. *Trends Biotechnol.*, **1996**, *14(1)*, 13-16.

CHAPTER

7

Preparative scale enantio-selective synthesis of vicinal diols using immobilized *Solanum tuberosum* epoxide hydrolase

7.1. INTRODUCTION

Epoxides and vicinal diols are valuable chiral intermediates because of their versatile reactivity [1, 2]. Enantiopure epoxides and vicinal diols have been used for synthesis of a variety of bioactive compounds such as β-3-adrenergic receptor agonists, anti-obesity drugs, N-methyl D-aspartate receptor antagonists, nematocides and anticancer agents [3, 4]. This is why, stereoselective synthesis of epoxides and vicinal diols has gained great commercial interest. In the past few years, different methods have been reported (mostly based on transition metal catalysis) for synthesis of chiral epoxides and vicinal diols [5-7]. However, the environmental concerns and the regulatory constraints faced in the chemical and pharmaceutical industries have spurred the quest for alternative biological methods that can offer clean and mild synthetic processes. One of the most promising methods to produce enantiopure vicinal diol involves use of epoxide hydrolase enzyme [8].

Epoxide hydrolase (EC 3.3.2.3) catalyzes the addition of a water molecule to the oxirane ring of epoxides leading to formation of the corresponding vicinal diols [9]. Epoxide hydrolases (EHs) are widespread in nature and readily available from plants, animals, insects and micro-organisms. The enzyme is co-factor independent and therefore suitable for operating even at larger scale [10]. More interestingly, a few EHs (e.g. that produced by *Solanum tuberosum*) possess complementary regioselectivity towards the two enantiomers of the same substrate. This unique catalytic property can be used to develop efficient one-pot enantioconvergent processes [3].

Among the several types of biocatalytic reactions, kinetic resolution of racemates is the most widely used method for synthesis of enantiopure compounds. Despite its widespread applications, the classical kinetic resolution is impeded by several limitations. The most crucial one is – the theoretical yield of each enantiomer can never exceed the limit of 50% of mole ratio. Enantioconvergent strategy is an efficient means to overcome the 50% yield limitation [11].

An enantioconvergent process essentially involves de-racemization. The de-racemization can be achieved by making use of two independent reactions where two enantiomers of a substrate are converted into a single enantiomer of product. An enantioconvergent production of (*R*)-vicinal diol by *Solanum tuberosum* epoxide hydrolase (*St*-EH) is given in Scheme 7.1. The enzyme preferentially attacks less-

substituted carbon in the oxirane ring of (*R*)-epoxide which retains its configuration to yield (*R*)-diol. Contrary to expectation, the enzyme preferentially attacks more-substituted carbon in the oxirane ring of *S*-epoxide which undergoes inversion of configuration to yield (*R*)-diol [11]. Thus racemic epoxide can be transformed to enantiopure vicinal diol via an enantioconvergent process.

Scheme 7.1: Enantioconvergent synthesis of (*R*)-vicinal diol catalyzed by *Solanum tuberosum* epoxide hydrolase (*St*-EH)

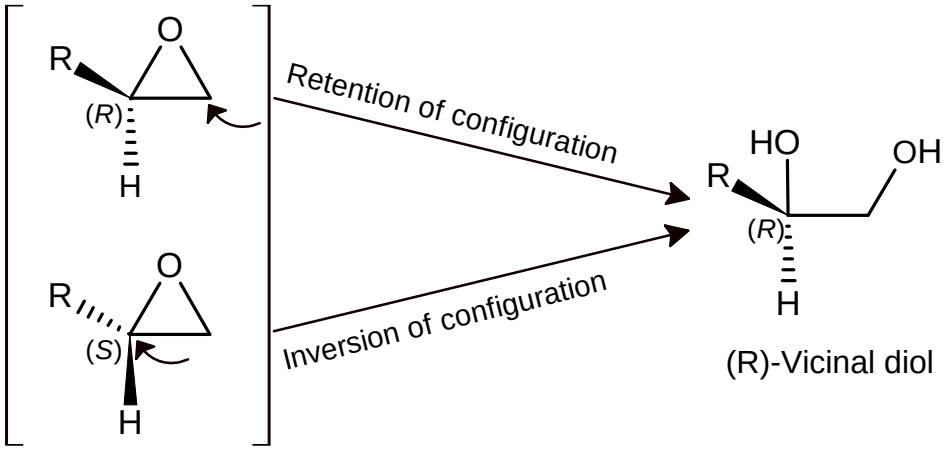

The present chapter deals with the enantioconvergent production of two vicinal diols (*namely*: phenylethane diol and *m*-chloro-phenylethane diol) using immobilized *St*-EH. To the best of our knowledge, a preparative scale enantioconvergent production of vicinal diols has not yet been reported. The enantioconvergent transformations are inherently complex and therefore difficult to scale-up.

The preparative scale process is difficult to implement mainly due to the instability and poor solubility substrates (epoxides) in the aqueous system. Epoxide hydrolase catalyzed biotransformations has generally been carried out in aqueous buffer systems in which most of the epoxides slowly undergo chemical hydrolysis [12]. The chemical hydrolysis of epoxide reduces the enantiomeric purity of the product (diol) as it yields racemic diol. One way to overcome this problem is to maintain the high rate of the enzymatic hydrolysis thereby finishing the biotransformation within short span of time. However, the epoxide hydrolase shows

competitive product inhibition. Thus as the reaction proceeds, more and more product is formed and the rate declines with time. Maintaining high rate of enzymatic hydrolysis throughout the reaction therefore becomes almost impossible especially when high substrate concentration is used.

In the present work, different strategies that can allow the transformation of substrate at higher concentrations have been studied. This chapter describes a method of preparative scale enantioconvergent synthesis of two vicinal diols (*namely*: phenylethane diol and *m*-chloro-phenylethane diol) using immobilized *Solanum tuberosum* epoxide hydrolase. *S. tuberosum* epoxide hydrolase was immobilized on glyoxyl agarose porous beaded polymers by multipoint covalent attachment. The high catalytic activity and stability of immobilized enzyme allowed reuse of the enzyme over repeated biotransformation cycles.

7.2. MATERIALS AND METHODS

7.2.1. Materials

The plasmid (pGEFII-*St*EH) containing the epoxide hydrolase gene from *S. tuberosum* was kindly provided by Prof. M. Arand (Institute of Pharmacology and Toxicology, Zürich, Switzerland). Ionic liquids *namely* 1-Butyl-3-methylimidazolium hexafluorophosphate i.e. [BMIm]PF_6, 1-Butyl-3-methylimidazolium tetrafluoroborate i.e. [BMIm]BF_4, 1-Butyl-3-methylpyridinium bis (trifluoromethyl sulfonyl) imide i.e. [BMPy] Tf_2N and 1-Butyl-1-methylpyrrolidium bis (trifluoromethyl sulfonyl) imide i.e. [BMP]Tf_2N were procured from Sigma-Aldrich, USA. Agarose-10 BCL was obtained from Iberagar S.A., Portugal and activated as described earlier [13]. All other chemicals were purchased from Sigma-Aldrich, USA.

7.2.2. Production of St-EH by recombinant E. coli cells

(a) Insertion of plasmid in E.coli BL21

Escherichia coli BL21 (DE3) cells were grown in LB broth (composition: casein peptone 10 g/L, yeast extract 5 g/L, NaCl 5g/L; pH 7.0 ± 0.2) at 37°C for 12h. 2 mL of broth was removed, centrifuged (at 1000 rpm for 5 min) and the cells were suspended in sterile TB buffer (KCl 18.65 g/L; $CaCl_2$ 2.2 g/L; 0.5 M solution of PIPES i.e. piperazine-N,N'-bis(ethanesulfonic acid) 20 mL in 1 L ; $MnCl_2$ 10.88 g/L; pH 6.7) Six µL of plasmid solution was added to the cell suspension. To facilitate the

insertion of plasmid into *E. coli* cells, the resultant solution was incubated at 0°C for 30 min, incubated at 42°C for 90 sec, kept at 0°C for 2 min and finally incubated at 37°C for 45 min under reciprocal agitation at ~ 200 strokes per minute. The cell suspension was poured on LB agar plate containing 200 μg/mL of carbenicillin. The presence of functional plasmid in the recombinant *E. coli* cells conferred resistance against carbenicillin while native cells were unable to survive. After 24 h, the cells from the individual colonies were sub-cultured on fresh LB agar media containing carbenicillin.

(b) Fermentative production of St-EH

Recombinant *E. coli* cells were grown in LB broth containing 200 μg/mL ampicillin in a 1 L fermenter at 20°C. After ~ 15 h of fermentation when broth OD_{600} > 1.5, production of EH was induced with 1 mL of 400 mM solution of IPTG. After ~ 20 h of fermentation, the cells were harvested by centrifugation, re-suspended in 20 mL of ammonium carbonate buffer (20 mM, pH 7.6) and then ruptured by using a French press. The cell debris was removed by centrifugation (20,000 rpm for 30 min) and the supernatant was freeze dried to produce crude extract of *St*-EH. From three batches of 1L fermenters, about 4.8 g of lyophilized crude *St*-EH was obtained having an activity of about 2 U/mg. This was used for the immobilization experiments.

7.2.3. Immobilization of St-EH

The immobilization of *S. tuberosum* epoxide hydrolase was carried out by the method described earlier by Mateo *et al.* [14].

(a) Preparation of the glyoxyl-agarose support (GA support)

Glyoxyl-agarose 10 BCL gels (agarose-O-CH_2-CHO) were prepared by etherification of agarose gels with glycidol (2,3-epoxypropanol) and further oxidation with sodium periodate [13].

(b) Immobilization of St-EH

GA support (2 g) was mixed with an enzyme solution (20 mL of 1 mg/mL water), 2 mL sodium bicarbonate solution (0.2 M, pH 10) and 20% (w/v) of 164 kDa dextran. The suspension was gently stirred for 1 h at 4°C. After this period, sodium

bicarbonate (6 mL of 0.2 M, pH 10) containing sodium borohydride (10 mg) was added and the suspension was stirred for 30 min. Finally, the immobilized beads were washed with an excess of 50 mM sodium phosphate buffer (pH 7).

7.2.4. Stability of immobilized epoxide hydrolase

(a) pH stability

The effect of pH on stability of free and immobilized *St*-EH was studied by incubating the enzyme at 20°C in buffers of varying pH in the range of 6-9 for 30 min. Residual activities were calculated as the ratio of the activity of immobilized enzyme after incubation to the initial activity at the optimum reaction pH.

(b) Temperature stability

The effect of temperature on stability of free and immobilized *St*-EH was tested by incubating the enzyme at varying temperatures in the range of 20-70°C for 30 min (at pH 7). Residual activities were calculated as mentioned above and plotted against temperature.

(c) Thermal stability as function of incubation time

The thermal stability of immobilized *St*-EH was tested by incubating the enzyme at varying temperatures in the range of 50-70°C for 2 h. The samples were withdrawn at regular time intervals, rapidly cooled to 25°C and immediately analyzed for residual EH activity.

(d) Solvent stability

(i) Stability of immobilized St-EH in water-miscible solvents

The immobilized *St*-EH was suspended in solution of equal volume of water-miscible solvent and phosphate buffer (50 mM, pH 7). After 24 h, the immobilized enzyme was washed thoroughly with phosphate buffer (50 mM, pH 7) and analyzed for residual EH activity.

(ii) Stability of immobilized St-EH in water-immiscible solvents

The immobilized *St*-EH was suspended in an emulsion of equal volume of water-immiscible solvent and phosphate buffer (50 mM, pH 7). After 24 h, the

immobilized enzyme was washed thoroughly with phosphate buffer (50 mM, pH 7) and analyzed for residual EH activity. Further, the stability of immobilized *St*-EH in ethyl acetate and iso-octane (50% mixture of each in phosphate buffer) was determined as a function of time.

7.2.5. Synthesis and characterization of substrates

(a) Synthesis of m-chloro-styrene oxide

m-Chloro-styrene oxide was prepared via Corey-Chaykovsky reaction [15]. In 250 mL round bottom flask, 6.96 g of trimethyl sulphonium iodide i.e. $(CH_3)_3SI$ was dissolved in 20 mL of dimethyl sulfoxide (DMSO) using a magnetic stirrer. To this, 0.83 g of sodium hydrate (NaH) was added slowly under gentle stirring conditions. (*Caution*: addition of NaH results in liberation of hydrogen gas). Four gram of *m*-chloro-benzaldehyde was dissolved separately in 40 mL DMSO and added drop-wise to the $(CH_3)_3SI$, NaH and DMSO mixture under gentle stirring. The reaction mixture was refluxed for 2 h. After 2 h, 100 mL cold water was added to the reaction mixture and the resultant solution was extracted thrice with 50 mL of *n*-hexane. The hexane phases were collected and pooled together and extracted with 50 mL cold water. The residual water in the hexane phase was removed using unhydrous $MgSO_4$. The solvent within the hexane phase was evaporated under vacuum using Rotavac® assembly (Buchi R-200, Switzerland) to obtain crude *m*-chloro-styrene oxide. Finally the crude *m*-chloro-styrene oxide was distilled using bulb-to-bulb evaporator (operated at 1 mBar vacuum at 100°C) to obtain pure product. The chemical reaction involved in synthesis of *m*-chloro-styrene oxide is given in Scheme 7.2.

Scheme 7.2: Chemical synthesis of *rac*- *m*-chloro-styrene oxide from *rac*- *m*-chloro-benzaldehyde

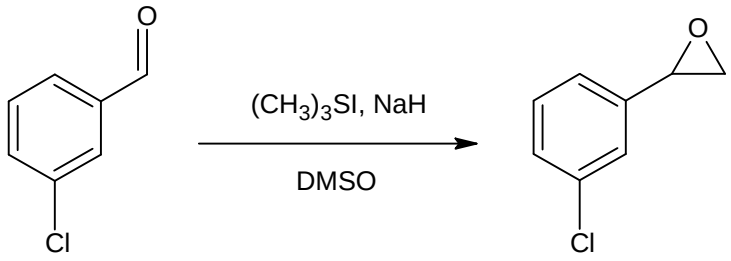

m-Chloro-benzaldehyde *m*-Chloro-styrene oxide

(b) Characterization

m-chloro-styrene oxide: Colourless liquid, boiling point range 120-121°C. ^{1}H-NMR (300 MHz): 7.24-7.56 (4H, aromatic *H*), 3.83 (1H, Ph-C*H*), 2.96-2.71 (2H, Ph-CH-CH_2).

7.2.6. Studies on product and substrate inhibition

(a) Product inhibition

The product inhibition of *St*-EH by diol was studied by the method described earlier [8]. The product inhibition of *St*-EH by phenylethane diol was studied in the range of 0-25 g/L. The enzymatic hydrolysis of epoxide was carried out in 20mL stoppered reaction tube (with conical bottom). To 10 mL of 0.05M phosphate buffer (pH 7.0), 0.1 g (i.e. 94.9 µL) of styrene oxide and different concentrations of phenylethane diol were added. The hydrolysis was initiated by addition of 100 µL of *St*-EH enzyme solution (prepared by dissolving 25 mg of lyophilized *St*-EH powder in 1 mL of 0.05M phosphate buffer, pH 7.0). The reaction mixture was maintained under continuous stirring with magnetic stirrer at 20°C. The samples were periodically withdrawn and analyzed for ee of styrene oxide by a GC method described in Section 7.2.10(b).

The product inhibition of *St*-EH by *m*-chloro-phenylethane diol was studied in the range of 0-15 g/L in a similar manner as described above. The samples were periodically withdrawn and analyzed for ee of *m*-chloro-styrene oxide by a GC method described in Section 7.2.10(b).

7.2.7. Strategies to minimize the product and substrate inhibition

(a) Use of resin as an adsorbent for product removal

(i) Adsorption of diol on resin

Fourteen commercial resins were studied for adsorption of phenylethane diol and *m*-chloro-phenylethane diol. In a 25 mL stoppered conical flask, a resin was suspended in a solution of known concentration of phenylethane diol. The flask was incubated on oscillatory shaker at 25°C at 120 rpm. After 1 h, the supernatant and resin were separated by filtration and the supernatant was analyzed for phenylethane

diol contents by HPLC. The amount of phenylethane diol adsorbed on the resin was calculated from the difference in concentration of phenylethane diol before and after treatment with resin.

A graph of amount of diol adsorbed verses amount of resin was used to select the resins having maximum binding capacity. Furthermore, the adsorption parameter (X) against the concentration of diol (mM) in the supernatant was used to study a pattern of diol adsorption on each resin. X is defined as mg of diol adsorbed per g of resin.

(ii) Selectivity of adsorption of diol on Lewatit VPOC 1163

The adsorption of phenylethane diol was studied in the presence of styrene oxide. Lewatit VPOC 1163 (2 g dry weight) was loaded in a glass column (6 cm × 2.5 cm). The resin was washed three times with 0.05 M phosphate buffer (pH 7). A solution of styrene oxide and phenylethane diol (5g/L of each in phosphate buffer) was passed through a bed of Lewatit VPOC 1163 resin using peristaltic pump with flow rate of about 5 mL/min. The eluent was collected and analyzed for the concentration of styrene oxide and phenylethane diol.

(b) Medium engineering

(i) Epoxide hydrolysis in buffer-ionic liquid biphasic reaction medium

The enzymatic hydrolysis of styrene oxide and *m*-chloro-styrene oxide was studied using 10 mg of immobilized *St*-EH in presence of 10% v/v of ionic liquids. The enzymatic hydrolysis of epoxide was carried out in 20mL stoppered reaction vessel. To 9 mL of 0.05M phosphate buffer (pH 7.0), 1 mL ionic liquid and 0.1 g (i.e. 94.9 μL) of styrene oxide were added. The hydrolysis was initiated by addition of 10 mg of immobilized *St*-EH. The reaction mixture was maintained under continuous stirring with magnetic stirrer at 20°C. The samples were periodically withdrawn and analyzed for ee of styrene oxide by GC.

(ii) Epoxide hydrolysis in buffer-organic solvent biphasic reaction medium

The enzymatic hydrolysis of styrene oxide and *m*-chloro-styrene oxide was studied using 10 mg of immobilized *St*-EH in presence of 10% v/v of different organic liquids. In a 20mL stoppered reaction tube, 9 mL of 0.05M phosphate buffer

(pH 7.0), 1 mL immiscible organic solvent and 0.1 g (i.e. 94.9 μL) of styrene oxide were added. The hydrolysis was initiated by addition of 10 mg of immobilized *St*-EH. The reaction mixture was maintained under continuous stirring with magnetic stirrer at 20°C. The samples were periodically withdrawn and analyzed for ee of styrene oxide by GC.

7.2.8. Determination of regioselectivity constants for immobilized St-EH

The regioselectivity constants of *St*-EH towards hydrolysis of styrene oxide and *m*-chloro-styrene oxide were determined by method described earlier by Karboune *et al.* [16].

(a) Regioselectivity towards hydrolysis of styrene oxide

To 2 μL of enantiopure (*R*)- or (*S*)-styrene oxide, 0.2 mL of iso-octane, 1.8 mL of phosphate buffer (10 mM, pH 7) and 100 mg of immobilized *St*-EH were added. The enzymatic hydrolysis was maintained at 20°C under gentle orbital staking. Three samples (10 μL) were withdrawn at different time periods; phenylethane diol formed was extracted with ethyl acetate. The ee of the diol was determined by GC.

(b) Regioselectivity towards hydrolysis of m-chloro-styrene oxide

To 2 μL of enantiopure (*R*)- or (*S*)-*m*-chloro-styrene oxide, 2 mL of phosphate buffer (10 mM, pH 7) and 300 mg of immobilized *St*-EH were added. The enzymatic hydrolysis was maintained at 30°C under gentle orbital shaking. Three samples (10 μL) were withdrawn at different time periods; *m*-chloro-phenylethane diol formed was extracted with ethyl acetate. The diol was derivatized into the corresponding acetonide using 2,2 dimethoxypropane in presence of *p*-chloro-sulphonic acid. The ee of derivatized product was determined by GC.

7.2.9. Preparative scale enantioselective production of vicinal diols

(a) Production of phenylethane diol

In a laboratory scale stirred cell (XFUF07601, Millipore Inc. USA), a macroporous filtration fabric cloth (76 mm diameter) was placed on the membrane support (Fig. 7.1).

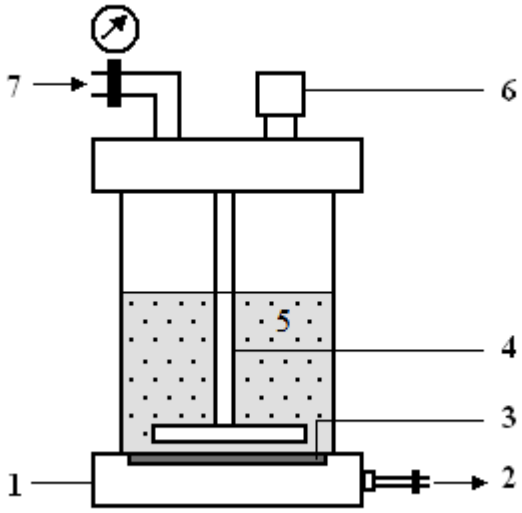

Fig. 7.1: Schematic representation of stirred cell bioreactor; 1: membrane support, 2: outlet, 3: macroporous filtration fabric cloth, 4: magnetic stirrer, 5: reaction mixture containing immobilized epoxide hydrolase, 6: sample port and 7: pressure gauze.

The reactor was charged with 85.3 mL of 0.05M phosphate buffer (pH 7.0), 10 mL of iso-octane and 5 g (4.7 mL) of *rac*-styrene oxide. The biotransformation reaction was initiated by addition of 10 g of immobilized *St*-EH. The reactor temperature was maintained at 20°C under constant stirring speed of 200 rpm. The samples were periodically withdrawn and analyzed by GC as described in Section 7.2.10(b).

The reaction was stopped by separating the reaction mixture. The reactor was thoroughly washed twice with a mixture of 50 mL of iso-octane:phosphate buffer (1:1 by volume) to ensure the complete removal of product and unreacted substrate. The washings and reaction mixture were pooled together. The iso-octane phase and aqueous phase were separated using separating funnel. The aqueous phase was extracted thrice with 30 mL of hexane. The hexane extract was mixed with iso-octane phase and solvent was evaporated under vacuum using Rotavac® assembly (Buchi R-200, Switzerland) to obtain styrene oxide. The aqueous phase was further extracted thrice with 30 mL of ethyl acetate. The solvent within the ethyl acetate phase was evaporated under vacuum using a Rotavac® assembly to obtain phenylethane diol.

(b) Production of m-chloro-phenylethane diol

A schematic diagram of stirred cell (XFUF07601, Millipore Inc. USA) which was used for production of *m*-chloro-phenylethane diol is given in Fig. 7.1. A macroporous filtration fabric cloth (76 mm diameter) was placed on the membrane support. The reactor was charged with 93.35 mL of 0.05M phosphate buffer (pH 7.0), 5 mL of iso-octane and 2 g (1.65 mL) of *rac*-*m*-chloro-styrene oxide. The biotransformation reaction was initiated by addition of 10 g of immobilized *St*-EH. The reactor temperature was maintained at 30°C under constant stirring speed of 200 rpm. The samples were periodically withdrawn and analyzed by GC as described in Section 7.2.10(b).

The reaction was stopped by separating the reaction mixture. The reactor was thoroughly washed twice with 50 mL of iso-octane:phosphate buffer (1:1 by volume) mixture to ensure the complete removal of product and unreacted substrate. The washings and reaction mixture were pooled together. Extraction of *m*-chloro-styrene oxide and *m*-chloro-phenylethane diol was carried out by the procedure mentioned for extraction of styrene oxide and phenylethane diol.

7.2.10. Analytical methods

(a) Enzyme activity assay

The enzymatic activity was measured spectrophotometrically using styrene oxide (at 25°C and pH 7) as substrate as described previously [17]. In a quartz cuvette, 1.8 mL of water, 100 µL of 40 mM sodium periodate solution and 100 µL of 360 mM styrene oxide solution (prepared in dimethyl formamide) were added. This reaction mixture was continuously mixed with magnetic stirrer and maintained at 25°C. The enzymatic reaction was initiated by addition of 20 µL of appropriately diluted *St*-EH solution (prepared in 0.05 M phosphate buffer, pH 7.0). The increment in the absorbance caused by the benzaldehyde formed was measured at 290 nm.

(b) GC analysis

All reaction profiles were monitored by GC (Shimadzu GC-20A, Japan) equipped with flame ionized detector (FID). The ee of the styrene oxide and phenylethane diol was determined by using a fast Cyclosil-B® GC column (13 m × 0.1 mm, 0.1 µm film, purchased from Agilent Technologies, Germany) while that of *m*-chloro-styrene oxide was determined by using a Lipodex-E® GC column (25 m ×

0.25 mm, 0.1 μm film, procured from Macherey-Nagel, Germany). *m*-chloro-phenylethane diol was derivatized by 2,2-Dimethoxy propane (98%) in presence of *p*-chloro-sulphonic acid and the enantiomeric excess of derivatized product (acetonide) was analyzed using a Chirasil-DEX® GC column (25 m × 0.25 mm, 0.1 μm film, purchased from Varian Inc. Canada).

(c) HPLC analysis

The quantitative analysis of phenylethane diol and *m*-chloro-phenylethane diol was carried out using a NUCLEODUR® C-18 column (125×4 mm, prepacked column supplemented with 8×4 mm guard column procured from Macherey-Nagel, Germany) isocratically eluted using acetonitrile-water mobile phase (30:70 v/v) with a flow rate of 0.5 mL/min. Peaks were detected by UV detector at 220 nm. Peak area was used as a measure to calculate the respective concentration.

(d) Determination of enantiomeric ratio

Enantiomeric ratio was determined by using Eq. 7.1 as described earlier [18].

$$E = \frac{\ln[(1-C)(1-\mathrm{ee_S})]}{\ln[(1-C)(1+\mathrm{ee_S})]} \qquad \text{– Eq. 7.1}$$

Where, C is conversion ratio and $\mathrm{ee_S}$ is enantiomeric excess of substrate. C and $\mathrm{ee_S}$ were calculated by using Eq. 7.2 and Eq. 7.3 respectively.

$$C = 1 - \left(\frac{c^S_{\mathrm{S(t)}} + c^R_{\mathrm{S(t)}}}{c^S_{\mathrm{S(0)}} + c^R_{\mathrm{S(0)}}} \right) \qquad \text{– Eq. 7.2}$$

Where, $c^S_{\mathrm{S(t)}}$ is concentration of *S*-enantiomer of substrate and $c^R_{\mathrm{S(t)}}$ is concentration of *R*-enantiomer of substrate at time, t. $c^S_{\mathrm{S(0)}}$ and $c^R_{\mathrm{S(0)}}$ are concentrations of *S*-enantiomer and *R*-enantiomer of substrate respectively at t = 0.

$$\mathrm{ee_S} = \frac{\left| c^S_{\mathrm{S}} - c^R_{\mathrm{S}} \right|}{c^S_{\mathrm{S}} + c^R_{\mathrm{S}}} \qquad \text{– Eq. 7.3}$$

Where, c_S^S is concentration of *S*-enantiomer of substrate and c_S^R is concentration of *R*-enantiomer of substrate.

7.3. RESULTS AND DISCUSSION

7.3.1. Immobilization of St-EH

The results of immobilization experiments are given in Table 7.1. The activity of free *St*-EH used for immobilization was 200 U/g of lyophilized enzyme powder while that of immobilized *St*-EH was 256.8 U/g of support. Total 8000 units of free *St*-EH were loaded on 22 g of GA support and 5650 units were recovered. Thus the immobilization gave 70% of activity recovery.

Table 7.1: Immobilization of *St*-EH on GA support

Parameter	**Free *St*-EH**	**Immobilized *St*-EH**
Activity (U/g)	2000	256.8
Amount (g)	4	22
Total units of *St*-EH	8000 [a]	5650 [b]
Activity recovery (%) [c]	–	70.62 %

[[a] Total units of free *St*-EH loaded; [b] Total units of immobilized *St*-EH recovered;

[c] $\text{Activity recovery}\,(\%) = \left(\frac{\text{Total units of immobilized } St\text{ - EH recovered}}{\text{Total units of free } St\text{ - EH loaded}} \right) \times 100$]

7.3.2. Stability of immobilized epoxide hydrolase

(a) Effect of pH on St-EH activity

Effect of pH on the residual activity of free and immobilized *St*-EH was studied for the pH range of 6 to 9 (Fig. 7.2). At pH 6, free *St*-EH and immobilized *St*-EH retained 86.75% and 92.70% residual activity. At pH 8 and 9, free enzyme retained 41.51% and 7.66% residual activity respectively while at same pH conditions, immobilized *St*-EH retained 67.38% and 47.05% residual activity respectively. Thus the immobilization improved the stability of enzyme in the alkaline range.

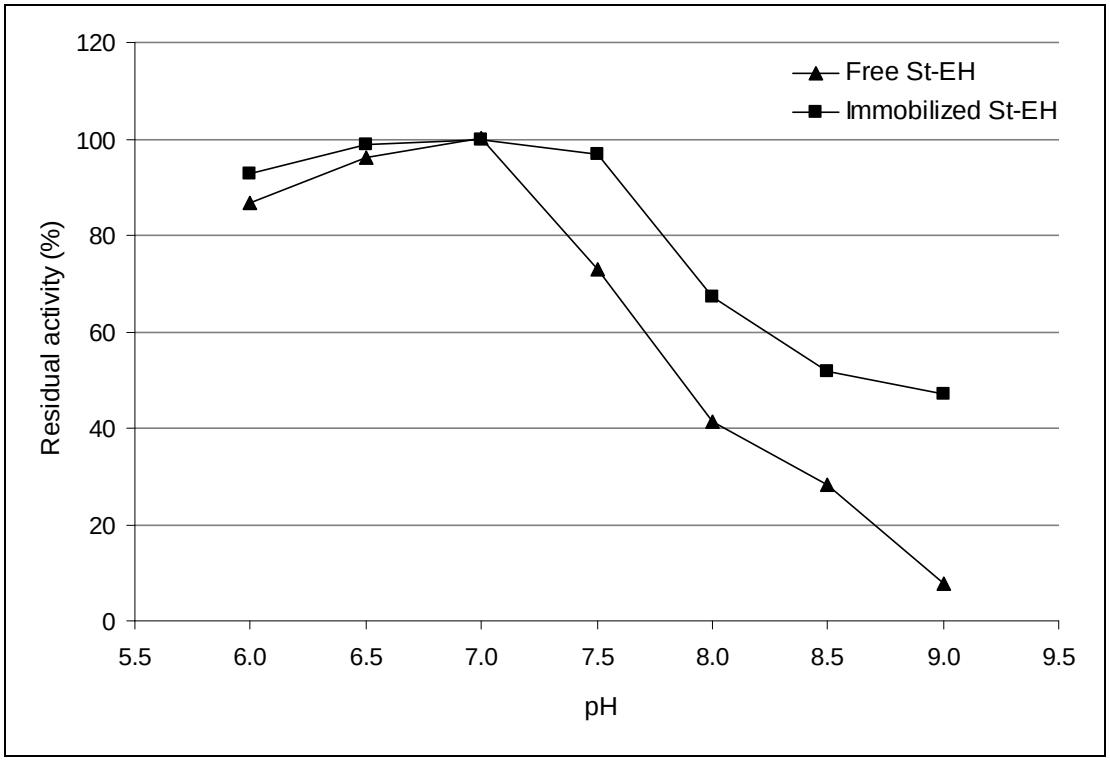

Fig. 7.2: pH stability of free and immobilized *St*-EH

(b) Effect of temperature on St-EH activity

The activity profiles of free and immobilized *St*-EH at different temperatures are presented in Fig. 7.3. At 20°C and 30°C free enzyme retained 77.99% and 85.93% residual activity respectively while immobilized *St*-EH retained 51.55% and 74.33% of its initial activity respectively.

The lower activities of immobilized enzyme than those of free enzyme could be ascribed to the reduced diffusion of substrate inside porous GA support due to higher viscosity of substrate at lower temperatures.

At 50°C and 60°C the free enzyme was found to retain 91.07% and 7.07% residual activity respectively while immobilized *St*-EH retained 97.65% and 70.72% of its initial activity respectively. These results indicate immobilization has conferred stability to the enzyme in the temperature range of 50-70°C.

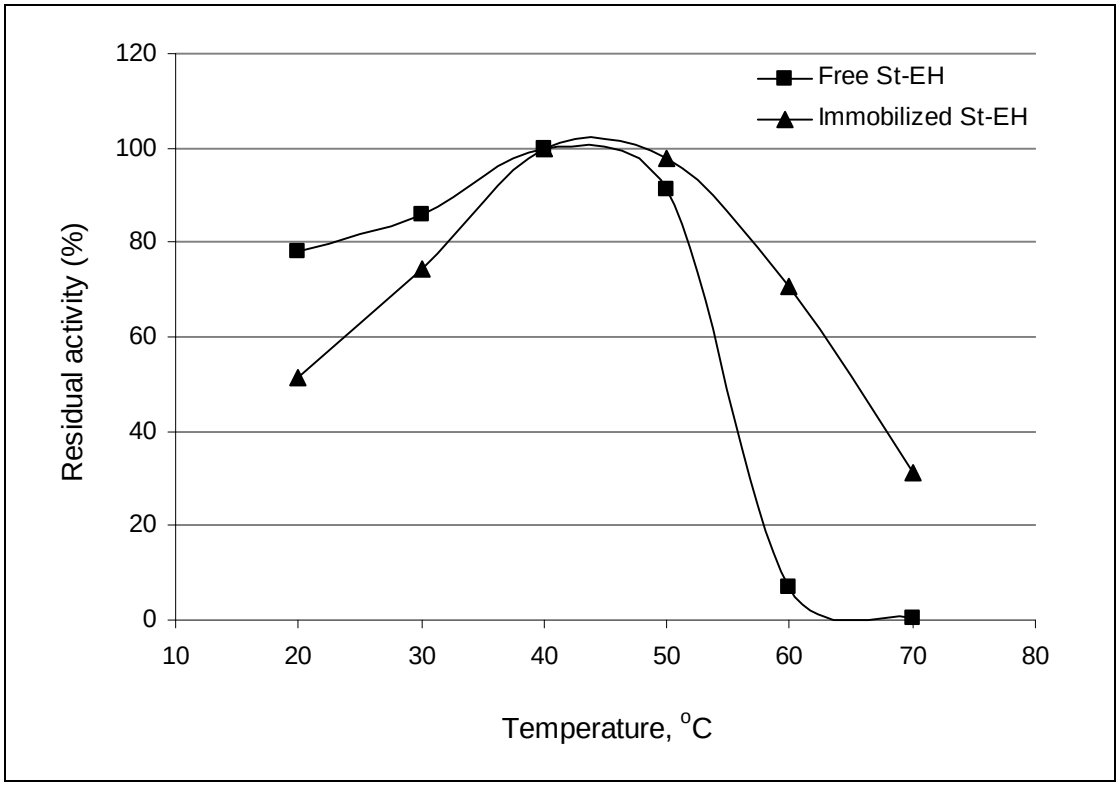

Fig. 7.3: Temperature stability of free and immobilized *St*-EH

(c) Thermal stability as function of incubation time

The thermal stability of immobilized *St*-EH is presented in Fig. 7.4.

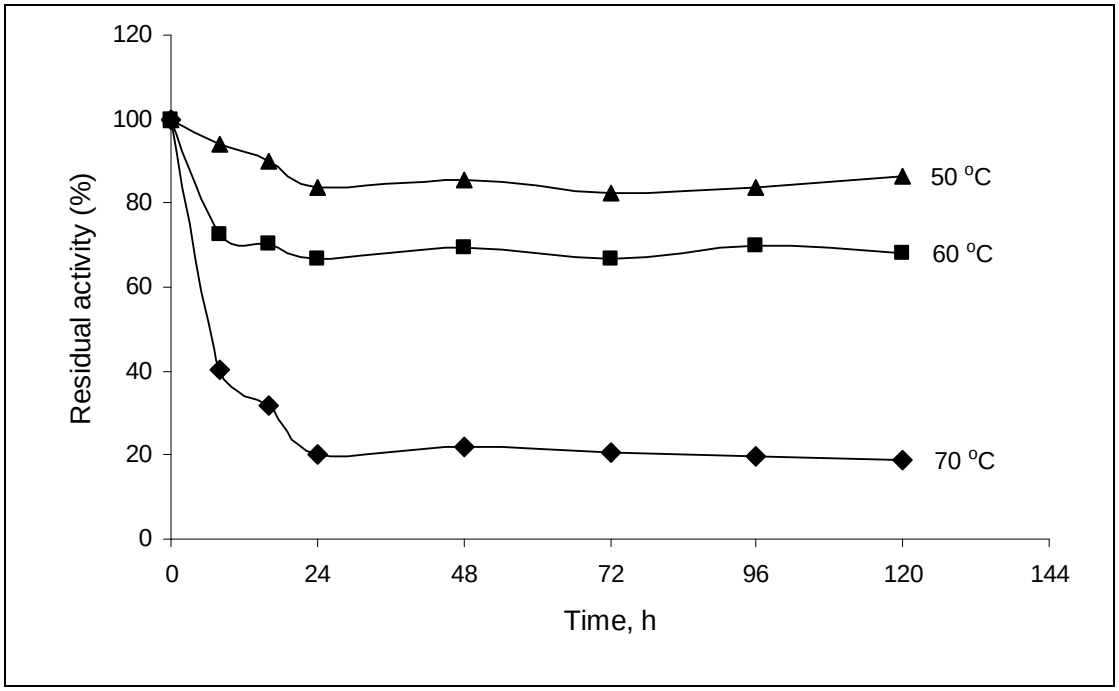

Fig. 7.4: Thermal stability of immobilized *St*-EH as function of incubation time

The residual activities of immobilized enzyme were found to decrease with increase in temperature. At the given temperature, the residual activity of immobilized enzyme showed gradual decrease up to 24 h incubation and thereafter it remained almost constant till 120 h.

(d) Solvent stability

(i) Stability of immobilized St-EH in water-miscible solvents

Stability of immobilized *St*-EH in different water-miscible solvents (*namely*: methanol, ethanol, iso-propyl alcohol, acetonitrile and dimethyl formamide) was studied. Incubation of immobilized enzyme in water-miscible solvents resulted in significant loss of *St*-EH activity (Fig. 7.5).

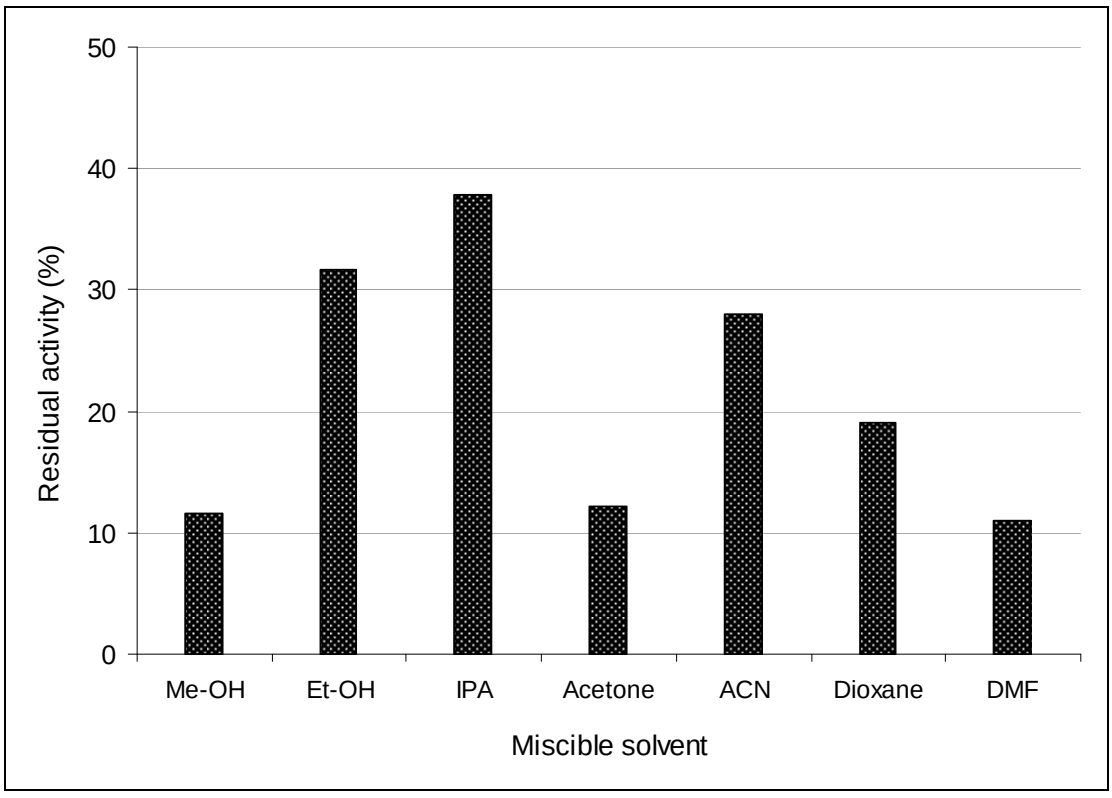

Fig. 7.5: Stability of immobilized *St*-EH in miscible solvents (Me-OH: methanol, Et-OH: ethanol, IPA: iso-propyl alcohol, ACN: acetonitrile, DMF: dimethyl formamide.)

The results suggest poor stability of immobilized enzyme in the water-miscible solvents. The immobilized enzyme incubated in iso-propyl alcohol (50% v/v in phosphate buffer) expressed maximum residual activity (i.e. 37.84%) while that

incubated in dimethyl formamide (50% v/v in phosphate buffer) expressed the least residual activity i.e. 10.96%.

(ii) Stability of immobilized St-EH in water-immiscible solvents

Stability of immobilized *St*-EH in different water-immiscible solvents (*namely*: carbon tetrachloride, cyclohexane, iso-octane, hexane and toluene) was studied. The result of water-immiscible solvent stability of immobilized *St*-EH is given in Fig. 7.6. The immobilized enzyme incubated in iso-octane (50% v/v in phosphate buffer) retained maximum residual activity i.e. 84.67% while that incubated in carbon tetrachloride (50% v/v in phosphate buffer) retained the least residual activity i.e. 30.60%.

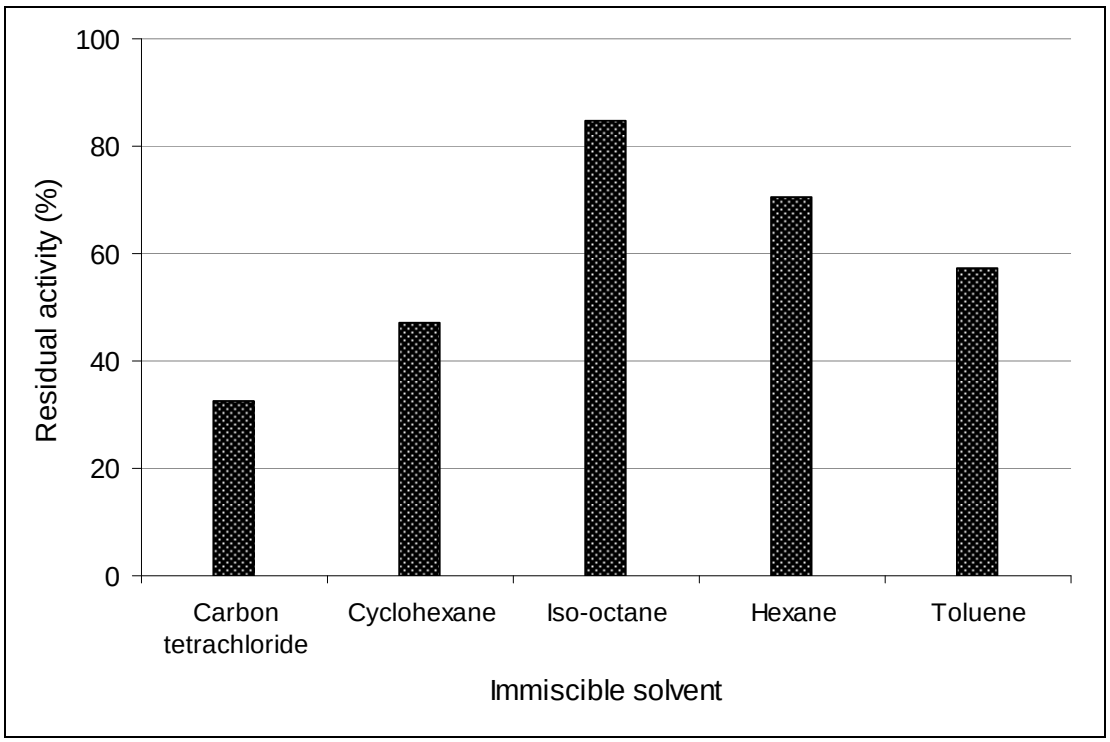

Fig. 7.6: Stability of immobilized *St*-EH in immiscible solvents

Furthermore, the activity profile of immobilized enzyme was studied in presence of iso-octane (50% v/v in phosphate buffer) for 120 h. Upon incubation in iso-octane-buffer emulsion, the residual activity of immobilized enzyme was found to decrease with time in initial 48 h of incubation and thereafter remained almost constant till 120 h (Fig. 7.7).

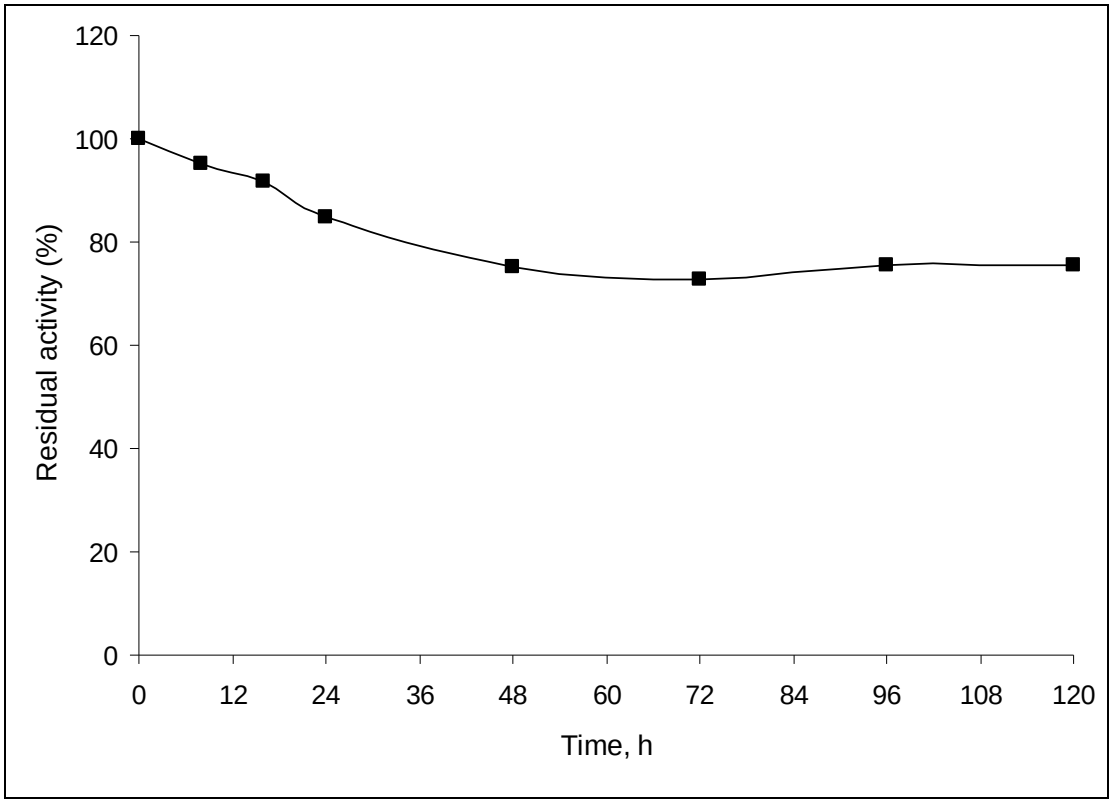

Fig. 7.7: Stability of immobilized *St*-EH in iso-octane

Several attempts have been made to immobilize epoxide hydrolases from different sources. For example: Karboune *et al.* compared different methods for immobilization epoxide hydrolase from the fungus *Aspergillus niger*. The highest retention of activity (65%) was obtained via ionic adsorption of the enzyme onto DEAE-cellulose compared to hydrophobic binding (onto porous polypropylene support) and covalent binding (onto Eupergit resin) [19]. In another report by same authors, immobilization of recombinant epoxide hydrolase from *Aspergillus niger* onto DEAE-cellulose is described [20]. Petri *et al.* reported a facile immobilization method of epoxide hydrolase from *Aspergillus niger* by covalent linking to epoxide-activated silica gel under mild conditions. About 90% retention of the initial enzymatic activity is reported. Though the immobilization did not improve pH and thermal stability, it considerably improved the storage and operational stability of the enzyme [21]. Ionic binding of *Nocardia* epoxide hydrolase on DEAE-cellulose showed 150-300% activity enhancement. Upon the covalent immobilization, marginal shift in pH optimum (from 7.5 to 8.0) and large shift in temperature optimum (from 35°C to 45°C) was observed [22]. Epoxide hydrolase producing cells of *Nocardia*

tartaricans ATCC 31191 were immobilized within sodium alginate−cellulose sulfate−poly(methylene-*co*-guanidine) capsules using a controlled encapsulation process [23]. Recently, Lee *et al.* have demonstrated immobilization of His-tagged epoxide hydrolases of *Rhodotorula glutinis* (produced by recombinant *Escherichia coli*) onto magnetic Fe_3O_4–silica–NiO nanoparticles. The binding affinity of NiO towards His-tagged proteins was utilized for the immobilization of the enzyme. More than 70% activity retention was observed after the immobilization [24].

7.3.3. Product inhibition

The enzymatic hydrolysis of styrene oxide was carried out in presence of different concentrations of phenylethane diol. The profiles of ee_S as a function of reaction time and respective initial reaction rates at different concentrations of phenylethane diol are given in Fig. 7.8. The initial reaction rate was found to decrease with increase in the concentration of phenylethane diol. The increase in phenylethane diol concentration from 0 g/L to 25 g/L, resulted in decrease in the initial reaction rate from 122.54 $\mu M.min^{-1}$ to 59.52 $\mu M.min^{-1}$.

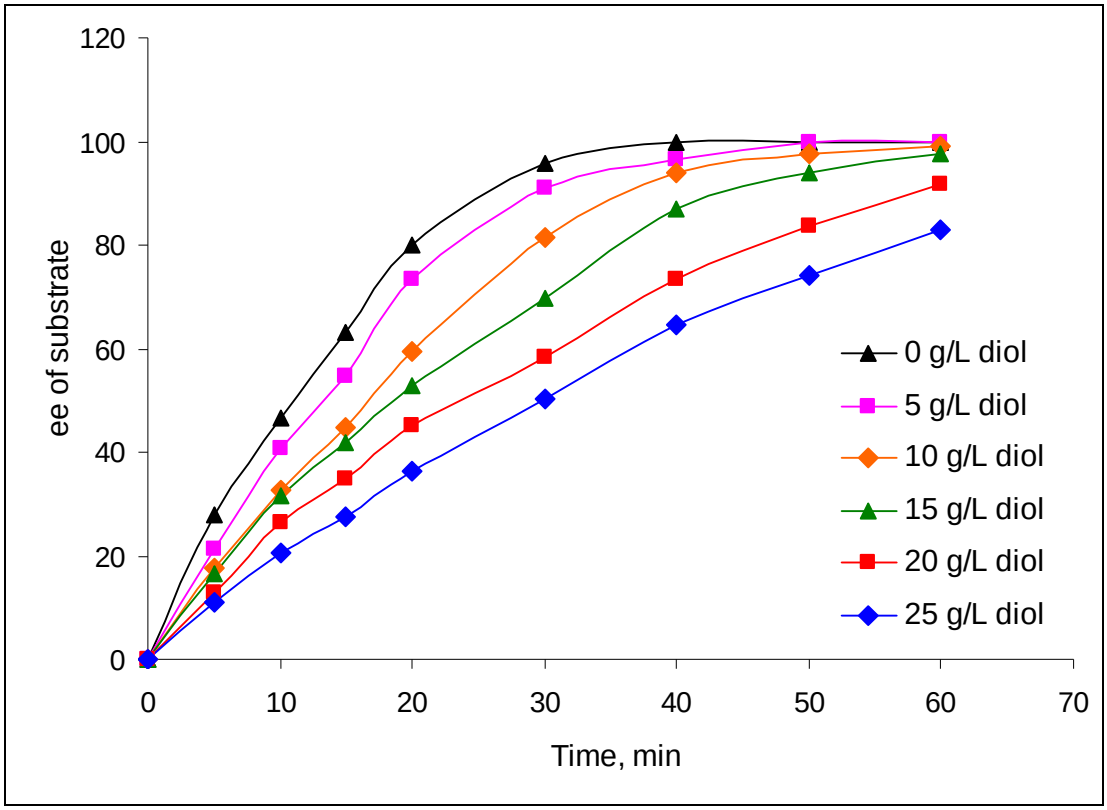

Fig. 7.8: Inhibition of *St*-EH by product (phenylethane diol)

Similarly, the ee_S as a function of reaction time and respective initial reaction rates at different concentrations of *m*-chloro-phenylethane diol are given in Fig. 7.9. The initial reaction rate was found to decrease with increase in the concentration of *m*-chloro-phenylethane diol. The increase in *m*-chloro-phenylethane diol concentration from 0 g/L to 15 g/L, caused decrease in the initial reaction rate from 36.33 $\mu M.min^{-1}$ to 17.84 $\mu M.min^{-1}$. The results indicate the predominant inhibition of *St*-EH by phenylethane diol and *m*-chloro-phenylethane diol.

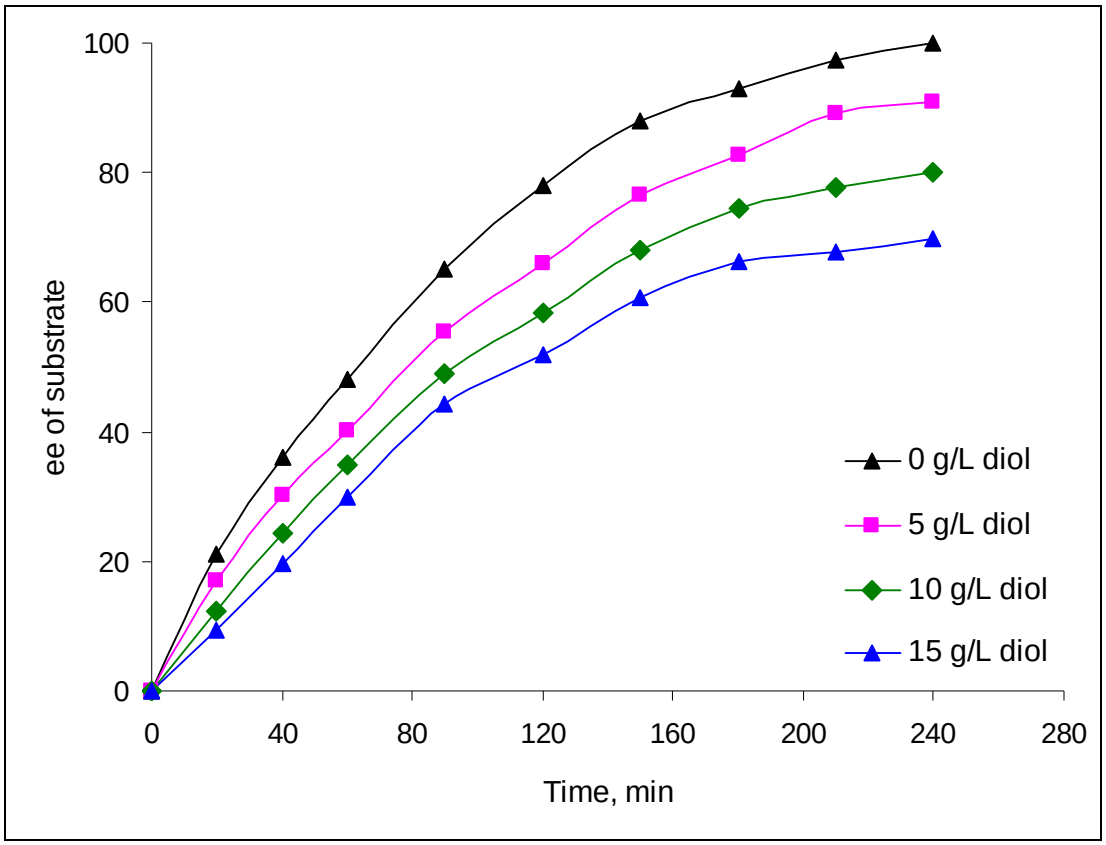

Fig. 7.9: Inhibition of *St*-EH by product (*m*-chloro-phenylethane diol)

7.3.4. Substrate inhibition

Both styrene oxide and *m*-chloro-styrene oxide are in liquid state at ambient temperature and pressure and have poor aqueous solubility. Hence, during the biotransformation reaction, a large fraction of the epoxide (styrene oxide or *m*-chloro-styrene oxide) remained insoluble in aqueous reaction medium. This insoluble substrate had an unfavourable effect on the rate enzymatic hydrolysis presumably because of two reasons: (i) owing to its corrosive nature, the insoluble substrate has some inhibitory effect on the enzyme and (ii) droplets of insoluble substrate typically

tend to adsorb on the immobilized enzyme matrix thereby limiting the rate of enzymatic hydrolysis. However, the exact implication of substrate inhibition is not fully understood and the work in this regard is in progress.

7.3.5. Strategies to minimize the product inhibition and substrate inhibition

(a) Use of resin as an adsorbent for product removal

An adsorbent resin which can selectively adsorb diol can be used to minimize product inhibition. Furthermore, at end of reaction the product recovery becomes easy as product is adsorbed on the resin. The concept of using an adsorbent resins for removal of product from the reaction medium has been reported for some biotransformations [25, 26]. A detailed study of adsorption of diol on resin and epoxide hydrolysis in presence of resin was carried out.

(i) Adsorption of diol on resin

The graph of amount of diol adsorbed against amount of resin is given in Fig. 7.10. Among the 14 resins studied, 3 resins *namely* Lewatit VPOC 1163, Dowex Optipore SD-2 and Dowex Optipore L-493 gave maximum adsorption of phenylethane diol. These three resins were selected for further studies.

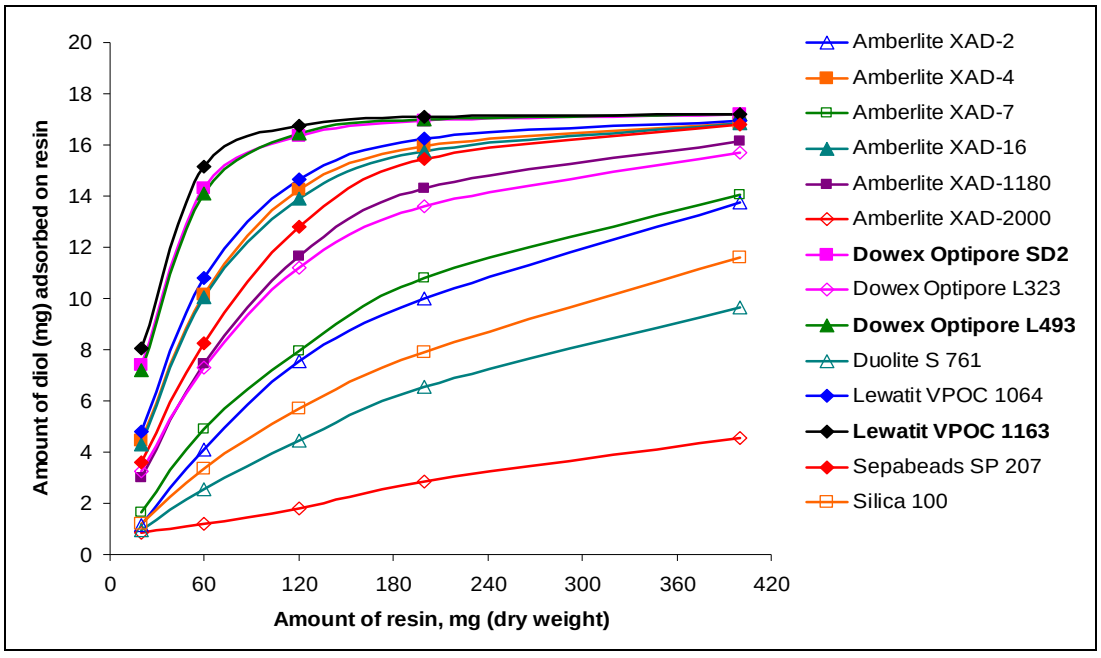

Fig. 7.10: Adsorption of phenylethane diol on commercial resins

Fig. 7.11 is a graph showing remaining concentration of diol in the aqueous phase verses X (i.e. mg of diol adsorbed per g of resin). Among three resins, Lewatit VPOC 1163 showed maximum capacity of diol adsorption and was therefore selected for further studies.

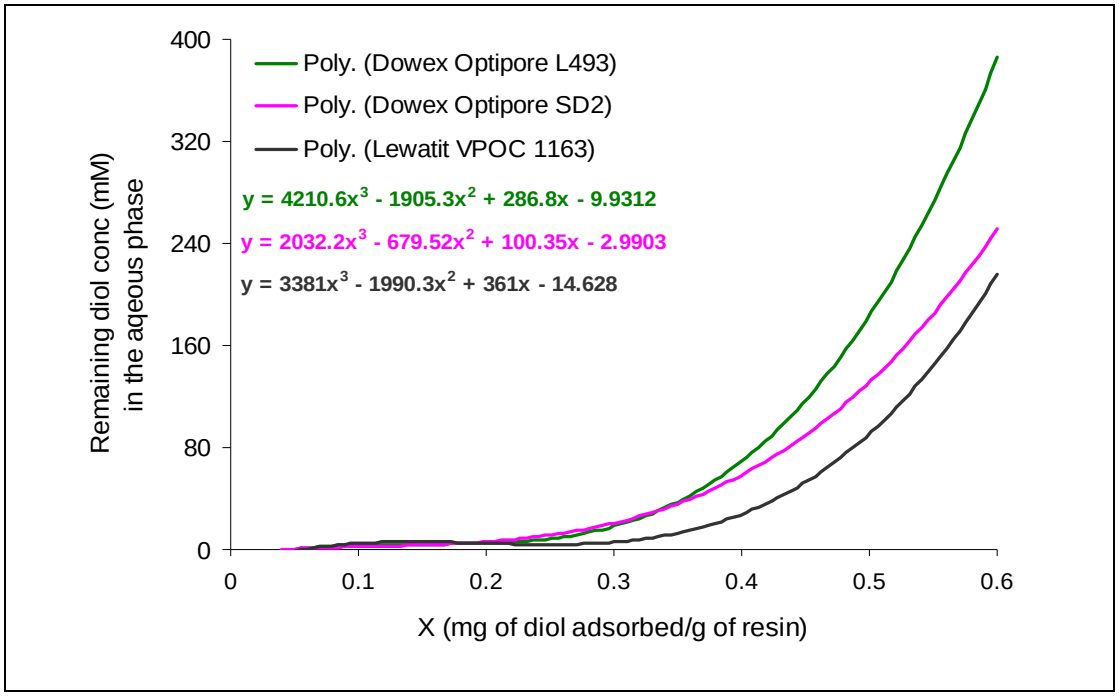

Fig. 7.11: Adsorption of phenylethane diol on commercial resins

(ii) Selectivity of adsorption

We decided upon a semi-continuous system of synthesis for vicinal diols. The enzymatic hydrolysis was carried out in stirred cell using immobilized *St*-EH. When the product concentration reached to a critical level that affected the rate of reaction, the reaction mixture was separated from immobilized enzyme and passed though the column containing an adsorbent resin which would selectively adsorb product (diol). The unreacted substrate was then recycled into the stirred cell for further conversion.

When solution of styrene oxide and phenylethane diol (5 g/L of each in phosphate buffer) was passed through a bed of Lewatit VPOC 1163 resin, styrene oxide was completely adsorbed on the resin while phenylethane diol showed partial adsorption (results not shown). The stronger adsorption of substrate on the resin rather than product ruled out the possibility of using Lewatit VPOC 1163 resin as selective adsorbent for product removal.

(b) Medium engineering

(i) Epoxide hydrolysis in phosphate buffer-ionic liquid biphasic reaction medium

Ionic liquids have been used to minimize the product inhibition in the epoxide hydrolase transformations [27]. Based on this report, we used four ionic liquids (in concentration of 10% v/v in 0.05 M phosphate buffer, pH 7.0) for the hydrolysis of styrene oxide.

The effect of ionic liquid as a reaction medium on ee of substrate and initial rate of reaction are presented in Fig. 7.12. The initial rates of *St*-EH catalyzed hydrolysis of styrene oxide in presence of all ionic liquids were very low.

This could be due to poor stability of enzyme in the ionic liquids and the inhibitory effects of ionic liquids on enzyme. Another possible reason of poor reaction rates could be due to high partitioning of substrate into ionic liquids with consequent low concentration of substrate in buffer phase where the enzymatic hydrolysis takes place. Detailed study in this regard is currently in progress.

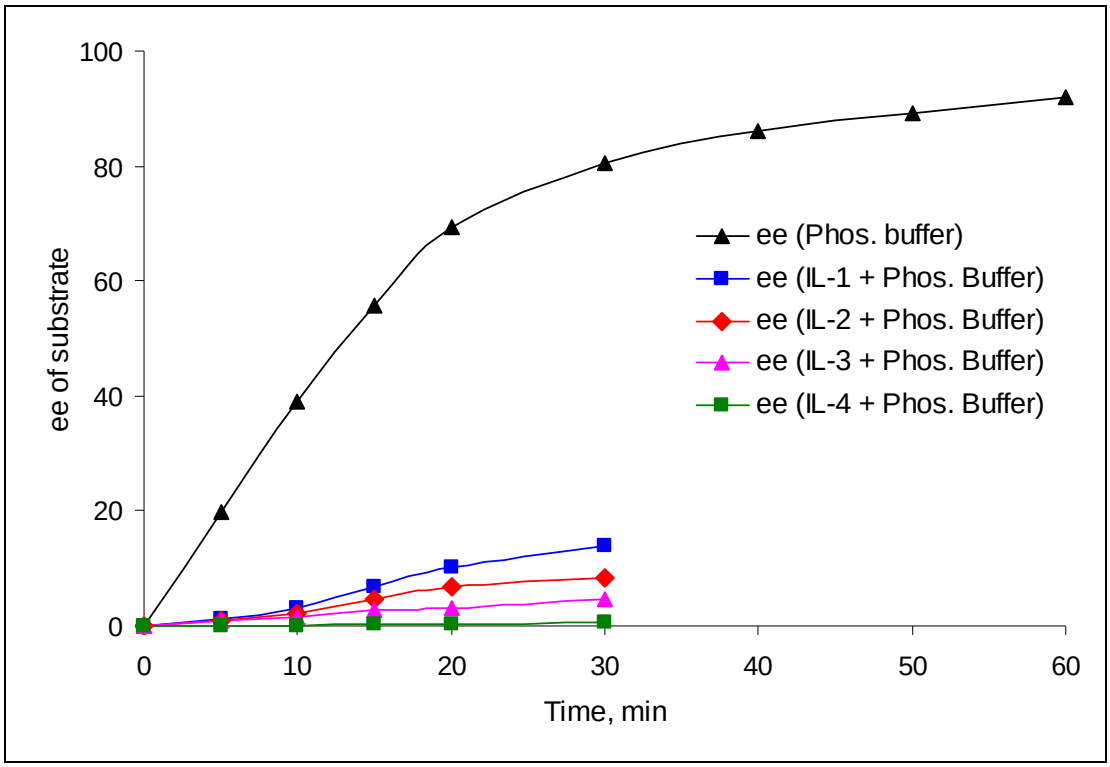

Fig. 7.12: Synthesis of phenylethane diol in (phosphate buffer + ionic liquid) biphasic reaction medium. (IL-1: [BMIm]PF_6, IL-2: [BMIm]BF_4, IL-3: [BMPy]Tf_2N and IL-4: [BMP]Tf_2N)

(ii) Epoxide hydrolysis in phosphate buffer-organic solvent biphasic reaction medium

Styrene oxide showed preferential partitioning in several water-immiscible organic solvents such as iso-octane, hexane and ethyl acetate. Hence organic solvent-phosphate buffer biphasic medium was used where the solvent phase acted as substrate reservoir and the enzyme was protected from the substrate inhibition. Among several immiscible solvents, *St*-EH showed maximum stability in the iso-ctane. Hence iso-octane was chosen for this study.

Several initial experiments were carried out to determine the optimum composition of biphasic medium (results not shown). The relative volumetric ratio of iso-octane to phosphate buffer in biphasic medium was found to be a critical parameter. At a higher ratio, a large quantity of styrene oxide partitioned into iso-ctane phase and resulted in decreased rate of reaction than that in plain phosphate buffer. At low ratio of iso-octane to buffer, due to high levels of styrene oxide in buffer phase, an improved rate of reaction could be achieved. However, this increased the extent of substrate inhibition. Also the rate of reaction was adversely affected due to loss of enzyme activity. Our study showed that 10:90 mixture of iso-octane-phosphate buffer give optimum results.

7.3.6. Determination of regioselectivity constants for immobilized St-EH

When unidirectional of bond-making or bond-breaking occurs preferentially over other possible directions, the reaction is said to be 'regioselective'. Reactions are termed completely (100%) regioselective if the discrimination is complete, or partially (*x*%), if the product of reaction at one site predominates over the product of reaction at other sites [28, 29].

The reaction medium can modulate the selectivity of an enzyme [30]. Therefore we studied the effect of iso-octane-buffer phase on regioselectivity of enzyme towards hydrolysis of styrene oxide and *m*-chloro-styrene oxide.

(a) Towards hydrolysis of styrene oxide

The regioselectivity constants for hydrolysis of styrene oxide in iso-octane-buffer biphasic medium are given in Table 7.4(a). The regioselectivity constants for hydrolysis of styrene oxide in biphasic medium were similar to that in phosphate

buffer. This suggests that use of biphasic medium did not affect the regioselectivity of *St*-EH.

(b) Towards hydrolysis of m-chloro-styrene oxide

The regioselectivity constants for hydrolysis of *m*-chloro-styrene oxide in iso-octane-buffer biphasic medium are given in Table 7.4(b). The regioselectivity constants for hydrolysis of *m*-chloro-styrene oxide in biphasic medium were similar to that in phosphate buffer. This suggests that use of biphasic medium did not affect the regioselectivity of *St*-EH.

Table 7.4: Regioselectivity constants [a] of immobilized *St*-EH

(a) For hydrolysis of styrene oxide

Reaction medium	***α-(S)***	***β-(S)***	***α-(R)***	***β-(R)***
Phosphate buffer	98	2	4	96
Iso-octane-phosphate buffer biphasic medium	98.5	1.5	3.6	96.4

(b) For hydrolysis of *m*-chloro-styrene oxide

Reaction medium	***α-(S)***	***β-(S)***	***α-(R)***	***β-(R)***
Phosphate buffer	97	3	5	95
Iso-octane-phosphate buffer biphasic medium	97.3	2.7	5.5	94.5

[[a] *α*-(*S*) and *β*-(*S*) represent regioselectivity constants for *S*-epoxide (indicating preference of attack on more substituted and less substituted carbon atom of the oxirane ring respectively) while *α*-(*R*) and *β*-(*R*) represent regioselectivity constant for *R*-epoxide (indicating preference of attack on more substituted and less substituted carbon atom of the oxirane ring respectively).]

7.3.7. Preparative scale enantioselective production of vicinal diols

(b) Production of m-chloro-phenylethane diol

The production of *m*-chloro-phenylethane diol was studied in repetitive batch mode. The initial reaction rate and reaction time of ten repeated cycles of hydrolysis of *m*-chloro-styrene oxide are summarized in Fig. 7.14. The first cycle proceeded with initial reaction rate of 18.4 $\mu M \cdot min^{-1} \cdot g^{-1}$ and reaction time was about 10 h. Thereafter

in each successive cycle, the initial reaction rate found to decrease steadily from 18.4 to 10.12 $\mu M \cdot min^{-1} \cdot g^{-1}$ indicating some loss of enzyme activity during each cycle. To attain complete conversion of *m*-chloro-styrene oxide to (*R*)-*m*-chloro-phenylethane diol in successive cycles, the reaction time was accordingly extended. The 10^{th} cycle therefore finished at 18 h and 10 min. The ee of product (ee_p) in each repetitive batch was found to be in the range of 95 to 96%.

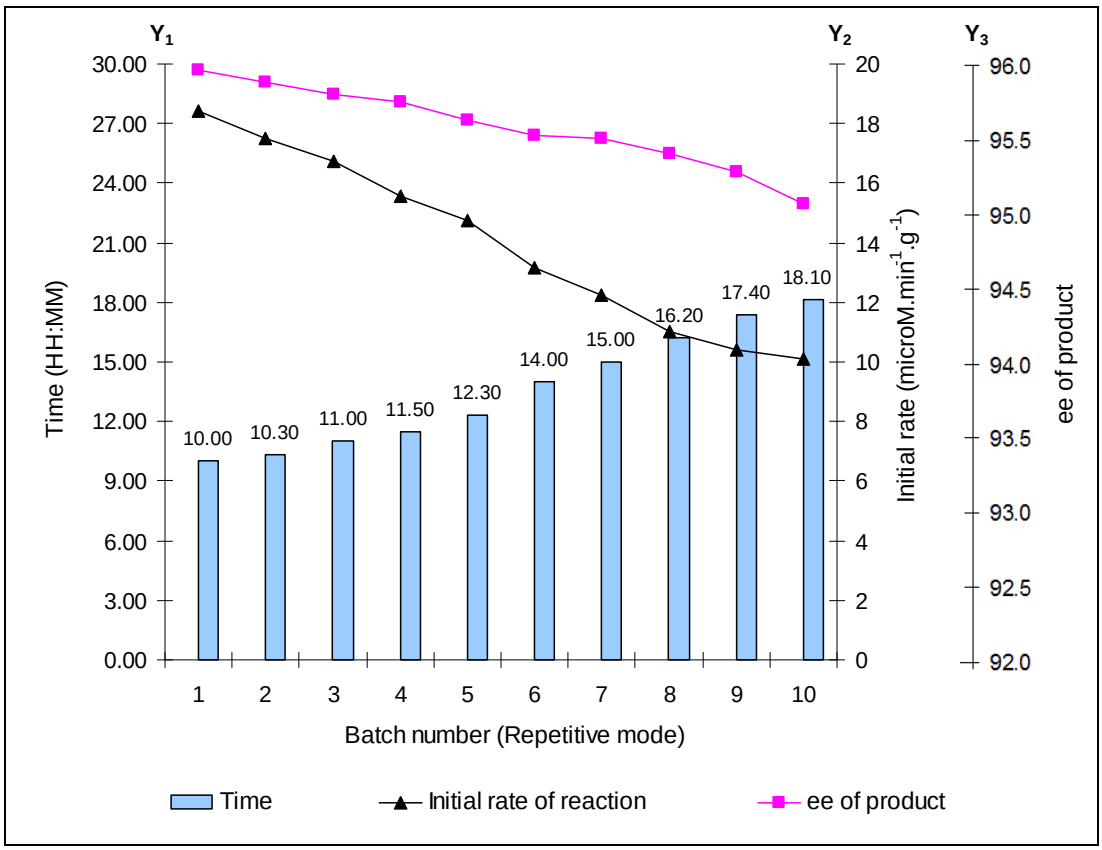

Fig. 7.14: Synthesis of *m*-chloro-phenylethane diol: Performance of stirred cell bioreactor over ten repeated cycles [Time is on Y_1 axis, Initial rate on Y_2 axis and ee of product on Y_3 axis]

(b) Production of m-chloro-phenylethane diol

The production of *m*-chloro-phenylethane diol was studied in repetitive batch mode. The initial reaction rate and reaction time of ten repeated cycles of hydrolysis of *m*-chloro-styrene oxide are summarized in Fig. 7.14. The first cycle proceeded with initial reaction rate of 18.4 $\mu M \cdot min^{-1} \cdot g^{-1}$ and reaction time was about 10 h. Thereafter in each successive cycle, the initial reaction rate found to decrease steadily from 18.4 to 10.12 $\mu M \cdot min^{-1} \cdot g^{-1}$ indicating some loss of enzyme activity during each cycle. To

attain complete conversion of *m*-chloro-styrene oxide to (*R*)-*m*-chloro-phenylethane diol in successive cycles, the reaction time was accordingly extended. The 10th cycle therefore finished at 18 h and 10 min. The ee of product (ee_p) in each repetitive batch was found to be in the range of 95 to 96%.

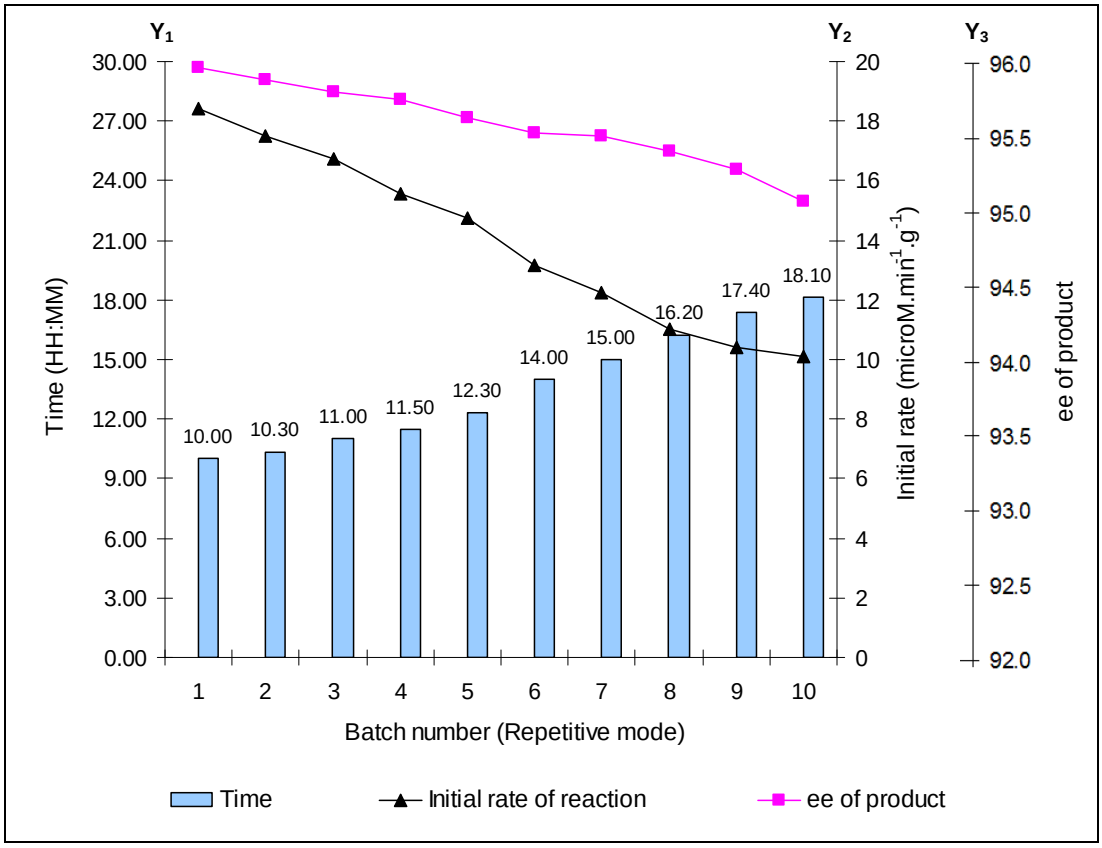

Fig. 7.14: Synthesis of *m*-chloro-phenylethane diol: Performance of stirred cell bioreactor over ten repeated cycles [Time is on Y_1 axis, Initial rate on Y_2 axis and ee of product on Y_3 axis]

The enantiomeric ratio (*E*) of the immobilized *St*-EH towards hydrolysis of styrene oxide was 27.2 while that of *m*-chloro-styrene oxide was 6.4. These observations are close to that reported in the literature [8].

Several epoxide hydrolases have been studied for enantioconvergent synthesis of (*R*)-phenyl-1,2 ethanediol and (*R*)-m-chloro-phenyl-1,2 ethanediol. For example: Pedragosa-Moreau *et al.* reported two epoxide hydrolases from *Aspergillus niger* and *Beauveria sulfurescens* that catalyzed the enantioconvergent synthesis of (*R*)-phenyl-1,2 ethanediol with an enantiopurity more than 90% ee and yield greater than 50% [31]. An enantioconvergent synthesis of (*R*)-phenyl-1,2 ethanediol using genetically

engineered epoxide hydrolases from *Agrobacterium radiobacter* and *Solanum tuberosum* gave 98% ee and 100% yield [32, 33]. Several epoxide hydrolases have been studied for enantioconvergent synthesis of (*R*)-phenyl-1,2 ethanediol and (*R*)-m-chloro-phenyl-1,2 ethanediol. For example: Pedragosa-Moreau *et al.* reported two epoxide hydrolases from *Aspergillus niger* and *Beauveria sulfurescens* that catalyzed the enantioconvergent synthesis of (*R*)-phenyl-1,2 ethanediol with an enantiopurity more than 90% ee and yield greater than 50% [31]. An enantioconvergent synthesis of (*R*)-phenyl-1,2 ethanediol using genetically engineered epoxide hydrolases from *Agrobacterium radiobacter* and *Solanum tuberosum* gave 98% ee and 100% yield [32, 33]. Hwang *et al.* employed two recombinant epoxide hydrolases from *Aspergillus niger* and *Rhodotorula glutinis* for enantioconvergent synthesis of (*R*)-phenyl-1,2 ethanediol. The product with 90% ee and 95% yield was obtained [34]. Kim *et al.* have recently demonstrated a enantioconvergent synthesis of (*R*)-phenyl-1,2 ethanediol by using two recombinant epoxide hydrolases from a bacterium (*Caulobacter crescentus*), and a marine fish (*Mugil cephalus*). The authors reported a conversion of *rac*-styrene oxide (at a concentration of 6g/L) into (*R*)-phenyl-1,2 ethanediol with 90% ee and 94% quantitative yield [35]. The enantioconvergent synthesis of (*R*)-*m*-chloro-phenyl-1,2 ethanediol using recombinant *Solanum tuberosum* epoxide hydrolase is reported by Monterde *et al.* The enantioconvergent transformation of *rac*-*m*-chloro-styrene oxide (at a concentration of 10 g/L) gave (*R*)-*m*-chloro-phenyl-1,2 ethanediol with 90% ee and 94% quantitative yield [8]. Enantioconvergent transformations of other epoxides such as *p*-chloro-styrene oxide [20, 36, 37] and *p*-nitro-styrene oxide [38] into their corresponding enantiopure diols has also been studied.

The maximum concentration of *rac*-styrene oxide used for EH-catalyzed enantioconvergent synthesis of (*R*)-phenyl-1,2 ethanediol is 6 g/L [35]. The present study reports enantioconvergent transformation of *rac*-styrene oxide at concentration of 50 g/L. Whereas, the maximum concentration of *rac*-*m*-chloro-styrene oxide used for EH-catalyzed enantioconvergent synthesis of (*R*)-*m*-chloro-phenyl-1,2 ethanediol is 10 g/L [8]. The present study reports enantioconvergent transformation of *rac*-*m*-chloro-styrene oxide at concentration of 20 g/L. Thus, the present study has shown enantioconvergent transformations of epoxides at much higher concentrations than those reported previously.

7.4. CONCLUSIONS

The immobilization of *St*-EH on GA support gave high activity recovery. The immobilization of *St*-EH on GA support increased the pH and temperature stability of enzyme. The immobilized enzyme had better stability in water-immiscible solvents than in water-miscible solvents. Use of 10:90 mixture of iso-octane-phosphate buffer biphasic medium was observed to be beneficial to minimize the substrate inhibition and chemical hydrolysis of substrate. The immobilized enzyme expressed high operational stability in repetitive hydrolytic batches of styrene oxide as well as that of *m*-chloro-styrene oxide.

REFERENCES

[1] Besse, P.; Veschambre, H. Chemical and biological synthesis of chiral epoxides. *Tetrahedron*, **1994**, *50*, 8885-8927.

[2] Kasai, N.; Suzuki, T.; Furukawa, Y. Chiral C3 epoxides and halohydrins: Their preparation and synthetic application. *J. Mol. Catal. B: Enzym.*, **1998**, *4*, 237-252.

[3] Archelas, A.; Furstoss, R. Synthetic applications of epoxide hydrolases. *Curr. Opin. Chem. Biol.*, **2001**, *5*, 112-119.

[4] Genzel, Y.; Archelas, A.; Broxterman, Q.B.; Schulze, B.; Furstoss, R. Microbiological transformation: 50. Selection of epoxide hydrolase for enzymatic resolution of 2-, 3-, or 4-pyridyloxirane. *J. Mol. Catal. B: Enzym.*, **2002**, *16*, 217-222.

[5] Nielsen, L.P.C.; Stevenson, C.P.; Blackmond, D.G.; Jacobsen, E.N. Mechanistic investigation leads to a synthetic improvement in the hydrolytic kinetic resolution of terminal epoxides. *J. Am. Chem. Soc.*, **2004**, *126*, 1360-1362.

[6] Jacobsen, EN. Asymmetric catalysis of epoxide ring-opening reactions. *Acc. Chem. Res.*, 2000, 33, 421-431.

[7] Tokunaga, M.; Larrow, J.F.; Kakiuchi, F.; Jacobsen, E.N. Asymmetric catalysis with water: Efficient kinetic resolution of terminal epoxides by means of catalytic hydrolysis. *Science*, **1997**, *277*, 937-938.

[8] Monterde, M.; Lombard, M.; Archelas, A.; Cronin, A.; Arand, M.; Furstoss, R. Enzymatic transformations Part 58: Enantioconvergent biohydrolysis of styrene oxide derivatives catalysed by the *Solanum tuberosum* epoxide hydrolase. *Tetrahedron: Asymmetr.*, **2004**, *15*, 2801-2805.

[9] Arand, M.; Cronin, A.; Adamska, M.; Oesch, F. Epoxide hydrolases: Structure, function, mechanism, and assay. *Methods Enzymol.*, **2005**, *400*, 569-588.

[10] Lee, E.Y.; Shuler, M.L. Molecular engineering of epoxide hydrolase and its application to asymmetric and enantioconvergent hydrolysis. *Biotechnol. Bioeng.*, **2007**, *98(2)*, 318-327.

[11] Strauss, U.T.; Felfer, U.; Faber, K. Biocatalytic transformation of racemates into chiral building blocks in 100% chemical yield and 100% enantiomeric excess. *Tetrahedron: Asymmetr.*, **1999**, *10*, 107-117.

[12] Choi, W.J. Biotechnological production of enantiopure epoxides by enzymatic kinetic resolution. *Appl. Microbiol. Biotechnol.*, **2009**, *84*, 239-247.

[13] Guisan, J.M. Aldehyde-agarose gels as activated supports for immobilization-stabilization of enzymes. *Enzyme Microb. Technol.*, **1988**, *10*, 375-382.

[14] Mateo, C.; Fernandez-Lafuente, R.; Archelas, A.; Guisan, J.M.; Furstoss, R. Preparation of a very stable immobilized *Solanum tuberosum* epoxide hydrolase. *Tetrahedron: Asymmetr.*, **2007**, *18*, 1233-1238.

[15] Corey, E.J.; Chaykovsky, M. Dimethyloxosulfonium methylide ($(CH_3)_2SOCH_2$) and dimethylsulfonium methylide ($(CH_2)_2SCH_2$): Formation and application to organic synthesis. *J. Am. Chem. Soc.*, **1965**, *87(6)*, 1353-1364.

[16] Karboune, S.; Archelas, A.; Furstoss, R.; Baratti, J.C. Immobilization of the *Solanum tuberosum* epoxide hydrolase and its application in an enantioconvergent process. *Biocatal. Biotransfor.*, **2005**, *23(6)*, 397-/405.

[17] Mateo, C.; Archelas, A.; Furstoss, R. A spectrophotometric assay for measuring and detecting an epoxide hydrolase activity. *Anal. Biochem.*, **2003**, *314*, 135-141.

[18] Straathof, A.J.J.; Jongejan, J.A. The enantiomeric ratio: origin, determination and prediction. *Enzyme Microb. Technol.*, **1997**, *21*, 559-571.

[19] Karboune, S.; Amourache, L.; Nellaiah, H.; Morisseau, C.; Baratti, J. Immobilization of the epoxide hydrolase from *Aspergillus niger*. *Biotechnol.*

Lett., **2001**, *23,* 1633-1639.

[20] Karboune, S.; Archelas, A.; Furstoss, R.; Baratti, J.C. Immobilization of epoxide hydrolase from *Aspergillus niger* onto DEAE-cellulose: enzymatic properties and application for the enantioselective resolution of a racemic epoxide. *J. Mol. Catal. B: Enzym.*, **2005**, *32*, 175-183.

[21] Petri, A.; Marconcini, P.; Salvadori, P. Efficient immobilization of epoxide hydrolase onto silica gel and use in the enantioselective hydrolysis of racemic *para*-nitrostyrene oxide. *J. Mol. Catal. B: Enzym.*, **2005**, *32*, 219-224.

[22] Kroutil, W.; Orru, R.V.A.; Faber, K. Stabilization of *Nocardia* EH1 epoxide hydrolase by immobilization. *Biotechnol. Lett.*, **1998,** *20(4),* 373-377.

[23] Bučko, M.; Vikartovská, A.; Lacík, I.; Kolláriková, G.; Gemeiner, P.; Pätoprstý, V.; Brygin, M. Immobilization of a whole-cell epoxide-hydrolyzing biocatalyst in sodium alginate-cellulose sulphate-poly(methylene-*co*-guanidine) capsules using a controlled encapsulation process. *Enzyme Microb. Technol.*, **2005**, *36*, 118-126.

[24] Lee, K.S.; Woo, M.H.; Kim, H.S.; Lee, E.Y.; Lee, I.S. Synthesis of hybrid Fe3O4–silica–NiO superstructures and their application as magnetically separable high-performance biocatalysts. *Chem. Commun.*, **2009**, 3780-3782.

[25] Hilker, I.; Wohlgemuth, R.; Alphand, V.; Furstoss, R. Microbial Transformations 59: First Kilogram scale asymmetric microbial Baeyer-Villiger Oxidation with optimized productivity using a resin-based in situ SFPR Strategy. *Biotechnol. Bioengg.*, **2005**, *92(6)*, 702-710.

[26] Mirata, M.A.; Heerd, D.; Schrader, J. Integrated bioprocess for the oxidation of limonene to perillic acid with *Pseudomonas putida* DSM 12264. *Process Biochem.*, **2009**, *44*, 764-771.

[27] Chiappe, C.; Leandri, E.; Hammock, B.D.; Morisseau, C. Effect of ionic liquids on epoxide hydrolase-catalyzed synthesis of chiral 1,2-diols. *Green Chem.*, **2007**, *9*, 162-168.

[28] IUPAC Compendium of Chemical Terminology. 2nd Edition, 1997; (URL: http://old.iupac.org/goldbook/R05243.pdf)

[29] Moussou, P.; Archelas, A.; Baratti, J.; Furstoss, R. Determination of the

regioselectivity during epoxide hydrolase oxirane ring opening: a new method from racemic epoxides. *J. Mol. Cat. B: Enzym.*, **1998**, *5*, 213-217.

[30] Sakurai, T.; Margolin, A.L.; Russell, A.J.; Klibanov, A.M. Control of enzyme enantioselectivity by the reaction medium. *J. Am. Chem. Soc.*, **1988**, *110 (21)*, 7236-7237.

[31] Pedragosa-Moreau, S.; Morisseau, C.; Zylber, J.; Archelas, A.; Baratti, J.; Furstoss, R. Microbiological transformations: 33. Fungal epoxide hydrolases applied to the synthesis of enantiopure parasubstituted styrene oxides. A mechanistic approach. *J. Org. Chem.*, **1996**, *61*, 7402-7407.

[32] Cao, L.; Lee, J.; Chen, J.W.; Wood, T.K. Enantioconvergent production of (*R*)-1-phenyl-1, 2-ethanediol from styrene oxide by combining the *Solanum tuberosum* and an evolved *Agrobacterium radiobacter* AD1 epoxide hydrolases. *Biotechnol. Bioeng.*, **2006**, *94*, 522-529.

[33] Rui, L.; Cao, L.; Chen, W.; Reardon, K.F.; Wood, T.K. Protein engineering of epoxide hydrolase from *Agrobacterium radiobacter* AD1 for enhanced activity and enantioselective production of (R)-1-phenylethane-1,2-diol. *Appl. Environ. Microbiol.*, **2005**, *71*, 3995-4003.

[34] Hwang, S.; Choi, C.Y.; Lee, E.Y. One-pot biotransformation of racemic styrene oxide into (*R*)-1,2-phenylethandiol by two recombinant microbial epoxide hydrolases. *Biotechnol. Bioproc. Eng.*, **2008**, *13*, 453-457.

[35] Kim, H.S.; Lee, O.K.; Hwang, S.; Kim, B. J.; Lee, E. Y. Biosynthesis of (*R*)-phenyl-1,2-ethanediol from racemic styrene oxide by using bacterial and marine fish epoxide hydrolases. *Biotechnol. Lett.*, **2008**, *30*, 127-133.

[36] Manoj, K.M.; Archelas, A.; Baratti, J.; Furstoss, R. Microbiological transformations. Part 45: A green chemistry preparative scale synthesis of enantiopure building blocks of Eliprodil: elaboration of a high substrate concentration epoxide hydrolase-catalyzed hydrolytic kinetic resolution process. *Tetrahedron*, **2001**, *57*, 695-701.

[37] Hwang, S.; Choi, C.Y.; Lee, E. Y. Enantioconvergent bioconversion of *p*-chlorostyrene oxide to (*R*)-*p*-chlorophenyl-1,2-ethandiol by the bacterial epoxide hydrolase of *Caulobacter crescentus*. *Biotechnol. Lett.*, **2008**, *30*, 1219-1225.

[38] Xu, W.; Xu, J.H.; Pan, J.; Gu, O.; Wu, X.Y. Enantioconvergent hydrolysis of styrene epoxides by newly discovered epoxide hydrolases in mung bean. *Org. Lett.*, **2006**, *8*, 1737-1740.

CHAPTER

8

Conclusions

8.1. CHAPTERWISE CONCLUSIONS

Chapter 2:

Epoxy-activated porous polymer beads of allyl glycidyl ether with ethylene glycol dimethacrylate as cross-linking agent and lauryl alcohol as porogen provided an excellent support for lipase immobilization. The immobilization of lipases (CRL and PPL) on AGE-(L)-100 polymer beads resulted in improved pH and temperature stability and extended storage half-life. Among the different lipases screened, CRL exhibited highest enantioselectivity towards hydrolysis of PG-ester, DOPA-ester and HPA-ester (E = 11.9, 9.6 and 15.6 respectively) while PPL exhibited highest enantioselectivity towards hydrolysis of NA-ester (E = 17.9). Both CRL and PPL preferentially hydrolyzed the *S*-enantiomer of unnatural amino acid ethyl esters. The immobilization of lipases (CRL and PPL) on AGE-(L)-100 polymer beads did not alter their enantioselectivity towards hydrolysis of unnatural amino acid ethyl esters.

Chapter 3:

A blend of polyurethane (meth)acrylate and GMA was coated and cured on a PP membrane to have better surface hydrophilicity, biocompatibility, strength and chemical stability. This membrane has excellent protein binding capacity hence can be used for enzyme immobilization. Under optimum conditions, the biocatalytic membranes (CRL-PUA-I and PPL-PUA-I), showed high activity recovery (about 90% and 91% respectively) and high retention of specific activity (about 92% and 96% respectively). Furthermore these biocatalytic membranes showed better stability over a wider range of pH and temperature than that of free enzyme. CRL-PUA-I showed maximum enantioselectivity towards hydrolysis of PG-ester, DOPA-ester and HPA-ester (E = 11.3, 10.3 and 14.4 respectively) while PPL-PUA-I showed maximum enantioselectivity towards hydrolysis of NA-ester (E = 15.2). Moreover, CRL-PUA-I and PPL-PUA-I exhibited high operational stability during repetitive hydrolytic cycles of HPA-ester and NA-ester respectively.

Chapter 4:

The production of amidase by *Rhodococcus erythropolis* MTCC 1526 was found to depend greatly on four media components (*namely*: sorbitol, yeast extract, meat peptone and acetamide). Using the RSM, it was possible to model individual and

interactive effects of media components on amidase production. The validity of the model was confirmed by the close agreement between experimental and predicted values. The media optimization by RSM effectively enhanced the amidase production by 6.88 fold. Among four methods of cell immobilization, entrapment of *R. erythropolis* cells in alginate gel (ALG-Re) and polyvinyl alcohol agar (PVA-Re) gave higher amidase activity. Amidase of *R. erythropolis* MTCC 1526 preferentially hydrolyzed *S*-enantiomer of unnatural amino acid amides. ALG-Re and PVA-Re biocatalytic matrices showed better enantioselectivity towards hydrolysis of PG-amide (E = 15.6 and E = 14.8 respectively) and HPA-amide (E = 11.5 and E = 10.6 respectively). These biocatalytic matrices showed poor enantioselectivity towards hydrolysis of NA-amide (E = 6.2 and E = 6.1 respectively).

Chapter 5:

The immobilization of L-aminoacylase on epoxy-activated porous polymer beads of styrene-glycidyl methacrylate-divinyl benzene ter-polymers has significantly improved the stability of aminoacylase with respect to pH, temperature and storage. Enantiomeric ratios of the immobilized enzyme were high ($E \approx 125$ to 200) towards hydrolysis of amides, moderate ($E \approx 22$ to 59) towards hydrolysis of N-acetyl derivatives and poor ($E < 15$) towards the hydrolysis of amino acid esters. Thus, the production of enantiopure amino acids via aminoacylase catalyzed hydrolysis of *rac*-amino acid amides appears to be an attractive alternative. However the operational stability of immobilized aminoacylase found to be inadequate for reuse of the enzyme in a repetitive batch mode.

Chapter 6:

In this work, we have demonstrated that co-aggregation of aminoacylase with an aminated polymer (e.g. PEI) facilitates formation of physically stable CLEA. The method described yields stable cross-linking and no release of enzyme was found upon storage. The cross-linking significantly improved the stability of aminoacylase with respect to pH, temperature and storage. Aminoacylase-PEI CLEA were able to hydrolyze different amino acid derivatives (*namely*: amino acid esters, N-acetyl amino acids and amino acid amides) in an enantioselective manner. The enantioselectivity however, was dependent on the type of amino acid derivative. The

enantioselectivity of CLEA was remarkably high towards hydrolysis of amides, moderate towards hydrolysis of N-acetyl derivatives and poor towards the hydrolysis of amino acid esters. Aminoacylase-PEI CLEA exhibited high operational stability in repetitive cycles of *rac*-HPA amide hydrolysis. Aminoacylase-PEI CLEA catalyzed hydrolysis of *rac*-amino acid amides gave best results for biocatalytic production of the given enantiopure amino acids.

Chapter 7:

The immobilization of *St*-EH on GA support gave high activity recovery. The immobilization of *St*-EH on GA support increased the pH and temperature stability of enzyme. The immobilized enzyme had better stability in water-immiscible solvents than in water-miscible solvents. Use of 10:90 mixture of iso-octane-phosphate buffer biphasic medium was observed to be beneficial to minimize the substrate inhibition and chemical hydrolysis of substrate. The immobilized enzyme expressed high operational stability in repetitive hydrolytic batches of styrene oxide as well as that of *m*-chloro-styrene oxide.

8.2. ENANTIOSELECTIVITY OF BIOCATALYSTS TOWARDS SYNTHESIS OF UNNATURAL AMINO ACIDS

In the present thesis, enantioselective synthesis of unnatural amino acids was studied using three immobilized biocatalysts *viz.* lipases (EC 3.1.1.3), amidase (EC 3.5.1, 3.5.2) and L-aminoacylase (E.C. 3.5.1.14). These biocatalysts were used for synthesis of enantiopure unnatural amino acids (*viz.* phenylglycine, homophenylalanine, 2-naphthylalanine). The different biocatalytic routes studied in the present thesis are schematically represented in Fig. 8.1.

Enantiomeric ratios (E) for lipase catalyzed hydrolysis of amino acid esters (route I) were in the range of 12-18 while that for amidase catalyzed hydrolysis of amino acid amides (route II) were in range of 6-16. Aminoacylase catalyzed hydrolysis of amino acid esters (route III) gave enantiomeric ratios in the range of 6-14 while that of N-acetyl amino acids (route IV) gave enantiomeric ratios in the range of 22-60. Aminoacylase catalyzed hydrolysis of amino acid amides (route V) gave maximum enantiomeric ratios ($E > 200$ for PG amide and HPA-amide while $E \approx 124$ for NA-amide). Thus among the different biocatalysts studied, immobilized

aminoacylase offered maximum enantioselectivity towards hydrolysis of amino acid amides.

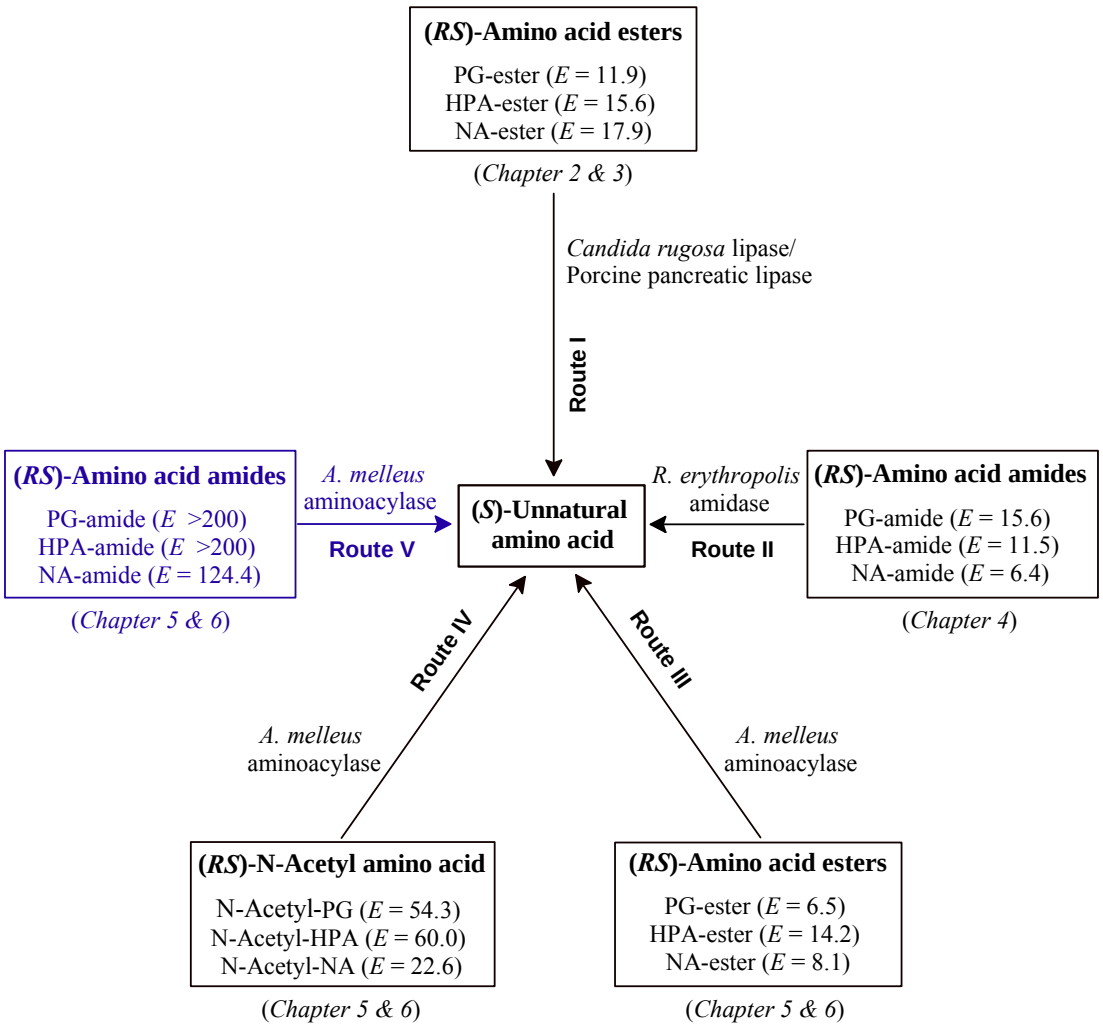

Fig. 8.1: Enantiomeric ratios (*E*) for different enzymatic resolution reactions studied in this thesis. (For the given amino acid derivative and for the given enzymatic route, *E* mentioned in this figure represents the maximum value experimentally obtained by using an immobilized enzyme preparation).

PUBLICATIONS, CONFERENCE PRESENTATIONS AND AWARDS

I. Publications from Ph.D. thesis work:

1. N.S. Pujari, **B.K. Vaidya**, S. Bagalkote, S. Ponrathnam, S.N. Nene; Poly(urethane methacrylate-*co*-glycidyl methacrylate)-supported-polypropylene biphasic membrane for lipase immobilization; ***Journal of Membrane Science,*** 285 (2006) 395-403. [*Received 8 citations**]

2. **B.K. Vaidya,** G.C. Ingavle, S. Ponrathnam, B.D. Kulkarni and S.N. Nene; Immobilization of *Candida rugosa* lipase on poly(allyl glycidyl ether-co-ethylene glycol dimethacrylate) macroporous polymer particles; ***Bioresource Technology***, 99 (2008) 3623-3629. [*Received 9 citations**]

3. **B.K. Vaidya**, S.R. Mutalik, R.M. Joshi, S.N. Nene, B.D. Kulkarni; Enhanced production of amidase from *Rhodococcus erythropolis* MTCC 1526 by media optimization using statistical experimental design; ***Journal of Industrial Microbiology and Biotechnology***, 36 (2009) 671-678.

4. **B.K. Vaidya**, S.N. Nene, B.D. Kulkarni; Enantioselective synthesis of unnatural amino acids using covalently immobilized L-aminoacylase; *Manuscript communicated*.

5. **B.K. Vaidya**, S.S. Kuwar, S.B. Golegaonkar, S.N. Nene, B.D. Kulkarni; Preparation and characterization of cross-linked enzyme aggregates of *Aspergillus melleus* L-aminoacylase; *Manuscript under preparation*.

6. **B.K. Vaidya**, A. Archelas; Preparative scale enantioselective production of vicinal diols by immobilized epoxide hydrolase in aqueous-organic biphasic reaction medium; *Manuscript under preparation*.

II. Other publications:

7. K.M. Desai, **B.K. Vaidya**, R.S. Singhal and S.S. Bhagwat; Use of an artificial neural network in modeling yeast biomass and yield of β-glucan; ***Process Biochemistry***, 40 (2005) 1617-1626. [*Received 14 citations**]

8. **B.K. Vaidya**, H.K. Suthar, S.M. Kasture, S.N. Nene; Purification of potato polyphenol oxidase (PPO) by partitioning in Aqueous Two Phase System; ***Biochemical Engineering Journal***, 28 (2006) 161-166. [*Received 11 citations**]

9. **B.K. Vaidya,** A.J. Karale. H.K. Suthar, G.C. Ingavle, T. Pathak, S. Ponrathnam, S.N. Nene; Immobilization of mushroom polyphenol oxidase on poly(allyl glycidyl ether-co-ethylene glycol dimethacrylate) macroporous beaded copolymers; ***Reactive and Functional Polymers***, 67 (2007) 905-915. [*Received 1 citation**]

10. **B. K. Vaidya**, R. S. Singhal; Use of insoluble yeast β-glucan as a support for immobilization of *Candida rugosa* lipase; ***Colloids and Surfaces B: Biointerfaces***, 61 (2008) 101-105. [*Received 2 citations**]

11. S.R. Mutalik, **B.K. Vaidya,** R.M. Joshi, K.M. Desai, S.N. Nene; Use of response surface optimization for production of biosurfactant from Rhodococcus spp. MTCC 2574; ***Bioresource Technology***, 99 (2008) 7875-7880. [*Received 1 citation**]

12. A.S. Deshpande, R.B. Khomane, **B.K. Vaidya,** R.M. Joshi, A.S. Harle, B.D. Kulkarni; Sulfur nanoparticles synthesis and characterization from H_2S gas, using novel biodegradable iron chelates in W/O microemulsion; ***Nanoscale Research Letters***, 3 (2008) 221-229. [*Received 1 citation**]

13. M.P. Pal, K.M. Desai, R.M. Joshi, **B.K. Vaidya**, S.N. Nene & B.D. Kulkarni; Media optimization for biosurfactant production by *Rhodococcus erythropolis* MTCC 2794: Artificial intelligence vs. a statistical approach; ***Journal of Industrial Microbiology and Biotechnology***, 36 (2009) 747-756.
    [* Source: www.scopus.com as on 01/12/2009]

III. Conference / Symposium Presentations:

1. Oral presentation on the topic 'Stabilization of aminoacylase via co-aggregation with polyethyleneimine' in the **International Symposium on Catalysis and Fine Chemicals (C&FC-2007)** held at Nanyang Technological University (NTU), Singapore.

2. Presented a poster on a topic 'Kinetic modeling of thermal inactivation of soluble and immobilized aminoacylase on poly(styrene- glycidyl methacrylate- divinyl benzene) macroporous beaded polymers' in the **International Conference on New Horizons in Biotechnology (NHBT-2007)** held at National Institute for Interdisciplinary Science and Technology (NIIST) Thiruvananthapuram, India.

IV. Awards:

1. Received '**Keerthi Sangoram Memorial Endowment Award**' for Best Research Scholar (in field of Engineering Sciences) for the Year 2008 [sponsored by NCL Research Foundation] on National Science Day (28th February 2009).

2. Received '**Best Poster Award**' for the poster entitled as 'Poly (urethane methacrylate -*co*- glycidyl methacrylate) -*supported*- polypropylene biphasic membrane for lipase immobilization' [sponsored by NCL Research Foundation] on National Science Day (28th February 2007).